The Roles of Phosphocholine Expressed on NTHi Bacteria and Host CRP in Acute Otitis Media

Gurpreet Kaur Bharj

St Cross College

University of Oxford

A thesis submitted for the degree of *Doctor of Philosophy*

Trinity 2022

Abstract

Otitis Media (OM) is inflammation of the middle ear (ME). Non-typeable *Haemophilus influenzae* (NTHi) is one of the leading otopathogens causing OM. Phosphocholine (PCho) on the NTHi lipopolysaccharide influences host-pathogen interaction. C-Reactive Protein (CRP), an acute phase protein, recognizes PCho and can mediate bacterial killing. However, some strains of NTHi survive well in the presence of CRP. We aimed to study the interaction of CRP with NTHi to understand its role in bacterial survival in acute OM (AOM). NTHi can efficiently infect the *Junbo* mouse, a characterised model of chronic and AOM. We developed a CRP ELISA that showed PCho off heptose III on NTHi surface enhanced CRP binding compared to PCho off heptose I. This increased interaction made the NTHi more susceptible to serum bactericidal killing. Gene expression analysis of macrophages infected with NTHi 375 strains confirmed that PCho influenced inflammatory cytokine gene expression whereby having no PCho or PCho off heptose III drove a M1 macrophage response. We inoculated the *Junbo* mouse with NTHi 375 strains and studied infection and immune responses at days 1-, 3- and 7- post NTHi inoculation. The highest levels of acute response were measured at 1-day post infection. A greater than 90% infection rate of the *Junbo* mouse was measured for NTHi bacteria expressing PCho compared to the PCho mutant, which had an infection rate of approximately 50%. Immune cell profiling of the innate and adaptive cells in the middle ear fluid (MEF), blood and nasal associated lymphoid tissue showed interesting cellular changes in response to PCho presence and position. NTHi promoted anti-inflammatory immune cell types in the MEF by activating M2-like macrophages and regulatory T cells. NTHi expressing PCho off heptose I survive in the MEF of the *Junbo* mouse even in the presence of a T cell cytokine/chemokine response. Together, these data confirm that the presence of CRP in the *Junbo* mouse MEF may not contribute to NTHi killing because it does not bind well to PCho off specific heptoses on the bacterial surface. Thus, NTHi bacteria can survive in the presence of CRP dependent upon the presence and position of PCho on their surface-expressed LPS.

Acknowledgements

I would like thank my supervisors for all the support and guidance they have provided me throughout this DPhil journey. Dr Derek Hood, thank you for giving me this opportunity to explore and grow independently. Thank you so much for your patience and supervision. Professor Timothy Hinks, thank you for letting me share my excitement about science with you. Despite the Covid-19 lockdowns and MRC Harwell closure, our conversations always kept the science alive. Professor Helen Christian, thank you so much your support over the years.

My first thank you, to my best friend and partner in crime, Dr Vineeth. Thank you for motivating me throughout the journey. Looking back, this DPhil seems almost incomplete without you. Thank you for our endless conversations, your motivation, being my soundboard, tiramisu-buddy, spontaneous trip partner and biggest drama queen. I fell in love with science even more through you. I look forward to seeing what the future holds.

To my sisters Harvinder and Moonsun Bharj. My backbone. My biggest thank goes to you both. Thank you for being my biggest cheerleaders and supporters. Thank you for the endless love, laughter and the madness. I could not have made it through this journey without you both.

To the rest of the drama queens, and to my most special friends – Nayan Waghmare, Sruthi Chandrasekar and Dillon Jagatia. Nayan, thank you for always asking the right questions and your positivity. Sruthi, thank you for your motivation and support. Dillon, thank you for your kindness, laughter and chaos.

To my best friend, Mary Benedict. Thank you for all your calls and listening to me talk for hours. To Harkirat Behl, thank you for your endless positivity, laughter and motivation through all those books you gifted me to read. To Rosaria, thank you so much for your kindness and motivation. To Nupur Patel, Aisha Ishaq, Yasmin Iqbal and Samantha Holderness, thank you for our trips and phone calls over the years. To Marius Weber, thank you for always being excited about hot chocolate with me. To Amy Southern and Louisa Zolkiewski, my girls, I am so grateful to have met you both and I am so excited to have completed this journey with you both.

Finally, to my parents, Mr Satpal Singh Bharj and Mrs Harjeet Kaur Bharj, thank you for your love, support, care, compassion and confidence in me. Papa ji, thank you for dreaming with me. This journey would have been impossible without you. Mummy, thank you for always pushing me to '*go for it'*. I love you both and I will forever be grateful to you both for being my pillars. I owe all my success to you both.

Statement of contributions

I, Gurpreet K. Bharj, confirm that the work presented in this thesis is my own. However, this thesis would not have been completed without the contributions of others.

In chapter 3, collaboration for immunogold staining and electron microscopy was setup with Dr Errin Johnson and Dr Charlotte Melia in the Department of Pathology, University of Oxford. Dr Melia kindly performed all the immunogold preparations and carried out the electron microscope imaging.

The Mary Lyon Centre provided all the animal care, and basic husbandry. All histological processes for fixing, wax embedding and sectioning were performed by the Histology Department in the MRC Harwell core histology facility.

In chapter 6, I am grateful for the help from Dr Emanuele Marchi who assisted in producing the heat-map for middle ear fluid samples from the *Junbo* mouse.

Chapter 6 is being prepared for a manuscript.

All contributions that have been made by others have been indicated in the thesis.

Gurpreet Kaur Bharj

Word count: Approximately 45,000

Publications

Vikhe, P., Tateossian, H., **Bharj, G**., Brown, S., Hood, D., Mutation in Fbxo11 Leads to Altered Immune Cell Content in *Jeff* Mouse Model of Otitis Media. Frontiers in Genetics (2020). DOI: 10.3389/fgene.2020.00050.

Brown, M., Jabeen, M, **Bharj, G.** and Hinks, T. Non-typeable Haemophilus influenzae airways infection: the next treatable trait in asthma? (2022). DOI: 10.1183/16000617.0008-2022

Conferences

Bharj, G., Vikhe, P, Brown, S. and Hood, D. Insights into Otitis Media: Dissecting the interaction of C-Reactive Protein with Non-Typeable Haemophilus influenzae. Access Microbiology (2022). DOI: 10.1099/acmi.ac2021.po0268 **Poster**

Oxford-MRC DTP Symposium. Insights into Otitis Media: Dissecting theinteraction of C-Reactive Protein with Non-Typeable Haemophilus influenzae. (2020) **Talk**

Bharj, G., Vikhe, P, Purnell, T., Martin-Fernandez, M, Brown, S. and Hood, D. C-Reactive Protein and Non-Typeable *Haemophilus influenzae*. 20th International Symposium on Recent Advances in Otitis Media. (2019) **Poster**

Other research activities

- 3-minute Thesis Runner up (2022). Mathematical, Physical and Life Sciences
- Co-chair. Microbiology Society Annual Conference Online 2021. Early career microbiologists forum. Co-chaired in the field of Infection
- Peer-review for Springer Nature Communications. One of 30 (out of 130 applications) to be selected to be mentored by an Editor at Springer Nature Communications. Voice of Young Scientists

Table of contents

List of figures

List of tables

Abbreviations

AOM	Acute otitis media
BHI	Brain heart infusion
BMDC	Bone marrow derived dendritic cell
BMDM	Bone marrow derived macrophage
BRS	Baby rabbit serum
BSA	Bovine serum albumin
cDNA	Complementary DNA
Co-IP	Co-immunoprecipitation
COPD	Chronic obstructive pulmonary disease
CRP	C-Reactive Protein
CSOM	Chronic suppurative OM
DCs	Dendritic cells
EDTA	Ethylenediaminetetraacetic acid
EGTA	Ethylene glycol-bis(β-aminoethyl ether)-N,N,N′,N′-tetraacetic acid
ELISA	Enzyme-linked immunosorbent assay
ER	Endoplasmic reticulum
ET	Eustachian tube
Evi1	Ecotropic viral integration site 1
FACS	fluorescence-activated cell sorting
FBS	Foetal bovine serum
GCSF	Granulocyte colony-stimulating factor
Glu	Glutamic acid
Gly	Glycine
GMCSF	Granulocyte-macrophage colony-stimulating factor
H&E	Hematoxylin and eosin
Hi	*Haemophilus influenzae*
Hib	Hi expressing a type b capsule
IDA	Industrial denatured alcohol
IFN	Interferon
IHC	Immunohistochemistry
iNKT cell	Invariant natural killer cells
Kdo	3-deoxy-D-*manno*-oct-2-ulosonic acid
LPS	lipopolysaccharide
M. catarrhalis	*Moraxella catarrhalis*
MAPK	Mitogen-activated protein kinase
MCP	Monocyte chemoattractant proteins
mCRP	Monomeric CRP
ME	Middle ear
MEE	ME effusion
MEF	Middle ear fluid
MHC	Major histocompatibility complex
MOI	Multiplicity of infection
NAD	Nicotinamide adenine dinucleotide
NALT	Nasal associated lymphoid tissue

NETs	Neutrophil extracellular traps
NHS	Normal human serum
NI	Non-inoculated
NK cell	Natural killer cell
NP	Nasopharynx
NPW	Nasal passage washes
NTHi	Non-Typeable *Haemophilus influenzae*
OD	Optical density
OM	Otitis media
OME	Otitis media with effusion
OPA	Opsonophagocytosis assay
PAFr	Platelet activated factor receptor
PBS	Phosphate buffered saline
PBS-T	Phosphate buffered saline - Tween
pCRP	Pentameric CRP
PCho	Phosphocholine
PCV	Pneumococcal conjugate vaccine
PEtn	Phosphoethanolamine
Phe	Phenylalanine
PI3K	Phosphoiositide-3-kinase
RBC	Red blood cell
rMoCRP	Recombinant mouse CRP
RNA	Ribonucleic acid
S. pneumoniae	*Streptococcus pneumoniae*
SAP	Serum amyloid protein
SBA	Serum bactericidal assay
SDS	Sodium dodecyl sulfate
SPF	Specific pathogen free
Thr	Threonine
TLR	Toll like receptor
TMB	3,3', 5,5;-tetramethylbenzidine
TNF	Tumour necrosis factor
Treg cell	T regulatory cell
URI	Upper respiratory infection
URT	Upper respiratory tract
VEGF	Vascular endothelial growth factor

Chapter 1. Introduction

1.1. Otitis Media

Otitis media (OM) is the inflammation of the middle ear (ME) (Schilder *et al.*, 2016). OM is among the most common diseases in young children globally. It is an umbrella term, which includes acute otitis media (AOM), OM with effusion (OME) (glue ear) and chronic suppurative OM (CSOM).

The focus of this thesis is on AOM, but other types of OM have been briefly described.

1.1.1. AOM

AOM occurs frequently in children and is less common in adults. AOM presents commonly in children from birth to 4 years of age: with most prevalent cases in children aged between 6 and 24 months old (Rosa-Olivares *et al.*, 2015; De Lusignan *et al.*, 2017). By the age of 3 years, 80% of children would have experienced one episode of AOM and by the age of 7 years, 40% of the children would have experienced >6 episodes of AOM (Monasta *et al.*, 2012). Criteria for AOM diagnosis include: (i) a red, yellow or cloudy tympanic membrane, (ii) moderate to severe tympanic membrane bulging or (iii) perforation of tympanic membrane and/or discharge from the ear (*Diagnosis* | *Diagnosis* | *Otitis media - acute* | *CKS* | *NICE*, no date). Prevalence of AOM varies globally, with 43.4 episodes per 100 people in Sub-Saharan West Africa and central Africa compared to 3.6 episodes per 100 people for central Europe (figure 1.1) (Schilder *et al.*, 2016).

Some patients can also develop recurrent AOM, which is defined as three of more episodes of AOM in six months, or four or more episodes in 12 months, with at least one episode of AOM in the past six months (Hampton *et al.*, 2021). Surgical grommets are often used for recurrent AOM.

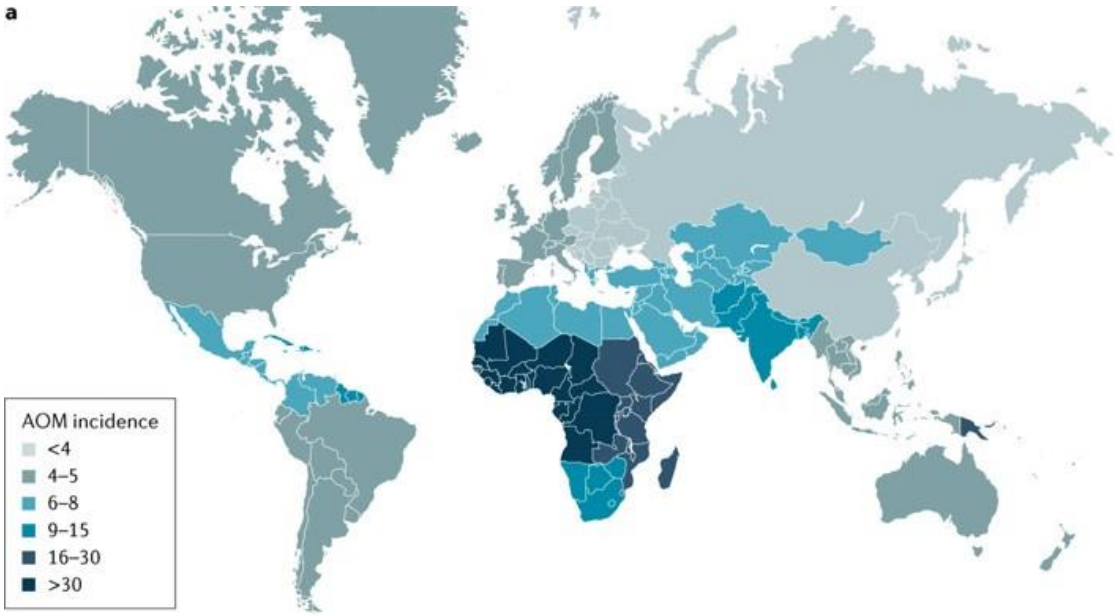

Figure 1.1. Global incidence rates estimate for AOM for 2005 per hundred people (Schilder et al., 2016a).

1.1.2. OME

OME is characterised by the presence of ME effusion (MEE) behind the intact tympanic membrane, and in contrast to AOM, OME is not associated with acute infection (Searight, Singh and Peterson, 2022). Approximately 50% of cases occur in children under the age of 1 year old and prevalence is higher in children with craniofacial malformations (Vanneste and Page, 2019). OME is initiated by inflammatory and immune reactions against nasopharyngeal infections. Prolonged inflammation leads to an increase in the number of mucus cells in the ME mucosa. The mucus trapped in the Eustachian tube induces a drop in pressure in the ME, which prevents the mucus being released from the ME (Vanneste and Page, 2019).

1.1.3.CSOM

CSOM is chronic inflammation of the ME in which the tympanic membrane is not intact and there is often discharge present (Verhoeff *et al.*, 2006). History of AOM and recurrent OM are the most prevalent causes of CSOM. In CSOM, bacteria (including *Pseudomonas aeruginosa*, *Staphylococcus aureus* and *Haemophilus influenzae*) can reach the ME through the nasopharynx and contribute to the disease prevalence. The most common consequence of CSOM is hearing loss, either conductive or sensorineural (Verhoeff *et al.*, 2006; Schilder *et al.*, 2016).

1.1.4. Hearing impairment

Global incidence of hearing loss due to OM is 30 per 10, 000 individuals. The presence of ME effusion in OME leads to hearing loss caused by impaired transduction of sound waves in the ME (Schilder *et al.*, 2016). As OM is a common disease in very young children, who are learning how to speak and communication, hearing loss due to OM can lead to a delay in learning development.

1.1.5. Environmental factors driving OM

A case-controlled study on 204 Sicilian children showed a strong link of OM development to large families, low parental educational background and children going to school within 3 years of life. Allergy and urban localisation increased the risk of OM in children exposed to smoke. Asthma, sleep apnoea, presence of pets and allergy were further risk factors for OM development (Martines *et al.*, 2016).

1.1.6. Genetic and anatomical risk factors of OM

Historically, multiple studies have been carried out that underline the genetic risk factors driving OM. A higher incidence of OM is associated with chromosomal abnormalities has been reported. This includes children with Down syndrome where the prevalence of OME is 38% (Austeng *et al.*, 2013). Down syndrome is a craniofacial syndrome and ontological examination in children show a narrow external auditory canal.

Genome wide association studies for AOM shows *Fndc1* (fibronectin type III domain containing 1) gene in disease contribution (Van Ingen *et al.*, 2016). *Fndc1* homologue is expressed in the ME tissue of mice and is upregulated in pro-inflammatory conditions such as treatment with lipopolysaccharide (LPS) treatment.

The anatomy of the Eustachian tube (ET) in children is different from adults, where it runs horizontally in children rather than a slope downward from the ME to the nasopharynx (NP) in the adults. Horizontal course of the ET allows easy transfer of the bacteria from the NP to the ME space. Furthermore, the ET lacks systemic immunity, thereby contributing as a risk factor for developing AOM (Marom, Nokso-Koivisto and Chonmaitree, 2012).

1.1.7. Viral and bacterial infections

Infection of the ME can be viral, bacterial or co-infection with both. The three common bacterial pathogens in AOM are *Streptococcus pneumoniae (S. pneumoniae), Moraxella catarrhalis (M. catarrhalis*) and Non-Typeable *Haemophilus influenzae* (NTHi), which colonise the NP during early childhood and are a part of the normal commensal flora. These bacteria do not cause any symptoms or disease unless there are changes in the NP environment, for example, after a viral infection, which can alter the bacterial adherence properties, lead to the dysfunction of the ET and promote bacterial colonisation in the ME. One in three young children with viral upper respiratory infections (URI) develop AOM within

4 weeks of URI (Nokso-Koivisto, Marom and Chonmaitree, 2015). Respiratory syncytial virus, influenza virus, rhinovirus, coronavirus, and adenovirus are some examples of viruses that have been strongly associated with URI. Viral URI causes inflammatory changes in the NP and ET, that providing easier access of bacteria present up the ET from the NP to the ME. Viral infections alter mucus properties and reduce normal mucociliary clearance of ET. This facilitates the entrance of bacteria and viruses present in the NP to the ME. ME inflammation leads to ME fluid (MEF) production, increased ME pressure and other signs and symptoms of developing AOM (Nokso-Koivisto, Marom and Chonmaitree, 2015). Respiratory viruses are found in up to 75% of MEF samples from AOM patients (Ruohola *et al.*, 2006; Chonmaitree *et al.*, 2008; Barenkamp, 2015; Ngo *et al.*, 2022). Co-infection with multiple bacterial pathogens and respiratory viruses contributes to the frequency of AOM and can influence the response to antibiotic treatment. A case study on Indigenous children with OM in Australia highlighted that an increase in individual NP bacterial load were apparent with worsening ME clinical state with a peak at AOM (Binks *et al.*, 2011).

Multiple studies have attempted to determine the threshold of commensal viral and bacterial loads driving the development of AOM. A comparison between aboriginal and non-aboriginal children in the Northern Territory of Australia showed a positive correlation between NP bacterial load and ME clinical state (Smith-Vaughan *et al.*, 2006). Further, comparison between the two groups demonstrated differences between bacterial loads, where higher numbers of *S. pneumoniae* and *M. catarrhalis* were present in aboriginal children. In addition to bacterial load, the socio-economic background also increased the risk of developing OM in aboriginal children. A systematic review on the microbiology of AOM from 1970 to 2014 globally reported a greater frequency of bacteria isolated from the MEF samples of patients with AOM than from other OM presentations (Ngo *et al.*, 2016). The authors confirm AOM frequently have bacteria present in the ME, while other forms of OM can be a consequence of previous AOM episode, or inflammation due to the presence

of biofilm or intracellular infection of cells within the MEF. Although bacterial loads are still unknown, this review highlighted *S. pneumoniae* and NTHi as the most frequently detected bacteria from AOM patients, with *S. pneumoniae* being prevalent in most continents. Changes in the vaccine composition and antibiotic use influences how the microbes evolve and is contributing to the resistance. For example, the replacement of pneumococcal conjugate vaccine (PCV7, provides protection against infections caused by seven serotypes of pneumococcal bacteria) serotypes by non-vaccine serotypes has shown the presence of resistant serotype, 19A that has been isolated from MEF samples of children with OM (Parra *et al.*, 2011; Ngo *et al.*, 2016).

AOM is the leading reason for antibiotic prescription in paediatric patients (Williams *et al.*, 2018). Children under the age of seven consume approximately 20% of the total antibiotics and over 50% of these children were prescribed antibiotics because they were diagnosed with AOM (Arason and Sigurdsson, 2010). A study on communities in Iceland showed that the likelihood of ear infections relapse and the need for grommets placement was higher in the communities with the highest antibiotic consumption (Arason *et al.*, 2005).

1.1.8. Microbiome and AOM

The polymicrobial colonisation of the upper respiratory tract (URT) is important in the development of URI and OM. Colonisation is described as a specific scenario where bacteria colonise into a new environment. Bacterial pathogens that are present in the URT differ during health and onset of infection. Along with the three major otopathogens mentioned so far, other microorganisms such as *S. pyogenes*, *C. otitidi, Turicella otitidis, Pseudomonas otitidis* and *Corynebacterium mucifaciens* have been isolated from the ME of patients with OM, but their significance in OM development remains unclear (Ngo *et al.*, 2016; Lappan *et al.*, 2018; Brugger *et al.*, 2019).

Microorganisms often coexist or compete with other microorganisms in their natural

environment. The NP and ME act as a polymicrobial pool harbouring multiple microbes. These polymicrobial interactions within NP and ME could be important in understanding differences between otitis prone and non-otitis prone patients (Xu *et al.*, 2017). Polymicrobial infections behave in synergy or compete with each other, and can drive the impact of infection by up- or down-regulating virulence factors. The ME infection by one microbe can facilitate other bacteria to establish themselves there. For example, NTHi, *S. pneumoniae* and *M. catarrhalis* have strong negative association with each other during AOM (Xu *et al.*, 2017). The strongest association was identified between AOM and NTHi presence in the NP (Xu *et al.*, 2017).

Further, the age of OM onset could influence bacterial colonisation. *S. pneumoniae* and NTHi colonisation in the NP and infection of ME is dominant between the ages of 6 month and 30 to 36 months (Kaur *et al.*, 2014). However, as the children get older, this relationship between the potential otopathogen in NP and MEF diminishes *i.e*. infection by NTHi or *S.pneumoniae* in older children and adults is lesser than younger children (Brugger *et al.*, 2019).

Thus, the polymicrobial colonisation in the NP is very complex, and the microbiome influences disease pathology. Amidst this, NTHi and *S*. *pneumoniae* remains the major bacterial otopathogens involved in AOM development, however, NTHi is dominant in causing recurrent AOM (Vergison, 2008; Lappan *et al.*, 2018; Ngo *et al.*, 2022).

1.1.9. Non-Typeable Haemophilus influenzae and AOM

Haemophilus influenzae (Hi) is a Gram-negative coccobacillus. Some strains of Hi are encapsulated while others are non-capsulated (NTHi). There are six serotypes of capsulated Hi designated a-f, based on their capsular polysaccharide. Hi is a common commensal of the human NP, and the respiratory tract is mainly colonised by NTHi (Slack, 2015) but despite this, NTHi is an underestimated pathogen. NTHi strains cannot be

serotyped by conventional method of agglutination using type-specific antisera (Slack, 2015). NTHi growth factor requirements are haemin and nicotinaminde adenine dinucleotide (Van Eldere *et al.*, 2014). NTHi bacteria grow aerobically or as facultative anaerobes and optimally between 35 and 37°C (Foxwell, Kyd and Cripps, 1998).

The introduction of invasive Hi expressing a type b capsule (Hib) vaccination in the early 1990s, led to a rapid and sustained reduction in Hib disease across all age groups (Peltola, 2000). NTHi strains are now one of the leading causative bacteria in AOM, recurrent AOM and OME (Behrouzi *et al.*, 2017). NTHi plays a critical role in many mucosal and some systemic infections, including, sinusitis, conjunctivitis (red/pink eye), cystic fibrosis, persistent bacterial bronchitis, meningitis and exacerbations of chronic obstructive pulmonary disease (COPD) (Van Eldere *et al.*, 2014; Behrouzi *et al.*, 2017). The lipopolysaccharide (LPS) is the major glycolipid of the NTHi cell surface and plays a significant role in host-pathogen interaction relevant to both the commensal lifestyle and disease.

1.1.9.1. NTHi LPS

LPS is a major virulence factor of NTHi and is responsible for much of the inflammatory responses associated with infection. NTHi LPS has two main covalently-linked constituents: (i) the core oligosaccharide linked with 3-deoxy-D-*manno*-oct-2-ulosonic acid (Kdo) residue with lipid A fixed into the outer membrane via electrostatic and hydrophobic interactions (Steimle, Autenrieth and Frick, 2016), and (ii) the three heptose residues (figure 1.2). Each of the three heptose residues can provide a point for elongation by oligosaccharide chains or the addition of non-carbohydrate substituents (Schweda *et al.*, 2003; Landerholm *et al.*, 2004; Elke K.H. Schweda1, Brigitte Twelkmeyer1, 2008; Gaultier *et al.*, 2017). Lipid A, which is conserved in all NTHi strains examined, is an endotoxin that provides targets for recognition by host immune system such as through Toll-like receptor (TLR) 4 (Wang *et al.*,

2002; Suzuki *et al.*, 2022).

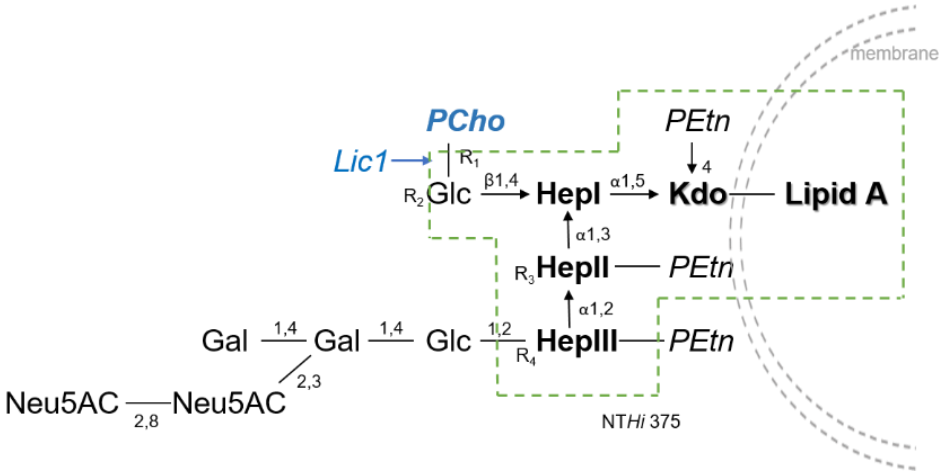

Figure 1.2. Schematic of NTHi 375 LPS structure. All NTHi tested have the conserved regions highlighted in green. These include lipid A, Kdo, phosphoethanolamine (PEtn) off Kdo and off heptose (hep) II. The *lic1* gene responsible for adding phosphocholine (PCho) onto the NTHi surface, which is highlighted in blue. Hep I-III are regions where PCho can be points of oligosaccharide extension.

Molecular structural studies on LPS from NTHi show additional conserved regions, for example the phosphoethanolamine (PEtn). The oligosaccharide extensions from heptoses on the NTHi LPS are highly variable (Månsson *et al.*, 2003) and contains antigens that imitate the phosphorylated sugars present within the host, enabling the bacteria to impede immune clearance. As well as carbohydrate molecules, NTHi LPS also harbours non-carbohydrate substituents (Månsson *et al.*, 2003). One such non-carbohydrate molecule is phosphocholine (PCho) which shows intra- and inter-strain variation in location and expression that can have a profound effect on virulence and commensal behaviour of NTHi (Schweda *et al.*, 2007).

1.1.9.2. Phosphocholine and its phase variable expression

PCho, a small zwitterionic molecule, is a common feature of *H. influenzae* LPS and is synthesised using choline obtained from the host. Choline is an essential nutrient and plays

a complex role in the host, including its use in neurotransmitter synthesis and signalling (phospholipids) (Zeisel and da Costa, 2009). Choline is not required for microbial growth, but it can provide a selective advantage to the pathogen (discussed in section 1.1.6.3 and 1.1.6.4). Choline turnover is continuous in eukaryotic cells during the production and recycling of main membrane lipid phosphatidylcholine (Clark and Weiser, 2013). Microbes, therefore have adapted strategies to scavenge host-accessible choline for use as nutrient source, osmoprotectant or to overcome the host immune response (Fitzsimmons, Hampel and Wargo, 2012; Clark and Weiser, 2013) .

NTHi uses choline from the host to synthesise PCho using the four genes of the *lic1* locus (figure 1.3). Each heptose residue on the LPS can permit the addition of a hexose residue, which can be terminal or act as a first step of oligosaccharide chain extension. A majority of the NTHi strains express PCho on hexose on heptose I. Rare NTHi strains have also been shown to carry two PCho substituents (Schweda *et al.*, 2007). For the remainder of the thesis, 'PCho off heptose' will be used and this is equivalent to 'PCho on hexose off heptose'.

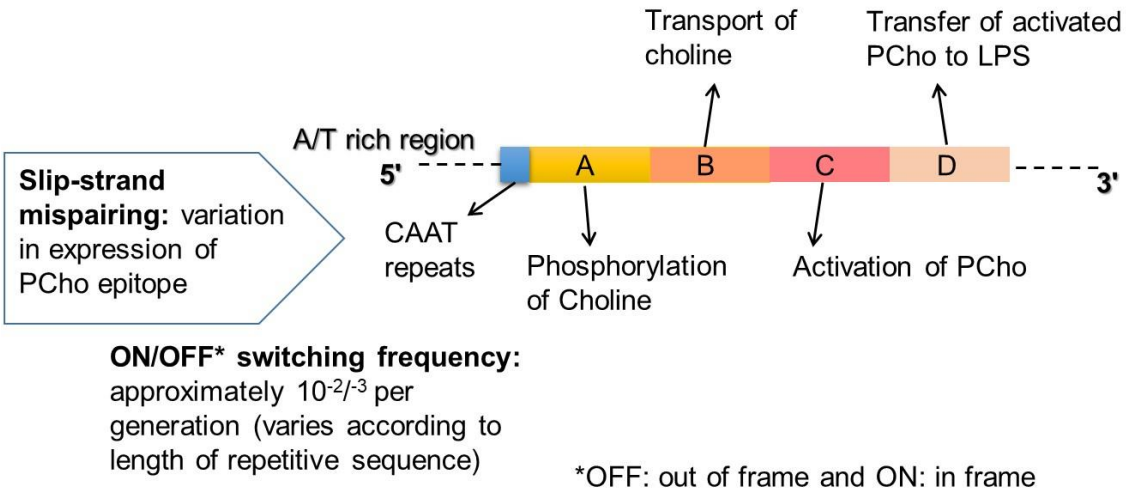

Figure 1.3. PCho synthesis in NTHi using choline from host. *Lic1* locus: Lic1A converts free choline to PCho. Lic1B is a transmembrane transporter. Lic1C synthesises CDP-choline from PCho and CTP in the cytoplasm. Lic1D is a PCho transferase which adds PCho to target glycans (Young, Foote and Wakarchuk, 2013).

The *lic1* locus is present in all NTHi isolates tested. A 5' CAAT tetranucleotide repeat tract is present within the 5' end of the *lic1A* reading frame. These repeats create a translational switch by shifting the upstream initiation codon in or out of frame with the main reading frame, making the addition of PCho to the NTHi LPS subject to phase variation (PV) (Weiser, Love and Moxon, 1989). The expression of PCho on LPS is dependent on the frequency of ON or OFF switching, which is approximately 10^{-2} to 10^{-3} per bacterium per generation. This varies in different strains due to the length of the repetitive sequence (Weiser *et al.*, 1998). PV permits NTHi to rapidly and randomly switch PCho expression within the population rather than controlling expression to the external stimuli. Published data clearly indicate that it can be advantageous to express PCho under some conditions and in some host compartments but a disadvantage in others (Langereis *et al.*, 2019).

1.1.9.3. Phosphocholine: adherence and uptake into host cells

The ability of NTHi to adhere to and invade the host epithelial cells is an important step in both colonisation and persistence, whether as a commensal or a pathogen. PCho on the bacterial surface influences both the commensal and pathogenic lifestyles of microbes (Clark and Weiser, 2013). PCho expression on the NTHi surface, reduces the potency of the LPS as an endotoxin and promotes bacterial adherence and invasion of host-immune cells. PCho-expressing NTHi strains are found in the human respiratory tract, which likely represents the mimicry ability of the bacteria to host epithelium and mucus layer where PCho is also found (Weiser *et al.*, 1998).

NTHi is an opportunistic pathogen. NTHi can adhere to multiple cells types of the epithelium through various mechanisms, including adhesion to mucins, binding proteins in the extracellular matrix and through interaction with host cell membrane receptors (Clementi and Murphy, 2011). One means by which, NTHi can adhere to epithelial cells via is platelet associated factor receptor (PAFr) (Swords *et al.*, 2000). PAFr is a G protein-coupled

receptor expressed on various host cell types. PCho can be incorporated and position on the NTHi LPS is dependent on the sequence of *lic1D* transferase. The position of PCho on the NTHi surface influences interaction with PAFr, where PCho-expressing NTHi co-localise with PAFr and stimulate PAFr-mediated endocytic signalling (Swords *et al.*, 2000, 2001; Avadhanula *et al.*, 2006; Iuchi *et al.*, 2019). Clathrin-mediated endocytosis (also known as receptor-mediated endocytosis), produces endosomes that are trafficked by the endolysosomal pathway. PAFr leads to downstream activation phosphoinositide-3-kinase (PI3K) and mitogen-activated protein kinase (MAPK) signalling. PI3K plays a critical role in bacterial engulfment through rearrangement of the host cell cytoskeleton, membrane ruffling and in protein and vesicle trafficking (Clementi and Murphy, 2011). PI3K is important for mouse alveolar and human epithelial cell invasion by NTHi (Martí-Lliteras *et al.*, 2009; Morey *et al.*, 2011).

As well as attachment and entry via PAFr, NTHi can enter host cells through alternative routes depending on the microenvironment. For example, phagocytosis and macropinocytosis. The ability of NTHi to exist both inside and outside of the host cell suggests it is able to function as an opportunistic intracellular pathogen. Phagocytosis and macropinocytosis are a type of endocytosis that requires non-specific uptake of extracellular material. Phagocytosis is a process carried out by phagocytic cells of the immune system and can play an important role in NTHi survival and killing (section 1.1.10.2). Macropinocytosis, on the other hand, is a mechanism that some NTHi can use under a transient nutrient deprived environment (Ketterer *et al.*, 1999; Hardison *et al.*, 2018). However, adherence and uptake by receptor mediated uptake is more efficient than macropinocytosis and could aid in NTHi survival (Swords *et al.*, 2001).

1.1.9.4. Immune evasion by Phosphocholine

NTHi possesses multiple factors that permit it to evade or impair the host immune response. Structures including PCho on the NTHi surface are an integral part of biofilm formation. Biofilms are defined as microbial communities, often enclosed within a matrix material (Costerton *et al.*, 1995). Structures on the NTHi LPS can play a role in the induction of biofilm formation, which can arise when NTHi undergo functional changes during infection, which can permit NTHi with basic attachment or nutrient sequestration (Duell, Su and Riesbeck, 2016). PCho expression can effect changes in bacterial aggregation and subsequent biofilm formation (Morey *et al.*, 2013). NTHi variants increase their PCho content during biofilm formation and within a mature biofilm, NTHi are predominantly expressing PCho on their surface. Within the biofilm, PCho decreases LPS bioactivity and reduces the innate immune response towards the bacteria, potentially by impeding the early stage Lipid A recognition or signalling (West-Barnette, Rockel and Swords, 2006).

NTHi have evolved mechanisms for evading host immune responses through changes in its outer surface molecules, including PCho (Clark *et al.*, 2012; Langereis, van der Pasch and de Jonge, 2019). LPS influences the ability to resist bacterial killing by naturally acquired PCho antibodies (Nishinarita, Sawada and Horie, 1990), complement proteins (Kerr, 1981), antimicrobial peptides such as LL-37 (E. S. Lysenko *et al.*, 2000; Majewski *et al.*, 2018) and pentraxins.

PCho expression on NTHi LPS decreases the bacterium's susceptibility to the antimicrobial peptide human cathelicidin LL-37. LL-37 is a 37 amino acid cationic peptide, which preferentially associates with negatively charged phospholipid membranes. This interaction allows for penetration of the molecule into the bacterial membrane, formation of transmembrane pores and bacterial lysis (Kahlenberg and Kaplan, 2013). Bacteria expressing PCho have 1000-fold greater survival in bactericidal assays compared to mutants without PCho (E. S. Lysenko *et al.*, 2000). Even though PCho is zwitterionic, decreased killing by cationic peptides could be due to positively charged quaternary amine

on choline, which is predicted to orient towards the exterior part of the NTHi surface (E. S. Lysenko *et al.*, 2000). PCho does not affect the quantity of peptide that associates with NTHi, but may interfere with the ability of the peptide to insert properly into the LPS membrane. In this respect, PCho on the NTHi behaves similarly to phosphatidylcholine on eukaryotic membranes, which are fundamentally more resistant to antimicrobial peptides (E. S. Lysenko *et al.*, 2000).

PCho on the surface of NTHi can also influence bacterial survival in the presence of host immune components, including complement proteins. As NTHi can express PCho off different heptoses on their LPS, the position of PCho can effect serum mediated killing of the bacteria (E. Lysenko *et al.*, 2000). NTHi PCho-expressing variants display an increased survival in the presence of antibody-dependent, complement-mediated killing (Clark *et al.*, 2012). The microenvironment in which NTHi are found shows differences in phase variation. For example, NTHi blood isolates are mainly not expressing PCho, whereas isolates from the ME are expressing PCho on their surface (Langereis *et al.*, 2019; Langereis, van der Pasch and de Jonge, 2019). Decreased expression of PCho on the NTHi surface leads to decreased binding of IgM (which can recognise PCho), and therefore permit bacterial survival, as observed for blood isolates collected from patients with bacteraemia (Langereis *et al.*, 2019).

Complement mediated killing can also occur through C-Reactive Protein (CRP), which has a binding specificity towards PCho (Weiser *et al.*, 1998; Langereis, van der Pasch and de Jonge, 2019).

1.1.10. C-Reactive Protein

CRP has the ability to recognise self and foreign antigens according to their pattern recognition (Sproston and Ashworth, 2018). It is an excellent marker for acute inflammation for many inflammatory conditions. Levels of CRP are elevated in infection (Sproston and

Ashworth, 2018; Pathak and Agrawal, 2019). In atherosclerosis elevated CRP is a biomarker for clinical progression and prediction of future cardiovascular disease (Singh, Suresh, Voleti, *et al.*, 2008; Badimon *et al.*, 2018). CRP is a prognostic marker in cancers (Watson *et al.*, 2019; Yoshida *et al.*, 2020; Suzuki *et al.*, 2022) and disease progression in age-related macular degeneration (Molins *et al.*, 2018; Swinkels *et al.*, 2018). Elevated plasma IL-6 and CRP levels are associated with disease severity in critically ill SARS-CoV-2 patients (Lavillegrand *et al.*, 2021) and a wide range of other pneumonic illnesses. Use of CRP as a marker for bacterial AOM has been investigated previously. Serum CRP levels have been used to investigate use of CRP for differentiating between viral and bacterial AOM (Tejani *et al.*, 1995). Use of CRP to make decisions regarding antimicrobial therapy for AOM in children has also been investigated previously, but serum CRP is not recommended for making antimicrobial therapy (Principi *et al.*, 1986).

CRP is an acute phase protein in the human, whose concentrations increase dramatically upon an inflammatory response. It is a highly conserved plasma protein that was initially discovered by Tillett and Francis in 1930 from serum of patients with acute inflammation by *S. pneumoniae* (Tillett and Francis, 1930). CRP has a high binding affinity towards PCho, although it can also bind to other ligands such as galactose and nuclear components, but with a lower affinity (Du Clos, 2000; Lee, Takagahara and Lee, 2002; Nehring *et al.*, 2021). PCho is usually exposed on damaged/dying cells in the host and on some microbes, which CRP can bind to and promote their clearance.

CRP is a pentameric protein made primarily by the liver, but also has been reported to be synthesised by other cell types including macrophages, lymphocytes, endothelial cells, adipocytes and smooth muscle cells (Sproston and Ashworth, 2018). Expression of CRP on human expiratory mucosal surfaces has been reported previously, where CRP gene has been shown to be expressed in epithelial cells of human respiratory tract (J. M. Gould and Weiser, 2001; Ramage, Proudfoot and Guy, 2004). CRP is first made as a monomer and is later assembled into its pentameric form in the endoplasmic reticulum (ER) of the cell.

Under non-inflammatory states, CRP is released slowly from the ER. In blood from a healthy young adult, the median concentration of CRP is 0.8 mg/l (Pepys and Hirschfield, 2003). Upon stimulus from the primary cytokine, IL-6, supported by TNF-α and IL-1β, the concentration of CRP can increase 1,000-fold. CRP concentrations rise significantly within 6 hours after receiving an inflammatory stimulus and peak around 48 hours post stimulation. The plasma half-life of CRP is approximately 19 hours and its rate of turnover is constant in health and disease (Pepys and Hirschfield, 2003).

CRP, a double edge-sword, plays both pro- and anti-inflammatory roles in disease pathogenesis and progression. The isoform of CRP can influence the biological activity of the protein. CRP can exist as two main types of isoform: pentameric (pCRP) and monomeric (mCRP). CRP is synthesised as monomers in the liver and assembled into pentameric protein in the endoplasmic reticulum (Sproston and Ashworth, 2018). The pCRP can irreversibly dissociate into mCRP. pCRP has anti-inflammatory properties, whereas mCRP is pro-inflammatory (Trial, Potempa and Entman, 2016; Rajab, Hart and Potempa, 2020). The mCRP isoform is short-lived, potent inflammatory protein and its activities are associated with earliest phases of acute inflammatory response (Wu *et al.*, 2015). The differences in the bioactivity of the two isoforms is related to their binding affinity for Fcγ receptors on host cells. The mCRP isoform binds to FcγIIIb on neutrophils and FcγIIIa on monocytes, whereas pCRP isoform binds to FcγIIa (Clos, 2013).

The alteration in cell membrane is necessary for CRP binding to PCho containing phospholipids or dying or altered cell membranes. The elevated CRP levels in inflammation leads to the activation of the classical complement pathway in a calcium dependent manner. CRP can also act as an opsonin and lead to the clearance of the pathogen/immune stimulus by activating phagocytes through Fc receptors and through the generation of chemotactic and convertases (Siegel *et al.*, 1975; Volanakis and Wirtz, 1979; Marnell, Mold and Du Clos, 2005).

1.1.10.1 C1q, CRP and classical complement pathway activation

CRP can activate the classical complement system after its binding to PCho in a calcium dependent manner (figure 1.4). PCho-complexed CRP is recognised by complement protein, C1q. Opposite the PCho binding site of CRP is a deep and narrow cleft which binds C1q, and its conformation is not affected by the absence or presence of calcium and PCho. Mutational analysis has demonstrated aspartic acid-112 and tyrosine-175 as major determinants for C1q binding (Agrawal *et al.*, 2001). Phenyalanine-66, threonine-76 and glutamic acid-81 form the PCho binding pocket (Gang *et al.*, 2012).

Binding of C1q to ligand-bound CRP activates the complement pathway. This leads to conformational changes in C1q, where two C1r and two C1s form the $C1qC1r_2s_2$ (C1 complex). Activation of the classical complement pathway by CRP is limited to the early components of the classical complement pathway cascade (C1, C4, C2), with minimal consumption of complement proteins C3 to C9 which leads to less formation of the membrane attack complex (MAC) (Siegel, Rent and Gewurz, 1974; Berman, Gewurz and Mold, 1986). CRP inhibits the alternative complement pathway by binding to the alternative complement pathway inhibitor factor H and decreasing C3 and C5 convertase activation, therefore inhibiting the complement amplification loop (Sproston and Ashworth, 2018) (figure 1.4). This is enough to initiate the clearance of the damaged cell/pathogen through C3b and iC3b, without releasing danger signals that could produce a more elaborate host immune response (Berman, Gewurz and Mold, 1986). The activation of only the early components of the classical complement pathways by CRP therefore protects against damage to the host cell while also leading to the clearance of a foreign molecule (Du Clos, 2000).

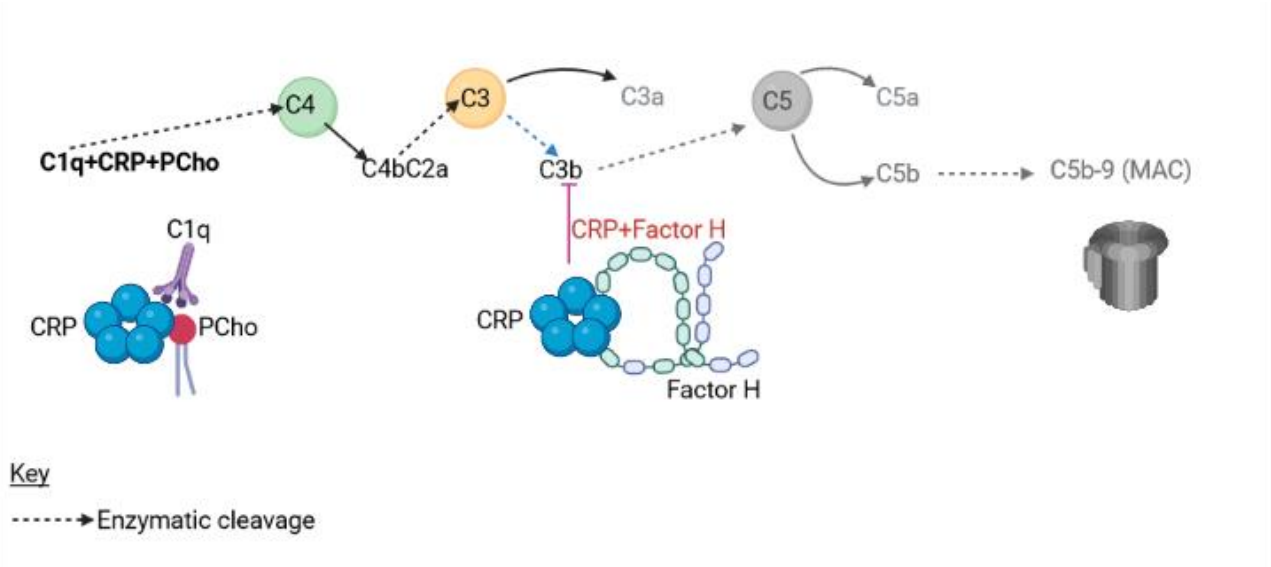

Figure 1.4. Classical complement pathway activation by CRP. PCho bound CRP can bind C1q. This leads to the activation of the classical complement pathway through C1q. This leads to conformational changes in C1q, where two C1r and two C1s form the C1 complex ($C1qC1r_2S_2$) which leads to the activation of C1s (Willrich, 2020). Activated C1s subsequently cleaves C4 to produce C4a (released into circulation) and C4b. C4b then recruits C2 that is cleaved by C1 complex. This releases C2b into the circulation and C2a, which remains associated with C4b (Willrich, 2020). CRP inactivated C3b molecules to iC3b. The increase in iC3b if high enough can lead to phagocytosis. In addition, CRP binds to factor H to block alternative complement pathway activation (Haapasalo and Meri, 2019).

1.1.10.2. Cell mediated opsonin response

CRP activation of complement can subsequently lead to opsonophagocytosis and this process does not require CRP to interact with Fcγ receptors on leukocytes (Marnell, Mold and Du Clos, 2005). In the absence of complement, CRP enhances leukocyte phagocytosis *in vitro* through its interactions with FcγRs (Black, Kushner and Samols, 2004).

CRP can interact with host cells through FcγRI and FcγRII receptors (already known receptors for IgG). FcγRIIa found primarily on human monocytes and neutrophils is the major receptor for CRP (Lu *et al.*, 2018). Both FcγRI and FcγRII are stimulatory receptors, categorized by the presence of a cytoplasmic immuno-receptor tyrosine-based activation motif (ITAM) sequence and inhibitory receptor, characterised by presence of an immuno-

receptor tyrosine-based inhibition motif (ITIM) sequence (Black, Kushner and Samols, 2004). These motifs control the phagocytic activity of CRP as an opsonin. Once CRP interacts with pathogen and Fcγ receptors, it induces a number of other cell types through the production of cytokines (Sproston and Ashworth, 2018).

1.1.10.3. CRP and NTHi

Phase variation of PCho on the bacterial surface contributes to the ability of NTHi to colonise and persist within the host. CRP deposition on NTHi surface through binding to PCho contributes to killing through complement mediated bactericidal activity (Weiser *et al.*, 1998). Further to the presence or absence, the position of PCho affects sensitivity to CRP binding. Lysenko and colleagues showed that exchanging the *lic1D* genes between two NTHi variants with PCho expressed at different locations in the LPS affected susceptibility to serum bactericidal activity (E. Lysenko *et al.*, 2000). PCho expressed on heptose III rather than heptose I made NTHi more sensitive to CRP-mediated serum killing. Thus, in addition to phase variable expression, the position of PCho contributes to evasion of CRP mediated killing. However, it is not clear what role CRP might play in the complex inflammatory circumstances found in AOM. While binding of CRP to NTHi may promote NTHi killing, it is still unclear how the presence or absence and position on the NTHi surface influences the NTHi surface in the presence of CRP. It is unclear if the amount of CRP binding is influenced by position of PCho on the bacterial surface. It also remains unclear if other molecules on the NTHi surface influence the CRP binding to PCho on the bacterial surface. For example, CRP recognises and binds to PEtn (in a calcium dependent manner), which is also found on the NTHi LPS (Black, Kushner and Samols, 2004).

The role of CRP in AOM is under-studied. The limited studies on CRP in AOM suggest there may be some correlations with AOM and serum CRP (Principi *et al.*, 1986) and that it is possible to distinguish between bacterial and viral OM using serum CRP levels (Tejani

et al., 1995). However, NTHi infect the ME in AOM, therefore serum CRP levels may not be the representative sample to measure CRP level changes following NTHi infection in AOM. The host-pathogen interaction is complex in AOM, where CRP may influence bacterial survival or killing in disease.

1.1.11. Immune cell response to NTHi in AOM

For the immune response to be generated, the host must first recognise the pathogen via pattern recognition receptors (PRRs). PRRs are located throughout the ME epithelium and are expressed on the cell surface of epithelial and antigen presenting cells. The initial innate immune response by PRRs activates multiple pathways via NF-κB, interferon response factors (IRFs) and AP-1 transcription factors (which respond to a variety of stimuli including cytokines, growth factors, stress, bacterial and viral infections). Signalling leads to the secretion of various cytokines, chemokines, interferons and antimicrobial peptides (Massa, Spann and Cripps, 2021).

NTHi induces weaker up-regulation of host immune responses in peripheral blood cells of young children with AOM compared to AOM caused by *S. pneumoniae* (Liu *et al.*, 2013). Children with NTHi infection have a dampened immune response where 90% of the genes involved in the pro-inflammatory response were downregulated. Further, genes involved in classical complement pathway were downregulated.

1.1.11.1 Toll-like receptors

TLRs play a critical role in innate immune responses. TLR expression in the normal ME is absent or weak, but is increased in MEF of AOM (Jung *et al.*, 2021). TLRs are responsible for recognising self from non-self and are found in immune cells including dendritic cells, macrophages, neutrophils, T cells and B cells. The role of TLRs are extensively studied in

animal models and defects in TLR signalling have been shown to affect the immune response in AOM. For example, mice with non-functional TLR4 presented with constant OM and an increasing bacterial titre from ME effusions compared to mice who had normal TLR4 function. TLR4 recognises LPS and stress induced endogenous ligands such as heat shock protein 60 and hyaluronic acid. Mice with non-functional TLR4 have impaired phagocytosis and phagosome maturation, which contributes to failed clearance of NTHi infection in OM (Hirano *et al.*, 2007). Polymorphisms in TLR4 predispose some children to OM, leading to attenuated production of TNF-α in dendritic cells (Hafrén *et al.*, 2015). TLR4 and TLR2 (which recognises various bacterial structures including lipoproteins and glycolipids) deficient mice lack tumour necrosis factor (TNF) induction during early stages of OM (Leichtle *et al.*, 2009).

1.1.11.2. Innate immune response in AOM

The innate immune response is different in children prone to OM from those not prone. The two populations have differential gene expression for inflammatory cytokines. Higher expression of IL-8, overstimulation and dysfunctional recruitment of neutrophils are observed in ME of OM prone children (Kaur, Casey and Pichichero, 2016). Phagocytes such as neutrophils and macrophages play a role in protecting the middle ear against pathogens (Mittal *et al.*, 2014). Phagocytosis is a cellular process of ingesting and eliminating foreign material and apoptotic cells larger than 0.5 μm in diameter (Uribe-Querol and Rosales, 2020). Foreign material is internalised into the phagosome (an organelle found within phagocytes). A phagosome undergoes maturation and fuses with lysosomes to become a phagolysosome. The phagolysosome contains enzymes that degrade the ingested particle. Neutrophils and macrophages are professional phagocytes found in middle ear effusions from children with OME (Lim *et al.*, 1979). Neutrophils are the most abundant leukocytes and form the first line of defence against invading pathogen. However,

even though they are one of the most abundant cells, NTHi can still persist within the host. In AOM, neutrophils form neutrophil extracellular traps (NETs) and are hypothesised to promote bacterial persistence, rather than clearance (Juneau *et al.*, 2011; Mittal *et al.*, 2014). NTHi ingested by neutrophils are not killed by neutrophils, but rather, the neutrophils themselves undergo cell death by necrosis following NTHi uptake (Naylor *et al.*, 2007). Macrophages play a central role in innate immunity in the ME and have been shown to be a major cellular component in ME effusions from human (Lim *et al.*, 1979). Single cell transcriptome analysis in a rat AOM model showed that macrophages may be master regulators of the inflammatory response in ME mucosa in AOM (Rao *et al.*, 2021). NTHi have been shown to survive in macrophages, which could be important in bacterial persistence and recurrent infections. Viable, intracellular NTHi have been recovered from macrophages up to 72 hours after phagocytosis (Craig *et al.*, 2001).

Other cells of the innate immune system involved AOM include natural killer cells and dendritic cells. Natural killer (NK) cells are effector white blood cells that control many tumours and pathogens by limiting their spread secreting cytokines such as interferon (IFN)-γ and TNF-α, thus controlling subsequent tissue damage. NTHi challenge increases NK cell numbers significantly in otitis-prone children (Seppanen *et al.*, 2018).

Dendritic cells (DCs) are antigen-presenting cells involved in orchestrating the immune response. DCs activate the naïve T cells through the antigen presentation receptor, major histocompatibility complex (MHC) II. DCs from blood samples from OM prone children have reduced levels of MHCII molecules on their surface (Sharma and Pichichero, 2013). This can compromise the priming of naïve T cells and effect memory T cell formation, thus influencing NTHi survival in AOM.

1.1.11.3. Adaptive immune response in AOM

Cells involved in adaptive immunity include T and B cells. Impaired T cell-mediated immunity is postulated to drive susceptibility to OM. Otitis prone children have reduced functional memory CD4+ T helper cells (Kodama *et al.*, 1999; Sharma, Casey and Pichichero, 2011). These children also develop a short-lived antibody response. Additionally, otitis prone children have a reduced number of B cells circulating in the blood (Sharma, Casey and Pichichero, 2012). Together with reduced memory B-cell and/or memory CD4+ T helper cells, otitis prone children are unable to sustain an adequate serum antibody level, thus becoming more prone to frequent AOM episodes.

Published literature suggests that the host-pathogen interaction in AOM development is complex. The role of PCho on the NTHi surface and host immune cell response during early infection remains unclear. It is not well understood why the immune system fails to clear away NTHi in AOM. The role of acute phase response by CRP in bacterial survival and killing during AOM is not well defined. The mechanisms by which NTHi survival *e.g.* through resistance to complement mediated killing or surviving in phagocytes by altering the phagocyte response, can help explain the host-pathogen interaction in AOM. Some of these questions will be discussed further in chapters 4, 5 and 6 of this thesis.

1.1.12. Animal models of AOM

Multiple animal models have been used to investigate the host-pathogen interaction in AOM. These models enable us to study specific immune cell responses, identify histopathological changes and evaluate the effect of treatments and vaccines.

1.1.12.1 Chinchilla

The chinchilla is a rodent that is a favoured model of OM due to its large ear and tympanic membrane size. NTHi does not naturally colonise chinchillas, however, intranasal adenovirus infection followed by NTHi inoculation directly into the MEF (via tympanic membrane) NTHi permits NTHi presence in the ME (Suzuki and Bakaletz, 1994). However, chinchillas are expensive to use and shed fur even at slightest signs of distress. Currently there are no specific pathogen-free, inbred or transgenic species available, and there is a lack of species-specific antibody reagents. Chinchillas have a higher rate of inner ear complications, and are prone to developing sepsis with high mortality rate (Davidoss, Varsak and Santa Maria, 2018).

1.1.12.3. Rat

The rat is another favoured AOM model due to the similarity of the histology and anatomy of its ME similarity to the human. Rat AOM resembles that of human (Hermansson *et al.*, 1988). Bacteria can be inoculated into the rat ME directly due to its large tympanic bulla. The rat also permits analysis of OME for greater than 16 days (Piltcher *et al.*, 2002). One of the drawbacks of the rat is the high frequency of naturally occurring infection in the ME with indigenous bacteria (Davidoss, Varsak and Santa Maria, 2018). Further, direct infection of the ME does not help study the commensal and pathogenic behaviour of NTHi in the rat. Direct infection in the ME of the rat is also not the natural way NTHi infects the human, therefore the immune cell response from the NP to the ME cannot be studied in these OM model.

1.1.12.4. Mouse

Mice are small, relatively inexpensive and easy to handle. Mice share many developmental

and physiological processes with human and 99% of mouse genes are homologous to human. Different transgenic and gene deletion strains can be developed, allowing us to study genetic susceptibility to AOM (Davidoss, Varsak and Santa Maria, 2018). However, there are multiple mouse lines and strains available and critical awareness needs to be taken into consideration when designing experiments, interpreting data and comparing between other studies (Trune and Zheng, 2009). Compared to the chinchilla and rat, mice have been used successfully to understand virulence factors, mechanisms of bacterial adherence and invasion, induction of inflammation by NTHi and also for vaccine studies (Trune and Zheng, 2009; Hood *et al.*, 2016; Kadry *et al.*, 2021). However, infection with human pathogens in most mouse models is short-lived and required experimentally induced conditions (Bhutta, 2012). For example, inoculation of the *Jeff* mouse (mouse model for CSOM) with NTHi showed very low infection rate of the ME (Kubinyecz *et al.*, 2020). Alternative mouse models have been developed and successfully used to study AOM. The *Junbo* mouse model is one such mouse model for OM that has been successfully used to study NTHi infection (Hood *et al.*, 2016).

1.1.12.5. The Junbo mouse model of OM

The *Junbo* mouse is an OM mouse model. The mouse harbours an Asn763Ile mutation in the gene encoding transcription factor ecotropic viral integration site 1 (*Evi1*), leading to chronic OME. The *Evi1* locus was first identified as a common site for retroviral integration (Sproston and Ashworth, 2018). *Evi1* is expressed in multiple cells in the ME *e.g.* neutrophils. It is a negative regulator of NF-κB expression. The loss of *Evi1* contributes to the OM phenotype and the mice are predisposed to developing OM without any external bacterial challenge (Hood *et al.*, 2016). Homozygote mice show prenatal lethality from cardiac failure (Parkinson *et al.*, 2006). Heterozygote mice are used for studying NTHi infection in OM and from this point, *Junbo* heterozygote mice will be referred as '*Junbo*

mice' for the remaining of the thesis. *Junbo* mice infected intranasally with NTHi show a persistent infection in the ME for at least 56 days. Inoculation of the *Junbo* heterozygote mouse shows high infection rate, giving a good immune response (Vikhe *et al.*, 2019), making it a good model to study NTHi infection in OM.

1.1.13. Aims

The presence or absence and position of PCho on the NTHi surface and its interactions with CRP within the host is poorly understood in AOM. The aim of this project was to understand this microbial-host interaction further. We aimed to investigate why some NTHi strains result in disease while other NTHi strains are cleared by the host immune response. We hypothesised that the role of CRP as an acute phase protein could influence NTHi killing and survival in AOM. We had the following objectives in this research.

1. Investigating the role of presence and position of PCho on the NTHi surface in CRP binding (chapter 3)

NTHi strains from human OM patients with characterised LPS structure and known PCho positions were used. We aimed to develop an ELISA-based binding assay to study interaction of CRP with different NTHi strains. We hypothesised that the presence and position of PCho on the bacterial surface effect CRP binding to NTHi (chapter 3)

2. Understanding the role of PCho presence and position on the NTHi surface on serum mediated killing (chapter 4)
    i. We aimed to confirm that PCho presence and position on the bacterial surface influences serum mediated killing
    ii. We hypothesised that the presence of CRP in the normal human serum may influence serum bactericidal activity. Therefore, we used CRP-depleted normal human serum to study the influence of CRP on bactericidal activity.

iii. We infected *Junbo* mice with NTHi 375 strains (from chapter 6) to investigate if PCho presence and position on the NTHi surface influences bacterial survival and host immune response *in vivo.* We hypothesised that serum from *Junbo* mice that had been inoculated with different NTHi 375 strains may lead to differences in NTHi killing in serum bacterial assay.

3. Investigating the role of PCho presence and position on uptake and cell response in opsonophagocytosis (chapter 5)

We aimed to investigate NTHi uptake in bone marrow derived macrophages. We hypothesised that the presence and position of PCho on the NTHi surface may influence uptake into macrophages. We also looked at the macrophage gene expression levels following NTHi infection to understand how PCho on the NTHi surface could influence survival in macrophages.

4. Mouse infection model: The *Junbo* mouse (chapter 6)

We aimed to investigate the role of PCho on the NTHi surface in host-immune response following infection with NTHi 375 strains.

a. We used PCho-expressing (NTHi 375sr and 375(2.8)sr and PCho mutant (NTHi 375*lic1*sr) to inoculate *Junbo* mice (C3H/HeH mice were used as controls)
b. We looked at the ME infection rates and ME bacterial titres in the *Junbo* mouse following infection with NTHi 375 strains
c. We aimed to determine the baseline CRP levels in the non-inoculated *Junbo* mice and C3H/HeH mice
d. We measured CRP levels in samples from different tissues of the mouse: nasal passage washes (NPW), middle ear fluid (MEF), blood and nasal associated lymphoid tissue (NALT) to study if CRP is a localised or a systemic response in the *Junbo* mouse
e. We looked at the infection rate, bacterial titre, and CRP levels in different

grades of *Junbo* MEFs (opacity and viscosity) to understand if this could influence NTHi survival in the *Junbo* MEF

f. We hypothesised that PCho presence and position on the NTHi surface may influence immune cell profiles in the MEF, blood and NALT of the *Junbo* mouse infected with NTHi. Therefore, we carried out immune profiling of the innate and adaptive cells in these tissues. We categorised the MEF according to grade to investigate if changes in MEF opacity and viscosity influence immune cell content. This can help us understand how PCho presence and position on the bacterial surface can influence bacterial survival in the presence of host immune cells.

Chapter 2. Methods

2.1. NTHi strains, growth/storage conditions

Table 2 1 NTHi strains

NTHi strain	**PCho position***
162sr	Heptose I
162srPCho^{-}	Phase variation off (Heptose I)
162*lic1*sr	PCho mutant, no PCho
1158sr	Two PCho: heptose III and heptose IV
1158*lic1*sr	PCho mutant, no PCho
285sr	Heptose I
285*lic1*sr	PCho mutant, no PCho
485sr	Heptose II
485*lic1*sr	PCho mutant, no PCho
176sr	Two PCho: heptose III and heptose IV
176(1c)sr	Two PCho: heptose III and heptose IV More highly PCho expressing than 176sr
375sr	Heptose I
375srPCho^{-}	Phase variation off (Heptose I)
375*lic1*sr	PCho mutant, no PCho
375(12.1)sr	Heptose II but NTHi 375sr does not have a hexose off heptose II to provide PCho extension
375(2.8)sr	Heptose III
375(7B.1)sr	Heptose I

375(lpt3)sr	PCho expressed off heptose I. Mutant that lacks phosphoethanolamine (PEtn) off heptose III (*lpt3* adds PEtn off heptose III)
375(lpt6)sr	PCho expressed off heptose I. Mutant that lacks PEtn off heptose II (*lpt6* adds PEtn off heptose II)
375(lpt3/lpt6)sr	PCho expressed off heptose I. Mutant that lacks PEtn off heptose III and heptose II.
375(lpt3/lic1)sr	Mutant that lacks PCho and PEtn off heptose III
375(lpt6/lic1)sr	Mutant that lacks PCho and PEtn off heptose II
375(lpt3/lpt6/lic1)sr	Mutant that lacks PCho and both PEtn off heptose III and heptose II

*PCho is expressed on a hexose off one of the heptoses on the NTHi LPS, table 2.1 shows which heptose the PCho on NTHi LPS is expressed off. All strains used were streptomycin (sr) resistant.

2.1.1. NTHi PCho mutants and PCho variants

NTHi 162*lic1*sr, a PCho mutant was constructed using DNA in which the whole *lic1* operon was disrupted by deletion of all of the *lic1A*, *lic1B*, *lic1C*, and *lic1D* open reading frames and replacement with a tetracycline resistance cassette. Various members of the research group created the respective *lic1* mutants for the other NTHi strains using the same method used to develop 162*lic1*sr. Successful deletion of the *lic1* gene was confirmed using polymerase chain reaction and gel electrophoresis by various members of the lab. Bacterial DNA was extracted using phenol/chloroform separation. Crude DNA was used for gel electrophoresis and polymerase chain reaction in which *lic1* mutant NTHi were compared with wild-type NTHi (with *lic1* present). DNA band sizes on gel electrophoresis were

compared. A complete deletion of the *lic1* gene resulted in various bands on gel electrophoresis depending on where the *lic1* gene was deleted. For example, complete deletion of *lic1* gene resulted in a band size of 3624 bp on the gel electrophoresis. Deletion of *lic1A*-*lic1B* (enzymes responsible for converting and transporting choline to PCho, figure 1.3) resulted in a band size of 1254 bp on the gel electrophoresis. Deletion of *lic1C-lic1B* (enzymes responsible for activation and transportation of PCho, figure 1.3) resulted in a band size of 1349 bp on the gel electrophoresis on the gel electrophoresis. Alternatively, immunoblots using anti-PCho antibody (TEPC15) was used consistently throughout various experiments to confirm the presence or absence of PCho on the NTHi surface.

NTHi 375 PCho variants were created using the *lic1D* gene from different NTHi strains. This gene encodes for transferase enzyme that adds PCho to different heptoses on the NTHi LPS. Immunoblots were used consistently through various experiments to confirm the presence or absence of PCho on the NTHi surface. Silver staining was used to confirm the LPS structures of the PCho variants.

2.1.2. NTHi storage conditions

All the NTHi strains used were clinical strains from OM children. All NTHi strains used in the study were grown from -80°C frozen stocks that were produced by various members of the research group over various years.

2.1.3. NTHi growth conditions

NTHi strains were inoculated onto brain heart infusion (BHI) streptomycin (300 µg/ml) agar plates (1% agar supplemented with 10% Levinthals base) overnight from frozen stocks (section 2.1.2). The following morning, NTHi were grown in liquid BHI broth supplemented with 10 µg/ml haemin and 2 µg/ml nicotinamide adenine dinucleotide (NAD) (Fox *et al.*, 2008), and incubated at 37°C at 250 rpm for 2 hours or until an optical density (OD) 490nm

of between 0.4 and 0.8 was achieved. OD490 was measured using a spectrophotometer. All NTHi strains used were normalised to OD490 of 0.5 and centrifuged for 3 minutes at 10 000 x *g*. The supernatant was discarded and the pellet was washed with PBS and centrifuged again for 3 minutes at 10 000 x g; this wash step was repeated three times. After the final wash, the pellets were ready to be used for various assays performed in the study.

2.2. Quantifying CRP interactions dependent upon PCho presence and position on NTHi surface

2.2.1. CRP Enzyme-linked immunosorbent assay (ELISA)

For the CRP binding assay, NTHi were mixed with 50 to100 ng/ml purified human CRP (Binding Site BP300.X; 99% pure) in CRP buffer (0.2 M Tris pH 7, 0.15 M NaCl and 10 mM $ZnCl_2$) or suspended in carbonate buffer (15 mM Na_2CO_3, 34.5 mM $NaHCO_3$ and 20 mM $MgCl_2.6H_2O$). The mixture was incubated in 1.5 ml Eppendorf tubes at 37°C for 30 minutes with shaking. Following this, the samples were centrifuged for 3 minutes at 10 000 x *g*. The pellet was resuspended in PBS and centrifuged for 3 minutes at 10 000 x *g*. The wash steps were repeated twice more. Finally, the CRP-treated NTHi samples were resuspended in carbonate buffer, and 100 µl of the sample was added to flat bottom 96-well plates and incubated overnight at 4°C. The next day, solutions from the wells of the 96-well plates were discarded and the plates were dried at 37°C for 1 hour. 300 µl of blocking buffer (2% bovine serum albumin (BSA) in PBS) was added to each well and incubated for 2 hours at room temperature. After 2 hours, blocking buffer was aspirated and the wells were washed three times with 300 µl/well of PBS-Tween (PBS-T). Any remaining solution in the wells was removed by gently tapping the inverted plate onto a tissue. 200 µl monoclonal anti-CRP antibody produced in mouse (clone CRP-8, Sigma, C1688) diluted 1/2000 in blocking buffer was added per well and incubated overnight at 4°C. The following day, wells were

aspirated and washed three times with 300 µl PBS-T. Any remaining solution in the wells was removed by gently tapping the plate onto a tissue. Wells were then incubated with 200 µl/well goat anti-mouse IgG (Abcam, ab205719) diluted 1:10,000 in blocking buffer for 1 hour at room temperature. Next, wells were aspirated and washed three times with 300 µl PBS-T. 100 µl 3,3', 5,5;-tetramethylbenzidine (TMB) solution (ThermoFiser Scientific, N301) was added to each well. The plate was incubated in the dark until the development of colour before 100 µl stop solution (1 M H_2SO_4) was added to each well. Plates were gently tapped on a flat surface for thorough mixing of solutions. Following this, OD was measured immediately after using an Epoch microplate spectrophotometer (Agilent Techonologies) and a wavelength of 450 nm.

Data from the microplate reader was exported to Excel Microscoft. ODs were measured for each sample after background deduction (OD from blank well treated with primary and secondary antibodies).

2.2.2 Immunogold labelling

Immunogold labelling is a staining technique, which makes use of colloidal gold particles attached to secondary antibodies. These antibodies bind to specific target antibodies, which in this case was primary antibody against human CRP. Gold has a high electron density and produced dark spots on the micrographs at sites where CRP bound to the bacteria. Each hCRP gold particle (seen as black spots on the electron micrographs) was counted manually using ImageJ analysis tool. The overall gold labelling was plotted as a bar graph after subtracting non-specific hCRP gold particle labelling from each electron micrograph. NTHi not treated with hCRP were used as a control to differentiate background noise from positive CRP signal on hCRP-bound NTHi samples.

Binding of CRP to NTHi bacteria was carried out as outlined in section 2.1.1. but using 500 ng/ml human CRP, NTHi were then washed twice with PBS. After the final wash, NTHi were fixed in 4% foetal bovine serum (FBS) and stored on ice for transport to the Department of Pathology, University of Oxford. The remaining steps required for imaging were kindly carried out by Dr Charlotte Melia and Dr Erin Johnson.

2.2.2.1. On grid method

Copper grids were glow discharged at 15 mA for 25 seconds. The grids were inverted onto 20 µl droplet of NTHi/CRP-NTHi sample (carbon-side down) and incubated for 5 minutes. The grids were transferred through 2 droplets of PBS; incubating for 2 minutes on each droplet. Grids were then transferred onto a droplet of blocking buffer (either 0.2% pork gelatine in PBS or 5% serum (goat or FBS) in PBS) for 5 minutes. Any excess liquid between each step was removed from the grids by gently blotting onto filter paper. The grids were incubated on a droplet of mouse anti-human CRP antibody (clone CRP-8, Sigma, C1688) for 60 to 90 minutes. Following this, grids were transferred through 6 droplets of blocking buffer, incubating for 2 minutes for each droplet. Gentle blotting on filter paper ensured removal of excess liquid on the grids. Grids were transferred through 3 droplets of blocking buffer, incubating for 2 minutes for each droplet. After blocking, the grids were incubated in 0.1% glutaraldehyde prepared in PBS for 15 minutes. Grids were washed with 3 droplets of milli-Q water, incubating for 2 minutes on each droplet. Finally, grids were blotted gently and air-dried prior to imaging.

2.2.2.2. Hybrid method

The NTHi/CRP-NTHi samples were centrifuged for 5 minutes at 14 000 x *g* and the pellets were resuspended in 500 µl PBS. The suspension was incubated for 5 minutes before repeating the wash twice more. After the final wash, pellets were resuspended in 500 µl

blocking buffer for 5 minutes. Then, the samples were centrifuged for 5 minutes at 14 000 x *g* and the pellets were resuspended in neat ((undiluted) 1 µl per sample) mouse anti-human CRP primary antibody (clone CRP-8, Sigma, C1688) and incubated for 1 hour. Next, samples were diluted with 450 µl blocking buffer and centrifuged for 5 minutes at 14 000 x *g*. Pellets were resuspended with 500 µl blocking buffer and incubated for 5 minutes before repeating this step twice more. Samples were centrifuged for 5 minutes at 14 000 x *g* and pellets were re-suspended in 400 µl blocking buffer. Then, the grids were glow discharged (300 mesh copper grids, C267/100) at 15 mA for 25 seconds. Grids were inverted onto 20 µl of re-suspended sample (carbon-side down) and incubated at room temperature for 5 minutes. Grids were transferred through 3 droplets of blocking buffer, incubated for 2 minutes on each droplet and gently blotted on filter paper between all transfers. After, the grids were incubated in 0.1% glutaraldehyde prepared in PBS for 15 minutes. Grids were washed with 3 droplets of milli-Q water, incubating for 2 minutes on each droplet. Finally, grids were blotted gently and air-dried prior to imaging.

2.3. Investigating uptake of NTHi by phagocytes

2.3.1 Generation of macrophages and dendritic cells from mouse bone marrow derived stem cells

All procedures were performed under laminar airflow.

C3H/HeH mice aged between 8 to10 weeks old were euthanized by cervical dislocation. The mice were sprayed with 70% ethanol prior to dissection. The hind-leg was cut just above the pelvic/hip joint using dissection scissors. Any remaining muscle/tissue on the femurs was removed using lint-free tissue. Both ends of the femurs were trimmed using a blade. Bone marrow stem cells from the centre of the femur were flushed using 1 ml for 50 mM EDTA prepared in PBS (for each end of the femur bone). Bone marrow washes were pooled and passed through a 70 µm cell strainer. The cells were centrifuged at 1200 x *g*, 5

minutes, 4°C (Heraeus Fresco 21). The supernatant was discarded and the pellet was resuspended in 2 ml red blood cell (RBC) lysis buffer (eBioscience™, 00-4333-57). Cells were incubated in RBC lysis buffer for 2 minutes before the addition of 33 ml 50 mM EDTA-PBS to stop each 2 ml reaction. The suspension was incubated for 5 minutes at room temperature before centrifuging at 1200 x *g*, 5 minutes, 4°C. The supernatant was discarded, and the pellet was resuspended in 1 ml complete media (bone marrow derived dendritic cell (BMDC) complete media (section 2.3.2) / bone marrow derived macrophage (BMDM) media (section 2.3.3)). To count cell numbers, 10 µl cell suspension was mixed with 10 µl trypan blue (Gibco™ 152500061), and 10 µl of the mixture was placed in a cell count using the Countess 3 FL Automated Cell Counter (Thermofisher).

2.3.2. Bone marrow derived dendritic cell (BMDC) preparation

Once the cell count was obtained, the cell density was adjusted to achieve a final density of 10 x 10^6 cell/ml using pre-warmed BMDC complete media (RPMI 1640 supplemented with L-glutamine (Gibco, 11875-093, Lot no. 2339171), 10% FBS, 10 ng/ml Penicillin – Streptomycin (Gibco, 15140-122, Lot no. 1835958), 0.05 mM 2-mercaptoethanol (Gibco™, 31350010) and 20 ng/ml granulocyte-macrophage colony-stimulating factor (GM-CSF) (Miltenyi Biotec, 130-095-746)**.** Cells were grown in sterile 90 mm petri dishes (non-tissue culture grade) at 37°C with 5% CO_2. On day 3, cells were provided with fresh complete media. On day 6, BMDCs from each petri dish were pooled in a 50 ml falcon tube; any loosely non-adherent cells were gently dislodged and added to the pooled cell suspension. The cells were centrifuged at 1200 x *g,* 5 minutes, 4°C. The supernatant was discarded and the cells were resuspended in 1 ml BMDC activation media (BMDC complete media + 100 ng/ml *E. coli* LPS (LPS from *E*. *coli* 055:B5, L2880-25 MG, Lot number 036M4018V). The cells were seeded at a cell density of 1 x 10^6 cell/ml per 1 ml in 24 well plate for 24 hours (activation) at 37°C with 5% CO_2.

2.3.3. Bone marrow derived macrophage (BMDM) preparation

After determining the number of bone marrow derived stem cells (2.3.1), cells were prepared in BMDM complete media RPMI 1640 supplemented with L-Glutamine, 10% FBS, 20 ng/ml gentamicin, 10 ng/ml Penicillin – Streptomycin and 10 ng/ml recombinant mouse macrophage colony stimulating factor (MCSF) (R&D systems, 416-ML-010/CF). Cells were plated at a final cell density of 1.5 x 10^6 cells/ml per 1 ml a 12 well plate and incubated at 37°C, 5% CO_2. Fresh complete BMDM media was provided every 2-3 days. On day 6, media from the wells was aspirated and cells were provided with complete BMDM media without recombinant MCSF. Cells were used on day 7 for the opsonophagocytosis assay (OPA) (section 2.3.4).

2.3.4. Opsonophagocytosis assay

All procedures were performed under laminar airflow.

Prior to the start of the assay, BMDMs were starved in RPMI 1640 supplemented with L-Glutamine, 0.01% FBS, 20 ng/ml gentamycin, 10 ng/ml Penicillin – Streptomycin. A cell count was obtained by scraping one of well from the 12-well plates. Simultaneously, as the cells were being starved, NTHi were grown in BHI liquid (section 2.1.3). BMDMs were infected with NTHi at a multiplicity of infection (MOI) of 1:100 for different periods of at 37°C, 5% CO_2 and 50 rpm. After incubation with NTHi, supernatant from the wells was aspirated and the cells were washed gently twice with sterile PBS. Extracellular NTHi were killed using gentamicin (50 µg/ml). Gentamicin is an antibiotic that kills Gram-negative bacteria by disrupting the ability of the bacteria to make proteins (Sojo-Dorado and Rodríguez-Baño, 2017), but which has poor intracellular penetration in eukaryotic cells. To measure intracellular survival and growth of NTHi, BMDMs were treated with 20 ng/ml gentamicin prepared in sterile PBS for 30 minutes at 37°C, 5% CO_2 and 50 rpm. After this, the supernatant was aspirated and the cells were washed twice with sterile PBS. After the final

wash, cells were dislodged from the wells using 200 µl cold, sterile PBS. NTHi survival and growth was measured by plating 50 µl of the suspension onto BHI and streptomycin plates and enumerating the resulting colonies following overnight inoculation at 37°C of 150 µl suspension was centrifuged at 10 000 x *g* for 3 minutes and the pellet was processed for analysis of gene expression quantitative polymerase chain reaction (qPCR) (section 2.3.5). Untreated cells were used as negative controls and to check for any contamination by plating out the cell suspension onto BHI plates following overnight incubation. *E.coli* LPS was used as a positive control for BMDM stimulation.

2.3.5. Quantitative PCR (qPCR): Determining mouse macrophage phenotype

2.2.5.1. RNA extraction

To measure changes in inflammatory gene expression in BMDMs stimulated with NTHi, qPCRs assays were carried out using RNA was isolated from BMDM pellets (section 2.3.4) using Maxwell® RSC simplyRNA cells kit (Promega, AS1390). Solutions provided by the manufacturer were used and the protocol was adapted as follows. Cells were homogenised in 200 µl chilled 1-thioglycerol/homogenisation solution (20 µl 1-thioglycerol in 1 ml homogenisation solution provided). The cells were then vortexed for approximately 30 seconds and stored on ice until needed. In the meantime, Maxwell cartridges were prepared. One cartridge was used per sample. To each cartridge, 5 µl DNase was added in well 4. A plunger was added to well 8, and an elution tube containing 40 µl RNase-free water placed in its respective position. Finally, 200 µl lysis buffer was added to 200 µl homogenised cells and the 400 µl solution was added into well 1 of the cartridge after brief vortexing. The cartridges were placed into a Maxwell® RSC instrument. The concentration of the resulting RNA concentration was measured using a NanoDrop.

2.3.5.2 cDNA synthesis

For complementary DNA (cDNA) synthesis, a high-capacity cDNA reverse transcription kit (Applied Biosciences™, 10400745) was used. For a 20 µl reaction, 1.5 µg ribonucleic acid (RNA) was used. In some circumstances when the RNA concentration was low, RNA samples were dried down and resuspended in a low volume (5 µl) of RNase-free water. For cDNA synthesis reaction was setup with the following synthesis programme: 25°C for 10 minutes, 50°C for 30 minutes, 85°C for 10 minutes and 4°C infinite hold (for overnight reactions).

2.3.5.3. PCR amplification

Debbie Williams kindly helped design the primers for the PCR amplification. The primers were tested using the macrophage test samples and SYBR Green Master mix (ThermoFisher Scientific, 4309155). Serial dilution of each primer pair was tested to obtain the primer pair concentration at which the Ct values were in measurable range. Non-template controls were used a negative control for amplification. Melting curves for each primer pair was set-up to see if there is a single temperature peak. Amplification curve for each of the dilutions tested along with the negative control was measured. Based on these analysis, we confirmed the concentration of each primer pair needed to measure macrophage phenotype following NTHi infection.

qPCR amplification reactions were set-up in 96 well plates. Each gene tested was quantitated in triplicate. A single 20 µl reaction was composed of 2.5 mM fast sybr, 18 µM forward and reverse primer reaction (table 2.2) 10 ng/ml cDNA and the remaining volume was made up with RNase free water. HPRT, HRAS and NRAS were used as internal controls. Reaction mixtures were centrifuged briefly to pool all the solution to the bottom of the wells before placing into the PCR thermocycler machine. The amplification programme was set to 95°C for 3 minutes, then 44 cycles of: 95°C for 30 seconds, 60°C for 30 seconds

and 72°C for 30 seconds, before a final step of 72°C for 4 minutes. Analysis of the cycling was carried out on 7500 Software v2.3 (Applied Biosciences®).

Table 2 2 Primers used in qPCR to measure inflammatory response in BMDMs

Primer name	Forward primer sequence 5′ to 3′	Reverse Primer sequence 5′ to 3′
IL-12β	GCGTTCCTCGTAGAGAAGACATC	GCTTGCACGCAGACATTCC
IL-10	CCAGCTGGACAACATACTGCTAA	TGGCAACCCAAGTAACCCTTA
TGF-β	CGGAGAGCCCTGGATACCA	GCCGCACACAGCAGTTCTT
IL-23a	ATCCAGTGTGAAGATGGTTGTGA	GCGGATCCTTTGCAAGCA
CD-80	TCATCGTTGTCATCATCAAATGC	CTGCTTGCCTCATTTCTTCTGA
IL-13	CGCAAGGCCCCCACTAC	AAAGTGGGCTACTTCGATTTTGG
IL-14	CGGCACCAGCGAGAGAAG	CTTCATCAGCTCGCACATCCT
iNOS	GCCATTGAGTTCATCAACCAGTAT	CTGGCCAGATGTTCCTCTATTTTT
CD206	CACGGAGATCCACGAGCAA	GTCCCGAGCTCAAGGAACTG
Arginase	TGGGCAACCTGTGTCCTTTC	AGAATCCTGGTACATCTGGGAACT
MHCII	GCCTGAAGAGCCCCATCAC	TGCCGCTCAACATCTTGCT
IL-6	GGGAAATCGTGGAAATGAGAAA	GCATCATCGTTGTTCATACAATCA
TNFα	CCACCCTCTTCTGTCTACTGAACTT	TGAGAGGGAGGCCATTTGG
IL-1β	CCTTCCAGGATGAGGACATGA	GAGTCACAGAGGATGGGCTCTT
MyD88	GCACCTGTGTCTGGTCCATTG	CATGCGGCGACACCTTTT
PRKCA	TATCTGAAGGCTGAGGTCACTGAT	GGGATTAGATTTTTTGCATCTCGTA
NFκB	CGGAGGAGACCGGCAACT	GCTGCCTGGCGGATGAT
HPRT	CCGAGGATTTGGAAAAAGTGTT	TTCATGACATCTCGAGCAAGTCTT
HRAS	ACCACTTTGTGGACGAGTATGATC	CCCATCAATGACCACCTGTTT
NRAS	CCAGAACCACTTTGTGGATGAA	TCACCACTTGCTTTCGGTAAGA

2.4. *Serum bactericidal assay*

To determine how the presence and position of PCho on the NTHi surface effects serum bactericidal assay (SBA), NTHi 375 strains were tested with normal human serum (NHS, Invitrogen, 31876) or pooled mouse serum from *Junbo* infection studies (section 2.6).

NTHi were prepared as described in section 2.1.3. NTHi bacteria were serially diluted to give a suspension of 2 x 10^4 CFU/ml in PBS-glucose (0.9 mM $CaCl_2$, 0.5 mM $MgCl_2$, 1 mM $MgSO_4$ and 0.1% (w/v) glucose). Reactions were setup in 0.5 ml tubes to give a final volume of 50 µl. This 50 µl volume was made up of 25 µl 2 x 10^4 CFU/ml NTHi (500 CFU). For SBA using mouse serum, pooled *Junbo* mouse serum (section 2.5) were supplemented with 2% baby rabbit serum (BRS, complement source). A decomplement control was prepared as control. For this, 2% BRS was heated at 56°C for 30 minutes. SBA was carried at 37°C, for 45 minutes. After brief mixing two 20 µl aliquots from each tube were plated onto BHI + streptomycin plates. Plates were incubated overnight at 37°C. The following day, the colonies from each plate were counted and percentage of NTHi survival was calculated using the decomplemented control as '100% survival'.

2.5. T cell induction by using NTHi 375 strains

2.5.1. Bead-isolation of mouse T cells

All procedures were performed under laminar airflow.

Whole fresh spleens were obtained from C3H/HeH mice of 8 to10 weeks of age following dissection. Spleens were placed into a petri dish with 5ml RPMI media. Spleens were mashed using the plunger from a 10 ml syringe. The cells were then passed through a 70 µm cell strainer, and the strainer was washed twice with 1 ml RPMI before centrifuging at 1200 x *g*, 5 minutes, 4°C (Heraeus Fresco 21). The supernatant was aspirated, and the red

blood cells were lysed using RBC lysis buffer (3 ml RBC lysis buffer was used for four spleens) for 2 minutes. Following this, the lysis reaction was stopped by adding 50 mM EDTA-PBS, and the cells were centrifuged at 1200 x *g*, 5 minutes, 4 °C. The supernatant was discarded and the splenocytes were then used for isolation of T cells using CD4+ and CD4+CD25+ isolation kits (section 2.5.2).

2.5.2. CD4+ T cell isolation

Mouse CD4+ T cells were isolated using magnetic beads kit (Miltenyi Biotec, 130-104-454) following the manufacturer's instructions. Splenocytes were resuspended in T cell isolation buffer (0.5% BSA, 2 mM EDTA in PBS). 40 µl of T cell isolation buffer was used per 10^7 total cells. 10 µl biotin-antibody cocktail (supplied by manufacturer) were added per 10^7 total cells. The suspension was pipetted gently a few times before incubating at 4 °C for 5 minutes. Following this, 30 µl of T cell isolation buffer and 20 µl of anti-biotin microbeads (supplied by manufacturer) were added per 10^7 total cells. The cells were mixed well and incubated at 4 °C for 10 minutes. In the meantime, LS columns (Miltenyi Biotec, 130-042-40) were prepared for the magnetic separation: the column was rinsed with 3 ml T cell isolation buffer. The final volume of the cell suspension was made up to 500 µl before applying T isolation cell buffer and it was applied onto the LS column. The supernatant from the LS column was collected and processed through the LS column once more. 10 µl of the supernatant was used to count the CD4+ T cells, and 100 µl was retained to check for the purity of the CD4+ T cells isolated. The cells were now ready for T cell CD4+CD25+ isolation.

2.5.3. CD4+CD25+ Regulatory T cell isolation

CD4+ T cells from negative magnetic bead purification were centrifuged at 300 x *g* for 10 minutes, 4°C. The supernatant was discarded and the cells were used for magnetic bead CD4+CD25+ T regulatory (Treg) cell isolation (Miltenyi Biotec, 130-091-041) following the manufacturer's protocol. The cell pellet was resuspended in 40 µl (per 10^7 total cells) T cell isolation buffer. To this, 10 µl CD4+CD25+ Treg cell biotin-antibody cocktail (supplied by the manufacturer) per 10^7 total cells was added and the cells were incubated for 10 minutes at 4°C. After this, 38 µl T cell buffer, 20 µl anti-biotin microbeads and 2 µl CD25-PE antibody (supplied by the manufacturer) per 10^7 cells was added to the suspension and the cells were incubated at 4°C for 15 minutes. In the meantime, LS columns were prepared for the magnetic separation: the column was rinsed with 2 ml T cell isolation buffer. T cell isolation buffer was added to the cell suspension to make the final volume to 500 µl and the cells were applied onto the LS column. Unlabelled cells were passed through the column, and the column was washed twice more with 1 ml T cell isolation buffer. Cells were centrifuged at 300 x *g* for 5 minutes, 4°C and the pellet was resuspended in 90 µl T cell isolation buffer per 10^7 total cells. 10 µl anti-PE microbeads were added to this suspension and the mixture was incubated at 4°C for 15 minutes. The final volume was made up to 500 µl using T cell isolation buffer and passed through a LS column. The column was rinsed twice using 500 µl T cell isolation buffer. The flow-through contained CD4+CD25- cells. These cells were kept aside for the Treg cell induction assay. 10 µl of the supernatant was used to count the CD4+CD25- T cells, and 100 µl was kept aside to check for the purity of cells. 10 µl of the supernatant was used to count the CD4+CD25+ T cells, and 100 µl was kept aside to check for the purity of the cells.

2.5.4. T regulatory cell induction assay

All procedures were performed under laminar airflow.

After 24 hour of pulsing the DCs (section 2.3.2), the activation media was removed from the cells. The DCs were then pulsed with NTHi bacteria with a MOI of 1:10 (DC:NTHi bacteria) or media only (untreated negative control) for a period of between 30 minutes and 4 hours. After pulsing DCs with NTHi, supernatant was aspirated from the wells. DCs were washed twice with sterile PBS. Following this, CD4+CD25- T (section 2.5.2) cells were added to the wells at a density of 2 x 10^6/ml. The assay was performed over 5 days at 37°C, 5% CO_2 incubator. On day 2, approximately 50% of the media was removed from the co-culture. Fresh pulsed DCs were resuspended in complete T cell media (RPMI 1640 supplemented with L-Glutamine, 20 ng/ml gentamycin, 10 ng/ml Penicillin – Streptomycin and 10^4 U/ml IL-2) and added to the original co-culture. As a positive control, control wells were coated with 5 µg/ml anti-CD3 and 5 µg/ml anti-CD28 in sterile PBS for 2 hours at 37 °C. Following this, the T cell suspension was added to the wells. After 5 days, cells were harvested and processed for T cell induction assay (section 2.5.5).

2.5.5. Flow cytometry: Measuring regulatory T cell induction

Table 2 3 T cell induction flow cytometry panel

Marker/ antigen	Fluorochrome	Final Dilution	Source	Catalogue number
Live/dead	APC-Cy7	1:1000	Invitrogen	65086514
CD4	FITC	1:800	BD biosciences	553047
CD25	PE-Cy7	1:400	BD biosciences	552880
FOXP3	PerCP-Cy5.5	1:200	BD biosciences	563902

CD4+CD25+ T cell induction was measured using flow cytometry. Supernatant in each well from Treg cell induction assay (section 2.5.4) was pipetted up and down gently a few times to dislodge the T cells. Supernatant was transferred to 1.5 ml Eppendorf tubes and centrifuged at 1200 x *g* for 5 minutes. Cells were washed twice with sterile PBS and centrifuged at 1200 x *g* for 5 minutes. After the final wash, all the T cells collected from Treg induction assay (section 2.5.4) were stained using the antibody panel in table 2.3 for 20 minutes at room temperature. Following this, cells were washed twice with sterile PBS and centrifuged at 1200 x *g* for 5 minutes. The cell pellets obtained were resuspended in fluorescence-activated cell sorting (FACS) buffer (5 mM EDTA and 0.5% FBS in PBS) for flow cytometry analysis using a CytoFLEX S machine (AD32087). FlowJo software (Tree Star) was used to analyse the data obtained.

2.6. Immune profiling of cells from tissues from Junbo mice infected with NTHi 375 strains

2.6.1. Generation of mouse cohorts

The *Junbo* mouse was generated through *N*-ethyl-*N*-nitrosourea (ENU) mutagenesis (Parkinson *et al.*, 2006); screening identified hearing loss as a phenotype. A deletion, A2318T, in the longest *Evi1* transcript was identified as being responsible for the observed phenotype. Homozygotes are lethal, and proceed to die between E18.5 to birth.

2.6.2. Animal care

Mice were housed in specific pathogen free (SPF) conditions in individually ventilated racks, within the environmental conditions outlined in the Home Office Code of Practices in the Mary Lyons Centre. The humane care and use of mice in this study were carried out under UK Home Office Project license number PPL3003280, Studies of Otitis Media in Mouse

Models, MRC Harwell Institute code 30/328, personal licence number I94E8E7B8. All animals and procedures used in this study; intranasal inoculation (1078/MLC), gaseous anaesthetic equipment (1104/MLC) and intraperitoneal injection (1083/MLC) were approved by the Animal Welfare Ethical Review Body, MRC Harwell Institute.

2.6.3. Inoculation of Junbo mice with NTHi

Heterozygote *Junbo* mice that were congenic on a C3H/HeH genetic background were used to study the importance of PCho on the bacterial surface in NTHi infection to obtain data on host immune cells. C3H/HeH mice, hereafter referred to as wild-type mice, were used as control mice for comparison of infection and cellular data obtained for the *Junbo* mouse.

NTHi strains 375sr, 375*lic1*sr and 375(2.8)sr were grown in BHI supplemented with Leventhal reagent at an OD490 of 0.4 to 0.5. NTHi were pelleted by centrifugation (13 000 x *g*, 3 minutes), washed with PBS and resuspended in PBS-1% gelatine before intranasal inoculation as described previously (Vikhe *et al.*, 2019). Briefly, *Junbo* mice were inoculated intranasally under gas anesthesia with10 µl NTHi (5 µl per nares) cell suspension at a concentration of 10^8 CFU/ml. NTHi CFU counts were obtained by plating NTHi inoculum onto BHI plates prior to and following inoculating the *Junbo* mice.

2.6.4. Collection and processing of mouse tissue and fluids

Middle ear fluid (MEF), nasal passage washes (NPW), nasal associated lymphoid tissue (NALT), blood and serum were collected at day 1-, 3- and 7- post NTHi inoculation from mice under terminal anaesthesia induced by an intraperitoneal overdose of sodium pentobarbital. The head was sprayed with 70% ethanol, and then the skin from the head and any material around the outer ear was carefully removed. The bottom jaw was removed

using sterile scissors to allow access to the NP and NALT. The malleus from the middle ear (ME) was removed using sterile forceps, creating a hole in the tympanic membrane for fluid collection.

MEF was collected with a pipette and micro-tip in up to 0.5 µl aliquots from the ME into 100 µl PBS. Wild-type mice do not develop OM and do not have MEF. Therefore, ME washes were performed, where the MEs were flushed with 2 µl PBS twice and collected in 100 µl PBS. ME washes were also performed in *Junbo* mice with clear MEs. This took place under a dissecting microscope, which allowed for grading of the fluid based on its viscosity and opacity (table 2.4). Two dilutions of MEF at 10^{-1} and 10^{-2} in PBS were prepared and 50 µl aliquot plated agar plates supplemented with streptomycin. The bacterial titre was calculated from the number of colonies and dilution factor following overnight growth. The remainder of the MEF in PBS was centrifuged at 800 x *g* for two minutes. Supernatant was collected for cytokine/chemokine and pentraxin analyses, while the pellet was kept aside for cellular phenotyping using flow cytometry using either the innate (P1) or the adaptive (P2) immune cell antibody panel (table 2.5).

NP sampling was carried out after dissecting, skinning and removal of the lower mouse jaw. The NP was rinsed with 200 µl PBS and collected into a 1.5 ml Eppendorf tube. 50 µl of neat NPW was plated agar plates supplemented with streptomycin. The bacterial titre was calculated from the number of colonies following overnight growth. The remainder of the NPW was collected for cytokine/chemokine and pentraxin analyses.

Blood was collected through retro-orbital bleeding under terminal anaesthesia in lithium heparin tubes and centrifuged at 800 x *g* for ten minutes. 50 µl of blood was resuspended in 1 ml red blood cell lysis buffer for 10 minutes on ice. The cells were centrifuged at 800 x *g* for two minutes. The supernatant was discarded and cells were washed twice with 1 ml PBS. Cells were then resuspended in FACS buffer (5 mM EDTA and 0.5% fetal bovine serum (FBS) in PBS) containing either the innate (P1) or the adaptive (P2) immune cell antibody panel (table 2.5).

NALT was dissected from the mice after the removal of the jaw and was incubated in 24 well plates, each containing 500 µl RPMI media containing 5% FBS for 24 hours at 37°C, 5% CO_2. Following the incubation, the media was collected and used for cytokine/chemokine and pentraxin analyses. NALT was collected in Precellys® ceremics 2 ml tubes containing 3 mL RPMI supplemented with 10 µg/mL collagenase II (ThermoFisher, 17101015) and 166 µg/mL DNase I (New England BioLabs, M0303L). NALT was homogenized in a Precellys® 24 homogenizer . The single cell suspension was passed through a 70-µm pore-size cell strainer to separate any debris. Cells were centrifuged at 800 x *g* for 2 minutes and resuspended in FACs buffer containing either the innate (P1) or the adaptive (P2) immune cell antibody panel (table 2.5).

Table 2 4 Grading of middle ear fluid

Grade	Middle ear fluid opacity and viscosity
1	Serous almost transparent fluid
2	Light fluid, limited opacity
3	Whitish free flowing fluid, 'bitty' opaque
4	White/cream opaque fluid, little viscosity (can be pipetted)
5	White/cream dense fluid, some viscosity (difficult to pipette in volume)
MEFs that were considered intermediate between two grades, were described as intermediate grades 2/3, 3/4, and 4/5.	

2.6.5. Flow cytometry: Immune profiling innate and adaptive immune cells

Immune profiling of the cells in the *Junbo* mouse MEF, NALT and blood (section 2.6.4) was performed using the antibody panel in table 2.5. Cells from each tissue or fluid were transferred to a 96-well plate. Cells were centrifuged, washed twice with FACs buffer then, cells were resuspended in either panel 1 or panel 2 antibody cocktail for 20 minutes at room temperature. Cells were then centrifuged and washed twice with FACs buffer and finally resuspended in SytoxBlue DNA stain. Flow cytometry was performed using a CytoFLEX S machine (AD32087). FlowJo software (Tree Star) was used to analyse the data obtained.

Table 2 5 Flow cytometry panel 1 (innate immune cells) and panel 2 (adaptive immune cells)

Panel 1: Innate immune cells				
Marker/ antigen	Fluorochrome	Final Dilution	Source	Catalogue number
Live/ dead	SytoxBlue	1:10,000	Invitrogen	S11348
CD5	BV421	1:200	BD biosciences	562739
CD4	FITC	1:800	BD biosciences	553047
CD8	PE-CF594	1:400	BD biosciences	562283
CD25	PE-Cy7	1:400	BD biosciences	552880
CD62L	APC-Cy7	1:1600	BD biosciences	560514
CD44	PE	1:200	BD biosciences	553134
TCR- δ	BV510	1:100	BD biosciences	563218
DX5	APC	1:200	BD biosciences	560628
Panel 2: Adaptive immune cells				
Live/ dead	SytoxBlue	1:10,000	Invitrogen	S11348
CD19	BV510	1:400	BD biosciences	562956
NK1.1	APC	1:200	BD biosciences	156505
LY6-C	FITC	1:400	BD biosciences	553104
LY6-G	BV421	1:400	BD biosciences	562737
CD5	BV421	1:200	BD biosciences	562739
CD11b	PE-CF594	1:800	BD biosciences	562287
CD11c	PE-CY7	1:400	BD biosciences	558079
MHCII	APC-CY7	1:200	BioLegend	107628

2.6.6. Mouse chemokine and cytokine array

Cytokine and chemokine levels were measured in the *Junbo* mouse MEF, NPW, serum and NALT. Three biological replicates were used for MEF samples, whereas only one biological sample for NPW, serum and NALT were tested (all the biological repeats have two technical repeats each). For MEF, high-grade fluids were used (grades >3/4) as we were primarily interested in investigating the immune responses in grades that had high NTHi titre and elevated/altered CRP levels. A mouse cytokine antibody array (mouse cytokine array C1, RayBiotech, Inc.) was used following the manufacturer's instructions. Samples were diluted prior to test: MEF, NPW and NALT = 1/25 and serum = 1/50 dilution in blocking buffer provided by the manufacturer. The following cytokines were analysed: granulocyte colony-stimulating factor (G-CSF), granulocyte-macrophage colony-stimulating factor (GM-CSF), and IL-2, IL-3, IL-4, IL-5, IL-6, IL-9, IL-10, IL-12p40/p70, IL-12p70, IL-13, and IL-17, along with IFN-γ, monocyte chemoattractant proteins 1 and 5 (MCP-1 and MCP-5), RANTES (T cell expressed and secreted), stem cell factor (SCF), soluble TNF receptor type I (sTNFRI), TNF-α, TPO, and vascular endothelial growth factor (VEGF). The signal intensities were measured using ImageJ 1.53e software and the values were input into an excel spreadsheet provided by the manufacturer for subsequent analysis.

2.6.7. Measuring cytokines: ELISA

Changes in CRP, C1q, C5a and serum amyloid protein (SAP) in *Junbo* NPW, MEF, NALT and serum were measured using commercial ELISA kits. NPW, MEF and NALT perfusion were diluted 1:50 and serum 1:100 in PBS. All the procedures were carried out according to the relevant manufacturer's instructions (table 2.6).

Table 2 6 ELISA kits used to measure immune proteins in the *Junbo* mouse tissues and fluids

Protein	ELISA kit	Source	Catalogue number
C1q	Wide-range ELISA Kit for Complement 1q	Cloud-clone corp.	WEA747Mu
C5a	Mouse complement C5a ELISA kit	Reddot biotech	EK5460
CRP	Mouse C-Reactive Protein/CRP DuoSet ELISA	Bio-techne	DY1829
SAP	Mouse Pentraxin 2/SAP Quantikine ELISA Kit	Bio-techne	MPTX20

2.6.8. Immunohistochemistry: Checking for CRP localisation in Junbo mouse MEF inoculated with NTHi

CRP and NTHi localisation was investigated qualitatively using immunohistochemistry (IHC) staining. *Junbo* mice were inoculated with NTHi 375sr as described in section 2.5.3. To make sure that the staining for CRP was specific, non-inoculated (NI) *Junbo* mice were used as negative controls. Wild-type mice were used as controls to measure baseline CRP levels.

Mice were culled as described in section 2.6.4 and the heads removed, deskinned and fixed in 10% neutral buffered formalin (formalin) (Leica) for at least 48 hours. The fixed heads were washed in PBS three times for 15 minutes before decalcification with 18% D.F.B

decalcifying agent (Kristensen, Pioneer Research Chemicals, PRC/R/12) for 3 days. Decalcified heads were processed for dehydration, clearance and paraffin wax impregnation in an Exelsior AS processor (ThermoScientific). Samples were dehydrated in increasing concentration of industrial denatured alcohol (IDA) (70%, 90% and 100%). 100% xylene was used for clearance; a process for lipid and residual alcohol removal. Finally, the heads were impregnated on molten paraffin wax under vacuum. Sections were cut using a Finesse ME+ microtome (ThermoFisher). Heads were cut in 5 µm transverse sections. Some sections were stained with haematoxylin and eosin (H&E) and others were left unstained for use with IHC antibodies. For H&E staining, sectioned heads were dewaxed using 100% xylene and rehydrated using 100% and 70% IDA before H&E staining. The Gram-stain was used to stain for bacteria in the ME. For CRP staining in the ME, 1/500 dilution rabbit anti-human CRP (DAKO, also works for mouse CRP) was used.

Sections were mounted in Clearium solution (Leica) and glass slides were applied. Images were taken using a NanoZoomer Digital Pathology scanner (Hamamatsu).

2.7. Co-immunoprecipitation

2.7.1. Magnetic bead co-immunoprecipitation

To test what target CRP binds to on the NTHi surface, co-immunoprecipitation was carried out.

NTHi strains were grown overnight on BHI agar plates. The following day, a 1 µl loop full of NTHi growth from the plates were re-suspended in PBS and bacterial suspension was normalised to OD490 of 0.2 for all the strains tested. Bacteria were treated with 100 ng/ml purified human CRP (BindingSite) for 30 minutes at 37°C. Following this, NTHi were centrifuged at 10 000 x *g* for 3 minutes and the pellets resuspended in PBS. The suspension was centrifuged at 10 000 x *g* for 3 minutes and the wash procedure repeated two more

times. After the final wash, CRP-bound NTHi bacteria were incubated with mouse anti-human CRP primary antibody conjugated Dynabeads (14321D, ThermoFisher Scientific).

The conjugation of Dynabeads was carried out as instructed by the manufacturer. Beads were conjugated with 7µl/ml mouse anti-human CRP antibody (clone CRP-8, Sigma, C1688). Samples were resuspended in lysis buffer: 50 mM Tris, pH 7.8, 150 mM NaCl, 1 mM EDTA, and the lysis of the samples was performed on ice for 30 minutes. 1% Triton X-100, 0.2% sodium deoxycholate, 0.1% sodium dodecyl sulfate (SDS). Following lysis, samples were incubated with conjugated dynabeads for 1 hour at 4°C to extract CRP-bound material, as instructed by the manufactuer. 'Pulled-down' samples were analysed by electrophoresis on SDS-PAGE gels.

2.7.2. SDS-PAGE LPS gels

Co-immunoprecipitation (Co-IP) samples were investigated using SDS-PAGE and 4-12% Bis-Tris gels (NUPAGE 4-12% Bis-Tris Gel 1.0 MM, NP0321BOX, Invitrogen). Samples were resuspended in 2X Laemmli loading buffer (50:50 mixture) (Bromophenol blue 0.004%, 2-mercaptoethanol 10%, Glycerol 20%, SDS 4%, Tris-HCl 0.125 M) and denatured for 10 minutes at 90°C. 15 µl of each sample was loaded into each well of the gel. NuPAGE MES SDS running buffer was used (NP0002, Invitrogen) to run gels for 30 minutes at 60V and then 40 minutes at 200V.

After electrophoresis, the gel was placed in a plastic tray and washed for 10 minutes with dH_2O. Gels were used either for silver-stain, western blotting or Coomassie staining to detect bands from Co-IP.

2.7.3. Silver staining for LPS

Following electrophoresis, gels were fixed in fixing solution (250 ml methanol, 50 ml glacial acetic acid and 200 ml water) for 30 minutes at room temperature. Following this, the fixing solution was discarded and replaced with fresh fixing solution and gels were incubated overnight at room temperature. The next day, fixing solution was removed and gels were washed with 30% ethanol followed by a wash with water for 10 minutes. The manufacturer's instructions were followed for the remainder of the silver stain procedure (ThermoFisher, 24612). Gels were visualised using Gel Doc XR+ Gel documentation system (Bio-Rad).

2.7.4. Western blot

The presence of CRP in *Junbo* mouse samples and the co-immunoprecipitation assay products was detected using western blot. Sample electrophoresed on PAGE-gels were transferred onto a nitrocellulose membrane via a Iblot gel transfer stack (IB201002, Invitrogen). Membranes were blocked with 5% BSA in PBS-T for 2 hours at room temperature. Following this, membranes were incubated in either 1/2000 dilution mouse anti-human CRP (clone CRP-8, Sigma, C1688), or rabbit anti-human CRP (DAKO, also works for mouse CRP) or goat anti-mouse CRP (AF1829-SP, R&D systems) antibody diluted in 5% BSA overnight at 4 °C. To detect PCho, 1/2500 dilution TEPC-15 antibody was used (IgA, Kappa from murine myeloma, M1421, Merck). Membranes were washed three times in PBS-T for 5 minutes each. Subsequently, membranes were incubated in anti-mouse (1/5000)/anti-goat (1/5000)/anti-rabbit (1/5000) diluted in 5% BSA-T for 1 hour at room temperature. Membranes were washed three times in PBS-T for 5 minutes and detected by an ultra-high sensitivity ECL-substrate kit (AB133409, Abcam). Membranes were visualised using a ChemiDoc machine.

2.7.5. Far western blot

To investigate CRP binding ligands on the NTHi surface, far western blot was used. NTHi lysates were electrophoresed on PAGE-gels as described in section 2.7.2. Sample electrophoresed on PAGE-gels were transferred onto a nitrocellulose membrane via a Iblot gel transfer stack (IB201002, Invitrogen). Membranes were blocked with 5% BSA in PBS-T for 2 hours at room temperature. The nitrocellulose membranes were incubated in 500 ng/ml human CRP (Binding Site BP300.X; 99% pure) prepared in CRP buffer (0.2 M Tris pH 7, 0.15 M NaCl and 10 mM $ZnCl_2$) for 1 hour at room temperature with agitation. Following this, the nitrocellulose membranes were washed three time with PBS-T for 5 minutes each. Following this, membranes were blocked with 5% BSA in PBS-T for 2 hours at room temperature. Next, membranes were incubated in 1/2000 dilution mouse anti-human CRP antibody (clone CRP-8, Sigma, C1688), diluted in 5% BSA overnight at 4 °C. The following day, membranes were washed three times in PBS-T for 5 minutes each. Membranes were then incubated in anti-mouse antibody (1/5000) diluted in 5% BSA-T for 1 hour at room temperature. Membranes were washed three times in PBS-T for 5 minutes and detected by an ultra-high sensitivity ECL-substrate kit (AB133409, Abcam). Membranes were visualised using a ChemiDoc machine.

2.8. Colony immunoblotting

To investigate PCho phase variation in a heterogeneous population of NTHi bacteria and PCho expression on NTHi grown from *Junbo* mouse MEF/NPW, colony immunoblotting was carried out. Bacteria were grown overnight on BHI agar plates. The following day, colonies were counted before placing a nitrocellulose filter on the surface of agar plate for 60 seconds. The filter was removed using clean forceps and air dried for 5 minutes before blocking in 2% BSA/PBS-T for 1 hour at room temperature. Filters were washed three times in PBS-T for 2 minutes each and incubated in 1/2500 dilution TEPC-15 antibody for 3 to 4

hours at room temperature or overnight at 4 °C. Filters were washed three times in PBS-T for 2 minutes each and incubated with 1/25000 dilution goat anti-mouse IgA peroxidase antibody (A4789, Merck) for 1 hour at room temperature. After washing three times in PBS-T, blots were developed by adding a 1:2 dilution of BCIP/NBT solution (chromogenic substrate for the enzyme label alkaline phosphatase (AP)) (AB7468, Abcam) for 15 minutes. Blots were rinsed in water and left to dry in the dark before evaluation.

Numbers of colonies on the immunoblot were counted manually. Levels of PCho on the NTHi surface was measured by counting colonies on the immunoblot that had positive staining for PCho/TEPC-15. Phase off variants did not stain with TEPC-15 or very faint colonies were visualised. Phase variation was calculated by counting number of colonies positive for PCho strain divided by the total number of colonies on the immunoblot.

2.9. Statistical Analyses

All statistical analyses were carried out using GraphPad Prism 9.3.1 software. One-way ANOVA or two-way ANOVA was used depending on one or two factors respectively. A threshold of $p < 0.05$ was used to measure if the differences obtained were statistically significant. Post-hoc analyses were carried out to determine where the differences truly came from. For the mouse studies, false discovery rate (FDR) correction was applied to measure accuracy. On the graphs, statistical significance is represented as: * = p <0.05, **= p <0.01, *** = p <0.001 and **** = p 0.0001. All results are shown as standard error of the mean, unless otherwise stated.

Chapter 3. Developing C-Reactive Protein Binding Assay to quantify binding to NTHi strains

3.1. Introduction

CRP levels have been correlated with NTHi infection in OM (E. Lysenko *et al.*, 2000; Jane M. Gould and Weiser, 2001; Langereis *et al.*, 2019; Langereis, van der Pasch and de Jonge, 2019). The presence and position of PCho on the NTHi surface have been shown to have an effect on CRP binding. Proteomic analysis of the MEF revealed CRP is present in the MEF of *Junbo* mice infected with NTHi (data not shown). While studies have investigated the role of CRP in bacterial AOM, the association between its level and outcome is not well understood. Published evidence indicates the relevance of PCho position on NTHi for preferential CRP binding. Lysenko et al., showed that CRP binding to PCho off heptose III on the NTHi LPS was stronger than PCho off heptose I (E. Lysenko *et al.*, 2000). However, the questions of how does this equate to the host-pathogen response and why do some NTHi strains survive while others are killed in the presence of CRP still need to be addressed.

An established enzyme based immunosorbent assay (ELISA) to measure CRP binding to NTHi to our knowledge does not exist. In research, several methodologies have been developed to study specific levels of CRP in disease and different biological settings (table 3.1). These methods differ in their sensitivities for measuring CRP levels. Furthermore, current methods used to measure CRP concentration do not quantify binding to whole bacteria. In this chapter, we aimed to develop an effective indirect ELISA to measure binding of CRP to whole NTHi bacteria. We aimed to quantify how presence or absence and position of PCho on different AOM NTHi clinical strains affects binding of CRP.

Table 3 1 Current methodologies used to measure CRP levels

Method	Use	Detection of limit	Reference
Agglutination reaction	CRP positive sera pooled from various inflammatory diseases. Studying to measure CRP induced agglutination of lipid suspensions and this reaction is inhibited more by PCho than phosphatidylcholine	-	(TSUJIMOTO, INOUE and NOJIMA, 1980)
Non-immunological assay enzyme linked sorbent assay (ELSA)	CRP binding to PCho is calcium dependent. Free CRP competes with immobilised CRP for PCho-BSA HRP conjugate	0.0011 mg/ml	(Deegan *et al.*, 2003)
Turbidity	CRP binding to PCho is calcium dependent	0.025 – 0.5 mg/ml	(Deegan *et al.*, 2003)
Turbidity	Measurement of CRP in serum and plasma	0.007 mg/ml	(Tugirimana *et al.*, 2009)
Protein-directed immunisation	Detecting pentametric CRP and thiolated PCho ligand on a gold surface	0.12 ng/ml	(Kim *et al.*, 2013)
Sandwich ELISA	In plasma of patients in renal allograft. Developed ELISA to study complement complexes with CRP	0.01 ng/ml	(Wolbink *et al.*, 1996)
	Quantification of monomeric CRP in plasma	1 ng/mL	(Zhang *et al.*, 2018)

Rapid enzyme immunoassay	Measuring CRP in human acute phase sera and purified human CRP	0.01 mg/ml	(Laurent *et al.*, 1985)
High sensitivity CRP assay	For predicting risks associated with chronic heart disease. Quantum dots-labelled immunoassay within a standard 96-well microplate.	60 ng/ml	(Luo *et al.*, 2012)
Fluorescent binding immunoassay	Detecting CRP in human and mouse sera	20 ng/ml	(Siboo and Kulisek, 1978)
Western blot	Detecting expression of CRP in the human respiratory tract	50 ng/ml	(Jane M. Gould and Weiser, 2001)
Multiplexed lateral flow strip	Detecting CRP in human serum and differentiate between viral and bacterial infections. Simultaneously detecting procalcitonin (PCT) and CRP which is relevant in sepsis	PCT = 0.5 ng/ml; CRP 500 ng/ml	(Cao *et al.*, 2022)

3.2. Developing indirect ELISA to measure CRP binding to NTHi bacteria

ELISA is a method used to detect the presence and amount of antigens and relies on antibodies specific to the target antigen. In in-direct ELISA, the antigen, which in this case is the bacteria, is immobilised onto the surface of a multi-well plate. The antigen can be immobilised onto the surface directly or using a capture antibody. An in-direct ELISA involves a two-step process for detection of a specific antigen. In the first step, a primary antibody binds to the antigen and in the second step; a labelled secondary antibody specific to the primary antibody is used for detection. The main advantage of this type of ELISA is that the signal is amplified as several secondary antibodies can bind to the primary antibody bound to the target antigen. It is an attractive method where the same secondary antibody can be used against many different primary antibodies. Disadvantages of the method include potential background signal from the secondary antibody. For this, a secondary only control is used and any signal produced by this control is deducted from the final values for all the samples. Another disadvantage is that it is a longer, more time-consuming process than other types of ELISA. However, despite these disadvantages, in-direct ELISA offers higher sensitivity and is more cost-effective (fewer labelled antibodies used) than other ELISA methods.

The development of in-direct ELISA for CRP binding to NTHi involved several optimisations, which are discussed in this chapter. The final method is detailed in chapter 2, section 2.2.1.

3.2.1. Optimising immobilisation of bacteria onto microtitre plate

In-direct ELISA required the immobilisation of NTHi bacteria onto a polystyrene surface. This step was crucial for the assay, as an improper immobilisation led to loss of bacteria during the subsequent steps of the assay. Bacteria can attach to the plastic surfaces through a variety of mechanisms which can be influenced by many factors such pH and temperature. Lipid symmetry of the outer membrane influences Gram-negative bacteria

function and attachment or detachment to/from polystyrene surfaces (Yuan *et al.*, 2017; Oh *et al.*, 2018). A strong correlation between cell surface hydrophobicity and affinity of bacteria for polystyrene has been reported (Rosenberg, 1981). Initial experiments tested different methods of immobilisation to enhance NTHi binding to 96-well plates. Antibody anti-162, which specifically detects strain 162sr, was used to measure NTHi 162sr adherence onto the 96-well plate. We tested different types of plate pre-coatings and bacterial preparations to determine which conditioned surface permitted the optimal NTHi adherence on the plate surface. This included, (i) preparation of NTHi in PBS, (ii) pre-coating the polystyrene surface with poly-L-lysine, (iii) dehydrating NTHi in 70% ethanol or pre-fixing bacteria with 0.08% PFA and, (iv) drying NTHi suspension plated onto the 96 well plates at 37°C.

Poly-L-lysine works by increasing the interaction between the positive charges on the polystyrene plate with negative charges on the bacterial cell surface. Once adsorbed onto the surface, it increases the availability of positively charged sites available for binding. Pre-coating with poly-L-lysine, dehydration and fixing bacteria with PFA did not improve coating of NTHi onto the polystyrene surface (figure 3.1A). We confirmed lack of NTHi adherence to the polystyrene surface using crystal violet staining (data not shown). To our knowledge this has not been reported for NTHi LPS, but similar effects have been reported for LPS from other bacteria *e.g. Pseudomonas aeruginosa*, another Gram negative bacteria (Bantroch, Buhler and Lam, 1994).

To improve NTHi attachment to the 96-well plates used in the assay, we tested the effect of drying the plates coated with NTHi. Drying the plates containing whole-bacteria suspension has been described previously and was adopted in our protocol (Elder, Boraker and Fives-Taylor, 1982). NTHi suspension was prepared in carbonate coating buffer prior to drying the plates. Carbonate buffer is commonly used in ELISAs to enhance the sensitivity of the assay (Bantroch, Buhler and Lam, 1994). Therefore, CRP-treated and NTHi only suspensions were coated onto the polystyrene plates overnight at 4°C in carbonate buffer. The following day, liquid (*i.e*. NTHi suspension) from the plates were

discarded and the plates was dried at 37°C for 30 minutes to 1 hour. The drying step significantly enhanced bacterial coating, which was confirmed by crystal violet staining (data not shown). This step was deemed critical for our in-house developed ELISA.

3.2.2. Testing different titres of bacteria for immobilisation step

The limit of detection for bacterial numbers was tested using different concentrations of whole NTHi 375 strains. Anti-162 antibody is specific to NTHi 162, and its binding with NTHi 375 strains produced a weak signal that was similar to background signal from secondary only control (data not shown). Therefore, primary antibody against PCho (which works well for all NTHi expressing PCho on their surface) was used to measure the optimum bacterial number for the assay (figure 3.1.B). Bacterial titres of between 10^2 and 10^8 CFU/ml were prepared and coated onto 96-well plates. 10^5 CFU/ml was the lowest bacterial titre that produced a detectable signal in the assay, whereas maximum signal intensity was obtained for 10^8 CFU/ml. For the remaining experiments, 10^8 CFU/ml was used to coat each well of the plate.

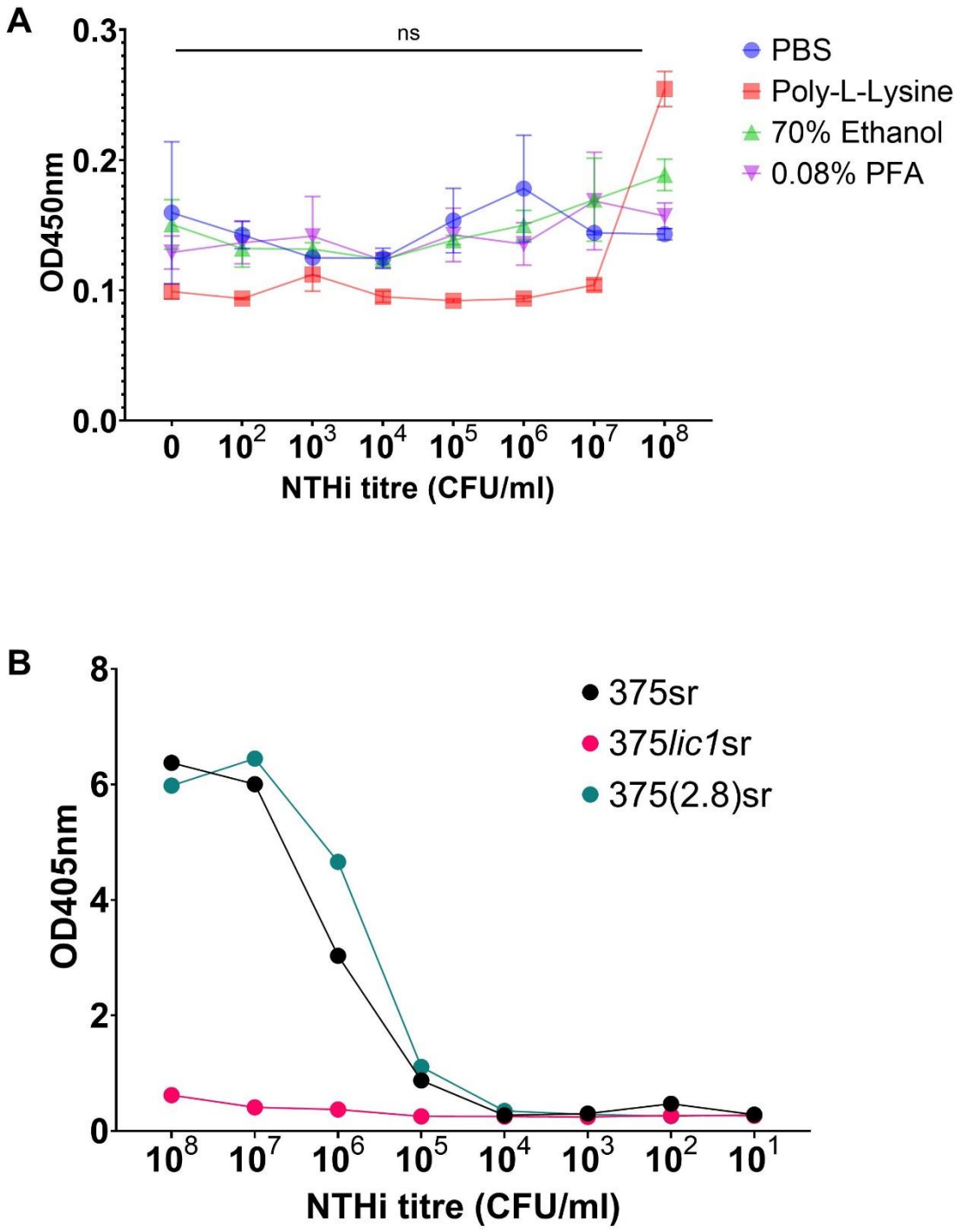

Figure 3.1. Optimising micro-titre plate coating and bacterial titre. (A) Coating conditions for NTHi 162sr. NTHi suspended in PBS, pre-coating the polystyrene surface with poly-L-lysine, dehydration of bacteria (70% ethanol) or fixation of bacteria (0.08% PFA). Final bacterial titre was prepared in carbonate buffer for coating. Anti-162 antibody was used as primary antibody for NTHi detection. HRP-conjugated secondary antibody used and the plate read out at OD 450nm (n = 2). One way ANOVA (p = 0.2314) (B) NTHi 375 strain titrations. TEPC-15 antibody used and AP-conjugated secondary antibody was used. Plate read at OD 405nm (n=2) One way ANOVA (p = 0.0647)

3.2.3. Testing CRP proteins

In the human, CRP is a major acute phase protein. We did not have access to human samples to study the host-pathogen interaction in AOM. Therefore, to study the role of CRP in NTHi survival in the presence of host-immune cells, we used the *Junbo* mouse model (as discussed in chapter 6). Mouse CRP also binds PCho (Ku, 1993). We hypothesised that PCho presence or absence and position on the NTHi surface may influence binding of human CRP (hCRP) and mouse CRP. Therefore, both human and mouse CRPs were tested in the ELISA. Both proteins are commercially available. Purified human CRP (Binding Site BP300.X; 99% pure) in its native pentameric form was obtained whereas; only recombinant mouse CRP (rMoCRP) (Bio-techne, 1829-CR-200) proteins can be tested. To our knowledge native purified mouse CRP is not commercially available. The mouse protein used in the experiments was from a mouse myeloma cell line, NS0-derived. Production of mouse CRP in mammalian expression system offers an advantage that the post-translational modifications and protein folding is similar to native protein. Commercially available rMoCRP exists as an oligomer as it contain multiple forms of the protein. The manufacturer claims that the protein is not entirely a dimer, trimer, or a pentamer and that the ratio of each oligomer may fluctuate between different batch lots. Furthermore, upon contacting the manufacturer, protein function does not seem to be affected by this although there is no published data to support this.

3.2.3.1. PCho on the NTHi surface may not be the main binding target for recombinant mouse CRP (rMoCRP)

NTHi 375 strains were used to investigate how PCho presence and PCho on bacterial surface influences rMoCRP binding. Our ELISA showed that rMoCRP bound all the NTHi strains tested (figure 3.2A). Furthermore, to our surprise, rMoCRP also bound NTHi 375*lic1*sr, a PCho mutant and this binding was much more than any other NTHi 375 strains.

The least amount of binding was evident for NTHi 375srPCho^{-} (phase variation 'OFF'), although binding to this variant was not statistically different compared to NTHi 375sr. Finally, to confirm if rMoCRP binds to PCho specifically, a titration assay to block PCho sites using TEPC-15 (a PCho specific antibody) was used to investigate the effect on rMoCRP binding. Prior treatment with TEPC-15 did not seem to affect rMoCRP binding, thus suggesting an alternative binding site/interaction (figure 3.2B).

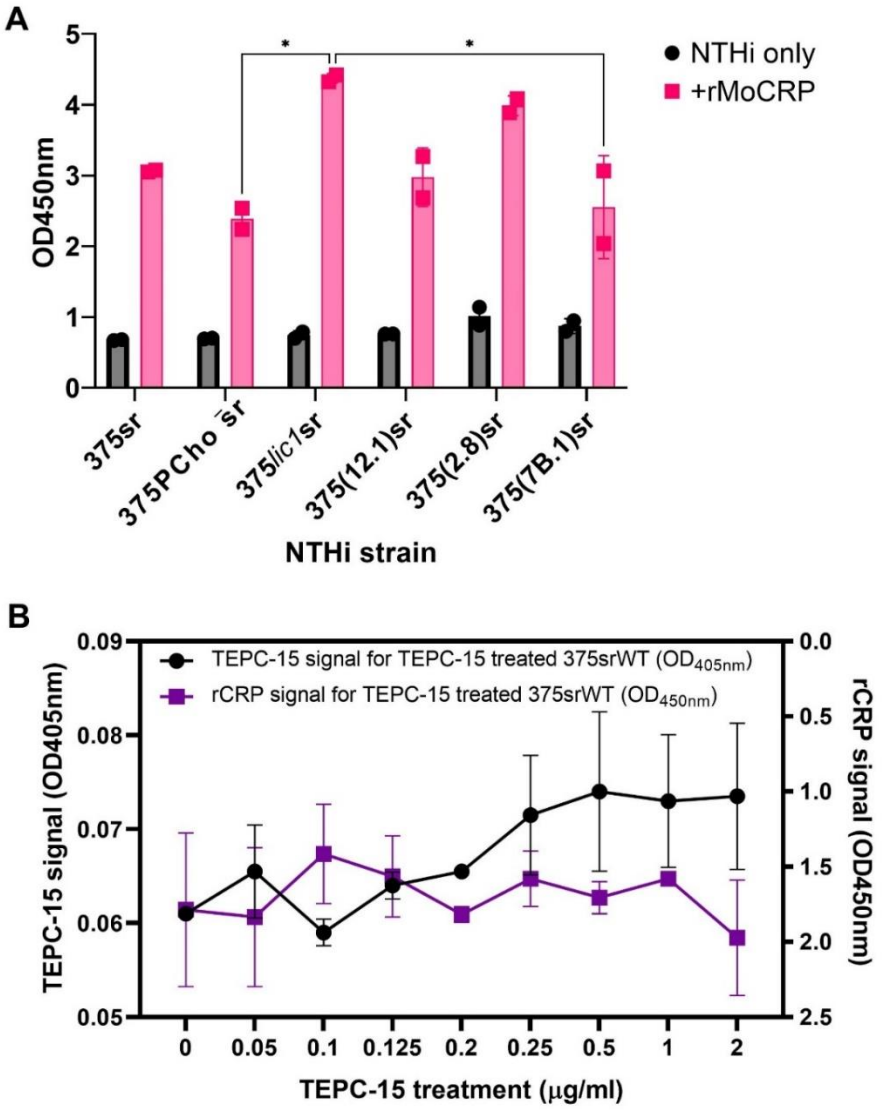

Figure 3.2. Recombinant mouse CRP (rMoCRP) binding to NTHi 375 strains. A) rMoCRP binding to NTHi 375 strains. NTHi only and rMoCRP bound NTHi were plated onto a 96-well plate. NTHi only was used to measure any non-specific secondary antibody binding (n=6). Two-way ANOVA followed by Sidak's multiple comparisons post-hoc test * p <0.05. (B) Saturation of PCho sites on the NTHi surface using TEPC-15 antibody and investigating rMoCRP binding (n=3).

3.2.3.2. Human CRP (hCRP) has preferential binding sites on the NTHi surface

The CRP binding was repeated on NTHi 375 strains. NTHi 375 strains only differed from each other by their surface PCho presence and positions. We also used other AOM NTHi strains in our binding assay. These bacterial strains also expressed PCho on their surface. Using NTHi 375 and other AOM NTHi strains, we investigated how the presence or absence and position of PCho on the NTHi surface affects hCRP binding. We showed that hCRP binds the most to PCho off heptose III (1158sr, 176sr (two PCho: heptose III and heptose IV) (figure 3.3A and 3.3B). The least amount of hCRP binding was observed for strains 375sr, 162sr and 285sr where PCho is expressed off heptose I. PCho off heptose II (NTHi 486sr) also had an increase in hCRP binding compared to PCho off heptose I. These data confirm PCho off heptose I is the least favourable site for hCRP binding.

We observed a similar PCho presence or absence and position specific effect on hCRP binding when NTHi 375 strains were used (figure 3.3C and 3.3D): PCho off heptose III had the highest level of hCRP binding and PCho off heptose I had the least (figure 3.3E and 3.3F). NTHi 375(12.1)sr also showed an increase in hCRP binding, however, it is not clear what hCRP is binding to on this strain because NTHi 375(12.1)sr does not have a hexose extension off heptose II to permit PCho binding. These data suggest that PCho presence and position influences hCRP binding to NTHi. Furthermore, immmunoblotting of NTHi 375 strains show that PCho expression levels vary between the NTHi 375 strains, where NTHi 375(2.8)sr which expressed of HepIII showed more extensively than other NTHi variants (figure 3.3D). Similar observation has been made previously by our group where upon western blotting of NTHi 375 variant LPS, higher levels of TEPC-15 was observed for NTHI 375(2.8)sr compared to other 375 variants. Structural analysis using electrospray ionisation mass spectrometry revealed that the amount of PCho incorporation into the NTHi 375 variants was equivalent (Cody *et al*., unpublished). Furthermore, sequencing of the tetranucleotide repeat tract within the *lic1A* (gene required for PCho synthesis) confirmed

that each 375 variant has 21 5´ -CAAT repeat units which permits the expression from the same start codon (Cody *et al*., unpublished).

PCho non-expressing strains (*lic1* mutant) were used to confirm if PCho on NTHi is the primary binding target for CRP. We did not have NTHi 176sr, 176(1c)sr and 162sr *lic1* mutants. NTHi 162 phase-off variant, NTHi 162srPCho¯ was used. NTHi 176(1c)sr is a variant of NTHi 176sr that expresses higher levels of PCho on its surface. In general, NTHi *lic1* mutants showed a decrease in CRP binding with exception of NTHi 486*lic1*sr where an increase in binding was observed (figure 3.3G). These data confirm that PCho is not the only binding site for human CRP on the NTHi bacterial surface.

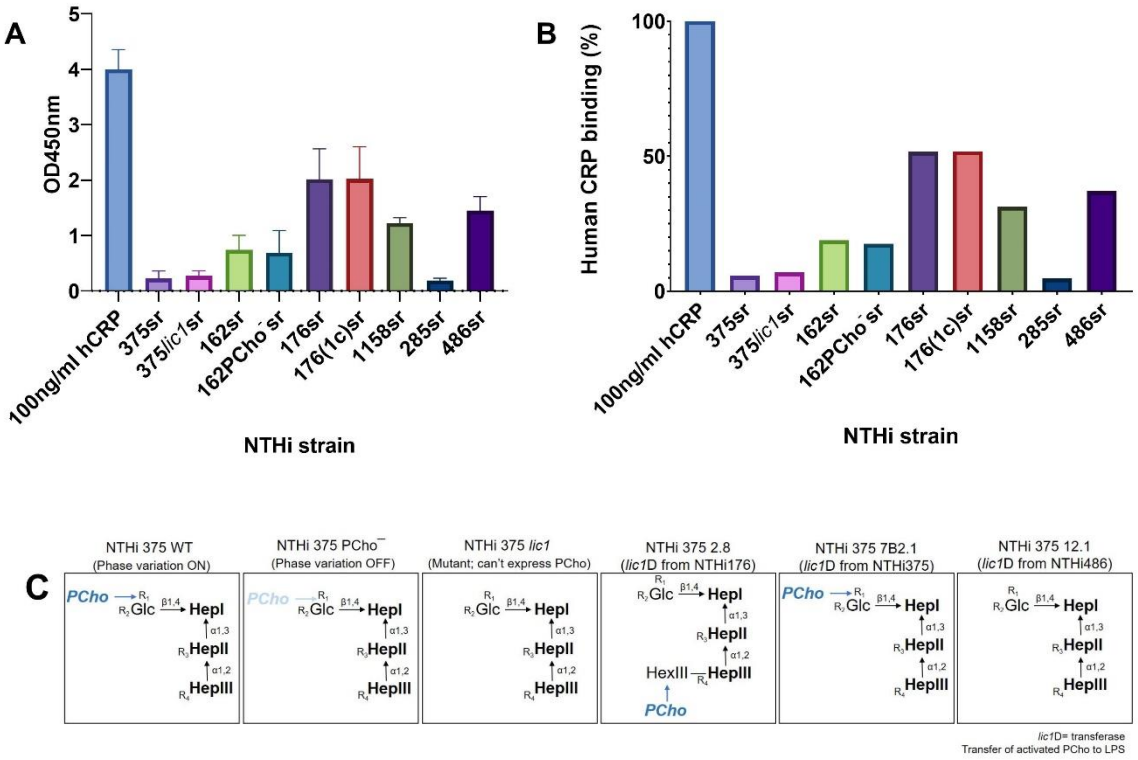
A
OD450nm
100ng/ml hCRP
375sr
375lic1sr
162sr
162PCho⁻sr
176sr
176(1c)sr
1158sr
285sr
486sr
NTHi strain
B
Human CRP binding (%)
NTHi strain

C
NTHi 375 WT
(Phase variation ON)
NTHi 375 PCho⁻
(Phase variation OFF)
NTHi 375 lic1
(Mutant; can't express PCho)
NTHi 375 2.8
(lic1D from NTHi176)
NTHi 375 7B2.1
(lic1D from NTHi375)
NTHi 375 12.1
(lic1D from NTHi486)
PCho
Glc
HepI
HepII
HepIII
HexIII
lic1D= transferase
Transfer of activated PCho to LPS

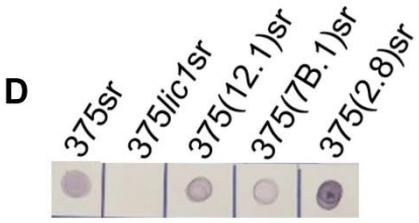
D
375sr
375lic1sr
375(12.1)sr
375(7B.1)sr
375(2.8)sr

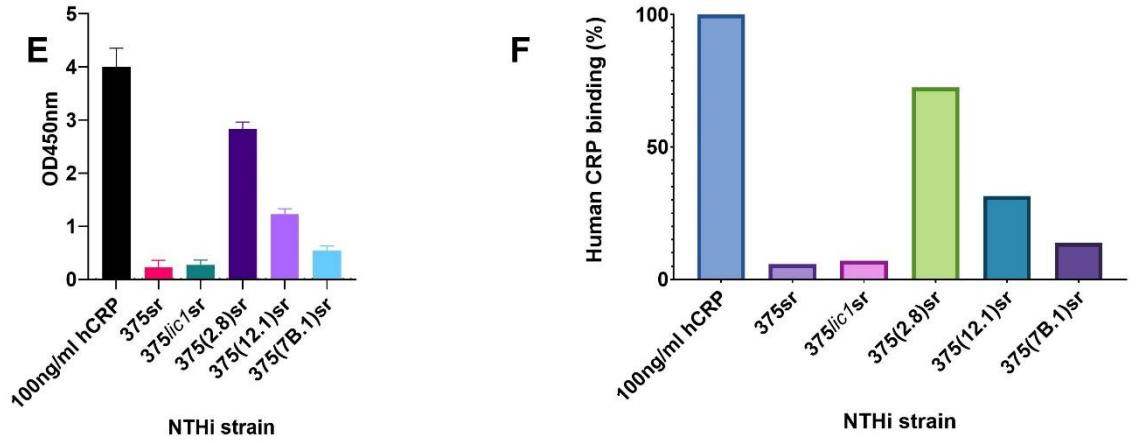
E
OD450nm
100ng/ml hCRP
375sr
375lic1sr
375(2.8)sr
375(12.1)sr
375(7B.1)sr
NTHi strain
F
Human CRP binding (%)
NTHi strain

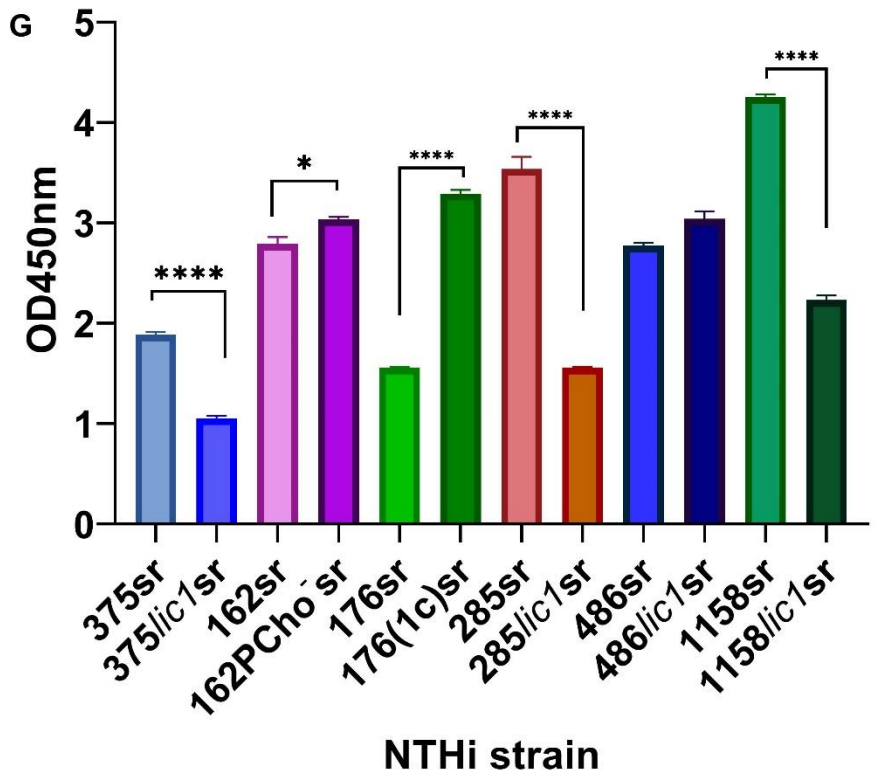

Figure 3.3. Quantifying human CRP (hCRP) binding to NTHi strains using indirect ELISA (A) hCRP binding to NTHi strains. (B) Percentage of human CRP bound to NTHi variants. This figure is a percentage of hCRP binding for NTHi strains in figure 3.3B. NTHi 375sr, 162sr and 285sr express PCho heptose I. NTHi 486sr expresses PCho off heptose II. NTHi 1158sr, 176sr and 176(1c)sr express PCho off heptose III. NTHi 176(1c)sr is expresses higher levels of PCho than 176sr. NTHi 176sr and 176(1c)sr express an addition PCho off heptose IV. (C) Schematic showing PCho on NTHi strains. (D) Immunoblot confirming expression of PCho on NTHi 375 strains. NTHi 375sr and 375(7B.1)sr express PCho off heptose I. 375*lic1*sr is a mutant with deleted *lic1* gene, thus does not express PCho. NTHi 375(2.8) expresses PCho heptose III. NTHi 375sr(12.1)sr does not express PCho due to no hexose extension off heptose II. (E) hCRP binding to 375 strains. (F) Percentage of hCRP bound to NTHi 375 strains. This figure is a percentage of hCRP binding for NTHi strains in figure 3.3E. (G) Binding of hCRP to NTHi expressing PCho and their respective PCho mutants. OD490nm values are plotted (n=3). Two way ANOVA followed by Sidak's multiple comparisons post-hoc test * = p <0.05 **** = p <0.0001

3.2.3.3. Phosphoethanolamine on NTHi surface interferes with CRP binding

We confirm that differences in CRP binding to NTHi strains is influenced by the presence and position of PCho on the NTHi surface. We hypothesised that the binding of CRP could be influenced by interactions or interferences from other ligands on the NTHi surface. The major binding ligand for CRP is PCho. In addition to this, CRP is also involved in binding to non-PCho ligands such as phosphoethanolamine (PEtn), which is also expressed on the surface of NTHi (figure 4.2A). To study what effect PEtn has on hCRP binding, we used NTHi 375sr mutants that lacked PEtn on their surface (figure 3.4b) (strain list in chapter 3, table 3.1). Our ELISA showed that the NTHi 375*lpt6*sr, a mutant lacking PEtn off heptose II increased hCRP binding to NTHi compared to wild-type NTHi. Loss of PEtn from heptose III in strain NTHi 375*lpt3*sr did not affect hCRP binding as levels of CRP binding were similar to wild-type NTHi 375sr. The double mutant strain, 375*lpt3/lpt6*sr showed an increase in hCRP binding with respect to the wild-type strain, NTHi 375sr. This increase in binding was probably due to mutation in *lpt6* rather than *lpt3*. These data confirm that PEtn off heptose II can influence hCRP binding to NTHi 375sr.

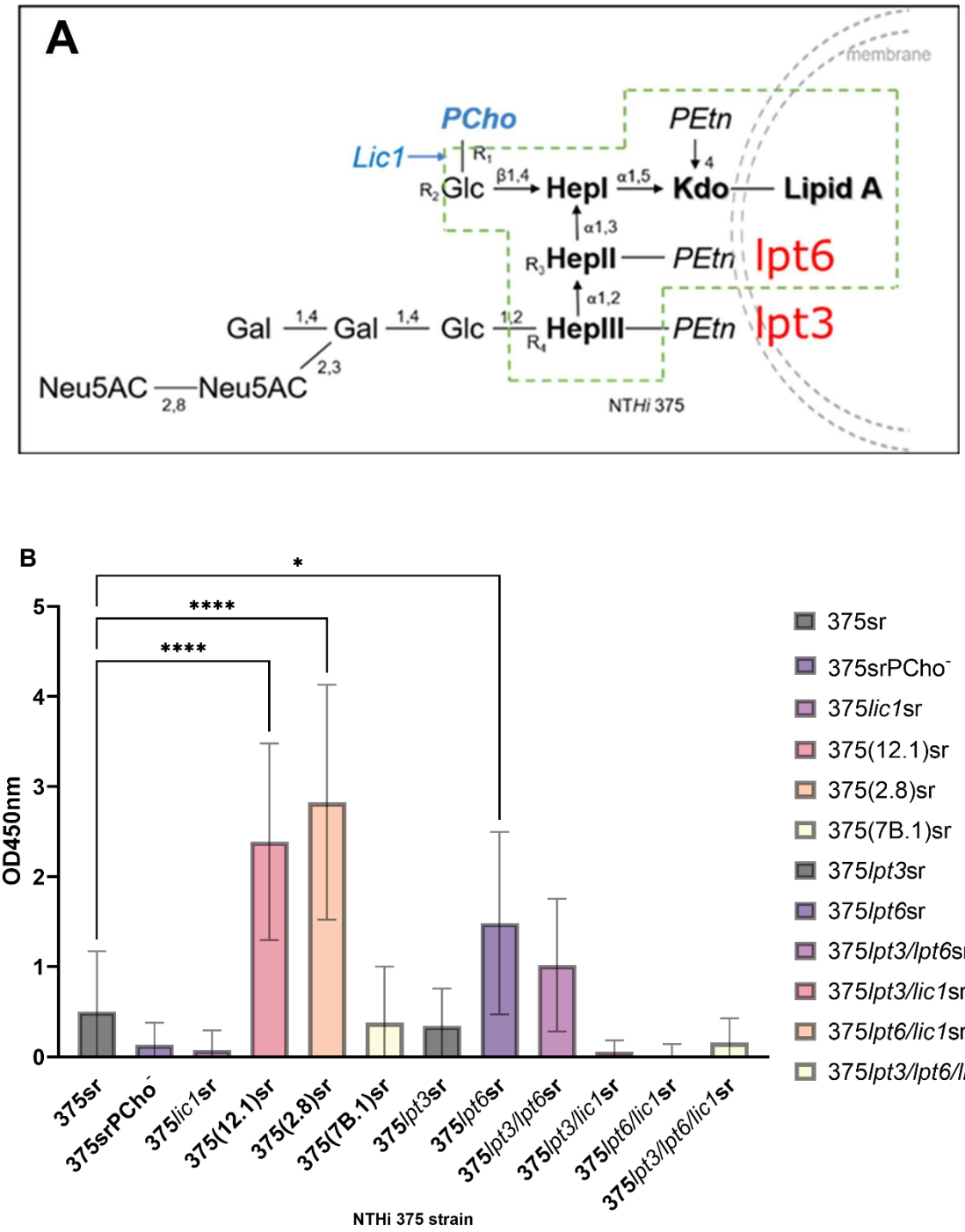

Figure 3.4. Investigating the role of phosphoethanolamine (PEtn) on human CRP (hCRP) binding. (A) Schematic and genes of NTHi 375 showing PEtn positions. (B) hCRP binding to NTHi strains, including PEtn mutants (n=4). One way ANOVA followed by Brown-Forsythe post-hoc test * p = <0.05 **** p = <0.0001

3.2.3.4. Mouse and human CRP show differences in PCho binding site

PCho binding by CRP is facilitated through calcium and hydrophobic pocket which contains the amino acids phenylalanine (Phe)^{66} and glutamic acid (Glu)^{81}. Glu^{81}interacts with the choline nitrogen atom. Both Phe^{66} and Glu^{81} are conserved in the CRP of human and other animals, including the mouse. In addition to Phe^{66} and Glu^{81}, threonine (Thr)^{76} also adds to the CRP hydrophobic pocket and aids in PCho binding (Shrive *et al.*, 1996).

The protein structure of hCRP is well characterised (Shrive *et al.*, 1996), however, details of the mouse CRP structure and PCho binding capacity are under reported. Protein homology modelling was performed using the Swiss-model (swissmodel.expasy.org) and the mouse CRP sequence (accession number Q91XB3) to predict the structure of mouse CRP. The human CRP structure was used as a template (P02741.1). Mouse CRP is a pentraxin and shares 71% sequence identity with hCRP. After aligning the protein models, PCho binding residues on hCRP were compared with PCho binding residues on rMoCRP (figure 3.5). Predictive analysis of the models revealed the Phe^{66} and Glu^{81} were indeed conserved in rMoCRP. However, in the rMoCRP, there is a glycine residue in the hydrophobic pocket instead of Thr^{76} **(**figure 3.5B). The structural modelling of hCRP and rMoCRP suggest that the two proteins have some differences in their PCho binding sites. This could explain the differences observed in the binding assays using the two proteins (figure 3.2A and 3.3E)

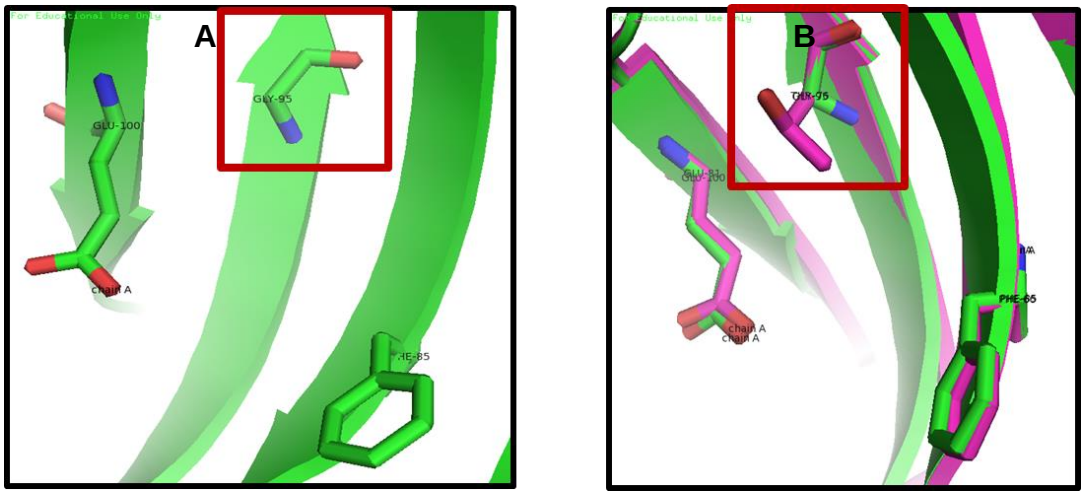

Figure 3.5. Predictive modelling of human and mouse CRP. (A) Human CRP showing PCho binding site containing the amino acids Phe[66], Thr[76], and Glu[81]. (B) Mouse CRP overlapped on human CRP. Phe[66]and Glu[81] are conserved in both human and mouse protein. Mouse CRP PCho binding site has a glycine instead of Thr (highlighted in red box).

3.2.4. Human and mouse protein storage conditions

Storage of CRP is can be critical for ensuring the reproducibility of the ELISA. Storage of hCRP at temperatures below 4°C dissociated the protein and hCRP no longer bound to NTHi bacteria. On the other hand, rMoCRP did not dissociate when stored at temperatures below 4°C. The CRP storage temperature therefore is important to ensure the CRP proteins do not dissociate, which can have an effect of the CRP binding assay.

3.2.5. Reducing background signal

In-direct ELISA involves multiple incubation steps and the use of secondary antibody. Insufficient washing can contribute to background signal and limit the strength of the assay. The bacterial growth broth, BHI also produced background signal during the ELISA. Thorough washing of the bacteria following growth in liquid BHI broth significantly reduced

background noise during the ELISA. Bacterial preparation for the assay and the wash steps during the ELISA are critical in ensuring that there is background signal.

3.2.6. Immunogold stain electron microscopy to visualise CRP binding to 375sr isogenic variants

The CRP binding ELISAs showed that PCho presence and position on the NTHi influences CRP binding. Furthermore, PEtn off heptose II also influenced hCRP binding to NTHi bacteria. We used the following NTHi 375 strains: 375sr, 375*lic1*sr, 375(2.8)sr and 375*lpt6*sr to measure CRP binding using immunogold labelling. NTHi 375sr, which expresses PCho off heptose I does not bind CRP well (figure 3.3E). NTHi 375*lic1*sr, a PCho mutant that had the least amount of hCRP binding compared to NTHi 375sr (figure 3.3E). NTHi 375(2.8)sr, which expresses PCho off heptose III and had the highest amount of hCRP binding compared to NTHi 375sr (figure 3.3E). NTHi 375*lpt6*sr expresses PCho off heptose I, and has PEtn off heptose II removed. It had higher hCRP binding than NTHi 375sr (figure 3.4B). As we had more data on hCRP binding to PCho and PEtn on NTHi compared to mouse CRP, initial experiments used hCRP for immunogold labelling. We aimed to visualise hCRP binding to NTHi 375 strains. We hypothesised that hCRP binding may be clustered around specific areas on the bacterial surface.

Similar to the data obtained from ELISA (section 3.2.3.2), NTHi 375(2.8)sr showed the highest level of hCRP binding to the bacterial surface. Very little CRP binding was observed for NTHi 375sr and no hCRP binding was measured for NTHi 375*lic1*sr (figure 3.6A and 3.6B). NTHi 375*lpt6*sr showed an increase in CRP binding as expected (figure 3.6A and 3.6B).

PCho off heptose III and PEtn mutation (*lpt6*) alone showed a general increase in hCRP detected on the bacterial surface. We did not observed any clustered hCRP binding on the

bacterial surface, suggesting PCho may be expressed all over the NTHi surface rather than being localised to specific areas on the NTHi LPS. In some of the electron micrographs, we observed that NTHi membrane seemed to bleb outwards and higher levels of hCRP particles were observed on these structures (figure 3.6C). More blebs were observed on hCRP-bound NTHi 375(2.8)sr and 375/*pt6*sr.

Overall, these data confirm previous ELISA data indicating that PCho presence and position on the NTHi surface influences hCRP binding and that PEtn can influence binding of CRP to PCho on NTHi.

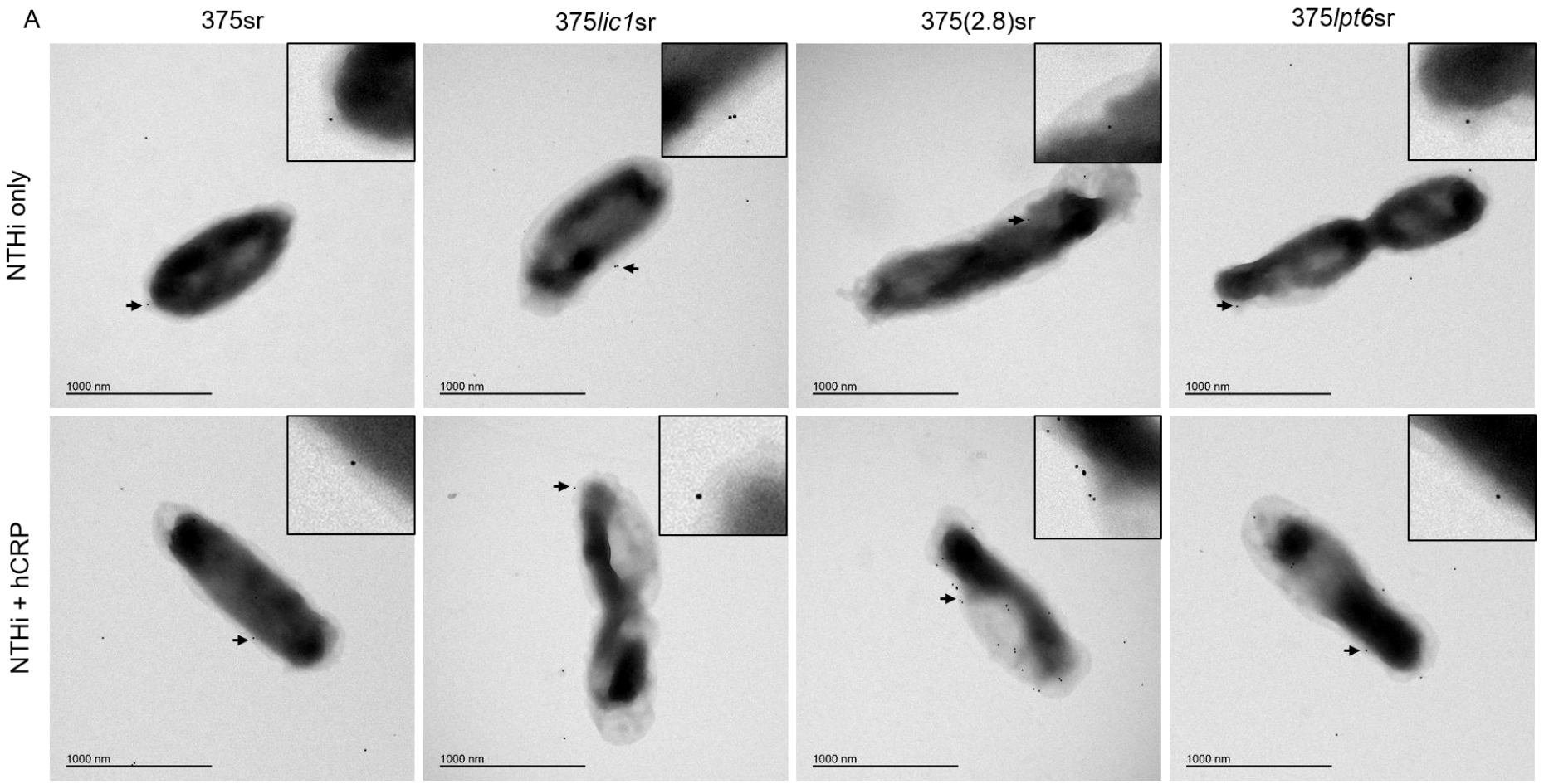
A
375sr
375lic1sr
375(2.8)sr
375lpt6sr
NTHi only
NTHi + hCRP
1000 nm

B

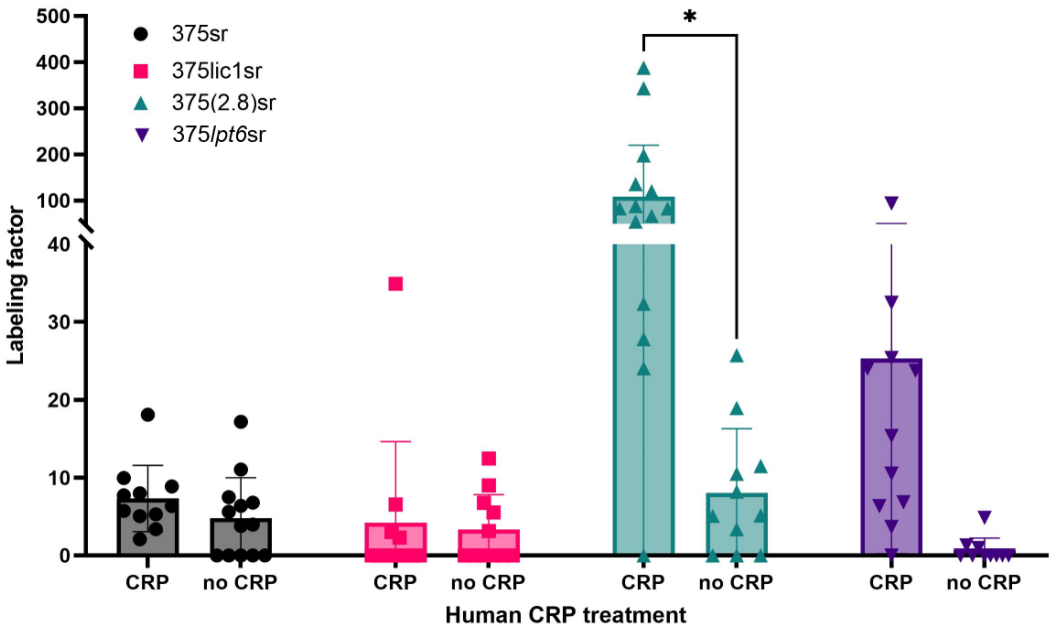
375sr
375lic1sr
375(2.8)sr
375lpt6sr
Labeling factor
500
400
300
200
100
40
30
20
10
0
*
CRP
no CRP
CRP
no CRP
CRP
no CRP
CRP
no CRP
Human CRP treatment

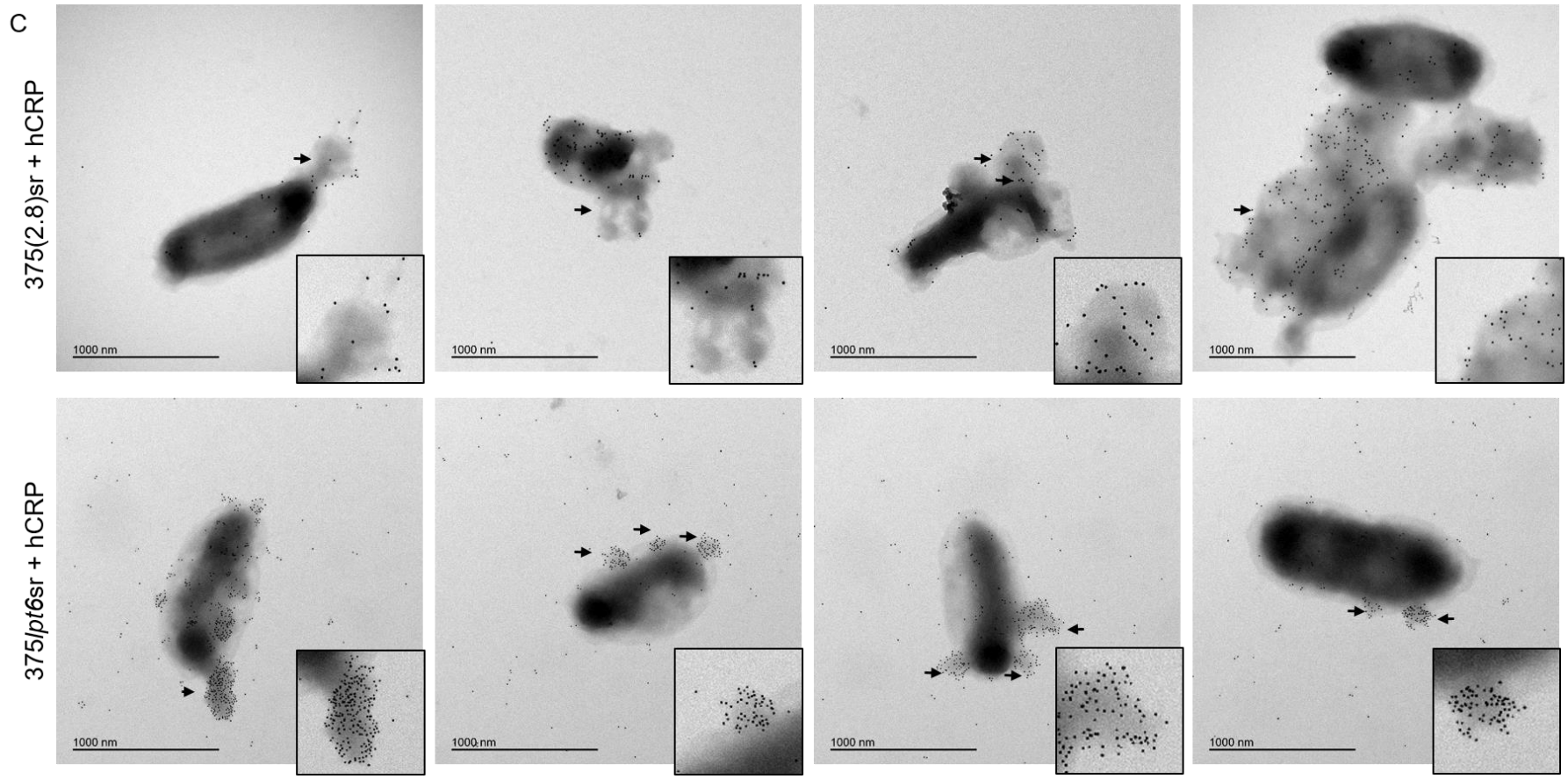

Figure 3.6. Immunogold labelling of NTHi 375 strains. (A) Immunogold electron microscopy images representing CRP particles on NTHi 375 strains. NTHi only are control bacteria not treated with hCRP. Any gold particles observed on these images are due to background noise due to non-specific hCRP antibody binding (B) Labelling factor of NTHi 375 strains. Labelling factor is the percentage of this labelling that is on the NTHi surface. It takes into consideration any background signal from non-specific binding by hCRP antibody. (C) Immunogold electron microscopy images showing blebbing of NTHi 375(2.8)sr and 375/*pt6*sr bacteria. hCRP binding was more pronounced on these structures. Electron microscopy image in box for each image zoomed in 3X. This experiment was repeated 4 times and approximately 20 images were taken per strain.

3.2.7. Identifying alternative CRP ligands on the NTHi bacterial surface

The ELISA and immunogold staining data confirm that CRP binds preferentially to particular PCho positions. Further, PEtn influences CRP interaction with NTHi. We have shown that rMoCRP behaves differently to hCRP and that rMoCRP binds NTHi 375*lic1*sr mutant bacteria more readily than 375sr and 375sr isogenic variants. However, it is evident from these combined data that PCho and PEtn are not the only targets on the NTHi bacteria for CRP binding, and that other ligands on the bacterial surface must exist. Therefore, we used co-immunoprecipitation (co-IP) to identify novel CRP binding targets on the NTHi surface.

We first aimed to look for any changes in the LPS signature on whole NTHi bacteria. PAGE- and silver staining confirmed NTHi 375 strains had some differences in their LPS patterns (figure 3.7A). Western blot with monoclonal antibody, TEPC-15 was used to confirm PCho expression, however, only NTHi strain 375(2.8)sr produced a clear band for PCho expression in the LPS (figure 3.7B). Further investigations is required to detect PCho bands on other PCho expressing NTHi 375 strains. Next, a far western blot was carried out to identify any differences in the hCRP binding pattern to NTHi strains (figure 3.7C). Following western blotting of NTHi lysates, membranes were incubated with hCRP and any hCRP binding was detected using mouse anti-human CRP antibody. A 'hCRP only' control produced two bands with molecular weights of approximately 24 kDa and 100 kDa. All NTHi 375 strains produced bands at approximately 40 kDa. Finally, we attempted to identify the inferred novel CRP ligand using co-immunoprecipitation. Magnetic beads were coated with anti-human CRP antibody overnight prior to the assay. CRP was bound to NTHi bacteria using method similar to that in the ELISA and then incubated with the anti-human CRP antibody coated magnetic beads. Next, SDS-gel electrophoresis and western blotting were carried out, but these investigations did not produce any significant results. Numerous background bands from anti-human CRP antibody were observed on the SDS-PAGE (appendix figure 1).

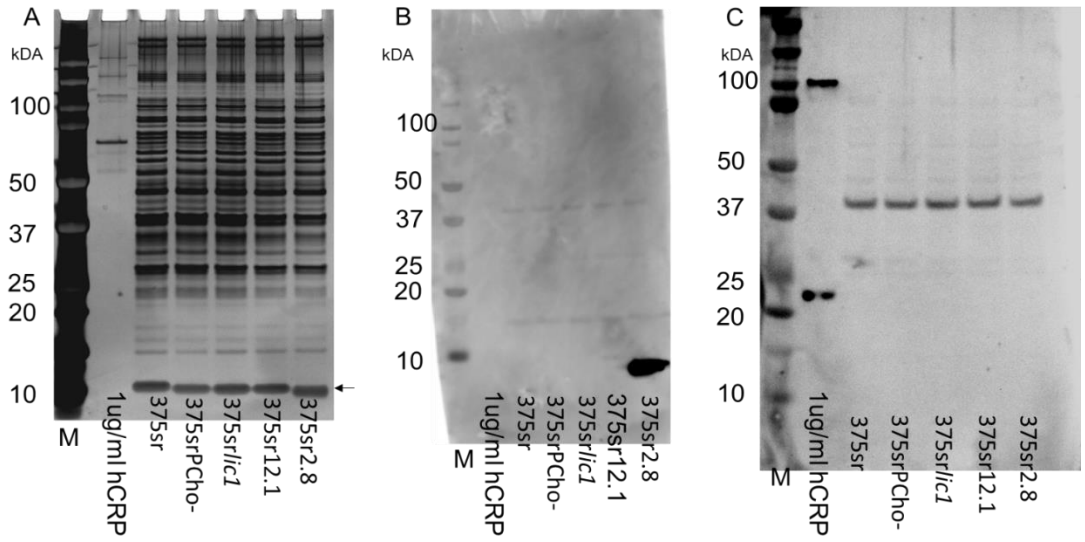

Figure 3.7. Binding of human CRP (hCRP) to NTHi 375 strains. (A) Silver stain 'LPS gel' confirming differences in LPS signature for NTHi 375 strains. (B) Confirming PCho expression using PCho specific antibody, TEPC15. (C) Far western blot. NTHi lysates were ran through gel electrophoresis using reduced conditions. CRP binding was visualized using Chemidoc (n=5).

3.3. Discussion

The aim of this section of the project was to develop a method to quantify CRP binding to different strains of NTHi with varying level of expression (presence or absence) and location of PCho on their LPS molecules. The central dogma in the literature is that CRP binds predominantly to PCho, though other binding targets are also known. Previous studies on NTHi and CRP have shown how the position of PCho on NTHi surface influences CRP binding (E. Lysenko *et al.*, 2000). Other NTHi strains have been used to explain how presence of PCho effects CRP binding/levels (Langereis, van der Pasch and de Jonge, 2019). In AOM, relevance of CRP in the presence of NTHi has also been studied (Principi *et al.*, 1986). However, it is not well understood how the position of PCho effects the fate of NTHi during host-pathogen interaction and disease. Previous studies performed on CRP and NTHi also do not quantify how levels of CRP vary for different PCho positions. Finally, CRP can also interaction and bind to other phosphorylated entities such as PEtn (Singh,

Suresh, Praythер, *et al.*, 2008). NTHi also express PEtn on their surface, but hCRP has a higher binding affinity for PCho (Gang *et al.*, 2012). However, there are no quantitative data on how the two phosphorylated entities influence each other's interaction with CRP.

We successfully developed an in-direct ELISA based binding assay which was used to study CRP binding on multiple NTHi strains at the same time. All assays were carried out in a 96 well ELISA plates, but have the capacity to be made more high-throughput and can be automated. The assay requirements are: (i) NTHi strains (can be optimised for other bacterial strains), (ii) purified CRP (can be from any animal species, and purified from serum or from a recombinant source), (iii) primary and secondary antibodies against CRP, (iii) TMB or other substrate (depending on the secondary antibody conjugate) for assay development and (iv) ELISA plate reader (photometer) and a computer with an evaluation software.

We showed that both human and rMoCRP can bind NTHi. We observed some difference in binding by the two proteins for example, rMoCRP binds to *lic1* mutant (NTHi 375*lic1*sr) as well as PCho expressing NTHi 375 strains, whereas hCRP does not. The reason for this is unclear and further experiments are needed to investigate this. The fact that rMoCRP exists as an oligomer may affect the binding ability of the protein; however, this needs to be further investigated. Using predictive modelling, we compared hCRP and rMoCRP PCho binding sites and showed a single amino acid change. The amino acid Thr^{76} in hCRP changed to gly in the rMoCRP. This is preliminary predictive modelling and expert guidance is required to confirm these observations.

The position of PCho on the NTHi surface is fundamental in permitting CRP binding (E. Lysenko *et al.*, 2000). We have confirmed PCho off heptose III binds 59 to 67% more human CRP than PCho off heptose I. These findings were further confirmed by immunogold labelling procedures. PCho is a terminal structure added to surface-exposed hexose residues on NTHi LPS. PCho off heptose III may permit better access for CRP binding than PCho off heptose I. In addition to position, number of PCho can also influence CRP binding

to NTHi. Presence of PCho increased CRP binding for NTHi 176sr. These data are consistent with published data (Fox *et al.*, 2008). CRP binding to NTHi could be influenced by PCho expression levels. We showed that NTHi 375 strains may have varying levels of PCho expression through immunobloting, for example, PCho might be more extensive on HepIII on the NTHi surface compared to PCho off heptose I and heptose II (figure 3.3D). However, structural analysis and sequencing of NTHi 375 variants by previous members of the lab have confirmed that all the NTHi 375 variants were similar in their 5'-CAAT repeat units that was permissive for the expression of PCho from the same initiation code. Future work should investigate why differences in immunoblot staining is observed even if the NTHi variants are structurally similar. Work should look at investigating if there is differences in accessibility to antibody when PCho is expressed off different heptose molecules on the NTHi surface. Further, future work should investigate if PCho accessibility influence CRP binding and NTHi clearance.

As well as PCho, CRP binding to other LPS structures is known, for example PEtn, galactosyl residues and polycations (Siegel *et al.*, 1975; Volanakis and Wirtz, 1979; Singh, Suresh, Praythe r, *et al.*, 2008; Gang *et al.*, 2012). We showed that presence of PEtn can influence CRP binding to NTHi. We used NTHi 375 strains with mutated *lpt* genes (*lpt3* or *lpt6*) that removed PEtn off ether heptose II (*lpt6*) and heptose III (*lpt3*). Absence of PEtn off heptose II increased hCRP binding to 375sr compared to wild-type NTHi 375sr, which had very little binding to human CRP. PEtn off heptose II may hinder CRP binding to PCho off heptose I. However, more in-depth structural analysis is needed to confirm the exact role of PEtn off heptose II on CRP binding to NTHi 375sr. Furthermore, the presence of other epitopes on the NTHi LPS and their effect on CRP binding should be investigated, for example galactose. Mutations in *lic2A*, a glycosyltransferase that adds galactose of α-Gal-(1-4)-β-Gal epitope to glucose on the LPS, enhanced CRP binding (Langereis *et al.*, 2019).

Immunogold labelling confirmed the ELISA binding assay findings. We did not observe any clustered CRP molecules on the NTHi surface, suggesting that PCho is expressed

generally all over the NTHi surface. We did however; observe more hCRP binding to NTHi cell membrane blebs. These blebs could be outer membrane vesicles, which are commonly produced by Gram-negative bacteria (Schwechheimer and Kuehn, 2015). More hCRP was observed on blebs from NTHi 375(2.8)sr than other NTHi 375 strains. It is unclear if more hCRP to NTHi 375(2.8)sr leads to the formation of these blebs, therefore, more work is needed to investigate this further.

We attempted to identify additional binding epitopes for CRP through co-immunoprecipitation experiments and far western blotting. Far western blotting showed human CRP binding to a molecular weighing approximately 40 kDa. These could be non-specific bands, which may have arisen due to the denaturing gel electrophoresis used for the experiment. Denatured proteins or proteins presented in non-native conformations may interact in artificial manner, leading to false positive interactions observed. Electrophoresis under native conditions, *i.e*. non-denaturing and without reducing agent could be used in the future to reduce non-specific bands. Duration of blocking step and concentration of CRP and anti-CRP antibody could also be further optimised in the future to reduce non-specific bands. Furthermore, appropriate protein controls should also be included in the future experiments to distinguish true interactions from non-specific artefacts. The LPS molecule weigh less than 10 kDa. Silver staining confirmed some variabilities in LPS signatures between NTHi strains, however, despite this, no hCRP binding was observed for these bands, even for the NTHi 375 strains that bound human CRP by ELISA. This could again be due to limitations of the assay where the samples are separated in a SDS gel under denaturing conditions. Denaturation profile of NTHi could be different for different NTHi strains, which could influence the LPS signature on obtained on the gels. Denatured NTHi could also influence interaction with CRP. Furthermore, denaturing of the sample (NTHi) leads to potential conformational changes, therefore affecting the binding affinity of the target to the bait protein. Denaturing conditions may hide the PCho binding site or make it less accessible to CRP, which could lead to failure of detection of interaction.

3.4. Future work

We confirm the presence and position of PCho on NTHi surface influences CRP binding. Furthermore, the presence of PEtn can influence CRP binding to the NTHi surface. Future work could use other range of wild-type and variant and mutant strains to confirm that CRP binding is influenced by PCho presence and position on the NTHi surface. In addition to this, further experiments should aim investigate the how the amount of CRP binding to PCho on the NTHi is influenced by other epitopes on the NTHi surface. For this, NTHi mutants for other epitopes such as galactose can be used. Binding inhibitors such as free PCho or PEtn can be used to investigate CRP binding affinity for PCho on the NTHi surface.

The co-immunoprecipitation assay did not identify any novel CRP binding molecule and due to time limitations, the assay could not be adjusted or optimised. Magnetic beads were conjugated with mouse anti-human CRP primary antibody prior to incubation with NTHi-bound CRP. However, there was a lot of false positive signal from the mouse anti-human CRP primary antibody; further testing of the assay would require optimisation of the antibody conjugation. Once the assay is optimised, novel CRP binding sites on the NTHi surface can be studied using mass spectrometry.

Chapter 4. Investigating how PCho presence and position on NTHi surface affects serum bactericidal activity

4.1. Introduction

CRP activates the classical complement pathway once bound to PCho (chapter 1, section 1.1.10.1). To investigate the role of PCho presence and position on the bacterial surface in complement-mediated killing, we used serum bactericidal assay (SBA). SBA measures the ability of antibodies or pentraxins, including CRP, to lyse bacteria in the presence of complement proteins.

As NTHi is a commensal and a pathogen in the human, we first used normal human serum (NHS) to study the influence of PCho presence and position on NTHi in sensitivity to serum mediated killing. To study the effect of serum sample from an OM inflammation, we used the *Junbo* mouse serum from day 1 post inoculation with NTHi. We used the mouse because we did not have access to OM patient serum samples. The mouse is a commonly used model for disease. We will discuss the use of the *Junbo* mouse its relevance as a model in studying CRP-NTHi interaction in AOM in chapter 6. *In vitro*, the mouse serum complement lacks activity that supports the formation of membrane attack complex (MAC) formation (Rowley and Wardlaw, 1958). Therefore, baby rabbit serum was used as an external complement source (Ercoli *et al.*, 2015) in our SBAs.

4.2. Results

4.2.1 Investigating the how PCho presence and position on NTHi surface affects bacterial survival using normal human serum

We used NTHi 375 strains (chapter 2, table 2.1) to investigate the influence of PCho presence and position on NTHi surface in serum mediated killing using NHS. We used NTHi 375 strains because PCho was the only variable that was altered on the NTHi surface (figure 4.1A). Therefore, the data obtained from the experiment was predominately a consequence of PCho alterations on the NTHi LPS.

Figure 4.1B shows that presence and position of PCho on NTHi LPS surface influenced serum bactericidal activity. A range of bacterial killing was noted; NHS killed all NTHi 375 strains, thus validating the SBA. NTHi strains 375sr and 375(7B.1)sr that express PCho off heptose I, were the most resistant strain in the SBA. NTHi 375(2.8)sr, which expresses PCho off heptose III, was the most sensitive strain in SBA. NHS concentration of 0.5% was enough to kill more than 50% of NTHi 375(2.8)sr whereas 5% NHS was needed to cause more than 50% killing of NTHi 375sr. These data suggested that position of PCho on the NTHi surface influences NTHi 375 killing in the SBA.

To investigate the role of CRP in serum bactericidal killing, CRP-depleted pooled NHS was used (unpublished, Cody *et al*.,) (figure 4.1B). The level of CRP in the pooled NHS was 1.23 mg/L, which is considered to be within the normal range in healthy adults. CRP was depleted from the pooled NHS using PCho-agarose beads. Following CRP depletion, CRP concentration in the pooled NHS was <0.12 mg/L. SBS using CRP-depleted NHS was compared with equivalent CRP-containing NHS. Pooled NHS shows similar killing to commercially available NHS, thus confirming that NHS from different sources can yield similar results. CRP-depleted NHS did not have a significant effect on NTHi 375sr and 375(7B.1)sr, which have PCho off heptose I on their surface. NTHi 375(2.8)sr was the most sensitive strain to killing by SBA with NHS. However, after treatment with CRP-depleted

NHS, NTHi 375(2.8)sr was as resistant to serum bactericidal killing as NTHi 375sr (figure 4.1B). This suggests that PCho off heptose III makes NTHi 375 more sensitive to bactericidal killing in SBA and this killing was most probably associated with CRP.

NTHi 375(12.1)sr was also one of the most sensitive strains in the SBA. After treatment with CRP-depleted NHS, its sensitivity to killing decreased. This strain cannot express PCho on its surface as there is no hexose off heptose II to permit the PCho linkage. Therefore, another moiety on the NTHi 375 surface could be influencing the serum bactericidal killing for this strain. However, further investigation is needed to confirm this hypothesis.

SBA using NHS showed that PCho position influences bacterial killing and that CRP in the serum can contribute significantly to serum mediated killing.

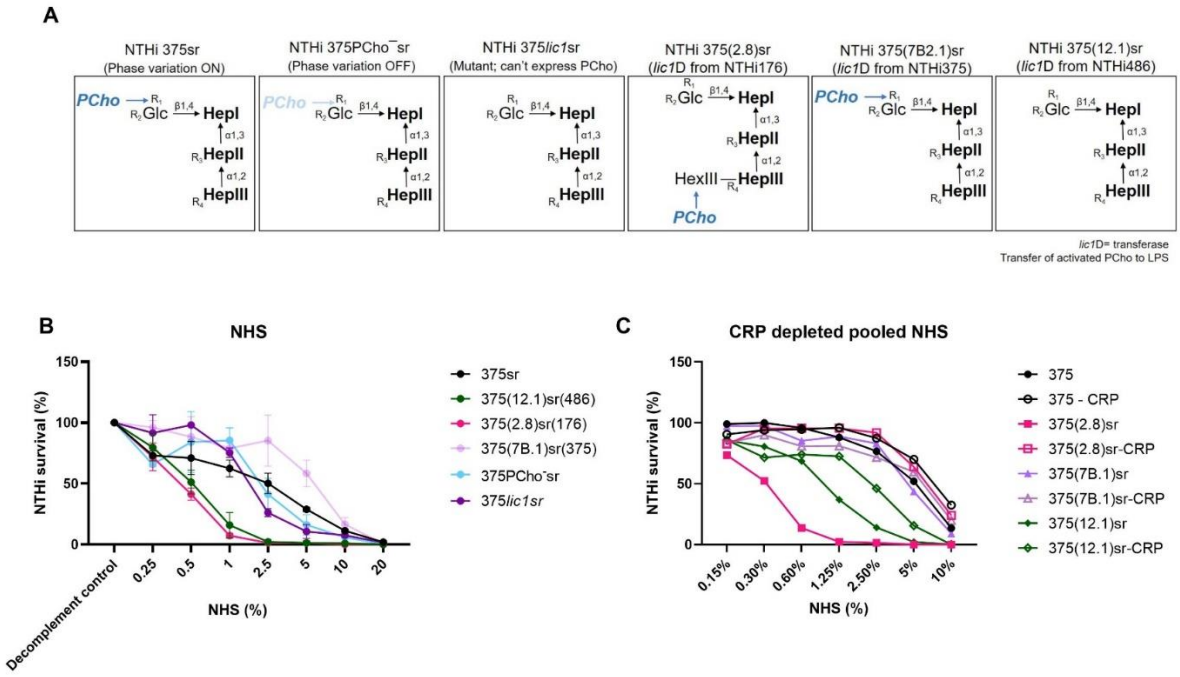

Figure 4.1. Serum bactericidal activity using normal human serum and 375 strains. (A) Schematic of PCho positions from LPS on NTHi 375 strains. (B) SBA using commercial normal human serum (NHS) against NTHi 375 strains (n=3). (C) SBA using CRP depleted and non-depleted pooled serum from healthy adults (unpublished, Cody *et al*.,). Unfilled boxes represent NHS that has CRP depleted and filled boxes are NHS with CRP.

4.2.2. Comparing SBA activity using NHS, NHS with spiked purified human CRP and day 1 NTHi 375sr inoculated Junbo mouse serum

During inflammation, CRP concentration in serum can increase to 500 mg/l (0.5 mg/ml) (Pepys and Hirschfield, 2003). As the NHS used in the SBA was from pooled healthy humans, where serum CRP concentrations are low (reported serum CRP in NHS is approximately 0.8 mg/l), we investigated the effect of adding more CRP to the SBA. We did this to understand how elevated CRP influences the serum bactericidal activity. To do this, we added two concentrations of purified hCRP into NHS: 0.1 mg/ml (100 mg/l) and 0.5 mg/ml (500 mg/l).

Figure 4.2 shows preliminary data on the effect of NTHi 375sr killing when NHS was spiked with purified hCRP. Compared to NHS only, both concentrations of purified hCRP reduced bacterial killing. This suggests that the addition of purified hCRP in NHS does not kill NTHi 375. This could potentially be due to the experiment design (discussed further in section 4.3).

As we did not have serum from AOM patients, we used serum from *Junbo* mice inoculated with NTHi 375sr to compare if sera sample from OM influences NTHi killing in the SBA. The average CRP concentration in the pooled *Junbo* mouse serum used was 88.8 ng/ml (0.09 x 10^{-3} mg/ml). Pooled serum from *Junbo* mice was collected day 1 post inoculation with NTHi 375sr. Baby rabbit serum (BRS) was used to provide complement source in the SBA using pooled mouse sera. Francis Anderson kindly provided the optimum concentration of baby rabbit serum to use for each NTHi strain.

Serum from OM patients may influence serum mediated killing of bacteria. CRP levels in the *Junbo* mouse rises during early infection, similar to human CRP (chapter 6, figure 6.1E). Therefore, we hypothesised that using serum from *Junbo* mouse could have a similar effect to serum from human with inflammation. Pooled mouse sera had higher NTHi killing than NHS spiked with hCRP (figure 4.2). However, pooled *Junbo* mouse serum and NHS had

similar NTHi killing activity in the SBA (one-way *ANOVA p = 0.0737*). This suggests that serum from day 1 inoculation with NTHi 375sr does not improve serum mediated killing for NTHi 375sr.

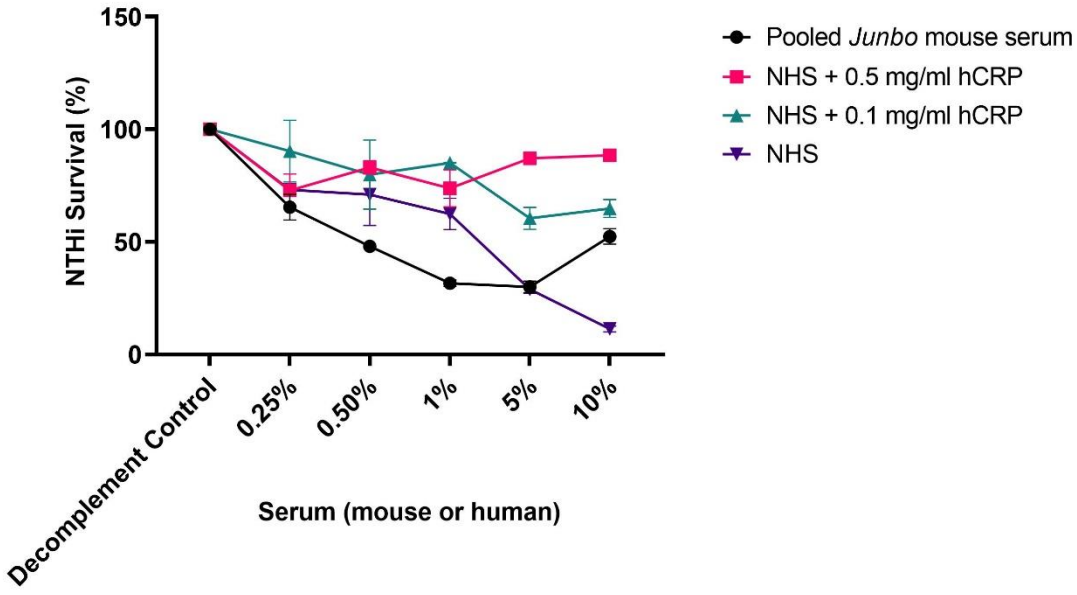

Figure 4.2. Serum bactericidal assay on NTHi 375sr using pooled *Junbo* mouse serum or NHS spiked with human CRP. Pooled *Junbo* mouse serum from day 1-inoculation with NTHi 375sr. Baby rabbit serum was used as an external source of complement component for the SBA. NHS was spiked with one of two concentrations of purified human CRP: 0.1 mg/ml and 0.5 mg/ml (n=2).

4.2.3. Investigating the role of PCho presence and position on serum bactericidal activity using Junbo mouse serum from NTHi inoculations

The *Junbo* mouse serum from day 1 post-NTHi inoculation killed NTHi 375sr similar to NHS (section 4.2.2). However, the presence and position of PCho on the NTHi surface also influences serum bactericidal activity (section 4.2.1). Therefore, we tested the pooled *Junbo* mouse serum against NTHi strains. We used NTHi 375sr, 375*lic1*sr and 375(2.8)sr to investigate the role of PCho presence and position on SBA activity using pooled *Junbo* mouse serum. In addition to this, pooled *Junbo* mouse serum following day 1 post-inoculation with NTHi 375*lic1*sr and 375(2.8)sr was also used. This was to determine how serum from different NTHi strain infections affects bactericidal killing. Pooled non-inoculated (NI) *Junbo* mouse serum had 153 ng/ml (0.15 x 10^{-3} mg/ml) CRP. NI *Junbo* mouse have OM but were not infected with NTHi. Pooled *Junbo* mouse serum from 1 day post-inoculation with NTHi 375sr had 88 ng/ml (0.09 x 10^{-3} mg/ml) CRP. Pooled *Junbo* mouse serum from post 1-day inoculation with NTHi 375*lic1*sr and 375(2.8)sr had 324 ng/ml (0.32 x 10^{-3} mg/ml) and 124 ng/ml (0.12 x 10^{-3} mg/ml) CRP respectively.

Figure 4.3 shows the preliminary SBA data for NTHi 375 strains using sera from different NTHi 375 inoculations in the *Junbo* mouse. All of the *Junbo* mouse sera tested (NI and NTHi inoculated) killed NTHi 375 strains. This confirm that the assay is valid to measure NTHi killing using serum from *Junbo* mice (figure 4.3).

NTHi 375sr was the most resistant to killing by NI serum from the *Junbo* mouse (figure 4.3A). Serum from NTHi 375(2.8)sr day 1 post-inoculation had the greatest killing for NTHi 375sr. Serum from NTHi 375sr and 375*lic1*sr had similar killing for NTHi 375sr. These data were not statistically significant (*one-way ANOVA p = 0.1*). NTHi 375*lic1*sr had similar bacterial killing for all the sera from the *Junbo* mouse (figure 4.3B). The data were not statistically significant (*one-way ANOVA p = 0.6*). The lowest amount of killing for NTHi 375(2.8)sr was measured using *Junbo* mouse serum from day 1 post-inoculation with NTHi

375(2.8)sr (figure 4.3C). *Junbo* mouse serum from the other NTHi inoculations (NTHi 375sr and 375*lic1*sr) and NI mice has similar serum bactericidal activity to each other. However, these data were not statistically significant (*one-way ANOVA p = 0.6*).

These data show that sera from different NTHi inoculations may influence serum mediated killing of NTHi 375 strains, but requires further optimisations to confirm this.

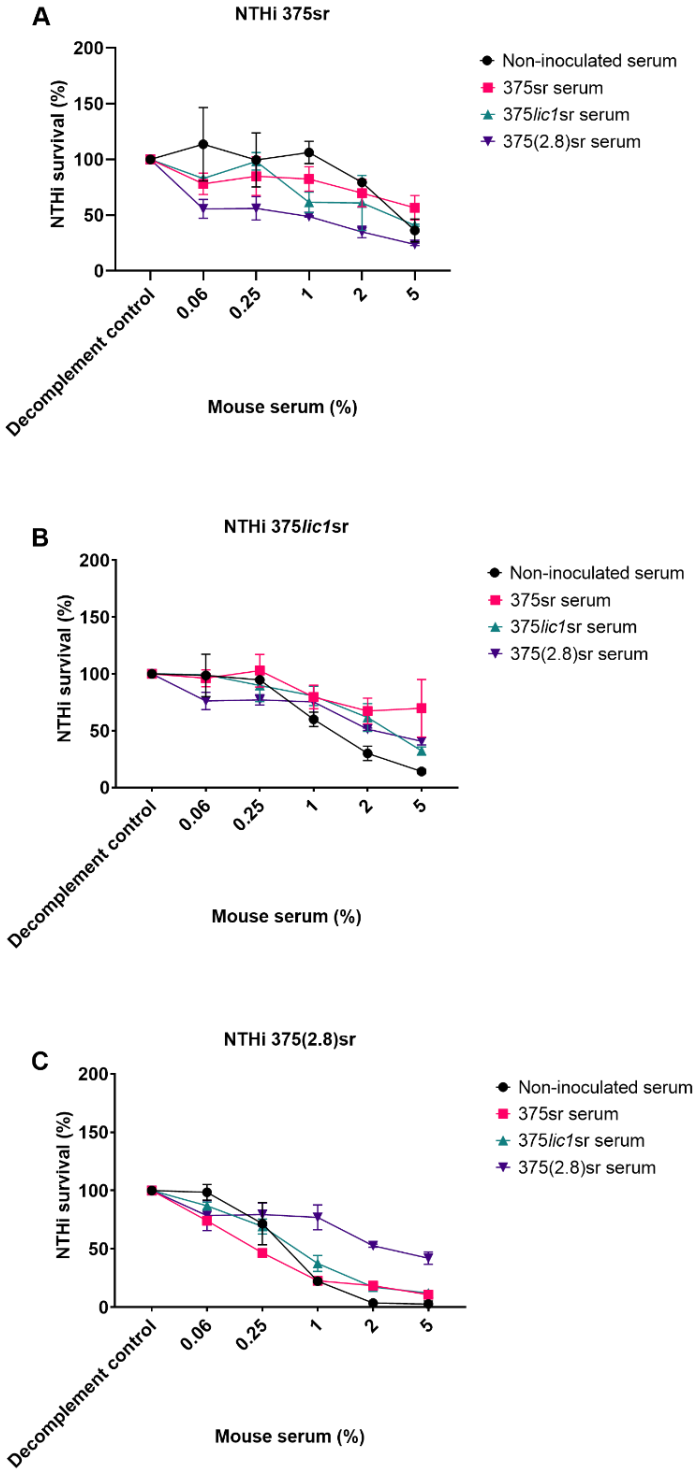

Figure 4.3. SBA on NTHi 375 strains using pooled *Junbo* mouse serum from day 1 post-inoculation with NTHi 375 strains. SBA was performed using 2% baby rabbit serum. (A) SBA of NTHi 375sr using serum from day 1 post-inoculation with NTHi 375 strains *Junbo* mouse (n=2). O*ne-way ANOVA p = 0.0957.* (B) SBA of NTHi 375*lic1*sr using serum from day 1 post-inoculation with NTHi 375 strains *Junbo* mouse (n=2). O*ne-way ANOVA p = 0.5942.* (C) SBA of NTHi 375(2.8)sr using serum from day 1 post-inoculation with NTHi 375 strains *Junbo* mouse (n=2). *One-way ANOVA p = 0.6122.*

4.2.4. Measuring C1q and C5a in serum from Junbo mouse inoculated with NTHi 375 strains

The SBA data thus far show that the presence and position of PCho on the NTHi surface influences serum bactericidal activity. Preliminary data using *Junbo* serum from day 1 post-inoculation with NTHi 375 strains showed some differences in bacterial survival in the SBA (section 4.2.3). NTHi 375sr was one of the most resistant strains in the SBA. NTHi 375sr treated *Junbo* serum from day 1 post-inoculation with NTHi 375(2.8)sr had higher killing than *Junbo* mouse serum from day 1 post-inoculation with NTHi 375sr. Therefore, we postulated if these differences could be driven by different concentrations of CRP and complement proteins in the *Junbo* mouse serum. We show that CRP levels increase in the *Junbo* mouse following NTHi infection (discussed further in chapter 6). We measured C1q protein in the serum from day 1 post-inoculations with NTHi 375sr, 375*lic1*sr or 375(2.8)sr (figure 4.4). CRP binds to C1q and activates the classical complement pathway. We also measured levels of C5a. C5 is a convertase produces C5a and C5b. C5a is a strong chemoattractant and is involved in recruiting inflammatory cells to the inflamed tissue (Guo and Ward, 2005).

The highest level of C1q was measured in the serum from the NTHi 375*lic1*sr inoculated *Junbo* mouse. NTHi 375sr inoculated serum had a 2-fold lower C1q concentration compared that from NTHi 375*lic1*sr (figure 4.4A). Serum levels of C1q was similar for day 1 post-inoculations with NTHi 375sr and 375(2.8)sr. The opposite trend for C5a was observed where serum from NTHi 375*lic1*sr had the 0.7-fold lower concentration than NTHi 375sr and 375(2.8)sr serum (figure 4.4B). CRP concentration followed the same observed trend as C5a (figure 4.4C). These data suggest that there are differences in CRP and immune complement proteins in the *Junbo* mouse serum from different inoculations with NTHi 375 strains. The differences in CRP, C5a and C1q could affect the SBA killing of NTHi

375 strains and could influence the results that we observed in section 4.2.3. However, further experiments are needed to confirm this.

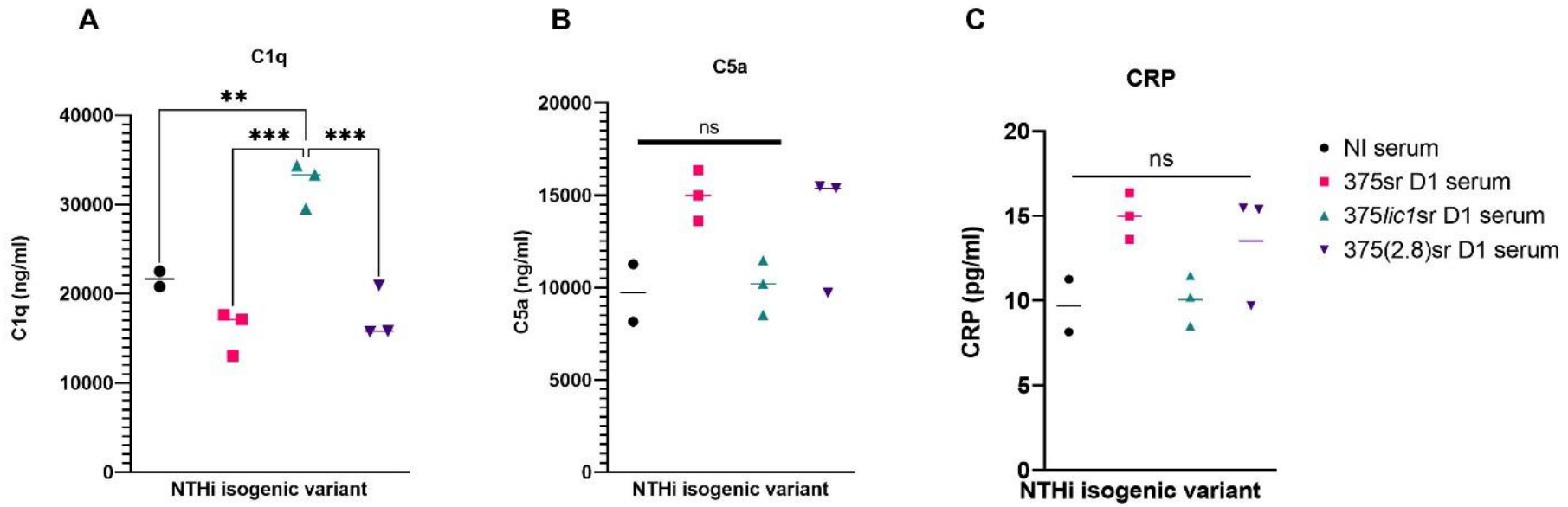

Figure 4.4. Measuring complement proteins in NTHi inoculated *Junbo* serum. (A) C1q (B) C5a (C) CRP. Sera from *Junbo* mice were inoculated with NTHi 375sr, 375*lic1*sr or 375(2.8)sr (n=3). Serum from the mice was collected day 1 post-NTHi inoculation. NI are non-inoculated *Junbo* mice that were not inoculated with NTHi. *One-way ANOVA* followed by Brown-Forsythe test. ** *p = 0.001* *** *p = 0.0001*

4.3. Discussion

SBA with NHS is a well-characterised assay for NTHI changes in LPS structure known to alter NTHi killing (Ercoli *et al.*, 2015). Expression of PCho on NTHi surface can effect serum mediated killing (Weiser and Pan, 1998). Furthermore, position of PCho on the NTHI effects binding and sensitivity to CRP mediated killing (E. Lysenko *et al.*, 2000). We investigated the role of PCho presence and position on serum bactericidal killing. We used serum from *Junbo* mice inoculated with NTHi 375 variants differing only in their PCho signature to investigate if differences in bacterial killing could be measured. We confirm PCho presence and position on the NTHi surface influences SBA. NTHi 375sr was killed the least in the SBA using NHS compared to NTHi 375*lic1*sr and 375(2.8)sr. NTHi 375(2.8)sr that expresses PCho off heptose III on its surface was the most sensitive. Removal of CRP from the NHS did not affect bacterial killing for NTHi 375sr, but made NTHi 375(2.8)sr as resistant to killing as NTHi 375sr. CRP activates the complement pathway and the depletion of CRP from NHS could affect complement activation. This could explain the lack of killing for NTHi 375sr and enhanced bacterial survival for NTHi 375(2.8)sr. Future work should investigate the role of CRP-depletion on complement activation. A control for mock CRP depletion without any PCho on the beads should be included in the future experiments.

During inflammation, acute phase proteins' including CRP are elevated which can promote killing or clearance of the inflammatory source or products. Levels of these proteins are not nearly as prominent in normal serum. We added purified hCRP to NHS to evaluate the effect of additional CRP on serum mediated killing. The addition of purified hCRP into NHS significantly reduced NTHi killing. This could be due to the assay design. The data suggest the addition of purified hCRP into SBA containing NHS may not work and requires further optimising. Future experiments can investigate if hCRP-bound NTHi has an effect in the SBA.

Serum from *Junbo* mice inoculated with NTHi 375sr had similar serum bactericidal activity against NTHi 375sr to NHS (figure 4.2) therefore suggesting *Junbo* mouse serum can also

lead to a range of NTHi killing and therefore could be used for future SBAs. Serum from *Junbo* mice (chapter 6), inoculated with NTHi 375 strains showed some variability in bactericidal activity against NTHi 375 strains. Future experiments are needed to optimise the assay and confirm these preliminary findings.

We observed differences in C1q and C5a levels in the different *Junbo* mouse sera. Serum from *Junbo* mice infected with NTHi 375*lic1*sr had more C1q, but reduced C5a and CRP levels. Whereas, NTHi 375sr and 375(2.8)sr infected *Junbo* mouse sera had lower C1q, but higher C5a and CRP levels. This could influence the serum mediated killing against different NTHi 375 strains we observed in our experiments. CRP and C5a have been positively correlated to each other in some infections such as COVID-19 (Prendecki *et al.*, 2020). However, further investigations are needed to confirm this. Serum resistance is crucial for NTHi to survive in the human host, and binding of complement proteins onto the NTHi surface could affect serum bactericidal activity. Future studies should investigate if CRP binds onto the surface of NTHi in SBA and if CRP-bound NTHi are more sensitive to serum-mediated killing. The accumulation of complement proteins in the surface of the NTHi should also be investigated. Other complement components such as C3 and MAC should also be studied. NTHi can avoid the consequence of classical complement activation by inhibiting the C3-convertase (chapter 1, figure 1.4), by binding to C4b binding protein to the surface (Riesbeck, 2020). This can contribute to serum resistance. Flow cytometry can be employed to study these questions (Ercoli *et al.*, 2015).

Similar As well as CRP, IgM in the serum from humans can influence complement mediated killing of NTHi (Langereis, van der Pasch and de Jonge, 2019). Both CRP and IgM can bind to PCho on bacterial surface. This can influence complement-mediated killing in the SBA. Future work should look at what antibodies are present in the serum used in the SBA and if these antibodies effect CRP-mediated SBA.

4.4. Limitations of the study and future experiments

The preliminary data suggest serum from different NTHi infections can have an effect on serum bactericidal activity. However, these experiments need more biological repeats to validate the results. NTHi is a human specific pathogen and does not naturally infect the mouse. Even though mouse and human CRP share similarities in their structure and binding PCho, their effect in the serum-mediated killing could be different from one another. Future work should look into investigating this.

PCho presence and position on the NTHI surface effects NTHi killing. However, the CRP-NTHi interaction in SBA is still unclear. Further work should look at rendering the activity of CRP from the NHS and mouse serum to study effect on NTHi killing.

Finally, other NTHi strains should be used to investigate if PCho presence and position on the NTHi surface effects serum bactericidal killing. This will require careful interpretation of the data because as well as there being differences in PCho position on these NTHi bacteria, other moieties of the bacterial surface could also influence bacterial killing. Therefore, these assays should also include their respective PCho mutants to compare how much of the bactericidal activity is due to changes in PCho on the NTHi surface.

Chapter 5. Role of PCho on NTHi surface on NTHi phagocytosis

5.1. Introduction

The multifaceted interplay between innate and adaptive immune mechanisms plays a role in host resistance against pathogens. Macrophages play a central role in innate immunity in the ME and have been shown to be a major cellular component in ME effusions from human (Lim *et al.*, 1979). NTHi have been shown to survive in macrophages, which could be important in bacterial persistence and recurrent infections. Viable, intracellular NTHi have been recovered from macrophages up to 72 hours after phagocytosis (Craig *et al.*, 2001). The role of PCho on NTHi surface and bacterial survival in macrophages is poorly understood. Therefore, we looked at the effect of PCho presence and position on NTHi surface in uptake and survival in macrophages. Macrophages are one of the key cells in AOM (Rao *et al.*, 2021). We used mouse bone marrow derived macrophages (BMDMs) as they have similar cell morphology, cell markers and cell functions as macrophage cells *in vivo*. The data obtained from using primary cells are more relevant and reflective of the *in vivo* environment.

5.2.1. Investigating uptake and survival of NTHi in BMDMs

To understand the role of PCho presence on NTHi surface and uptake into macrophages, we infected BMDMs with NTHi 375sr (PCho off heptose I) and 375*lic1*sr (PCho mutant). We infected the macrophages for 30 minutes. After killing extracellular NTHi using gentamicin, BMDMs were incubated for 24 hours to measure bacterial persistence. To study the effect of CRP as an opsonin, recombinant mouse CRP (rMoCRP)-bound NTHi were also used. We used rMoCRP because we used the *Junbo* mouse (chapter 6) to study the role of PCho on NTHi surface in infection and immune response. Purified mouse CRP is currently not commercially available. Therefore, we used recombinant protein. We

aligned the sequence of rMoCRP with native mouse CRP sequence using NCBI Basic Local Alignment Search Tool (BLAST) and they were similar, thus validating the use of recombinant protein for our investigations.

Initial observations on NTHi uptake were made using confocal microscopy (figure 5.1A). Large aggregates observed in BMDMs treated with NTHi 375*lic1*sr compared to NTHi 375sr. Larger aggregates were observed for NTHi 375sr pre-treated with rMoCRP compared to unbound NTHi 375sr. This suggests CRP may influence uptake of NTHi 375sr into BMDMs. Z-stacks of the images showed that the bacteria were internalised. To measure the bacterial survival in BMDMs before and after rMoCRP treatment, we also cultured the bacteria from the OPA onto BHI streptomycin plates (figure 5.1B). Addition of rMoCRP decreased bacterial titre for both NTHi 375sr and 375*lic1*sr, although these differences were not statistically significant. These are preliminary data suggest PCho presence and absence may influence uptake into macrophages. Once inside the macrophage, the PCho presence or absence may influence cellular response to NTHi, which could explain the variation in the NTHi aggregates observed in the confocal microscopy. However, it is worth noting that the absolute numbers of bacteria are not synonymous with CFU. If many bacteria are aggregated, they produce only a single CFU, even though there may be more bacteria present in absolute numbers than those in less aggregated clumps. The resolution of confocal microscopy could limit the size of aggregate/bacteria detection. Colony counts following uptake into macrophages show that both NTHi 375sr and 375*lic1*sr are internalised. NTHi 375sr may form smaller aggregates that were not visible at the magnification used. Finally, rMoCRP binding to NTHi did not affect NTHi uptake into BMDMs.

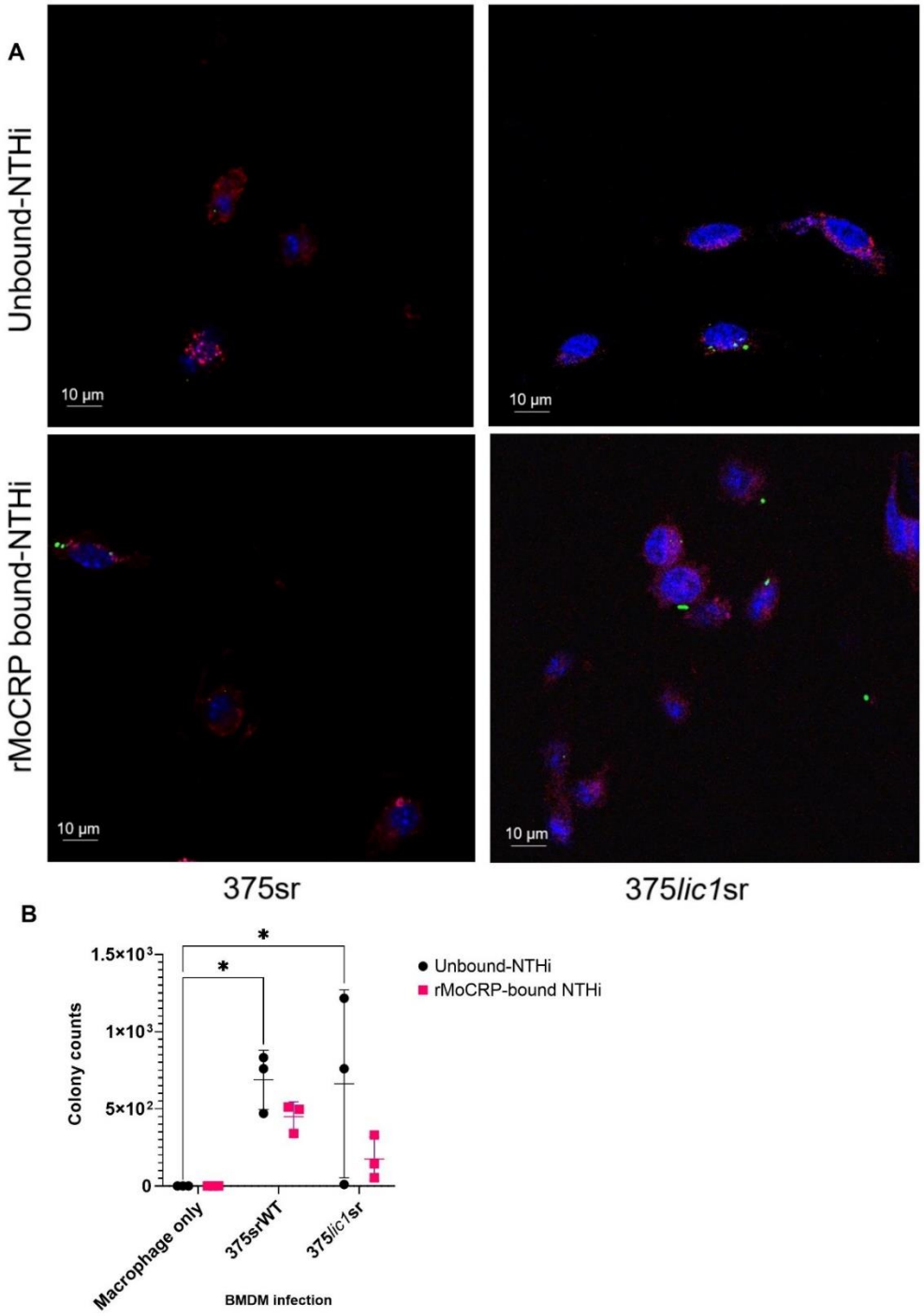

Figure 5.1. Uptake of NTHi into bone marrow derived macrophages and bacterial survival. (A) Confocal images of NTHi 375sr and 375*lic1*sr in bone marrow derived macrophages (BMDMs). Images are representative of n=10 images taken, n=2 biological replica. NTHi are in green, white arrow; labelled using PKH67 fluorescent cell linker kit that stains cell membranes. Nuclei in blue and macrophages are labelled using macrophage marker, F4/80 PE (red). (B) NTHi 375sr and 375*lic1*sr survival in BMDMs with and without bound-recombinant mouse CRP (rMoCRP). For CRP treatment, NTHi were incubated with 50 ng/ml rMoCRP for 30 minutes at room temperature before being added to BMDMs for 30 minutes (n=3). *Two-way ANOVA followed by SIdak's multiple comparisons test * p <0.05*

5.2.2. Investigating uptake of NTHi into BMDMs over 4-hours

PCho on the NTHi surface may influence uptake into BMDMs. Figure 5.2 shows uptake and survival of NTHi in BMDMs over 4-hour time period. Highest bacterial colony counts for NTHi 375sr were measured at 60-minutes, whereas for NTHi 375*lic1*sr, the highest bacterial colonies were measured at 20 minutes post-macrophage infection. After the 20-minute time period, we did not measure any colonies for NTHi 375*lic1*sr suggesting 375*lic1*sr were cleared by BMDMs. For NTHi 375sr, bacteria were present over the 4-hour time period. The highest NTHi 375sr colony counts were measured at 60-minutes and 210-minutes post BMDM infection. The uptake of NTHi by BMDMs is influenced by PCho expression on the NTHi surface. Our data suggests PCho expression on NTHi surface promotes uptake of bacteria into BMDMs.

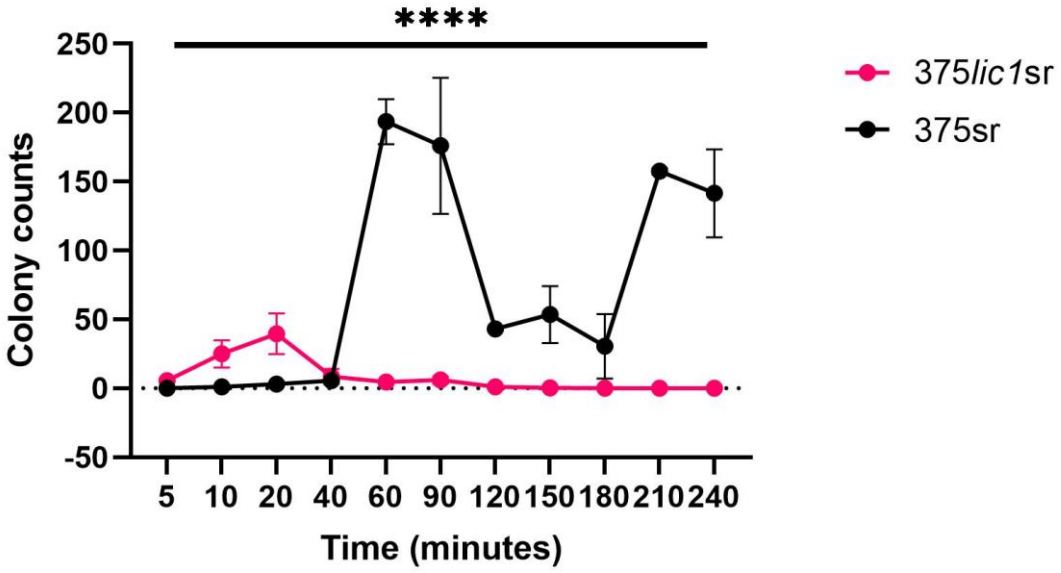

Figure 5.2. Uptake of NTHi in BMDMs over a 4-hour time-period. BMDMs were infected with NTHi 375sr and NTHi 375*lic1*sr over 4-hour time period (n=2). NTHi colony counts were obtained at each time point over the 4-hour time period. More NTHi 375sr colony counts were measured over the 4-hour time period compared to NTHi 375*lic1*sr. *Two way ANOVA **** p = <0.0001*

5.2.3. Investigating cytokine gene expression following uptake of NTHi by BMDMs

In section 5.2, we observed that PCho expression influences uptake into BMDMs. The uptake of NTHi into BMDMs may trigger macrophage activation and eventually lead to phagocytosis. PCho on the surface of NTHi may influence the macrophage activation and phenotype. This could aid in NTHi survival within the macrophages. Once macrophages are activated, they can polarise towards a spectrum of phenotypes, which includes two main subtypes: M1 (pro-inflammatory) and M2 (anti-inflammatory, pro-healing). The polarisation determines the macrophage cellular response.

Our OPA data so far suggests that the presence or absence of PCho on the NTHi surface affects uptake of NTHi into BMDMs. We included NTHi 375(2.8)sr to investigate if PCho position change on the NTHi surface affects NTHi uptake and macrophage response. We measured changes in the macrophage inflammatory gene expression using quantitative PCR (qPCR) to investigate if macrophage phenotype (M1 (pro-inflammatory) or M2 (anti-inflammatory)) may influence bacterial survival in BMDMs. For M1 macrophage response, we measured changes in iNOS, IL-12β, TNF-α, IL-1β, CD80, IL-6 and MHCII. For M2 macrophage response, we measured changes in CD206, TGF-β and IL-10. BMDMs were infected with NTHi 375 strains for 30 minutes. The BMDMs were then incubated to allow phagocytosis to take place. After 2-hour post NTHi infection, an increase in bacterial colony count was measured when BMDMs were infected with NTHi 375sr compared to infection with NTHi 375*lic1*sr and 375(2.8)sr (figure 5.3A). We studied the cytokine gene expression 45-minute and 2-hour post BMDM infection with NTHi 375 strains to investigate if PCho presence and position influences macrophage response and bacterial survival (figure 5.3B).

In section 5.2.2, we observed a decrease in bacterial colony count for NTHi 375 compared to earlier time-points for the same strain. Our gene expression analysis at 2-hour post BMDM infection with NTHi 375sr shows that the M1 gene expression markers, MHCII, iNOS, TNF-α, iNOS, IL-12β and CD80 were all elevated (figure 5.3). An increase in CD206,

TGF-β and IL-10 gene expression markers for M2 macrophage was also observed at the 2-hour time-point.

For NTHi 375*lic1*sr, M1 gene expression markers, iNOS, TNF-α, iNOS, IL-12β and CD80 were elevated 2-hours post NTHi infection, similar to NTHi 375sr. The level of TNF-α gene expression was higher in BMDMs treated with NTHi 375*lic1*sr than 375sr. This suggests NTHi 375*lic1*sr elicits more M1-like macrophage response than PCho expressing, NTHi 375sr.

For NTHi 375(2.8)sr, like NTHi 375sr, iNOS, TNF-α, iNOS, IL-12β and CD80 gene expression levels were elevated. However, unlike NTHi 375sr the M2 markers TGF-β and CD206 were downregulated 2-hours post BMDM infection with NTHi 375(2.8)sr. IL-10 gene expression was sustained between the 45 minute and 2-hour time-points. This suggests PCho off heptose III on the NTHi surface predominantly promotes a M1 macrophage phenotype.

The absence or presence and position of PCho on the NTHi surface influences the macrophage response. All three NTHi 375 strains elicited both M1 and M2 macrophage gene expression.

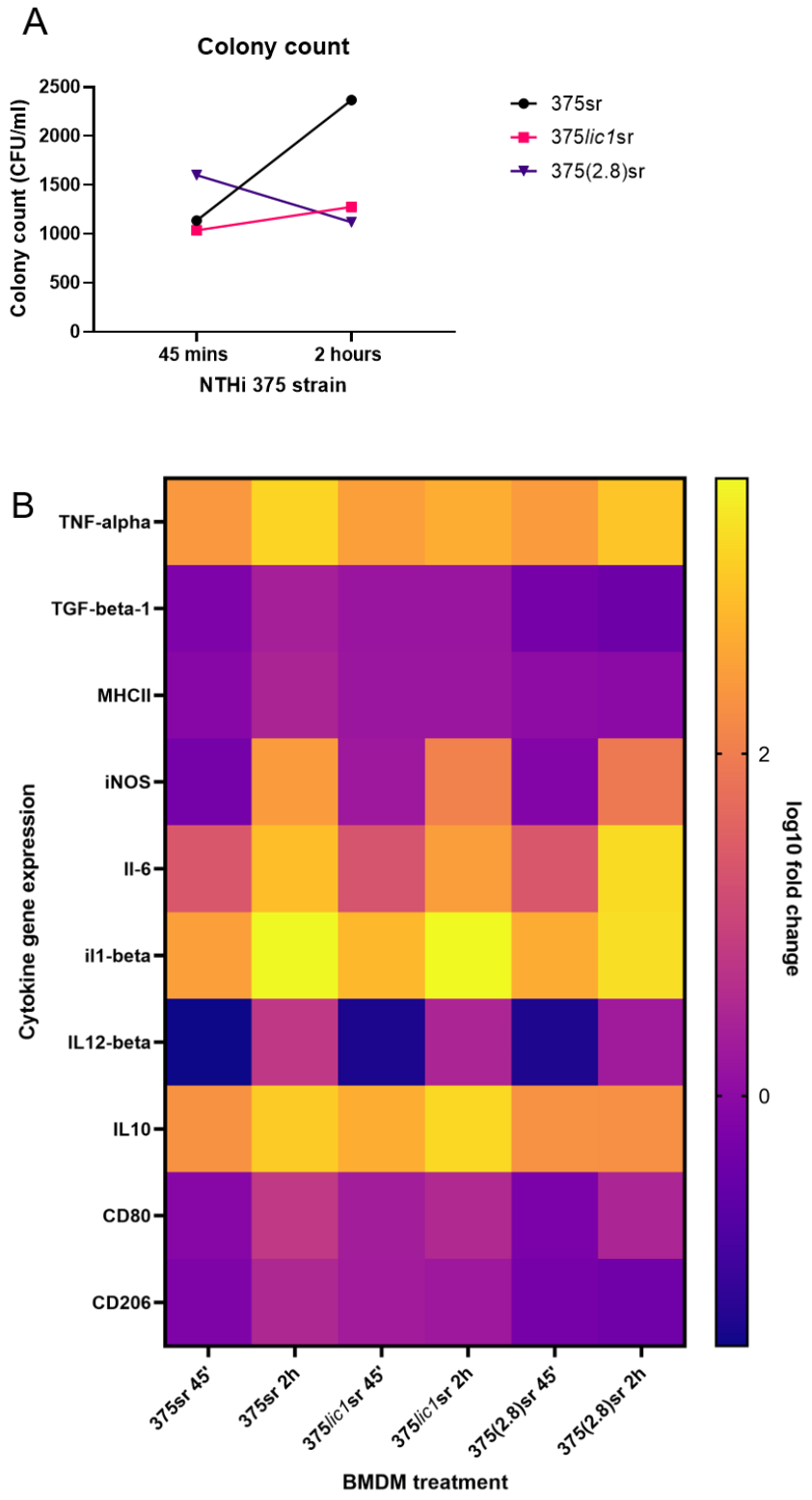

Figure 5.3. Cytokine gene expression following uptake of NTHi 375 strains into BMDMs. (A) Bacterial colony counts post 45-minute and 2-hour BMDM infection. (B) Heat hap of gene expression changes following 45 minute and 2 hour BMDM infection (n=2). BMDMs were treated with NTHi 375sr, 375*lic1*sr and 375(2.8)sr for 30 minutes. Following this, extracellular NTHi was killed using gentamicin and the cells were incubated for further 45 minutes and 2 hours in fresh BMDM media (n=2).

5.2.4. Initial investigation using serum from NTHi inoculated Junbo mice influences macrophage response to NTHi

In vivo, the host milieu following NTHi infection is much more complex than our *in vitro* OPA. Therefore, we investigated the effect of adding serum to the BMDMs infected with NTHi. As we did not have access to AOM patient serum samples, we used serum from the *Junbo* mouse infected with NTHi (chapter 6). The same pooled serum used in chapter 4, section 4.2.3 was used in the OPA. This was carried out to understand how the PCho presence or absence and position on the NTHi surface influences macrophage gene expression in the presence of serum. BMDMs were infected with NTHi for 1 hour and any extracellular NTHi was killed using gentamicin. We then studied the macrophage gene expression analysis post 1-hour BMDM infection with NTHi 375 strains (figure 5.4). We chose to study 1-hour post infection because the highest NTHi 375sr colony counts were measured at this time point in section 5.2.2. We compared NTHi 375sr BMDM infection with NTHi 375*lic1*sr and 375(2.8)sr BMDM infection.

After 1-hour uptake of NTHi 375 strain into BMDMs, differences in macrophage gene expression were observed. NTHi 375*lic1*sr had lower gene expression levels of M1 macrophage genes IL-1β, TNF-α, IL-6 and iNOS (for which we did not observe any gene expression) (figure 5.4A and 5.4C). However, M1 macrophage gene, MHCII was 5.8 times higher than NTHi 375sr. Macrophages use MHCII to present processed antigens to CD4+ T cells. This shows that absence of PCho on the NTHi surface influences the macrophage response to process and present NTHi antigens on its MHCII. IL-10 gene expression in BMDMs treated with NTHi 375*lic1*sr was 10 times higher than BMDMs treated with NTHi 375sr. MYD88, a major adaptor molecule for all toll-like receptors (TLRs), except TLR3, was 12 times more highly expressed in BMDMs infected with NTHi 375*lic1*sr than NTHi 375sr. This suggests that NTHi 375*lic1*sr may interact with macrophages differently to NTHi 375sr, which could be influenced by the presence or absence of PCho on the NTHi surface.

BMDM infection with NTHi 375(2.8)sr had a similar effect on the macrophage gene expression as NTHi 375*lic1*sr. Compared to infection of BMDMs with NTHi 375sr, infection with NTHi 375(2.8)sr caused an increase in IL-10, MHCII and MYD88 gene expression levels (figure 5.4E). This suggests that PCho off heptose III on NTHi surface may induce a similar macrophage gene response as NTHi 375*lic1*sr.

The presence of serum immune proteins and components could influence the clearance of bacteria by macrophages. To test this, we added serum from day 1 post NTHi infection of *Junbo* mouse (chapter 6) to the OPA. We observed a decrease in M1 macrophage genes IL-1β, TNF-α, IL-6 and iNOS when 375sr D1 serum was added to BMDMs infected with NTHi 375sr compared to BMDMs infected with NTHi 375sr alone (figure 5.4A and 5.4B). IL-10 gene expression level 3.2 fold elevated with 375sr D1 serum was added to BMDMs infected with NTHi 375sr compared to BMDMs infected with NTHi 375sr alone. MHCII was also 1.4 fold increased after 375sr D1 serum was added to BMDMs infected with NTHi 375sr compared to BMDMs infected with NTHi 375sr alone. This suggests that the addition of 375sr D1 serum influences macrophage response to NTHi.

The presence and position of PCho on the NTHi surface influences bacterial uptake and survival (section 5.2.2 and 5.2.3). In chapter 6, we discuss how presence and position of PCho on the NTHi surface influences the host immune response. We used the serum from *Junbo* mice infected with NTHi 375sr or 375(2.8)sr to investigate if *Junbo* mouse sera from different NTHi infections can influence the macrophage response in the OPA. BMDMs infected with NTHi 375*lic1*sr with 375sr D1 serum (figure 5.4D) had similar macrophage gene expression levels as BMDMs infected with NTHi 375*lic1*sr only (figure 5.4C). This suggests that the *Junbo* serum from day 1 post-inoculation with NTHi 375sr does not influence the OPA for BMDMs infected with NTHi 375*lic1*sr. A similar observation was observed for BMDMs infected with NTHi 375(2.8)sr (figure 5.4D) and NTHi 375(2.8)sr+375sr D1 serum (figure 5.4F), with the exception of iNOS. Levels of iNOS were undetectable in BMDMs infected with NTHi 375(2.8)sr+375sr D1 serum compared to

BMDMs infected with NTHi 375(2.8)sr alone. iNOS is a M1 macrophage cytokine. This suggests *Junbo* mouse serum from day 1 post-inoculation with NTHi 375sr influences M1 gene expression levels in the BMDMs. To investigate if the change in macrophage response to NTHi 375(2.8)sr is due to *Junbo* mouse serum from day 1 post-inoculation with NTHi 375sr, we compared the macrophage response following NTHi 375(2.8)sr infection in the presence of *Junbo* mouse serum from day 1 post-inoculation with NTHi(28)sr (figure 5.4G). We did not observe any major changes in the macrophage response, except an elevation in TNF-α expression compared to NTHi 375(2.8)sr only. Unlike BMDM infection with NTHi 375(2.8)sr+375sr D1 serum (figure 5.4F), iNOS gene expression was sustained when serum from *Junbo* mice inoculation with NTHi 375(2.8)sr.

Together these data show that PCho presence or absence and position on the NTHi surface influences macrophage response post 1-hour infection with NTHi 375 strains. Regardless of the NTHi infection and/or addition of serum from the *Junbo* mouse, IL-10 gene expression was sustained.

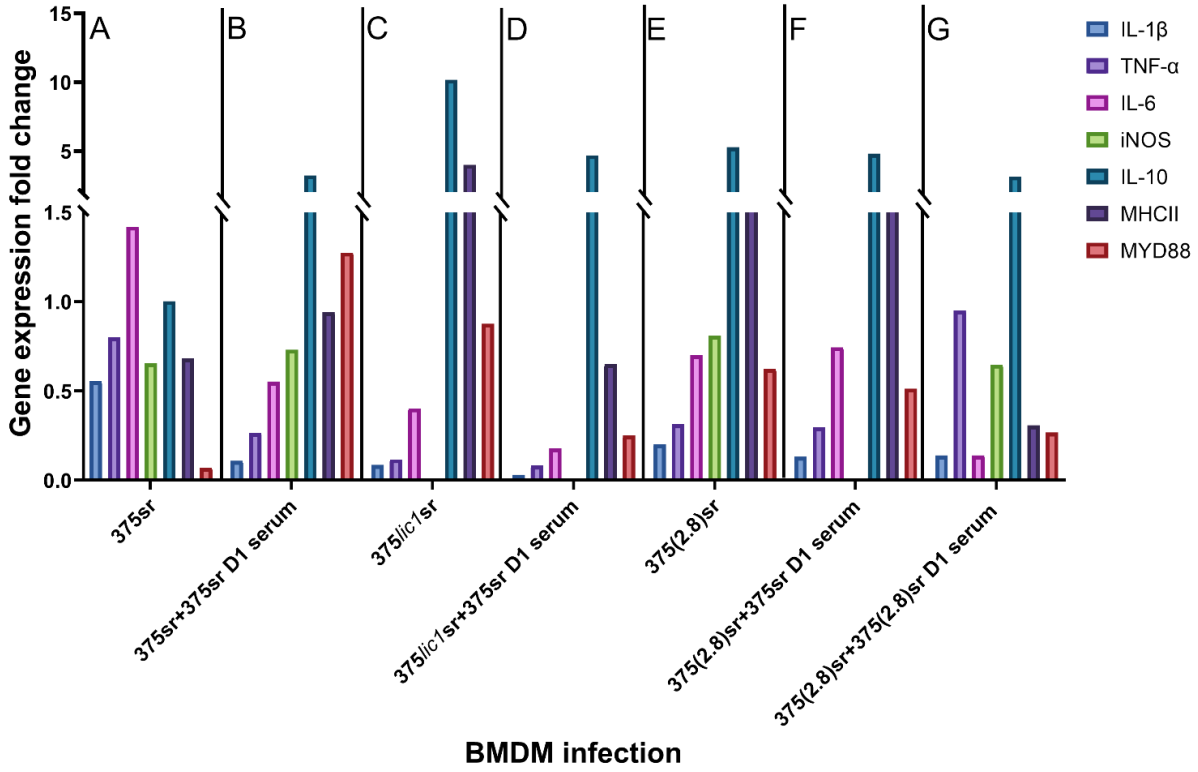

Figure 5.4. Cytokine gene expression following uptake of NTHi 375 strains into BMDMs treated with *Junbo* mouse serum. (A) BMDMs infected with NTHi 375sr (B) BMDMs infected with NTHi 375sr in media containing serum from day 1 post NTHi 375sr inoculation of *Junbo* mice (C) BMDMs infected with NTHi 375*lic1*sr (D) BMDMs infected with NTHi 375*lic1*sr in media containing serum from day 1 post NTHi 375sr inoculation of *Junbo* mice (E) BMDMs infected with NTHi 375(2.8)sr (F) BMDMs infected with NTHi 375(2.8)sr in media containing serum from day 1 post NTHi 375sr inoculation of *Junbo* mice (G) BMDMs infected with NTHi 375(2.8)sr in media containing serum from day 1 post NTHi 375(2.8)sr inoculation of *Junbo* mice. BMDMs were treated with NTHi at a MOI of 1:100 for 30 minutes. Following this, extracellular NTHi were killed using gentamicin treatment. The macrophages were incubated were incubated for further 1 hour in fresh BMDM media. NTHi were treated with 5% *Junbo* mouse serum and 2% baby rabbit serum. *Junbo* mouse serum from day 1 (D1) post inoculation with NTHi 375sr or 375(2.8)sr were used. Data is represented as relative fold gene expression of samples. Each sample had 3 technical repeat and 1 biological repeat.

5.3. Discussion

Expression of PCho on the NTHi surface influences uptake of bacteria into macrophages. PCho expressing NTHi persist longer in BMDMs, whereas 375*lic1*sr are cleared almost by 20 minutes following uptake. NTHi expressing PCho off heptose I on the NTHi surface persists longer in the BMDM than PCho off heptose III on the NTHi surface and elicits a similar macrophage response as PCho mutant.

Confocal microscopy showed larger bacterial aggregates after infection with NTHi 375*lic1*sr than NTHi 375sr. Bacterial loads in the macrophages could be a confounding factor, however due to the limit of detection of confocal microscopy, only larger aggregates were observed. The size of the aggregate formation could be influenced by multiple factors. One such factor is that PCho is zwitterionic; thus, lack of PCho on NTHi 375*lic1*sr could promote larger aggregate formation.

The aggregates could also be products of phagocytosis where after bacteria interact with macrophage receptors, it leads to activation of the phagocytic receptor. The activated phagocytic receptors may have then aggregated with bound NTHi. Receptor aggregation (also known as cross-linking) is a common process of phagocytosis and is promoted by the active process of phagocytes (Rosales and Uribe-Querol, 2017). We hypothesise these aggregates could be enhanced during interaction of NTHi 375*lic1*sr through toll-like-receptors (TLRs).

NTHi LPS can interact also with platelet activating factor receptor (PAFr, chapter 1, section 1.1.9.3) and lead to the activation of PI3-K (Erwin and Smith, 2007). Infection of BMDMs with NTHi 375 strains did not induce gene expression of PI3-K gene expression (data not shown as we did not get any gene amplification), suggesting this could may not be the major receptor by which NTHi are taken up. Ligand binding to TLRs triggers MYD88-mediated signalling (Deguine and Barton, 2014), which was expressed in high levels following BMDM infection with NTHi 375*lic1*sr and NTHi 375sr+375sr D1 serum. MYD88-

dependent signalling is important for clearance of infection and resolution of acute due to OM (Wieland *et al.*, 2005; Hernandez *et al.*, 2008). The pro-inflammatory response can mediate a macrophage response that can promote NTHi clearance. However, as these are preliminary findings, further optimisations and biological repeats are needed to understand the cellular response to NTHi uptake and survival into BMDMs in the presence and absence of serum.

Even though MYD88 was elevated for both NTHi 375*lic1*sr and NTHi 375sr+375sr D1 serum, it is not clear what enables the NTHI 375sr to survive in macrophages. IL-10 may influence bacterial survival in macrophages. IL-10 is anti-inflammatory; it down-regulates cellular expression of MHCII (Thomssen, Kahan and Londei, 1995) and inhibits TNF-α (Oswald *et al.*, 1992). IL-10 production facilities bacterial persistence and dissemination within the host (Peñaloza *et al.*, 2018). Transcriptomic studies on NTHi persistence in macrophages have shown increased levels of IL-10 along with IL-1β, IL-6 and TNF-α (Ackland *et al.*, 2021). IL-10 prevents excessive production of inflammatory cytokines during tissue injury and infection. LPS has been shown to induce expression of IL-10, and certain pathogens persist or evade the immune system by elevating IL-10 expression (Barsig *et al.*, 1995; Ernst *et al.*, 2019). . IL-10 was consistently elevated for all NTHi 375 strains, even when BMDMs were treated with serum from *Junbo* mice. IL-10 could influence bacterial killing and persistence in BMDMs.

NTHi 375sr bacterial colonies were measured at each time point 1-hour post infection of BMDMs with NTHi. We hypothesize uptake of NTHi 375sr by macrophages happens between 5-60 minutes following adherence. After this, increase in NTHi 375sr colony numbers in the macrophages happens between 60 and 90 minutes. Between 120 and 180 minutes, NTHi 375sr bacterial colonies decreased, but some colonies were still present. These could be the population of NTHi which survive phagocytosis and/or enter a senescence state and are not actively dividing. Between 210 and 240 minutes, NTHi 375sr colony numbers increased again, and these could be the population that are undergoing

bacterial division within the macrophages. A similar effect has been observed in macrophages for other Gram-negative bacteria (Mestas and Hughes, 2004).

Uptake of NTHi 375sr bacteria promoted M1 cytokine gene expression 2-hour post-BMDM infection. Some M2 macrophage cytokine genes were also expressed at low levels, which can help NTHi 375sr survive and persist within the macrophages. NTHi 375*lic1*sr promoted mainly M1 cytokine gene expression, explaining why this variant did not survive very well shortly after uptake. NTHi 375(2.8)sr elicited M1 cytokine gene expression, as with NTHi 375*lic1*sr. M2 cytokine gene expression was down regulated and this may explain why NTHi (2.8)sr was cleared away by 2-hours post-macrophage infection. However, further investigation is needed to understand how macrophage phenotype influences NTHi survival in BMBMs. At 2-hour post-infection of BMDM, MHCII gene expression was upregulated in macrophages infected with NTHi 375sr. This suggests PCho expression and position affects the antigen presentation ability of macrophages. We observed a higher MHCII gene expression for NTHi 375(2.8)sr 1-hour post-macrophage infection, but not at the 45-minute and 2-hour time points. This further supports macrophage response maybe NTHi strain specific, and therefore future work should study the theory that macrophage responses are NTHi strain specific. PCho presence or absence and position influenced macrophage responses. NTHi 375(2.8)sr behaved more similarly to NTHi 375*lic1*sr (PCho mutant) and NTHi 375sr (PCho expressing). PCho position on the NTHi surface is critical in promoting the type of (M1 or M2) macrophage response. Further work should investigate NTHi 375(2.8) uptake, and gather bacterial colony counts for BMDM infection with NTHi 375(2.8)sr. This should be compared to NTHi 375sr and 375*lic1*sr to compare how PCho position on the NTHi 375(2.8)sr influences the OPA.

These data suggests that PCho off heptose I on the NTHi surface plays a role in bacterial persistence in the macrophage and dampening of the macrophage response. PCho on heptose III on the NTHi surface altered the macrophage response where it was similar to PCho mutant strain, NTHi 375*lic1*sr. The addition of *Junbo* mouse serum from day 1 post

inoculation with NTHi 375sr or 375(2.8)sr influenced the macrophage response, where serum from NTHi 375sr reduced the M1 gene expression levels post NTHi 375sr and 375(2.8)sr BMDM infection compared to NTHi 375sr and 375(2.8)sr alone. Whereas NTHi 375(2.8)sr serum led to an increase in M1 macrophage gene expression (TNF-α) compared to NTHi (375(2.8)sr. These data suggest the NTHi-macrophage response is complex and is influenced by the presence or absence of PCho on the NTHi surface. The addition of serum from different NTHi infections influenced the macrophage response following BMDM infection with NTHi. The presence of CRP in the serum could influence the macrophage response. However, we did not include a 'serum only' control in our assays and it is unclear how 'serum only' influences macrophage activation. A 'serum only' control should be used to study the effect of *Junbo* mouse serum on macrophage activation. Furthermore, due to time limitations, we could not complete the preliminary experiments to investigate the role of CRP as an opsonin in the OPA. This should be followed up in the future work.

5.4. Future experiments

In the chapter, we show preliminary data that the presence or absence and position of PCho on the NTHi surface influences the macrophage response to NTHi infection. We have optimised a number of experimental systems, and so future work should collect more biological repeats to permit adequate statistical analysis. The role of CRP as an opsonin should be investigated where purified human CRP (hCRP) and recombinant mouse CRP (rMoCRP) could be used to compare mouse and human CRP. We supplemented our OPA with serum from the *Junbo* mouse, however, as the NTHi is a human specific pathogen, the effect normal human serum on the OPA should be studied. Flow cytometry based OPA can be used to measure interaction of serum components *e.g.* CRP and complement proteins C1q during the OPA .This will provide information on what role the immune components in

the serum play in bacterial killing or persistence during an OPA. Further optimisations of confocal microscopy could also provide insight into where the NTHi localise within the macrophages. Organelle markers such as lysosome and endosome could be used to see if NTHi 375 strains undergo phagolysosome formation.

We used NTHi 375 strains where only the PCho on the surface was altered. Other NTHi strains that have PCho expressed on different positions on their surface naturally should be used to confirm that the effects we measured are also true for other bacterial strains.

The presence or absence of PCho on the NTHi surface influenced the macrophage response, where lack of PCho on the NTHi surface led to more bacterial killing by the macrophages. Even though we infected the BMDMs with PCho expressing NTHi 375sr (Phase variation ON), it would be interesting to see what the PCho expression is over time in uptake and phagocytosis. Future experiments could use a mixture of phase variation ON or OFF strains to investigate which PCho phase variation is dominant after OPA. This will further confirm the relevance of PCho on NTHi survival in macrophages.

Future work should follow phagocytosis for strain specific time-points. Studies have shown that macrophage inflammatory responses to NTHi are strain-dependent (Ackland *et al.*, 2019)

We used macrophages for my OPAs. Other phagocytes such as neutrophils (which are the most abundant cells in the MEF (chapter 6)) could also play a role in bacterial persistence. OPAs could be performed using other phagocytes.

Chapter 6. Presence and position of PCho on the NTHi surface affects immune response in the Junbo mouse

6.1. Introduction

The acute phase response is a prominent systemic response preceding specific immune responses associated with local or systemic homeostatic disturbances caused by infection and other pathologies, including tissue injury or other immunological disorders. This leads to the production of cytokines and other inflammatory mediators. Acute phase proteins have a general function in opsonisation and trapping pathogens, in activating the complement pathways and modulating the immune response in the host. Proteomic analysis of the MEF conducted by our group revealed CRP is present in the MEF of *Junbo* mice infected with NTHi (data not shown). The interaction of CRP, an acute phase protein and NTHi has been studied, however, it is still unclear why, in the presence of CRP, NTHi can survive and persist. NTHi expresses PCho on its surface in a phase variable manner. In chapter 3, we showed the CRP binding was affected by the presence or absence and position of PCho on the NTHi surface. Presence and position of PCho has been shown to influence persistence in the respiratory tract and sensitivity to serum mediated killing associated with antibody and CRP (Weiser *et al.*, 1998; E. Lysenko *et al.*, 2000; Langereis *et al.*, 2019; Langereis, van der Pasch and de Jonge, 2019). Chapters 4 and 5 demonstrate that the presence and position of PCho on the surface of NTHi affects bacterial survival in serum bactericidal and opsonophagocytic assays. However, mimicking complex host-pathogen interactions in disease and commensal behaviour is non-trivial and hard to mimic *in vitro*. We aimed to understand how the presence and position of PCho on the NTHi surface influences infection with NTHi *in vivo*. We inoculated the *Junbo* mouse with NTHi 375 strains (375sr, 375*lic1*sr and 375(2.8)sr) and studied the how the presence and position of PCho on the NTHi surface influences infection rates in the ME, bacterial titres in the ME and the CRP levels in various *Junbo* tissues and fluids at day 1, 3 and 7 post-NTHi

inoculation. Specifically, we investigated the cellular immune response after day 1 post-infection with NTHi 375 strains. Finally, we studied the immune cell cytokine and chemokine profiles in the *Junbo* mouse nasal passage washes (NPW), middle ear fluid (MEF), serum, and nasal associated lymphoid tissue (NALT) day 1 post-inoculation with NTHi 375 strains to get a better understanding of the inflammatory response following infection with NTHi 375 strains.

6.2. Results

6.2.1. C-Reactive Protein concentration is highest at day 1 of infection with NTHi 375sr strains in the Junbo mouse

The role of CRP as an acute phase protein is understudied in the mouse. We hypothesized that, the interaction of CRP with PCho on the bacterial surface can potentially influence NTHi infection. CRP levels under healthy and inflammatory conditions have not been characterized thoroughly in the mouse. Some studies report CRP upregulation, following LPS stimulation in a few mouse models (N O Ku 1, 1993; Huang *et al.*, 2019). For example, It has been reported that mouse serum CRP levels at baseline are 5-9 mg/L and peak at 17 mg/l after LPS injection (Paul Simons *et al.*, 2014). However, CRP levels in the *Junbo* mouse have not been studied. Specifically, we were interested in the influence of NTHi infection, MEF grade and pre-inflammatory state of the *Junbo* mouse on CRP levels.

First, to determine if the *Junbo* mouse can be infected with NTHi, we used wild type C3H/HeH mice as a control and measured infection rate and bacterial titre following NTHi infection. The C3H/HeH mouse does not develop OM and therefore did not present with MEF. Therefore, NTHi strains do not infect the C3H/HeH mouse as no bacteria were detected from the respective ME washes. *Junbo* mice were inoculated with NTHi 375sr and the bacterial infection was investigated at day 1, 3 and 7 post-inoculation (figure 6.1A).

Junbo mouse infection rates were monitored primarily through testing MEF for the presence of NTHi bacteria; the rate being determined as the proportion of MEF tested that contain detectable bacteria. The infection rate at the three time-periods were each over 90%. Furthermore, there was an increase in ME bacterial titre over the days of infection. An average of 13,900 CFU/µl MEF was measured for day 1 and 16,350 CFU/µl for day 3 post-inoculation. The highest level of NTHi counts were obtained at day 7 post-inoculation with an average of 51,250 CFU/µl in MEF, showing evidence of bacterial proliferation and persistence in the ME for strain NTHi 375sr. The MEF fluid of the *Junbo* mouse is heterogeneous in its opacity and viscosity. Therefore, we graded the MEF 1 to 5 according to its opacity and viscosity, where MEF grade 1 MEF is the least opaque and grade 5 was the most opaque and viscous (chapter 2, table 2.4**.**). Higher bacterial titre was obtained from higher grade MEF (MEF grade >3/4) (figure 6.1A, B, C and D). For each time-period, some very high bacterial counts were observed for individual MEFs. For example, in MEF grades 3/4, 4 and 4/5, MEF grade 3/4 for day 3 and MEF grade 4/5 for day 7, which could be due to the heterogeneity of the MEF. Overall, MEF opacity and viscosity increased with time post-NTHi infection. Moreover, there is an increase in NTHi titre in a MEF grade dependent manner, except for a few outliers and this is consistent with previously reported infection studies in the *Junbo* mouse for other NTHi strains (Vikhe *et al.*, 2019).

Next, we investigated CRP levels in the *Junbo* mouse. As a control, we again studied C3H/HeH mice following NTHi infection. Again the C3H/HeH mouse does not develop OM and there was no MEF from these mice, we performed ME washes to study CRP levels. CRP levels were measured at day 1, 3 and 7 post-NTHi inoculation of the *Junbo* and C3H/HeH (figure 6.1E and appendix figure 2). CRP levels were highest at day 1 post-NTHi infection. Average CRP levels at day 1 post-NTHi infection of the *Junbo* mouse was 3770 pg/µl. Whereas in the C3H/HeH mice day 1 post-NTHi, the inoculation average CRP level were 1145 pg/µl. This suggested that the *Junbo* mouse is a good mouse model for studying CRP level changes following NTHi infection. Therefore, given the relevance of *Junbo*

mouse for the study of AOM, for the future experiments, we only used *Junbo* mice. The average CRP concentration at day 3 and 7 post-NTHi infection in the *Junbo* mouse was 1898 pg/µl and 1177 pg/lµl respectively. Non-inoculated (NI) CRP levels in the *Junbo* mouse were 743 pg/µl. This confirms that CRP levels in the *Junbo* mouse are influenced by NTHi infection. Levels of CRP appeared to normalise after day 1 as we did not observe any significant changes in the concentration at days 3 and 7 post-infection. Given the influence of the MEF grade on NTHi infection, we were interested in the relationship between MEF grade, CRP levels and NTHi titre. We categorized the data into the different grades of MEFs according to their opacity and viscosity. At day 1 post-inoculation, CRP levels were highest in higher grade MEFs and the lowest levels were measured in lower grade MEF (figure 6.1F). Higher CRP levels were measured when MEF had lower bacterial titre and the higher CRP levels in higher grade MEF correlated with higher NTHi titre (figure 6.1B). Consistent with the above observations, a negative regression correlation with a R^2 value of -0.24 between CRP levels and NTHi titre was calculated at day 1 post-NTHi 375sr inoculation. However, this was not statistically significant ($p = 0.29$). Intriguingly, there were certain mice with very high CRP levels, which presented with higher grade MEF and were outliers (figure 6.1E, 6.1F, 6.1G). This observation was similar to certain mice presenting with increased MEF bacterial titre counts (figure 6.1B, 6.1C). However, there was no correlation between the two outliers. Most importantly, the levels of CRP were highest at day 1 of NTHi infection in the *Junbo* mouse.

In addition, we hypothesized that CRP may localise with bacteria in the MEF. We used immunohistochemistry to stain for CRP and Gram-negative bacteria and confirmed that CRP is found predominately in the MEF with NTHi (figure 6.I). Together, this suggested that despite the CRP and NTHi both being present around the MEF, CRP levels do not directly influence NTHi survival.

The CRP levels in the *Junbo* mouse could be influenced by the pre-existing inflammation of the ME due to background chronic OM in the *Junbo* mouse. The *Junbo* mice starts to

develop OM spontaneously at 4 to 5 weeks of age (Hood *et al.*, 2016). We investigated the CRP level changes in the 5-week old *Junbo* mice. We hypothesised that during the onset of OM, CRP levels in the MEF higher be higher than in the 11-week old *Junbo* mouse and that levels would further increase in the 5-week old *Junbo* mouse MEF upon infection with NTHi. NTHi infection rates in the 5-week old *Junbo* mice were 50% and not all mice had developed OM at this age. The levels of CRP in 5-week old *Junbo* mice was elevated in mice that had developed OM. The levels of CRP in NI *Junbo* mice were approximately 2-fold higher than in 11-week old NI *Junbo* mice, thus confirming levels of CRP are higher at the onset of OM (figure 6.2). A 5.4-fold increase in CRP concentration was measured when 5-week old *Junbo* mice were inoculated with NTHi 375sr. In 11-week old *Junbo* mice, levels of CRP were 5.1-fold higher after NTHi infection. We showed that the levels of CRP increased even more after NTHi inoculation compared to NI *Junbo* mice with OM. This confirmed that the increase in CRP was due to the presence of bacteria in the MEF at the onset of OM and also in the 11-week old *Junbo* mice. The 11-week old *Junbo* mouse is good to study NTHi infection because at this age, more of the mice have stable OM (which is bilateral) compared to 5-week old *Junbo* mice. The infection rate is higher in 11-week old *Junbo* mice because more mice have developed OM, making the 11-week old mice more useful for studying NTHi infection. Finally, CRP levels are influenced by the NTHi infection in the 11-week old *Junbo* mice. In conclusion, age dependent pre-inflammatory conditions in the *Junbo* mouse influence CRP levels. These observations support the use of 11-week old *Junbo* mice to study CRP levels in the context of OM.

From the above observations, we can conclude that the CRP levels are highest day 1 post-infection in the *Junbo* mouse and that the 11 week old mouse facilitates an ideal inflammatory state and relevance to the study of AOM, Therefore, for the reminder of the chapter, we will discuss data on the 11-week old *Junbo* mouse and samples obtained at day 1 post-infection.

CRP levels are influenced by NTHi infection. However, the survival and persistence of NTHi in the MEF in the presence of CRP suggests that the host-pathogen interaction is complex. NTHi 375sr expresses PCho even in the presence of CRP in the NP (appendix figure 3) and in MEF samples from *Junbo* mouse infection (appendix figure 3). As shown in the previous chapters, CRP binding to NTHi is dependent on PCho presence or absence and position on the NTHi surface. The host-pathogen interaction in disease and the commensal lifestyle can be influenced by cellular response *in vivo*. The immune cell profile during NTHi infection in AOM could be vital in providing an understanding of NTHi survival in the presence of CRP.

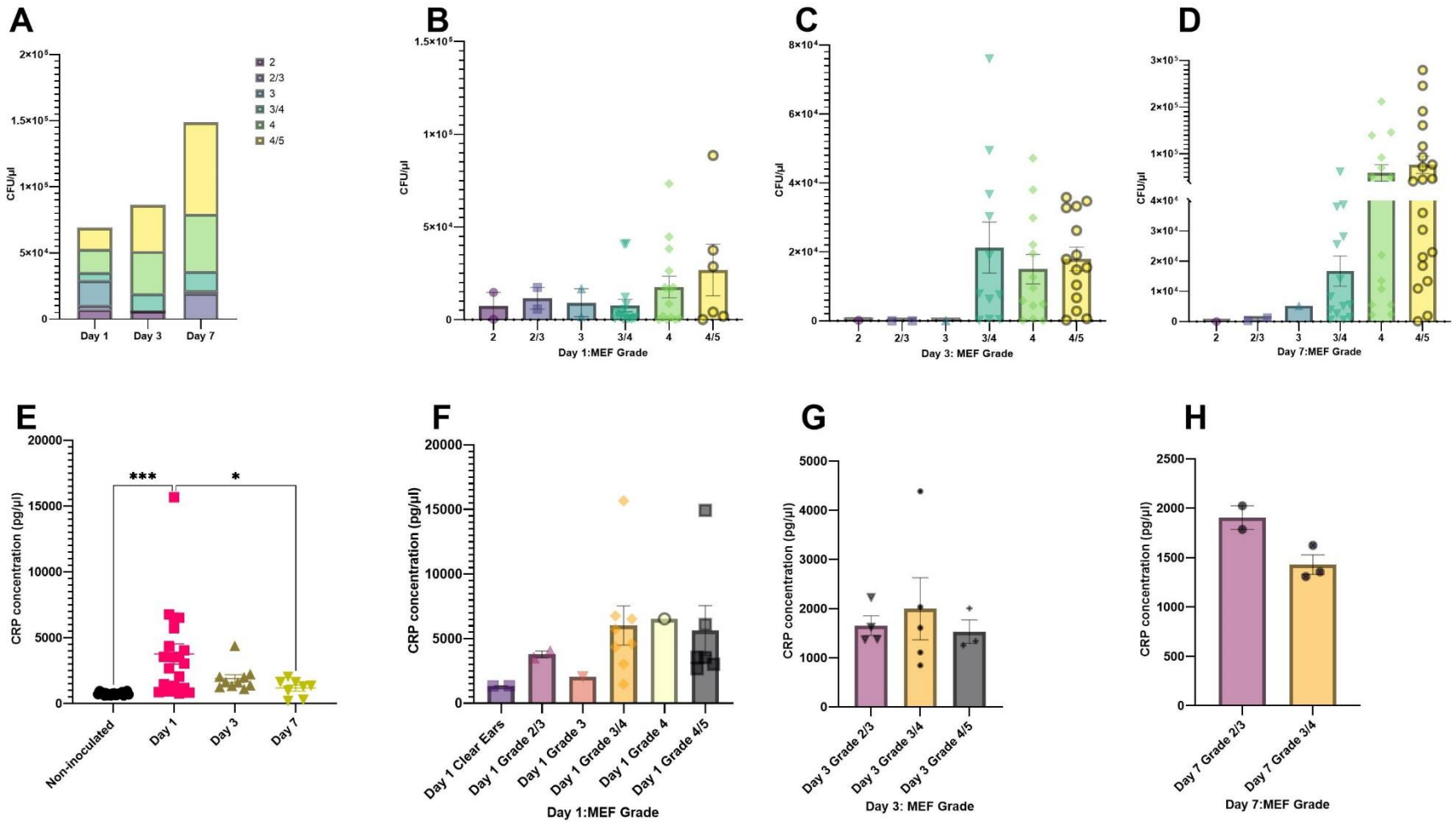
A
B
C
D
CFU/µl
2
2/3
3
3/4
4
4/5
Day 1
Day 3
Day 7
Day 1:MEF Grade
Day 3: MEF Grade
Day 7:MEF Grade
E
F
G
H
CRP concentration (pg/µl)
***
*
Non-inoculated
Day 1
Day 3
Day 7
Day 1 Clear Ears
Day 1 Grade 2/3
Day 1 Grade 3
Day 1 Grade 3/4
Day 1 Grade 4
Day 1 Grade 4/5
Day 3 Grade 2/3
Day 3 Grade 3/4
Day 3 Grade 4/5
Day 7 Grade 2/3
Day 7 Grade 3/4

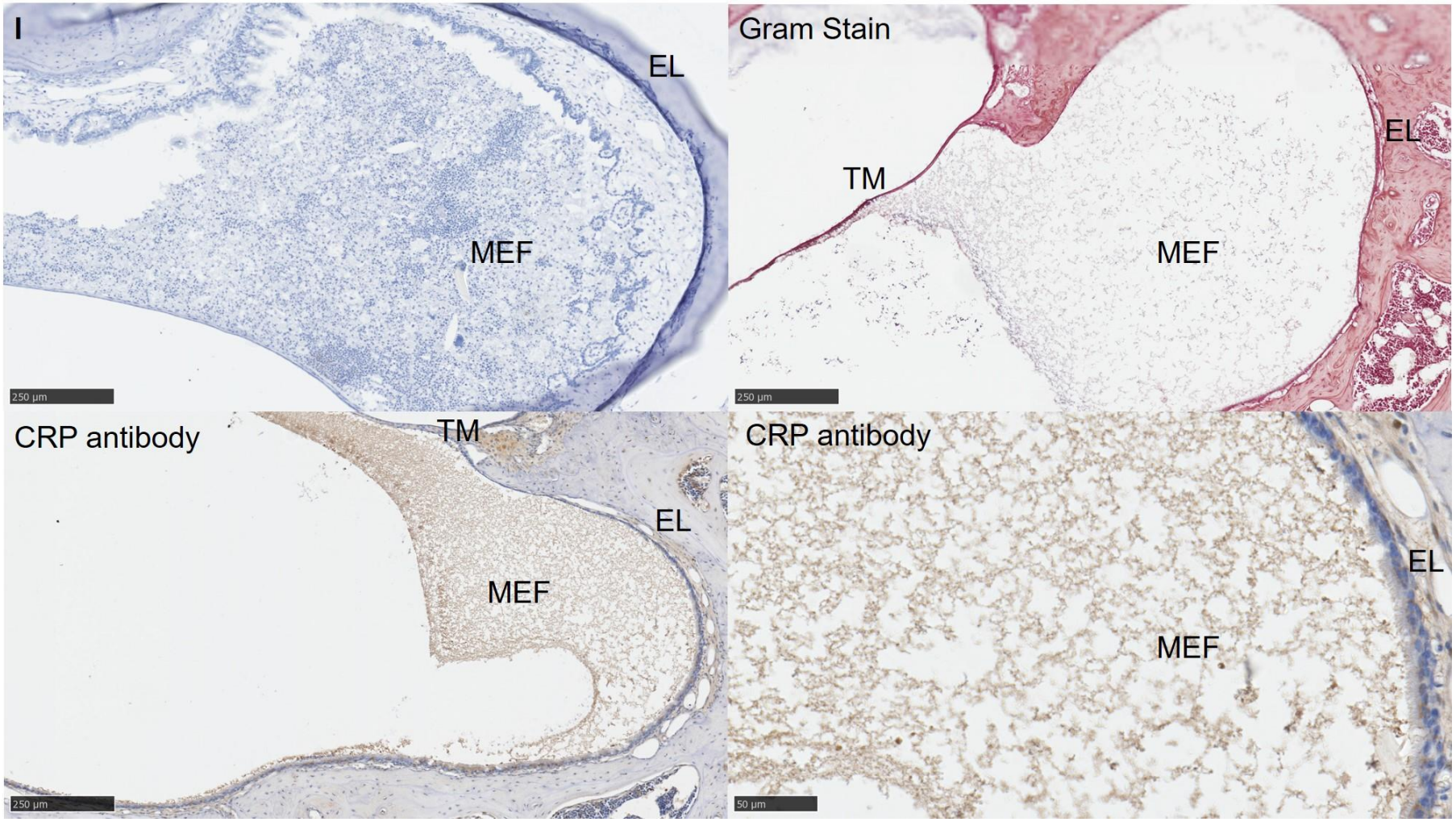
I
EL
MEF
250 µm
Gram Stain
EL
TM
MEF
250 µm
CRP antibody
TM
EL
MEF
250 µm
CRP antibody
EL
MEF
50 µm

Figure 6.1. CRP in the *Junbo* mouse MEF days 1, 3 and 7 post-inoculation with NTHi 375sr. The *Junbo* mouse was inoculated with 375sr and MEF was collected days 1 (n=16 *Junbo* mice), 3 (n=10 *Junbo* mice) and 7 (n= 5 *Junbo* mice) post-infection. The levels of CRP were measured in the different grades of MEF collected. CRP levels were normalised to per µl MEF. Non-inoculated (NI) *Junbo* mice were used as controls for NTHi infection and CRP concentration (n=10 *Junbo* mice). (A) Bacterial colony counts in the MEF of *Junbo* mouse days 1, 3 and 7 post-NTHi infection represented as a stacked bar chart. The stacked bar chart was used to represent the proportional contribution of individual data points for grade of MEF in comparison to a total MEF. (B) Range of bacterial colony counts per µl of MEF for different grades at day 1 post-375sr infection (n=10 *Junbo* mice). (C) Bacterial titre per µl MEF for different grades at day 7 post-NTHi 375sr infection (n=5 *Junbo* mice). (D) Bacterial titre per µl MEF for different grades at day 7 post-NTHi 375sr infection (n=4 *Junbo* mice). (E) CRP concentration per µl MEF day 1, 3 and 7 post-NTHi 375sr inoculation*. (F) CRP levels in different grades of MEF for day 1 post-inoculation with NTHi 375sr. (G) CRP levels in different grades of MEF for day 7 post inoculation with NTHi 375sr. (H) CRP levels in different grades of MEF for day 7 post-inoculation with NTHi 375sr. (I) Immunohistochemistry staining of *Junbo* ME. Sectioned *Junbo* ME were stained for CRP using a polyclonal CRP antibody and the Gram stain was used to stain for bacteria. EL = epithelial lining, MEF= middle ear fluid and TM = tympanic membrane. *Number of *Junbo* mice was different for figure 6.1A and 6.2D because these are two different studies. The first study aimed to understand the infection rate of NTHi 375sr and look at the bacterial titres in different grades of MEF in the *Junbo* mouse. The second study looked at investigating CRP levels following NTHi 375sr infection. Further, we were limited by the number of mice. This is the reason why there are fewer CRP data points for day 3 and day 7 post-NTHi infection. One-way ANOVA was performed for each data set followed by Brown-Forsythe test. Analysis was corrected for multiple comparisons by controlling the False Discovery Rate. *p <0.05, **p <0.01, ***p <0.001

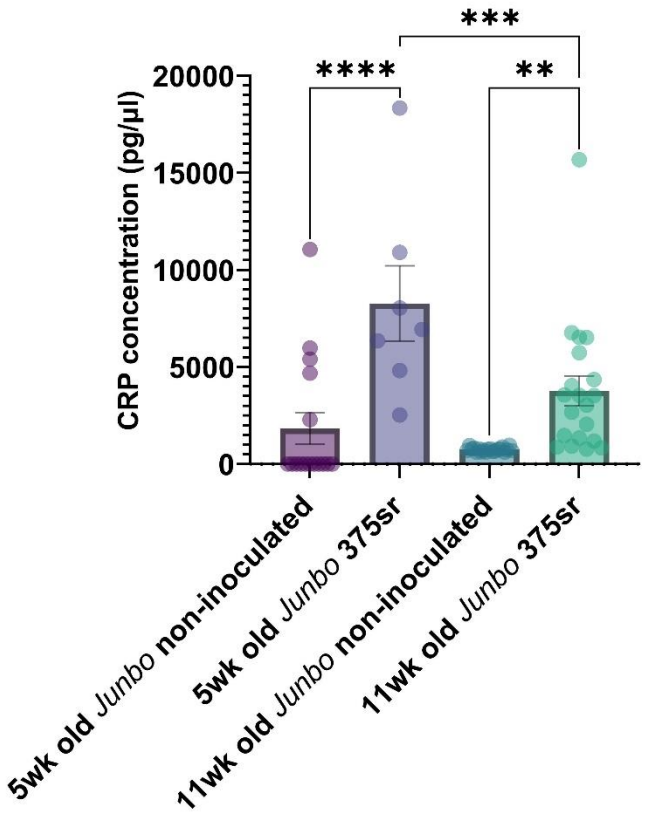

Figure 6.2. CRP levels at onset of OM in the *Junbo* mouse ME compared to the adult *Junbo* mouse. Non-inoculated *Junbo* mice were used as controls of NTHi infection for both age groups *Junbo* mice were inoculated with 375sr and MEF samples were collected day 1 post-inoculation with NTHi. CRP concentration was calculated for per µl MEF. (n= 8 NI 5-week old *Junbo* mice infected with NTHi 375sr, n = 6 for 5-week old *Junbo* mice, n=10 for 11-week old NI *Junbo* mice and n = 10 for 11-week old *Junbo* mice infected with NTHi 375sr. One-way ANOVA was performed followed by Brown-Forsythe test. Analysis was corrected for multiple comparisons by controlling the False Discovery Rate. **p* <0.05, ***p* <0.01, ****p* <0.001, *****p* <0.0001

6.2.2. Cellular response in the Junbo mouse is influenced by the expression and position of PCho on the NTHi surface

CRP plays an essential role in recognition of self and foreign molecules. CRP interaction with foreign molecules contributes to the activation of the immune response early during inflammation or infection. We aimed to understand how the presence and position of PCho on the NTHi surface influences infection with NTHi *in vivo*. Therefore, we inoculated the *Junbo* mouse with NTHi 375 strains (375sr, 375*lic1*sr and 375(2.8)sr) and studied the immune response at days 1, 3 and 7 post-NTHi inoculation. Specifically, we investigated the cellular immune response after 1 day of infection with NTHi 375 strains. We investigated a range of immune cells in the *Junbo* mouse MEF to determine, which cell types were altered upon NTHi infection. Using flow cytometry, both cells of the innate immune and adaptive immune system were immunophenotyped in the *Junbo* mouse tissues and fluids (gating strategy in appendix figure 4, appendix figure 5 and appendix table 1).

Neutrophils were the most abundant immune cells in the *Junbo* mouse MEF. This is consistent with previous literature where infection of the *Junbo* mouse with another NTHi strain also had abundant neutrophils present in the MEF (Vikhe *et al.*, 2019). Neutrophils are typically the first immune cells to respond to a microorganism when infecting the host. In NI *Junbo* mice, neutrophils made up 35.0% of the total live cell populations in MEF. Proportion of neutrophils did not change when *Junbo* mice were inoculated with NTHi 375*lic1*sr (35.4% live cells) compared to NI mice. The proportions of neutrophils were somewhat elevated in MEF infected with NTHi expressing PCho (*i.e*. 375sr (41.0% live cells) and 375(2.8)sr (43.8% live cells) compared to NI mice, although this difference was not statistically significant (figure 6.3A).

Monocytes travel via the blood to tissues where they develop into macrophages or dendritic cells (DCs). In NI *Junbo* mouse MEF, monocytes made up 0.9% of total live cells. A slightly lower proportion of monocytes were obtained for *Junbo* mice inoculated with NTHi 375sr

(0.6% live cells) and 375(2.8)sr (0.7% live cells) compared to NI mice. The proportion of monocytes were slightly elevated in mice infected with 375*lic1*sr compared to NI mice (1% live cells). However, none of the differences in monocyte proportions were statistically significant (figure 6.3B).

DCs capture, process, and present antigens to cells of the adaptive immune system. We phenotyped two subtypes of classical DCs to see which kind of antigen presenting DC was dominant: $CD11b^+$ classical DC (cDCs) and $CD8^+$ type DCs. In NI *Junbo* MEF, 2.4% of total live cells were $CD11b^+$ DCs and 2.2% of total cells were $CD8^+$ DCs. $CD11b^+$ cDCs were reduced in MEF from *Junbo* mice inoculated with NTHi 375sr (1% live cells) and 375*lic1*sr (0.3% live cells) compared to NI MEF (figure 6.3C). *Junbo* mice inoculated with NTHi 375(2.8)sr had similar proportions of DCs to NI MEF (2.5%). The proportion of $CD8^+$ DCs decreased for all strains compared to NI *Junbo* mice (375sr (0.5% live cells), 375*lic1*sr (0.4% live cells), and 375(2.8)sr (0.5% live cells) (figure 6.3D).

Macrophages are phagocytes with a critical role in host defence towards foreign material. In NI *Junbo* mice, macrophages made up 0.42% of total live cells. Macrophage proportions reduced when *Junbo* mice were inoculated with NTHi 375sr (0.2% live cells) and 375*lic1*sr (0.3% live cells) compared to NI mice, although these data were not statistically significant (figure 6.3E). However, when *Junbo* mice were inoculated with NTHi 375(2.8)sr, 0.5% of total live cells were macrophages. The proportion of macrophages were elevated for NTHi 375(2.8)sr infection compared to NI mice and the other NTHi 375 strain infected mice used. The difference in macrophage proportions in MEF of the *Junbo* mouse inoculated with NTHi 375sr and 375(2.8)sr were statistically significant.

B1a cells were selected for their CD5+ surface marker. These are innate-like B cells that have a bias towards bacteria and self-antigens, promoting the clearance of apoptotic cells and bacteria (Wong *et al.*, 2019). The proportions of B cells were 0.7-fold lower in *Junbo* mice inoculated with NTHi 375sr compared to NI mice; however, this was not statistically significant (figure 6.3F). Proportions of B1a cells were similar for NTHi 375*lic1*sr (1.5% live

cells) and NI mice (1.3% live cells). Finally, levels of B cells were significantly reduced following 375(2.8)sr (0.6% live cells) inoculation, therefore suggesting PCho position on the NTHi surface could influence the distribution of immune cell types observed in the MEF of infected *Junbo* mice.

Invariant natural killer T (iNKT) cells are a dissimilar population of T cells that express αβ T-cell receptor and some surface markers similar to natural killer (NK) cells. iNKT cells can play an immunoregulatory role. iNKT cells made up 1.5% of total live cells in MEF from NI mice (figure 6.3G). In mice inoculated with NTHi 375sr, 1% of the total live cells were iNKT cells. In MEF from 375*lic1*sr inoculated *Junbo* mice, 1.7% of total live cells were iNKT. iNKT cells were highest in MEF from NTHi 375(2.8)sr inoculated *Junbo* mice (2.6% live cells).

Natural killer (NK) cells belong to the same family as T- and B-lymphocytes; however, they are classified as cells of the innate immune system because they can respond quickly to infections and other pathological conditions such as cancer. NK cells were elevated 2-fold in MEF from mice inoculated with NTHi 375sr and 2.2-fold for 375*lic1*sr compared to NI *Junbo* mouse MEF (figure 6.3H). NTHi 375(2.8)sr inoculation led to a reduction in NK cell proportions (0.5% live cells) compared to NI mice, again differences in the immune cell response corresponded to differences in the PCho expressed on NTHi bacteria.

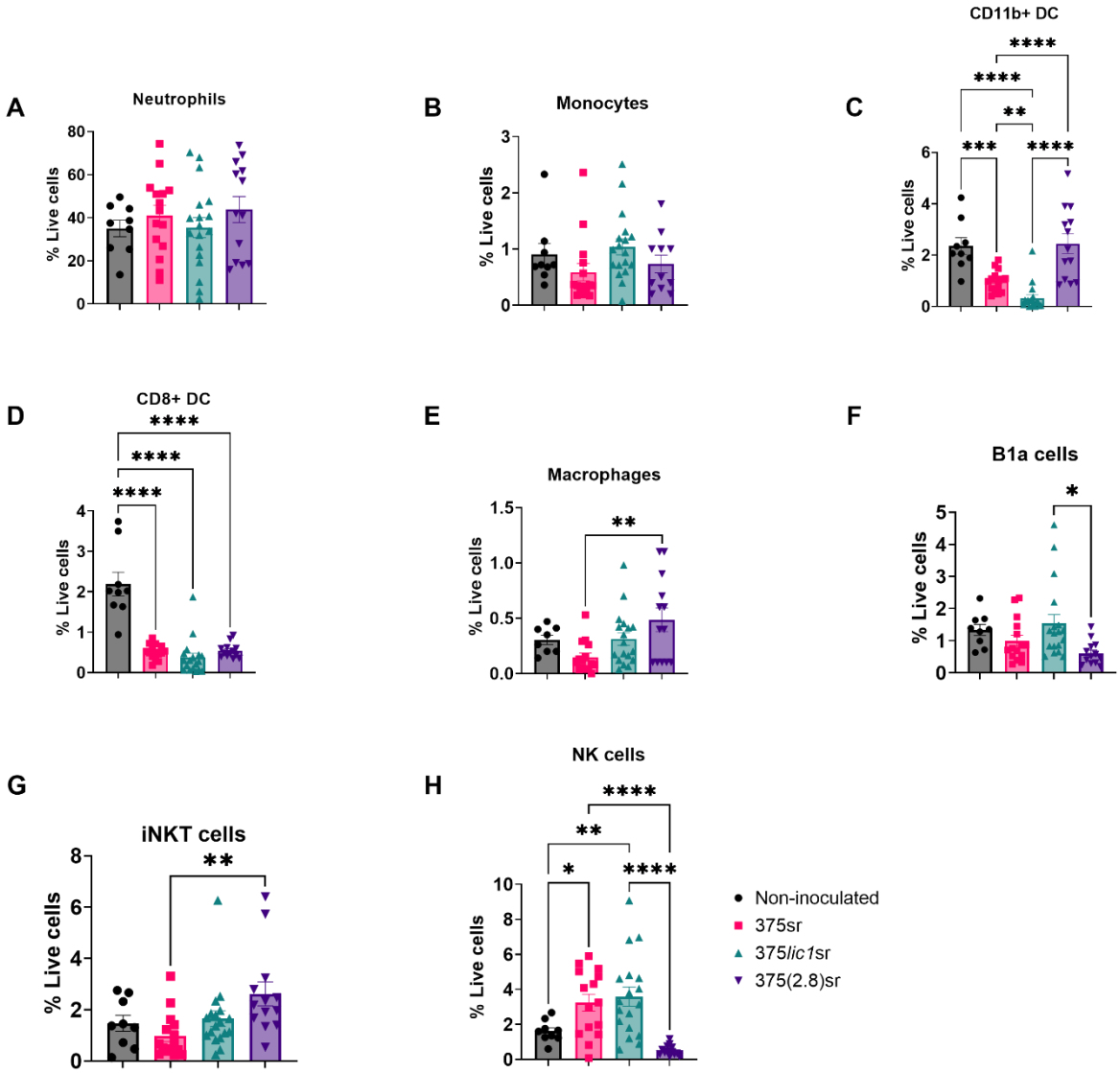

Figure 6.3. MEF innate immune cell profiling following inoculation of *Junbo* mice with NTHi 375 strains. Mice were inoculated with 375sr strains (375sr (n=8), 375*lic1*sr (n=9) and 375(2.8)sr (n=7) for day 1 prior to sampling. MEF samples were collected day 1 post-inoculation and analysed for innate immune cell populations. Non-inoculated *Junbo* mice were used as controls (n=5). (A) Neutrophils (B) Monocytes (C) CD11b+ type DC (D) CD8+ type DC (E) Macrophages (F) B cells (G) iNKT cells (H) NK cells. One-way ANOVA was performed followed by Brown-Forsythe test. Analysis was corrected for multiple comparisons by controlling the False Discovery Rate. **p* <0.05, ***p* <0.01, ****p* <0.001, *****p* <0.0001.

CD4+ T helper (CD4+ T cells), regulatory T cells (Treg) and CD8+ cytotoxic T (CD8+ T cells) cells were profiled for the adaptive immune populations. CD4+ T cells made up 3.2% of the total live cells in MEF samples from NI *Junbo* mice. Inoculation with NTHi 375sr strains caused a 1.4% increase CD4+ T cells compared to NI *Junbo* MEF (figure 6.4A). The highest proportion of CD4+ T cells was found following inoculation with NTHi 375(2.8)sr (6.3% live cells), followed by 375sr (4.6% live cells) and 375*lic1*sr (4.7% live cells). CD4+ T cells recognise antigens presented on MHC II by antigen presenting cells and play a role in activating and influencing the immune response. PCho position and presence seems to affect CD4+ T cell proportions. CD4+ T cells can differentiate into Treg cells. These cells play a role in regulating or suppressing other cells of the immune system. Treg cells control the immune response to self and foreign antigens. We observed differences in Treg cell proportions when *Junbo* mice were inoculated with alternative NTHi 375 strains. The highest proportion of Treg cells was measured with NTHi 375sr where there was a 1.4-fold increase compared to NI mouse MEF (figure 6.4B). For NTHi 375*lic1*sr and 375(2.8)sr, a 1.3-fold and 1.5-fold increase in Treg cell proportions compared to NI samples was measured. There was a slight increase in Treg cell populations when *Junbo* mice were infected with PCho expressing NTHi 375 strains (*i.e*. 375sr and 375(2.8)sr). However, the differences observed between NTHi 375 strains was not statistically significant. This could be because day 1 post-infection is too early to measure any statistically significant changes in Treg cells. We collected samples at day 1 post-inoculation when a sufficient adaptive immune response against NTHi may not yet be induced. Finally, levels of CD8+ T cells was measured (figure 6.4C). NI *Junbo* mice had 0.1% CD8+ T cells. The highest proportion of CD8+ T cells were measured after inoculation with NTHi 375(2.8)sr, where an average of 0.6% live cells were made up of CD8+ T cells. Proportion of CD8+ T cells following day 1 post-inoculation with NTHi 375sr and 375*lic1*sr did not change compared to NI MEF samples from the *Junbo* mouse.

In conclusion, we identified that the presence and position of PCho influences immune cell phenotypes in the *Junbo* mouse MEF. In addition to this, the bacterial titre in the MEF could be a confounding factor that could be influencing the number of immune cells we measured. This has been previously reported by our group where higher NTHi titre in higher grades MEF resulted in higher number of immune cells (Vikhe *et al.*, 2019). Specifically, NTHi 375*lic1*sr influences levels of CD11b+ DCs. This shows that the presence and absence of PCho on the NTHi surface influences immune cell phenotype. NTHi 375(2.8)sr affects iNKT, NK, macrophage, B1a and CD8+ DC cell proportions and this is a novel finding, showing PCho position influences immune cell phenotype. The respective macrophage phenotype and T cell subtypes need further investigation.

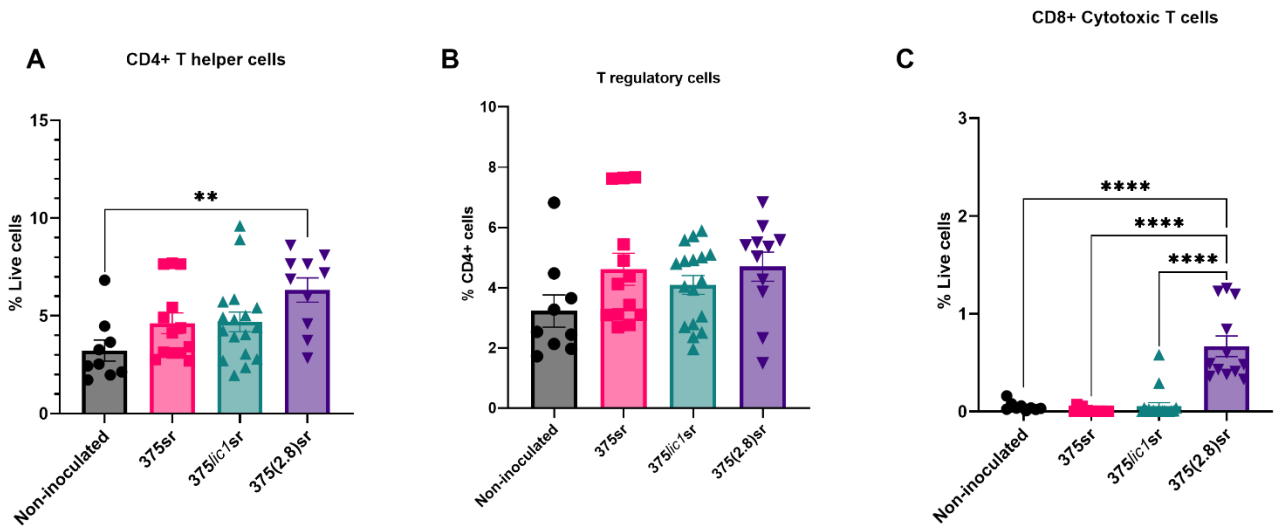

Figure 6.4. MEF adaptive immune cell profiling following inoculation of *Junbo* mice with NTHi 375 strains. MEF samples from *Junbo* mice day 1 post-inoculation with NTHi 375 strains (375sr (n=8), 375*lic1*sr (n=9) and 375(2.8)sr (n=7)) for 1 day. MEFs were collected and the cells of adaptive immune system were analysed. Non-inoculated *Junbo* mice were used as controls (n=5). (A) CD4+ T helper cells (B) Regulatory T cells (C) CD8+ cytotoxic T cells. One-way ANOVA was performed followed by Brown-Forsythe test. Analysis was corrected for multiple comparisons by controlling the False Discovery Rate. *p <0.05, **p <0.01, ***p <0.001.

6.2.3. Immune profiling Junbo mouse MEF according to grade MEF following infection with NTHi 375sr strains

The grade of the MEF may influences the immune cell profile in the *Junbo* mouse infected with NTHi. Vikhe (2019) showed persistence of NTHi at day 7 depends on the grade of the fluid, where NTHi were present in the most opaque and viscous MEF. We investigated if there are changes in the different grades of MEF at day 1 post-NTHi inoculation had differences in the immune cell content, and whether this depends on PCho position and presence. This could provide insight into immune cell changes in early infection that could lead to bacterial survival and persistence later in the disease.

6.2.3.1. Higher grade MEF day 1 post-infection NTHi 375sr have more neutrophils and lower Tregs

Neutrophils (41% live cells) were the dominant innate immune cells in MEF of *Junbo* inoculated with NTHi 375sr, followed by NK cells (3.2% live cells) (figure 6.5A). B1a cell (1% live cells), $CD11b^{+}$ DC (1% live cells), iNKT cells (1% live cells) also made up the immune cell profile of the *Junbo* mouse MEF. Eosinophils were the least abundant cells in the MEF (0.04% live cells).

The innate immune cell profiles were categorised into different grades of MEF (figure 6.5B). The opacity and viscosity of the MEF influenced the immune cell profile following NTHi 375sr inoculation in the *Junbo* mouse. The proportion of neutrophils were higher in higher grade MEF, whereas a decrease in proportion of macrophages and B1a cells was observed in the same higher grade MEFs.

In the adaptive immune cell population, CD4+ T helper cells were the most abundant T cell type (5.6% live cells) and majority of these CD4+ T cells were made up of effector Tregs (5% CD4+ cells) (figure 6.5C). Effector Treg cells play a role in dampening the immune

response. The grade of MEF did not influence overall proportion of CD4+ T cells (figure 6.5E). However, the proportion of effector Treg cells decreased as the grade of the MEF increased (figure 6.5F). The most opaque and viscous MEFs also had the highest proportion of CD8+ T cells (figure 6.5E).

Overall, we noted that the higher grade MEF are enriched with neutrophils and have low Treg cells 1 day post-infection, thus showing that grade of the fluid influences the immune phenotype during early infection and could have implications for bacterial survival and persistence with disease progression.

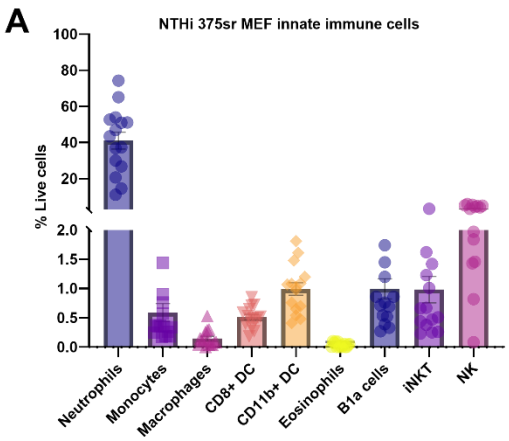
A
NTHi 375sr MEF innate immune cells
% Live cells
100
80
60
40
20
2.0
1.5
1.0
0.5
0.0
Neutrophils
Monocytes
Macrophages
CD8+ DC
CD11b+ DC
Eosinophils
B1a cells
iNKT
NK

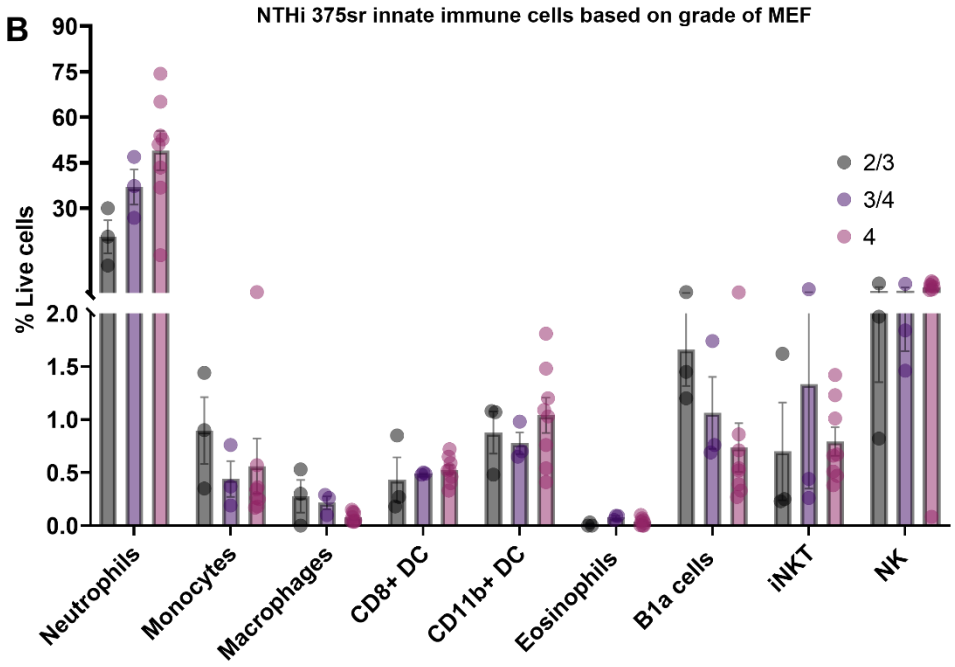
B
NTHi 375sr innate immune cells based on grade of MEF
% Live cells
90
75
60
45
30
2.0
1.5
1.0
0.5
0.0
2/3
3/4
4
Neutrophils
Monocytes
Macrophages
CD8+ DC
CD11b+ DC
Eosinophils
B1a cells
iNKT
NK

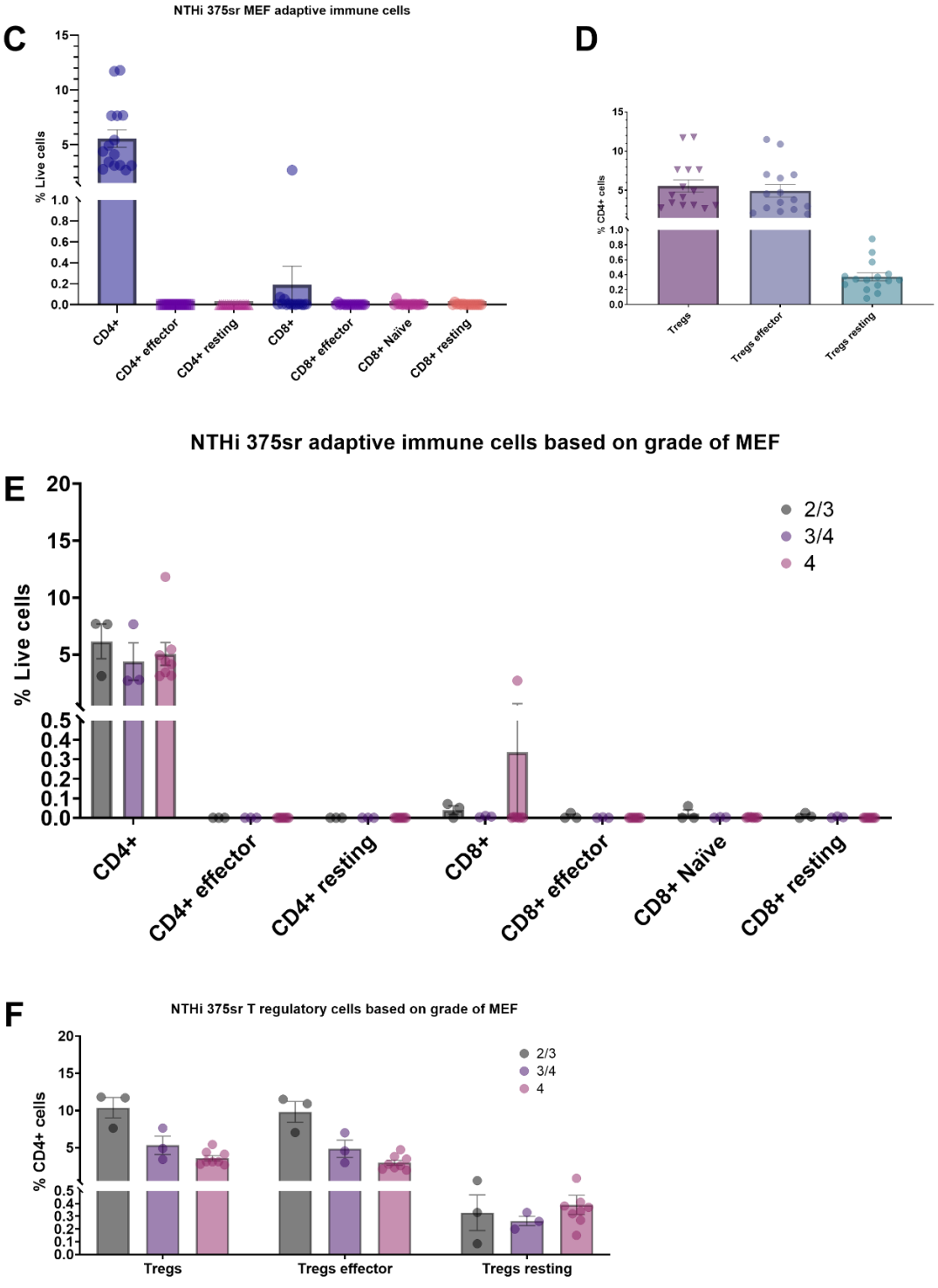

Figure 6.5. Immune profiling of cells in the *Junbo* mouse grades of MEF day 1 post-inoculation NTHi 375sr. (A) Innate immune profiling day 1 post-inoculation of the *Junbo* mouse with NTHi 375sr. (B) Innate immune cell populations for each grade categorisation of *Junbo* mouse MEF. (C) Immune profiling of adaptive immune cells day 1 post-inoculation of *Junbo* with NTHi 375sr. (D) Treg cells (E) Adaptive immune cell populations for each MEF grade categorisation of *Junbo* mouse MEF. (F) Treg cell populations for each MEF grade (n = 8). One-way ANOVA was performed followed by Brown-Forsythe test. Analysis was corrected for multiple comparisons by controlling the False Discovery Rate.

6.2.3.2. NTHi lacking PCho on its surface leads to lower bacterial survival in the Junbo mouse ME and is possibly influenced by immune cell phenotype in a MEF grade dependent manner

Studies up to now had focused on immune profiling on *Junbo* mice following infection with NTHi 375sr, a strain that expresses PCho. To understand the role of PCho on the NTHi surface in the immune cell response to the bacteria, we inoculated the *Junbo* mouse with NTHi 375*lic1*sr, a PCho non expressing mutant. *Junbo* mouse MEFs were collected day 1 post-NTHi inoculation.

Inoculation of the *Junbo* mouse with NTHi 375*lic1*sr resulted in a lower infection rate of the *Junbo* mouse ME at day 1 post-inoculation (54%) than did NTHi 375sr (92%). The bacterial titre for NTHi 375*lic1*sr day 1 post-inoculation was lower than for NTHi 375sr, with an average of 2647 CFU/µl MEF. The *Junbo* mouse MEF CRP levels after NTHi 375*lic1*sr infection were 1.3-fold higher than the infection with NTHi 375sr. A regression correlation with a R^2 value of 0.01 between CRP levels and NTHi titre was calculated at day 1 post-NTHi 375*lic1*sr inoculation. However, this was not statistically significant (*p 0.65*).

As observed for NTHi 375sr infection, higher bacterial titres were observed in the higher grades of MEF (figure 6.6A). Unlike NTHi 375sr, infection with NTHi 375*lic1*sr resulted in higher CRP levels in lower grade MEFs from the *Junbo* mouse, where bacterial titres were lower (figure 6.6B).

Neutrophils were the most abundant cells in the MEF from *Junbo* mice inoculated with NTHi 375*lic1*sr, making up an average of 35.4% of total live cells (figure 6.6C). Neutrophil proportions were an average of 5.6% lower than seen infection of the *Junbo* mouse with NTHi 375sr. Similar to NTHi 375sr inoculation, NK cells were the second most abundant cells in the *Junbo* mouse MEF (3.6%). iNKT (1.7%), B1a cells (1.5%) and monocytes (1%) were present in the *Junbo* mouse MEF day 1 post-inoculation with NTHi 375*lic1*sr.

Eosinophils were the least abundant cells in the MEF of *Junbo* mice infected with NTHi 375*lic1*sr.

The proportion of neutrophils increased in higher grade MEF (figure 6.6D). $CD8^+$ DC and $CD11b^+$ DC cell proportions also increased in higher grade of MEFs. There was a general increase the in proportion of iNKT cells as the grade of MEF increased with the exception of grade 4 where the iNKT cell proportion decreased. Proportion of macrophages decreased in higher grades of MEF and B1a cells decreased as the grade of MEF increased. This is the opposite of what was observed for NTHi 375sr infection (figure 6.5B).

CD4+ T cells made up a majority of the adaptive immune cells in the MEF (figure 6.6E). An average of 5.5% of the total live cells were made up of CD4+ T cells. Effector Treg cells accounted for 4.2% of the CD4+ T cell population (6.6F). Adaptive immune cells did not differ significantly when the grades of MEF were categorised (figure 6.6G and 6.6H).

A

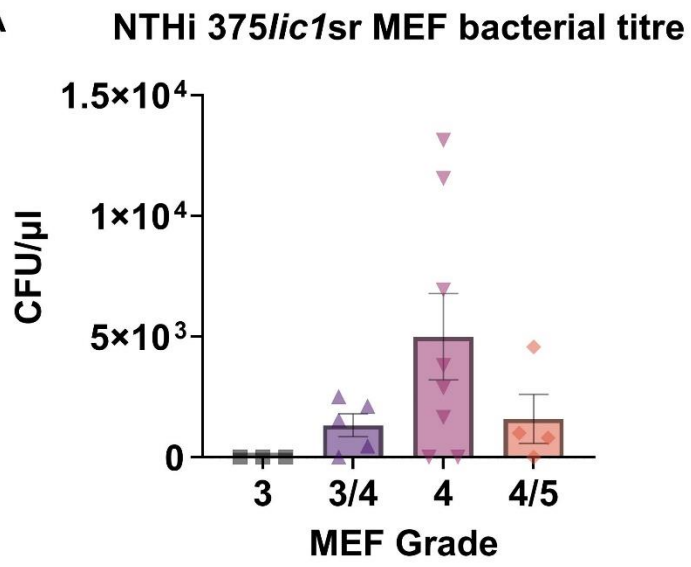
NTHi 375lic1sr MEF bacterial titre
1.5×10⁴
1×10⁴
5×10³
0
CFU/µl
3
3/4
4
4/5
MEF Grade

B

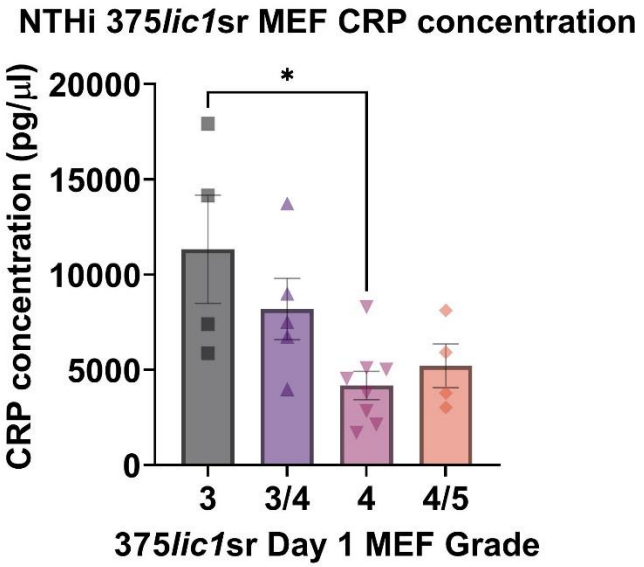
NTHi 375lic1sr MEF CRP concentration
CRP concentration (pg/µl)
20000
15000
10000
5000
0
*
3
3/4
4
4/5
375lic1sr Day 1 MEF Grade

C

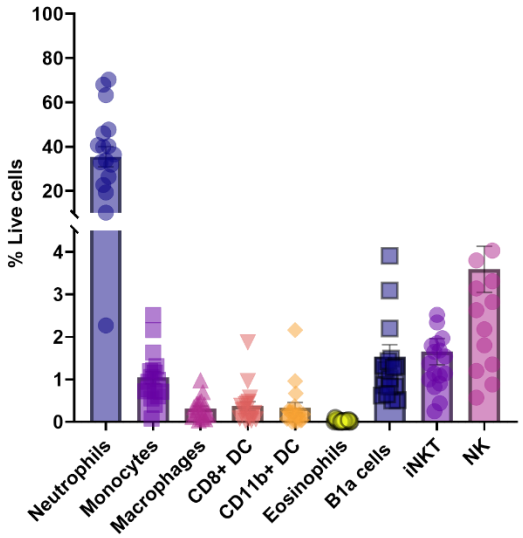
NTHi 375lic1sr MEF innate immune cells
% Live cells
100
80
60
40
20
4
3
2
1
0
Neutrophils
Monocytes
Macrophages
CD8+ DC
CD11b+ DC
Eosinophils
B1a cells
iNKT
NK

D

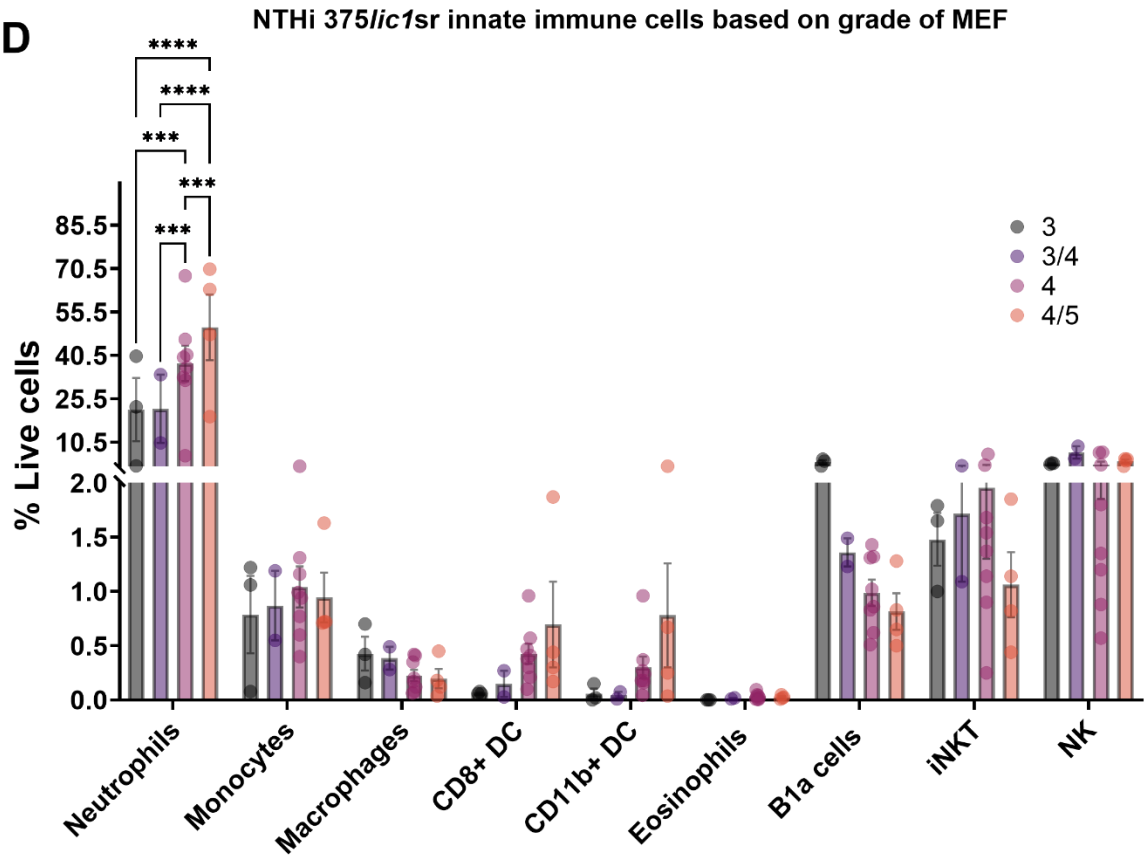
NTHi 375lic1sr innate immune cells based on grade of MEF
****
****
***
***
***
% Live cells
85.5
70.5
55.5
40.5
25.5
10.5
2.0
1.5
1.0
0.5
0.0
3
3/4
4
4/5
Neutrophils
Monocytes
Macrophages
CD8+ DC
CD11b+ DC
Eosinophils
B1a cells
iNKT
NK

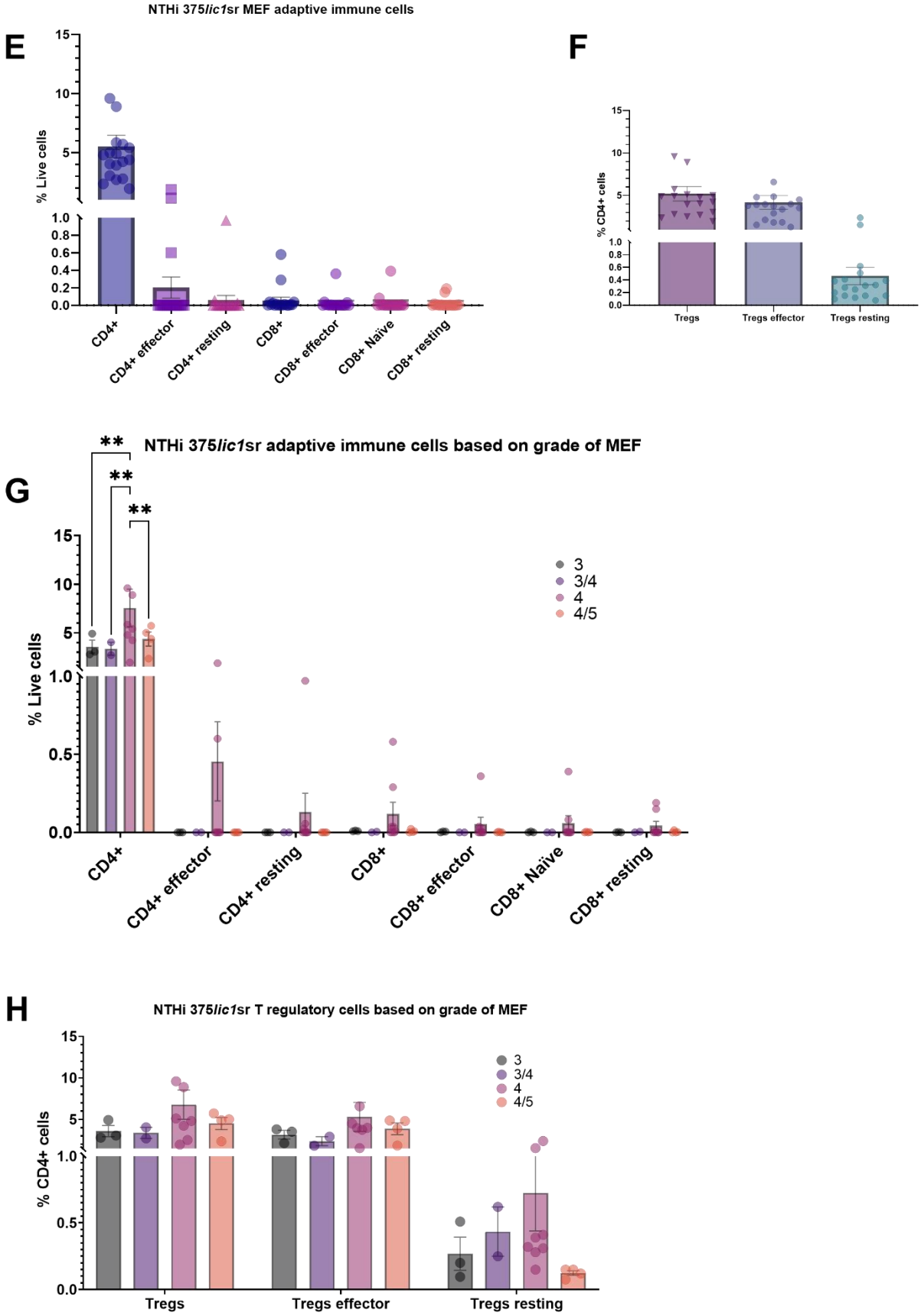
E
NTHi 375lic1sr MEF adaptive immune cells
% Live cells
CD4+
CD4+ effector
CD4+ resting
CD8+
CD8+ effector
CD8+ Naïve
CD8+ resting
F
% CD4+ cells
Tregs
Tregs effector
Tregs resting
G
NTHi 375lic1sr adaptive immune cells based on grade of MEF
**
**
**
% Live cells
3
3/4
4
4/5
CD4+
CD4+ effector
CD4+ resting
CD8+
CD8+ effector
CD8+ Naïve
CD8+ resting
H
NTHi 375lic1sr T regulatory cells based on grade of MEF
% CD4+ cells
3
3/4
4
4/5
Tregs
Tregs effector
Tregs resting

Figure 6.6. Acute phase response and immune profiling of *Junbo* mouse MEF day 1 post-inoculation of *Junbo* mice with NTHi 375*lic1*sr. CRP levels were normalised to per µl MEF (n=11). A) Bacterial titre per µl middle ear fluid for different grades day 1 post-inoculation of the *Junbo* mice with NTHi 375*lic1*sr. (B) CRP levels in different grades of MEF day 1 post-inoculation of the *Junbo* mice with NTHi 375*lic1*sr (n=11). (C) Innate immune profiling day 1 post-inoculation of *Junbo* mouse with NTHi 375*lic1*sr. (D) Innate immune cell populations for each grade categorisation of *Junbo* mouse MEF. (E) Immune profiling of adaptive immune cells day 1 post-inoculation of *Junbo* with NTHi 375*lic1*sr. (F) Treg cells (G) Adaptive immune cell populations for each grade categorisation of *Junbo* mouse MEF. (H) Treg cell populations for each grade categorisation of *Junbo* mouse ME (n = 9 mice). One-way ANOVA was performed followed by Brown-Forsythe test. Analysis was corrected for multiple comparisons by controlling the False Discovery Rate.

6.2.3.3 PCho off heptose III on NTHi 375 affects the acute phase response and immune cell profile in the different MEF grades from Junbo mice

The *lic1D* gene is a transferase that adds PCho to different hexose sugars off different heptoses on the LPS presented on the NTHi surface. The majority of the NTHi bacteria studied have preference to carry PCho on hexose I off heptose III (Schweda *et al.*, 2007). Other NTHi strains carrying PCho on different hexose sugars off different heptoses have also been reported. We investigated the effect of changing PCho position on the same NTHi strain on the cellular response in the *Junbo* mouse MEF. NTHi 375(2.8)sr, expresses PCho off heptose III, whereas NTHi 375sr expresses PCho off heptose I.

At day 1 post-inoculation of the *Junbo* mouse with NTHi 375(2.8)sr, the ME infection rate was 94%. This infection rate was similar to that observed for NTHi 375sr infection, where a 92% ME infection rate was found. The average NTHi 375(2.8)sr bacterial titre was 17.6% higher than that for NTHi 375sr at day 1 post-infection. An average of 52790 CFU/µl in the MEF was measured (figure 6.7A). The MEF CRP levels after NTHi 375(2.8)sr inoculation were also elevated at day 1 post-NTHi infection, similar to that observed for NTHi 375*lic1sr*. There was 1.5-fold increase in MEF CRP concentration compared to MEF CRP levels in *Junbo* mice infected with NTHi 375sr. NTHi levels were higher in higher grades of MEF, where CRP levels were lower (figure 6.7A-B). A negative regression correlation with a R^2 value of -0.81 between CRP levels and NTHi titre was calculated at day 1 post-NTHi 375(2.8)sr inoculation and this was statistically significant (*p 0.001*). This means there is an inverse relationship between NTHi 375(2.8)sr bacterial titre and CRP concentration in the *Junbo* mouse MEF.

Neutrophils were the most prevalent innate immune cells in the MEF, making up 43.8% of the total live cells (figure 6.7C). Neutrophil proportions increased as the grade of MEF increased (figure 6.7D), a trend similar to that observed for NTHi 375sr (6.5B). A decrease in the percentage of B1a cells in higher grade MEF was also observed similar to NTHi 375sr

(figure 6.7D), however the difference was not as prominent as that for infection with NTHi 375sr (figure 6.5B). A decrease in macrophage and iNKT cell proportions were also observed in higher grade MEFs, however these were 1.7-fold greater than that observed for NTHi 375sr infected mice. iNKT, $CD11b^+$ DCs and monocytes made up 2.6%, 2.4% and 2% of the total live cells (figure 6.7C). Monocytes proportion increased in higher grade MEFs, an observation similar to that made for NTHi 375*lic1*sr (figure 6.6C). The proportion of $CD11b^+$ cells were 1.5-fold greater when the PCho position was moved to heptose III compared to heptose I. A dramatically lower proportion of NK cells were also observed when PCho position was moved to heptose III.

For the adaptive immune cell populations in the *Junbo* mouse MEF, CD4+ T helper cells, and Tregs were the most prominent cell (figure 6.7F), similar to NTHi 375sr (figure 6.5D) and 375*lic1*sr (figure 6.6F) infection. There no significant difference in the adaptive immune cell profiles in the different grades of MEF (figure 6.7G and 6.7H).

These data suggest that there are similarities between immune cell profiles of NTHi 375sr and 375(2.8)sr inoculated *Junbo* mice. However, some differences were also observed between NTHi 375sr and 375(2.8)sr infected mice, for example an increase in $CD11b^+$ DCs and iNKT cells. Finally, an increase in CD4+ and CD8+ T cells was observed when the PCho position was moved to heptose III, compared to being on heptose I.

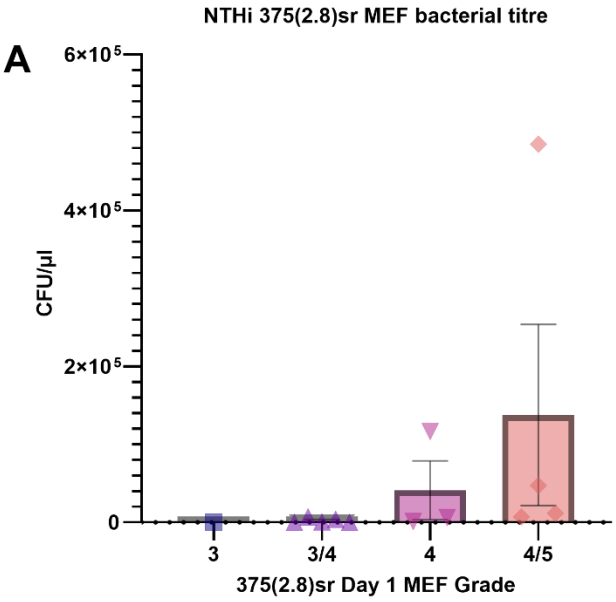
A
NTHi 375(2.8)sr MEF bacterial titre
6×10⁵
4×10⁵
2×10⁵
0
CFU/µl
3
3/4
4
4/5
375(2.8)sr Day 1 MEF Grade

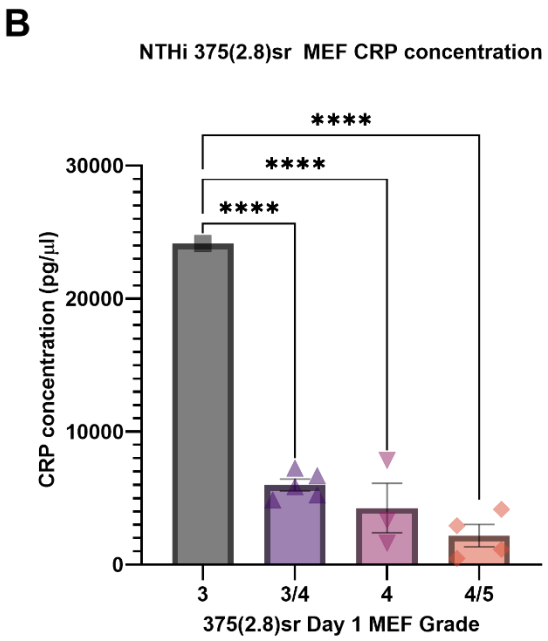
B
NTHi 375(2.8)sr MEF CRP concentration
****
****
****
30000
20000
10000
0
CRP concentration (pg/µl)
3
3/4
4
4/5
375(2.8)sr Day 1 MEF Grade

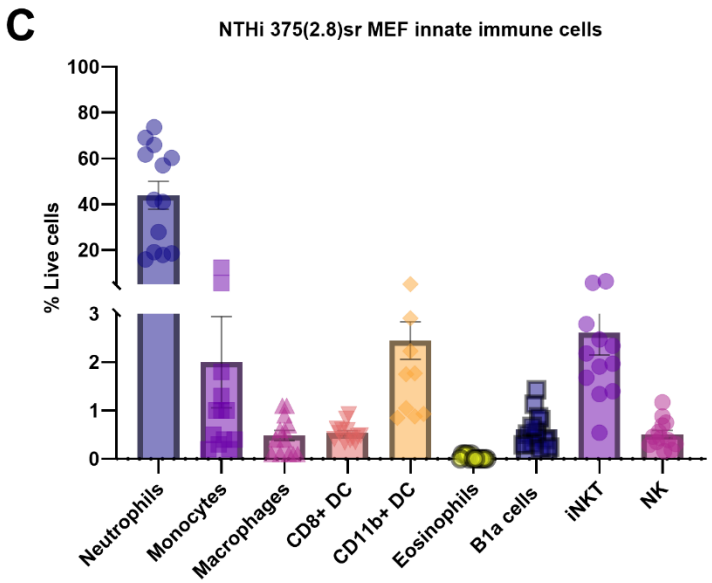
C
NTHi 375(2.8)sr MEF innate immune cells
% Live cells
100
80
60
40
20
3
2
1
0
Neutrophils
Monocytes
Macrophages
CD8+ DC
CD11b+ DC
Eosinophils
B1a cells
iNKT
NK

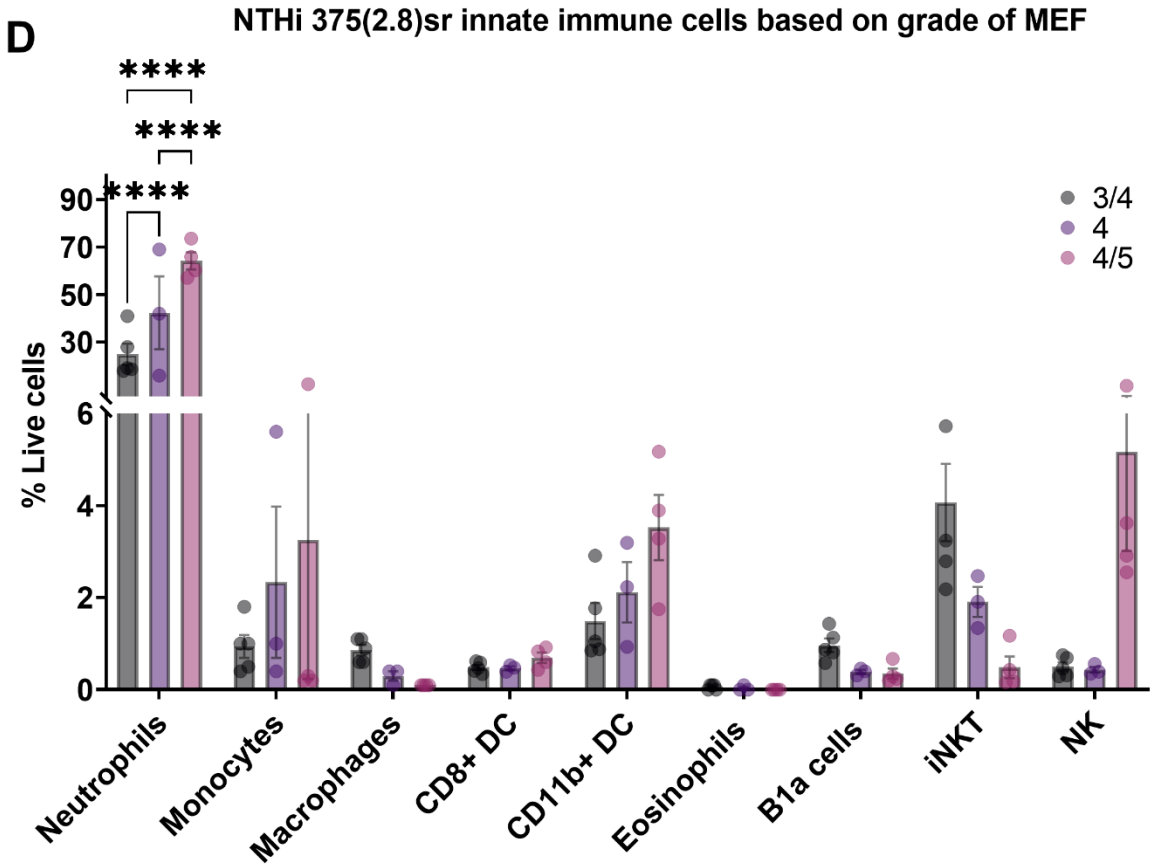
D
NTHi 375(2.8)sr innate immune cells based on grade of MEF
****
****
****
% Live cells
90
70
50
30
6
4
2
0
3/4
4
4/5
Neutrophils
Monocytes
Macrophages
CD8+ DC
CD11b+ DC
Eosinophils
B1a cells
iNKT
NK

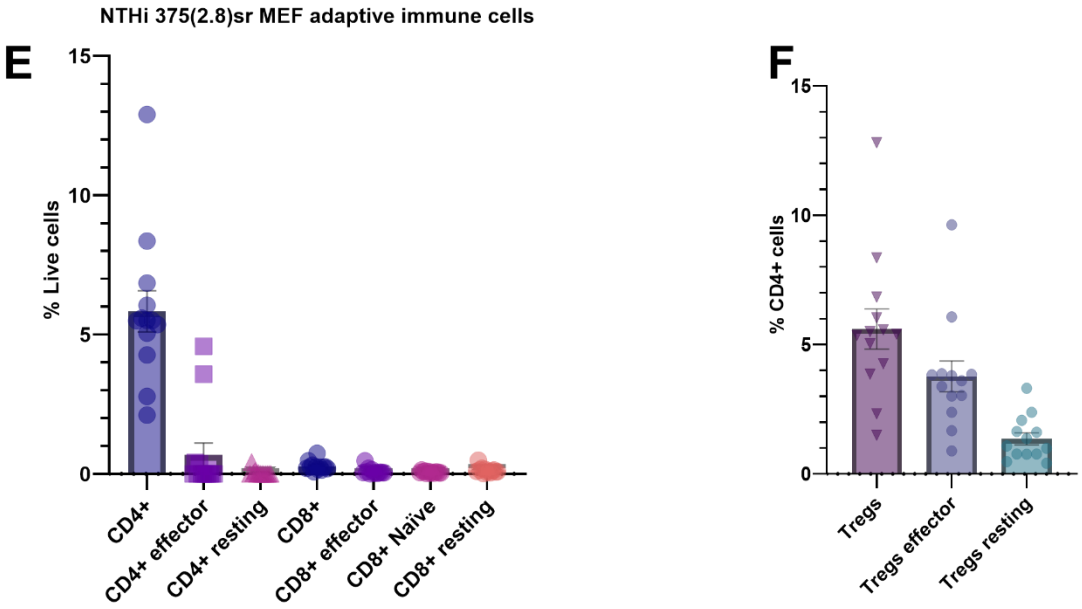
E
NTHi 375(2.8)sr MEF adaptive immune cells
% Live cells
15
10
5
0
CD4+
CD4+ effector
CD4+ resting
CD8+
CD8+ effector
CD8+ Naïve
CD8+ resting
F
% CD4+ cells
15
10
5
0
Tregs
Tregs effector
Tregs resting

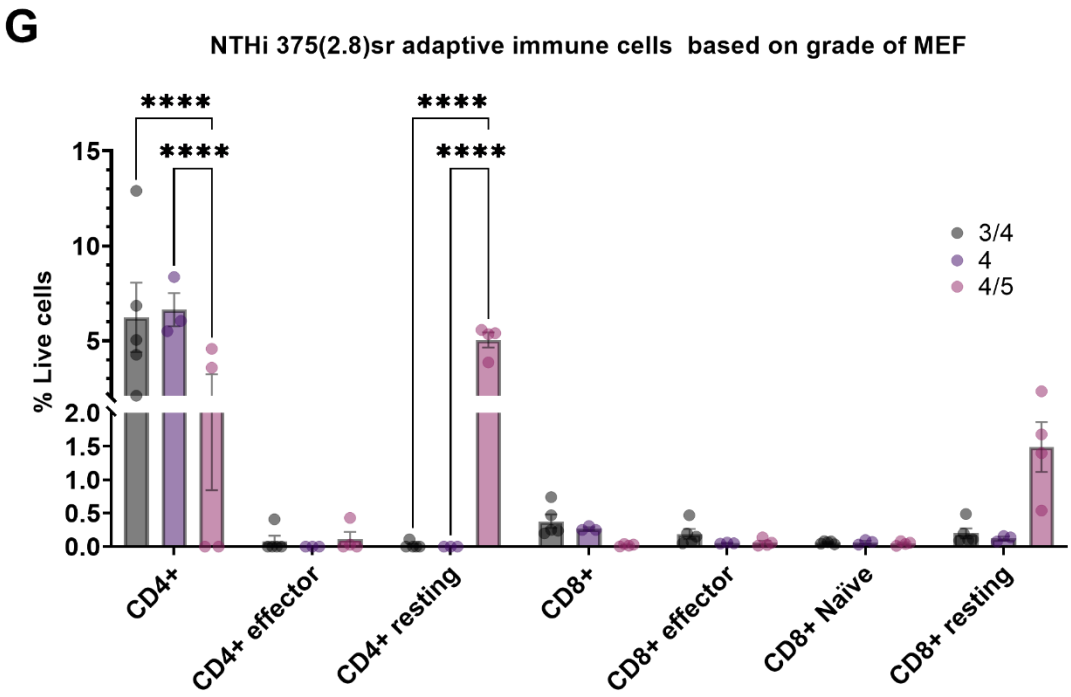
G
NTHi 375(2.8)sr adaptive immune cells based on grade of MEF
****
****
****
****
% Live cells
15
10
5
2.0
1.5
1.0
0.5
0.0
3/4
4
4/5
CD4+
CD4+ effector
CD4+ resting
CD8+
CD8+ effector
CD8+ Naïve
CD8+ resting

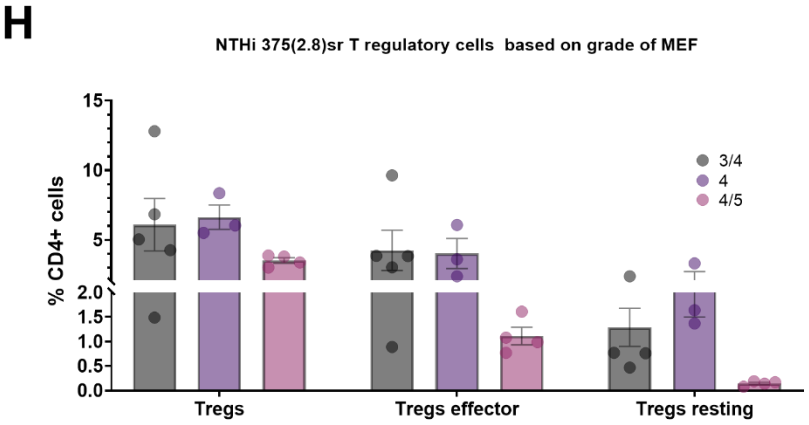
H
NTHi 375(2.8)sr T regulatory cells based on grade of MEF
% CD4+ cells
15
10
5
2.0
1.5
1.0
0.5
0.0
3/4
4
4/5
Tregs
Tregs effector
Tregs resting

Figure 6.7. Acute phase response and immune profiling of *Junbo* mouse MEF day 1 post-inoculation of *Junbo* mice with NTHi 375(2.8)sr. CRP levels were normalised to per µl MEF. A) Bacterial titre per µl MEF for different grades day 1 post-inoculation of the *Junbo* mice with NTHi 375(2.8)sr. (B) CRP levels in different grades of MEF day 1 post-inoculation of the *Junbo* mice with NTHi 375(2.8)sr. (C) Innate immune profiling day 1 post-inoculation of *Junbo* mouse with NTHi 375(2.8)sr. (D) Innate immune cell populations for each grade categorisation of *Junbo* mouse MEF. (E) Immune profiling of adaptive immune cells day 1 post-inoculation of *Junbo* with NTHi 375(2.8)sr. (F) Treg cells (G) Adaptive immune cell populations for each grade categorisation of *Junbo* mouse MEF (H) Treg cell populations for each grade categorisation of *Junbo* mouse MEF (n = 7 mice). One-way ANOVA was performed followed by Brown-Forsythe test. Analysis was corrected for multiple comparisons by controlling the False Discovery Rate.

6.2.4. PCho presence and position affects CRP levels and immune cell profile in the blood from Junbo mice infected with NTHi

To investigate the systemic response to NTHi and understand how it is different from the previously studied localized response in the MEF, we measured the CRP levels in the blood and next compared the immune response in the blood to NTHi 375 strain inoculation of the *Junbo* mouse. The immune response was studied day 1 post-inoculation with NTHi 375 strains.

Serum is the fluid and solute part of the blood that does not play a role in clotting, and it is where CRP is found normally after its production in the liver. In the serum, higher levels of CRP were measured in NI mouse serum compared to NTHi-inoculated serum. Overall, there was significantly less CRP upon NTHi infection in the blood compared to NI serum (figure 6.8A). Furthermore, CRP levels in the serum were lower than CRP levels in the MEF following infection with NTHi 375 strains (figure 6.5E, 6.6A, 6.7A, 6.8A).

To understand the effect of NTHi PCho position and expression on the innate immune system, we immunophenotyped innate cells in the blood. The proportion of dendritic cells (CD11b+ and CD8+ type) was highest in blood from NTHi 375(2.8)sr inoculated *Junbo* mice and lowest in blood following NTHi 375sr infection, although these differences for both subtypes were not statistically significant (figure 6.8B). Neutrophils were drastically elevated in blood from NTHi 375*lic1*sr infection compared to NI mice and mice infected with other NTHi 375 strains. They made up approximately 22.5% of the total live cells. This was 100-fold and 11-fold greater than blood samples from NTHi 375sr and 375(2.8)sr infected mice respectively. Eosinophils were the least abundant cells in the blood collected from any of the NTHi 375 strain infected mice. Monocytes were elevated most in blood from NTHi 375(2.8)sr (6.4% of total live cells) infected *Junbo* mice compared to other NTHi 375 strains and NI mouse samples. Blood from NTHi 375*lic1*sr infected mice had the second highest monocyte levels (3% total live cells) compared to NI and other blood samples from NTHi

375sr and NTHi 375*lic1*sr inoculated mice. Monocyte cell levels were similar between blood from NTHi 375sr infected mice (1.8% total live) and NI blood samples (1.4% total live cells). The highest proportion of macrophages were measured in blood from NTHi 375(2.8)sr infected mice (0.6%) compared to 0.04% and 0.1% in blood from NTHi 375sr and NTHi 375*lic1*sr infected mice. B1a cells were most elevated in blood from NTHi 375*lic1*sr (3.8% total live cells) and NTHi 375(2.8)sr (3.5% total live cells) infected mice, whereas for NTHi 375sr infected mice only 1.2% of total live cells were B1a cells. The above data suggests that PCho position and expression uniquely influenced innate immune cell phenotypes in the blood. Blood neutrophilia was markedly different between NTHi 375sr and 375*lic1*sr, where neutrophil numbers were highest in blood samples from 375*lic1*sr infection. This implies that PCho is inhibiting the neutrophilia.

Next, we looked at how PCho position and expression influences adaptive immunity in the blood. We immunophenotyped the cells of the adaptive immunity in the blood of *Junbo* mice. Most of the cells from the blood were NKT cells, making up 7.4% of the total live cells in NI blood samples. NKT cell numbers decreased in blood samples from NTHi 375sr and 375*lic1*sr infected mice compared to NI blood samples, but were elevated in blood from NTHi 375(2.8)sr infected mice. CD4+ T helper cells were the most dominant T cells in the blood, with the highest proportion in blood from NTHi 375*lic1*sr infected mice (7.3% of the total live cells, figure 6.9A). CD4+ T helper cells were slightly increased for NTHi 375(2.8)sr infection, however, for NTHi 375sr infection, the CD4+ T helper cells did not change compared to NI. The majority of the CD4+ T helper cells in the blood from NTHi 375*lic1*sr infected mice were Treg cells (figure 6.9B). This is the opposite of what we observed in the MEF (figure 6.4B), where Treg cells were lowest for NTHi 375*lic1*sr. NTHi 375*lic1*sr infected mice also had the highest proportion of CD8+ cytotoxic T cells, making up 4.2% of CD4+ cells compared to inoculation with NTHi 375sr (1.7% CD4+ T cells) and 375(2.8)sr (2.4% CD4+ T cells). The above data suggests that, PCho presence and position influences neutrophil proportions in the blood.

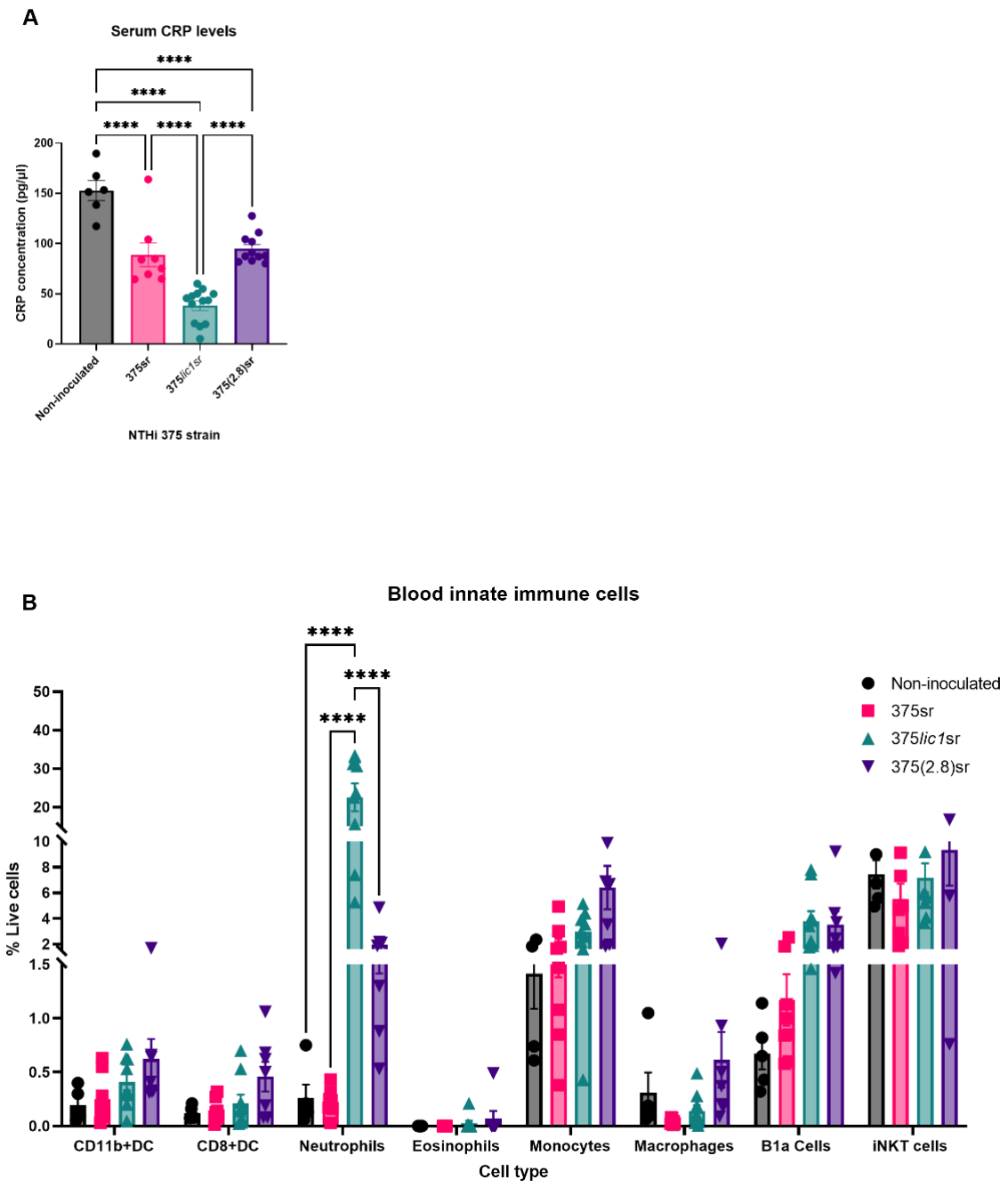

Figure 6.8. Acute phase and innate immune response in blood day 1 post-inoculation of *Junbo* mice with NTHi 375 strains. (A) Serum CRP levels day 1 post-inoculation of *Junbo* mice with NTHi 375 strains (NTHi 375sr (n=8), 375*lic1*sr (n=9) and 375(2.8)sr (n=6)) (B) Innate immune cells. Blood collected from mice via retro-orbital bleed. Non-inoculated *Junbo* mice were used as controls (n=5). Two-way ANOVA was performed followed by Brown-Forsythe test. Analysis was corrected for multiple comparisons by controlling the False Discovery Rate. *p <0.05, **p <0.01, ***p <0.001, ***p <0.0001

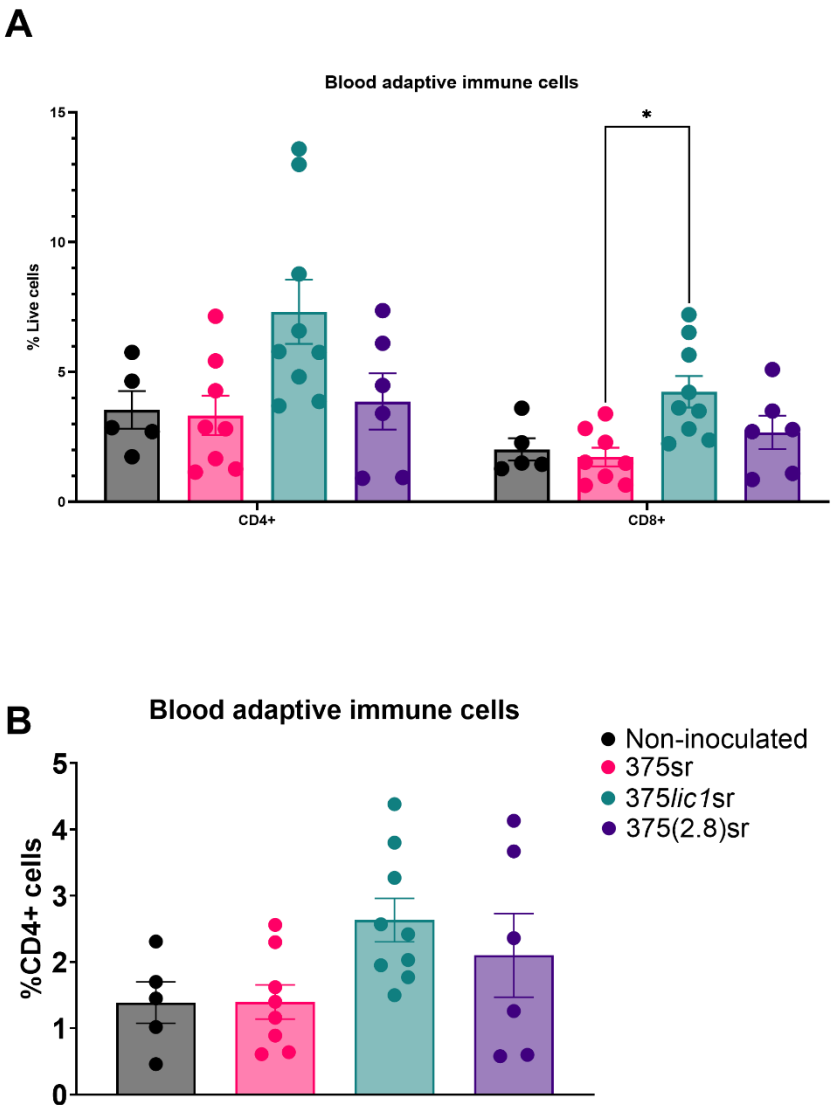

Figure 6.9. Adaptive immune response in blood day 1 post-inoculation of *Junbo* mice with NTHi 375 strains. (A) CD4+ and CD8+ T cell proportion in the blood. (B) Treg cell proportion in the blood. Blood collected from mice via retro-orbital bleed. Blood from day 1 post inoculation of *Junbo* mice with NTHi 375 strains (NTHi 375sr (n=8), 375*lic1*sr (n=9) and 375(2.8)sr (n=6)). Non-inoculated *Junbo* mice were used as controls (n=5). Two-way ANOVA was performed followed by Brown-Forsythe test. Analysis was corrected for multiple comparisons by controlling the False Discovery Rate. **p* <0.05, ***p* <0.01

6.2.5. Antigen presenting cells are the dominant cells in the NALT from NTHi 375sr infected Junbo mice

NALT represents the immune system of the nasal mucosa and plays a role in the protective immune response. In mice, NALT is described as a tonsil-like aggregation of adaptive immune tissue and is equivalent to the Waldeyer's ring in human (Debertin *et al.*, 2003). It is a poorly studied tissue with respect to infection. To understand the response to NTHi infection in the NALT of the *Junbo* mouse, and compare it to the previously studied systemic and localized response, we measured CRP abundance in the NALT followed by immunophenotyping of the NALT in response to NTHi 375 strains infecting the *Junbo* mouse, with the same mice used for systemic and localized response studies.

CRP levels were similar in NALT across mice infected with all the NTHi 375 strains, with slight elevation for NTHi 375(2.8)sr (figure 6.10). Compared to the MEF (figures 6.1E, 6.6A and 6.7A) and serum (figure 6.8), CRP levels in the NALT were drastically lower compared to other tissues and fluid from the *Junbo* mouse. This could largely be due to the way we collected the NALT sample and therefore needs further investigation (chapter 2, section 2.6.4).

We immunophenotyped the NALT, to understand the influence of PCho position and expression on the innate and adaptive cell composition in the NALT. CD8+ type DCs dominated the innate cell content in the NALT, making up 29% of total live cells in NI mouse samples (figure 6.10B). The highest proportion of CD8+ type DCs were measured in samples from mice infected with 375sr (57% total live cells), followed by 375*lic1*sr (49% total live cells) and 375(2.8)sr (34% total live cells). CD11b+ type-DCs were one of the least abundant cell types in the NALT. Neutrophil proportions decreased following NTHi 375 strain infection of the *Junbo* mice. A total of 3.3% of live cells in the NI NALT comprised of neutrophils. However, neutrophil proportions were much lower in *Junbo* mice infected with NTHi 375 strains mice where only 0.3% for NTHi 375sr, 0.68% for NTHi 375*lic1*sr and 0.1%

NTHi 375(2.8)sr neutrophils were present. Eosinophils levels increased following NTHi 375 strain infections, making up 5% of total live cells for NTHi 375*lic1*sr, 4.6% for NTHi 375(2.8)sr and 2.2% for NTHi 375sr. Monocytes were the next most dominant cell type in the NALT. We observed changes in eosinophil levels related to PCho expression and position changes. Infection with NTHi 375(2.8)sr led to a 3.3% decrease in eosinophil levels, whereas infection with NTHi 375sr and 375*lic1*sr led to a 6.3% and 2.3% increase. Similarly, PCho position and expression also drove a change in macrophage cell number in the NALT, where strikingly elevated numbers of macrophages was observed for infection with NTHi 375sr (48% total live cells). Finally, adaptive immune cells made up the lowest proportion of cell types in the NALT and we did not measure any significant cell type changes in infected mice (table 6.1).

The above data suggests that, PCho position influenced macrophage (and to a lesser extent, CD8+ DCs) proportions in the NALT. The highest proportion of macrophages (and CD8+ DCs) were observed for NTHi 375sr infection compared to infection with NTHi 375*lic1*sr and 375(2.8)sr in the *Junbo* mouse. Interestingly, PCho did not influence adaptive immune cell content of NALT. This suggests that PCho presence and position on the NTHi bacterium influences innate immune cells in the NALT.

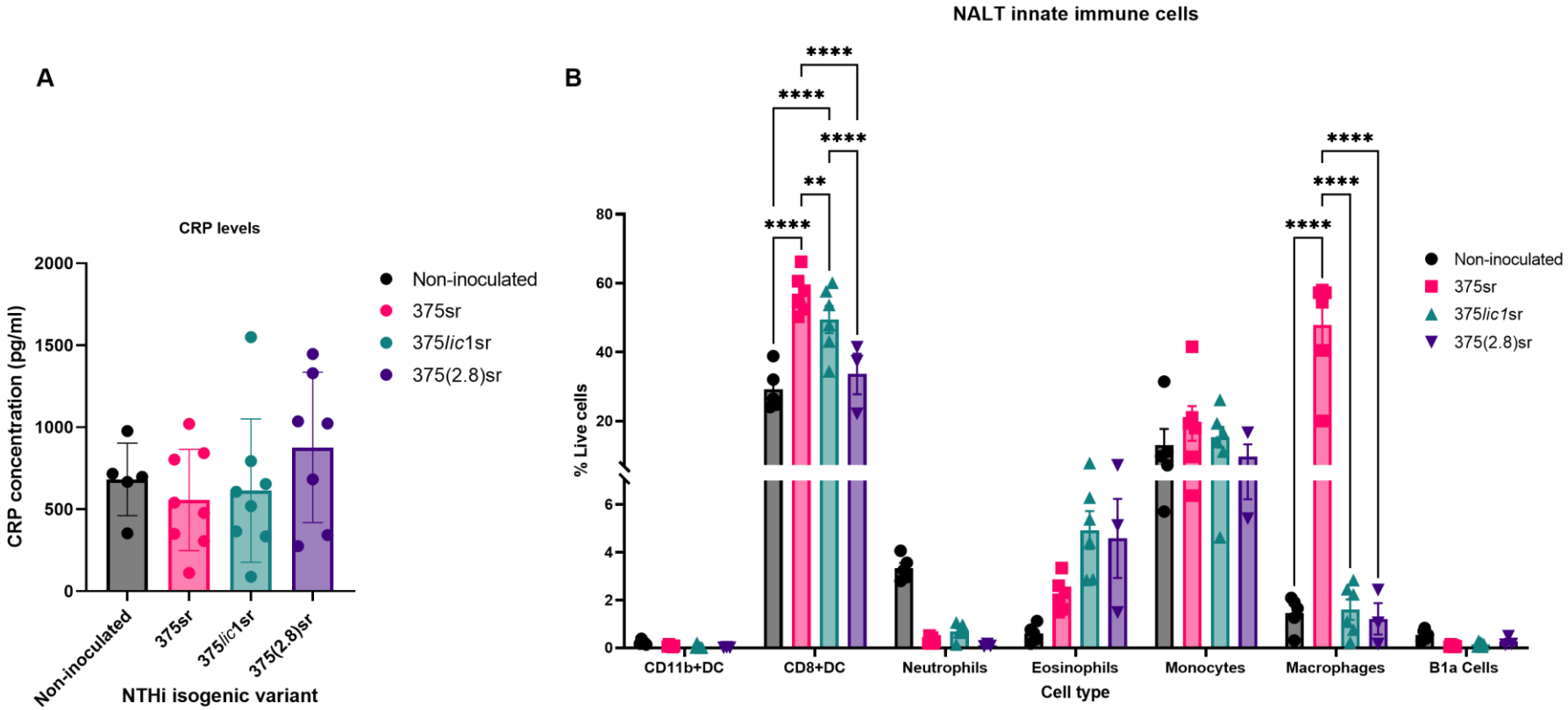

Figure 6.10. Acute phase and innate immune response in the NALT day 1 post-inoculation of *Junbo* mice with NTHi 375 strains. (A) NALT CRP levels day 1 post-inoculation of *Junbo* mice with NTHi 375 strains (NTHi 375sr (n=8), 375*lic1*sr (n=9) and 375(2.8)sr (n=6)) (B) Innate immune cells. Non-inoculated *Junbo* mice were used as controls (n=5). Two-way ANOVA was performed followed by Brown-Forsythe test. Analysis was corrected for multiple comparisons by controlling the False Discovery Rate. *p <0.05, **p <0.01, ***p <0.001, ***p <0.0001

Table 6 1 Adaptive immune cells in the NALT day 1 post-inoculation of *Junbo* mice with NTHi 375 strains

	Non-inoculated		375sr Day1		375*lic1*sr Day 1		375(2.8)sr Day1	
	% total live cells	±SEM	% total live cells	±SEM	% total live cells	±SEM	% total live cells	±SEM
CD4+	0.49	0.12	0.14	0.09	0.31	0.11	0	0
CD8+	0.01	0.01	0	0	0	0	0	0
	% CD4+ cells	±SEM	% CD4+ cells	±SEM	% CD4+ cells	±SEM	% CD4+ cells	±SEM
Treg cells	0.12	0.05	0.04	0.03	0.1	0.04	0	0

6.2.6. The presence and position of PCho on the NTHi surface influences macrophage phenotype in the tissues collected from Junbo mice

Previously, we observed similar macrophage numbers in the MEF of the NI, NTHi 375*lic1*sr and NTHi 375(2.8)sr infected *Junbo* mice. Macrophage numbers were lower in MEF from mice infected with NTHi 375sr (section 6.2.2., figure 6.3E). Macrophage phenotype (M1/M2) can contribute towards NTHi survival and persistence depending on its phenotype. For example, macrophage isolated from ME effusions from human release suppressive factors, leading to hyper-responsiveness, thus contributing to an increased risk of recurrent OM (Yamanaka *et al.*, 1982; Mittal *et al.*, 2018). In chapter 4, bone marrow derived macrophages infected with NTHi 375 strains showed differences in inflammatory response according to PCho presence and position. Therefore, we investigated how the macrophage phenotype, rather than the number varies across tissues in response to infection with NTHi 375 strains, with different levels PCho expression and positions. We investigated the macrophage phenotype in samples obtained from the *Junbo* mouse by calculating the M1/M2 ratio. This was calculated by dividing the proportion of M1-macophages with M2-like macrophages. M1 and M2 type macrophages were determined according to the expression of major histocompatibility complex II (MHCII) marker on the surface of the cells. MHCII is highly expressed on M1 macrophages. M1 macrophages are pro-inflammatory and M2 are anti-inflammatory. *Junbo* mice inoculated with NTHi 375 strains had a lower M1/M2 ratio compared to NI mice; *i.e*. the macrophages from these mice skewed towards M2-like macrophages (figure 6.11A). Inoculation with NTHi 375*lic1*sr had a higher M1/M2 ratio compared to NTHi 375sr and 375(2.8)sr, *i.e*. the macrophages from *Junbo* mice inoculated with NTHi 375*lic1*sr had a more M1-like phenotype compared to mice infected with NTHi 375 strains expressing PCho.

In the blood, mice infected with NTHi 375(2.8)sr had a 5-fold greater M1/M2 ratio than NTHi 375sr (figure 6.11B). Thus, blood macrophages were more M1-like following NTHi

375(2.8)sr inoculation compared to other NTHi 375 strain inoculations. NTHi 375sr and 375*lic1*sr had a lower M1/M2 ratio compared to NI serum, thus, similar to the MEF, these NTHi strains induce a more M2-phenotype in the blood.

For the NALT, all of the NTHi inoculation of mice induced a M2-like phenotype compared to NI NALT from the *Junbo* mice (figure 6.11C).

Together, we conclude that, NTHi drives a M2-like phenotype in the MEF, serum and NALT, with the exception of NTHi 375(2.8)sr in serum, where a more M1-like macrophages were present. We are first to report these findings that the presence and position of PCho on the NTHi surface influences macrophage phenotype in the MEF, serum and NALT of NTHi infected mice.

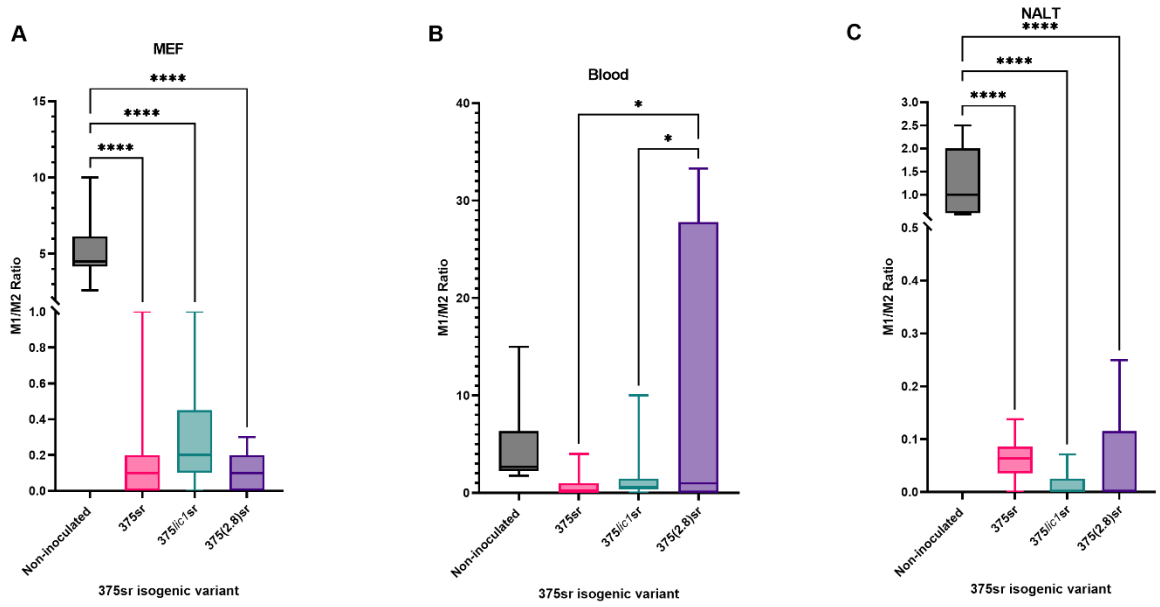

Figure 6.11. Macrophage phenotype in tissues collected from *Junbo* mice day 1 post-inoculation with NTHi 375 strains. (A) M1/M2 phenotype in the *Junbo* mouse MEF (B) M1/M2 phenotype in the *Junbo* mouse blood (C) M1/M2 phenotype in the *Junbo* mouse NALT. All tissues were collected from *Junbo* mice day 1 post-inoculation with NTHi 375 strains (NTHi 375sr (n=8), 375*lic1*sr (n=9) and 375(2.8)sr (n=6)). Non-inoculated *Junbo* mice were used as controls (n=5). Box plot displaying data as minimum to maximum. One-way *ANOVA* was performed followed by Brown-Forsythe test. Analysis was corrected for multiple comparisons by controlling the False Discovery Rate. *p <0.05, **p <0.01, ***p <0.001, ***p <0.0001

6.2.7. NTHi induces T regulatory cells

CD4+ T cells were the dominant T cell type in both, the NI and NTHi inoculated MEF and blood samples from the *Junbo* mice. Notably, most of the CD4+ T cells in the MEF were Treg cells (section 6.2.2). In the MEF, a higher proportion of Tregs was found following inoculation with NTHi strains (figure 6.4B). Although these data were not statistically significant, we hypothesised that NTHi could induce Treg cells and that Treg cells may add to dampened killing of NTHi in the *Junbo* mouse. Therefore, we carried out a Treg induction experiment to confirm if NTHi can induce a Treg cell response. Purified CD4+ T cells from the C3H/HeH mouse spleen were infected with NTHi 375sr, 375*lic1*sr or 375(2.8)sr. Treg markers CD25+ and FOXP3+ were used to measure Treg cells induction after 5 days of NTHi infection.

We observed an increase in Treg cell induction upon infection with NTHi (figure 6.12). Compared to untreated cells, NTHi 375sr had a 3.7-fold increase in Treg cells whereas both NTHi 375*lic1*sr and 375(2.8)sr had 2.7-fold increase. Overall, these data confirm that the NTHi can directly induce Treg cells.

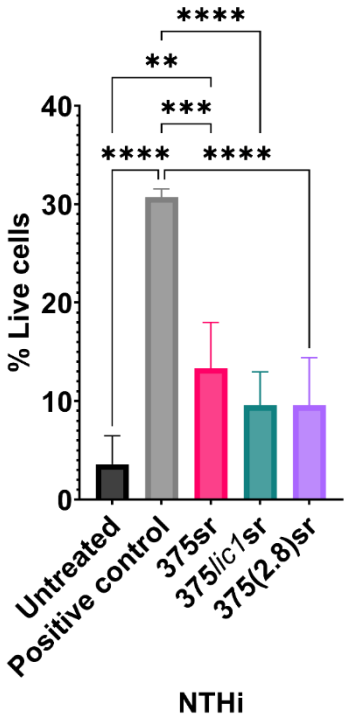

Figure 6.12. T regulatory cell induction. CD4+ T cells were incubated with NTHi 375sr, 375*lic1*sr and 375(2.8)sr for 5-days (n=3). CD25+ and FOXP3+ were used as markers for Treg cells. For positive control of Treg cell activation, CD4+ T cells were activated CD3 and CD28 antibodies. Cells are displayed as proportion of live cells. One-way *ANOVA* was performed followed by Tukey's post-hoc test. **p <0.01, ***p <0.001, ***p <0.0001

6.2.8. PCho presence and position on the NTHi surface influences cytokine and chemokine response in higher grade MEFs

Junbo mice inoculated with NTHi 375sr have a high ME infection rate and have higher bacterial titre in the higher grade MEFs (figure 6.1F) compared to NTHi 375*lic1*sr and NTHi 375(2.8)sr infected mice. NTHi 375*lic1*sr infection rate is over 40% lower than that for NTHi 375sr and the bacterial titre in the MEF of the *Junbo* mouse is 5.4-fold lower than for NTHi 375sr. NTHi 375*lic1*sr titre was greatest in higher grades of MEF (figure 6.6A). *Junbo* mice inoculated with NTHi 375(2.8)sr have a similar ME infection rate and bacterial titre to those mice inoculated with NTHi 375sr. However, differences were observed between the two strains when examining the different grades of MEF, where in higher grade MEF, NTHi 375(2.8)sr had lower average bacterial titre compared to similar grade MEF from NTHi 375sr infected mice (figure 6.7.A).

NTHi 375sr survived best in higher grade MEFs where there was higher CRP levels compared to NTHi 375(2.8)sr which survived better in high grade MEFs that had lower CRP levels. Therefore, we hypothesised that immune cell responses may be different in higher grade MEF from day 1 post-inoculations with NTHi 375 strains which could influence bacterial survival in the MEF of the *Junbo* mouse. Hence, we selected MEF fluids that were graded 3/4 and higher to study. To understand the immune cell cytokine/chemokine response to NTHi infection, we examined specific levels of cytokines and chemokines that could modulate the functional response of respective immune cells. Following the infection of the *Junbo* mouse with NTHi 375 strains, we analysed the cytokine and chemokine levels using a mouse cytokine and chemokine array.

Figure 6.13 shows the cluster analysis of 3 cytokine signatures. Cluster 1 included tumour necrosis factor- alpha (TNF-α), interleukin (IL)-12 p40/p70, IL-12p70, IL-2, MCP-5 and thrombopoietin (TPO). Cluster 2 included granulocyte-colony stimulating factor (GCSF), Granulocyte macrophage colony-stimulating factor (GM-CSF), IL-3, IL-5, IL-4, vascular

endothelial growth factor (VEGF), IL-17 and interferon gamma (IFN-γ). Cluster 3 included IL-10, IL-13, stem-cell factor (SCF), soluble tumour necrosis factor receptor I (sTNF RI), IL-6, macrophage chemoattractant protein-1 (MCP-1), IL-9 and RANTES. We looked at the cytokine and chemokine levels in each individual *Junbo* mouse for NI and NTHi 375sr inoculated cohorts. This is because each mouse had a variable cytokine and chemokine response. Emanuele Marchi kindly carried out cluster analysis for each test condition to identify subgroups based on the respective cytokine profile.

Infection of the *Junbo* mouse with NTHi 375sr resulted in MEF with elevated cytokines in clusters 2 and 3 compared to NI *Junbo* mice (figure 6.13). NTHi 375sr mice 1 and 2 had similar cytokine profiles to each other compared to NTHi 375sr mouse 3. MEF from day 1 post-inoculation with NTHi 375sr *Junbo* mouse 3 cytokine profile was similar to NI *Junbo* mouse 2. NTHi was present in all the MEFs from day 1 post-inoculation with NTHi 375sr. Cluster 2 and 3 includes T helper (Th) 1 and Th2 cytokines. IFN-γ is a key cytokine in the Th1 response, whereas IL-4 is a one of the dominant Th2 cytokines. Other Th2 cytokines, IL-5, IL-13 and IL-10 were also elevated in day 1 post-NTHi 375sr inoculated *Junbo* mouse 1 and 2 compared to NI MEF. CD4+ T helper cells can be subdivided into Th1, Th2 and Th17 depending on the cytokines they produce (Berger, 2000). Th1 cytokines are produced in a response to intracellular pathogens. IFN-γ is a Th1 cytokine and was elevated in day 1 post-NTHi 375sr inoculated *Junbo* mice 1 and 2 compared to NI MEF. Th2 cytokines are involved in the eradication of extracellular pathogens. IFN-γ and IL-4 were both equally elevated in the MEF of NTHi 375sr inoculated *Junbo* mouse 1 and 2. This suggests neither Th1 nor Th2 response is dominant yet at day 1 of NTHi 375sr infection. Th17 cells protect against extracellular pathogens that Th1 or Th2 immunity are not suited for (Tesmer *et al.*, 2008). Th17 produce IL-17 that recruits neutrophils. Th17 cytokine, IL-17 was detected in *Junbo* mice 1 and 2.

GCSF and GM-CSF cytokines were elevated in NTHi 375sr *Junbo* mouse 2. GCSF is produced by macrophages and neutrophils. It promotes proliferation and differentiation of

mature granulocytes. GM-CSF is produced by macrophages, T cells and NK cells to recruit neutrophils and monocytes. IL-3 was elevated in MEF from day 1 post-NTHi 375sr inoculated *Junbo* mice. IL-3 is secreted by activated T cells and activates mature neutrophils and macrophages. Neutrophils (figure 6.3A), macrophages (figure 6.3E), NK cells (figure 6.3I) and T cells (figure 6.4) were detected in the *Junbo* MEF following day 1 post-infection with NTHi 375sr. VEGF levels were elevated at day 1 post-inoculation with NTHi 375sr in *Junbo* mice1 and 2 compared to NI MEFs. VEGF increases vascular permeability and plays a role in the generation of ME effusion during OM (Husseman *et al.*, 2012). The cytokine and chemokine profiles in MEFs of NTHi 375sr infected *Junbo* mice suggest NTHi 375 increase T cell response compared to NI mice. Th1, Th2 and Th17 cytokines were elevated in the MEF in a response to NTHi, but day 1 post-infection may be too early to confirm which Th response is dominant.

In day 1 post-NTHi 375*lic1*sr inoculated *Junbo* mouse 1 MEF, IL-12 p40/70 and IL12p70 in cluster 1 were elevated the most compared to 375*lic1*sr inoculated *Junbo* mouse 2 and 375*lic1*sr inoculated *Junbo* mouse 3 MEF. IL-12 p40p70 was elevated the most in this cluster followed by IL-12p70. IL-12 p70 cytokine is composed of two heterodimers, p40 and p35 and is the active form of IL-12. IL-12 p40/p70 is composed of both p70 and the heterodimers (p40 and p70). Macrophages and dendritic cells produce IL-12 p70 and IL-12 p40/p70 cytokines and both of these cell types were observed in the MEF of *Junbo* mice inoculated with NTHi 375*lic1*sr (figure 6.3C, D and E). MCP-5 in cluster 1 was the most elevated cytokine in day 1 post-375*lic1*sr inoculated *Junbo* mouse 1 MEF compared to 375*lic1*sr mice 2 and 3. MCP-5 is a potent chemoattractant and is expressed in activated macrophages (Sarafi *et al.*, 1997). A rise in IL-12 p40/p70, IL-12 p70 and MCP-5 could influence survival of NTHi 375*lic1*sr in the MEF of *Junbo* mice. NTHi 375(2.8)sr inoculated mouse 1 also had a similar increase in the cluster 1 cytokines to NTHi 375*lic1*sr mouse 1 (although the cytokine/chemokines were not as highly expressed as NTHi 375*lic1*sr). This suggests that 375(2.8)sr (PCho off heptose III) may induce a cytokine/chemokine response

more similar to NTHi 375*lic1*sr (PCho mutant) than NTHi 375sr (PCho off heptose I). Activated phagocytes (macrophages and dendritic cells) and the pro-inflammatory cytokine response may lead to clearance of NTHi 375*lic1*sr and NTHi 375(2.8)sr in the *Junbo* mouse MEF.

For NTHi 375(2.8)sr, IL-10 was elevated in MEFs of the *Junbo* mice compared to NI mouse MEFs. IL-10 levels were not detected in MEF from NTHi 375*lic1*sr infected mice. Only mouse 3 from NTHi 375sr infected *Junbo* mouse had elevated IL-10.

NTHi 375*lic1*sr infection in the *Junbo* mouse did not activate the cytokine and chemokine response as strongly as NTHi 375sr. The cytokine and chemokine levels following NTHi 375(2.8)sr infection of the *Junbo* mouse were generally higher than those for NTHi 375*lic1*sr infection. However, levels of cytokines and chemokines following NTHi 375(2.8)sr infection were generally lower than those seen for NTHi 375sr.

Together, these data suggest that NTHi 375 strains elicit different inflammatory cytokine/chemokine response in the *Junbo* mouse MEF. As well as influencing the infection rates, bacterial titres, CRP levels and cellular responses, PCho presence and position on the NTHi surface can influence the cytokine/chemokine response in higher grade MEFs. This can help explain the differences observed in bacterial titre between the NTHi strains in higher grade MEF.

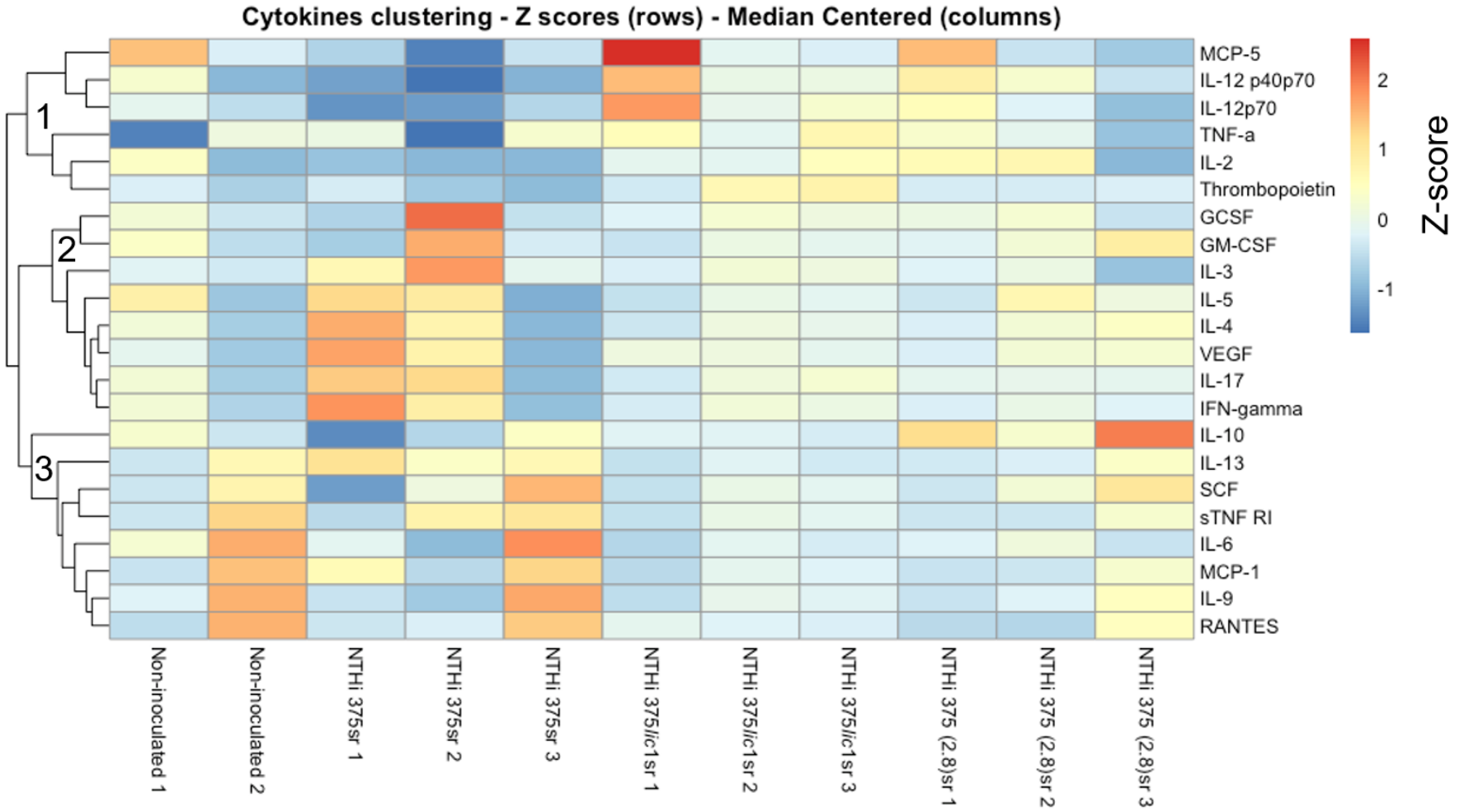

Figure 6.13. Clustering chemokine and cytokine levels in *Junbo* mouse MEF day 1 post-inoculation with NTHi 375 strains. Immunoblot to measure cytokine/chemokine levels was performed on MEF from *Junbo* mice infected with NTHi 375 strains. Distribution of each sample was centralised across each row and column for each cytokine/chemokine (Z score by row). Data was normalised to the number of NTHi using the median in the *Junbo* mouse MEF. (n=3 for each condition tested).

6.2.9. PCho presence and position on the NTHi surface influences inflammatory response in the NP of the Junbo mouse

The cytokine and chemokine profile was different in the high viscosity MEFs following 1 day of infection of NTHi 375 strains in the *Junbo* mouse. NTHi 375sr survived in the presence of inflammatory cytokine/chemokines compared to NTHi 375*lic1*sr and 375(2.8)sr. Cytokine and chemokine responses in other tissues, including the NP, could influence the bacterial survival in the NP and therefore affect infection to the MEF. Cytokine and chemokine levels in the NP might help explain a link between the commensal and pathogenic behaviour of NTHi

Appendix figure 4 shows the preliminary cytokine and chemokine profile from NI and NTHi strain 375sr NP *Junbo* mouse NP samples. We compared the cytokine/chemokine levels in the NP following 1 day of infection with NTHi 375*lic1*sr or NTHi 375(2.8)sr with NTHi 375sr infection. We inoculated the *Junbo* mice intranasally and performed nasal passage washes (NPW) at 1 day post-inoculation. We cultured bacteria from the NPW on BHI plates to estimate the bacterial titres. However, very few colonies were detected (data not shown due to very low numbers). This suggests that NTHi in the NP of the *Junbo* mouse may behave similarly to commensal bacteria (in human). The immune response in the NP could influence the NTHi infection of the ME and bacterial titres in the MEF.

Figure 6.14 shows the cytokine/chemokine profiles in the NP. Each cytokine/chemokine was plotted as log fold-change to quantify the changes observed between NTHi 375sr and 375*lic1*sr or 375(2.8)sr. Cytokines/chemokines that were 1.5-fold different compared to NTHi 375sr were classified as significant changes in the cytokine/chemokine profile. NTHi 375*lic1*sr in the NP had 3.6- and 3.8- fold lower Th2 cytokines IL-6 and IL-10 respectively, than NTHi 375sr infected mice, suggesting PCho presence or absence can have some influence on factors relevant to commensal behaviour in the NP. IL-12 p40/70 was 3.7-fold lower in the NP after 1-day of infection with NTHi 375(2.8)sr compared to NTHi 375sr

infection. IL-12 p40/70 drives the humoral response. This suggests that the position of PCho on the NTHi surface can influence the cytokine/chemokine response in the NP.

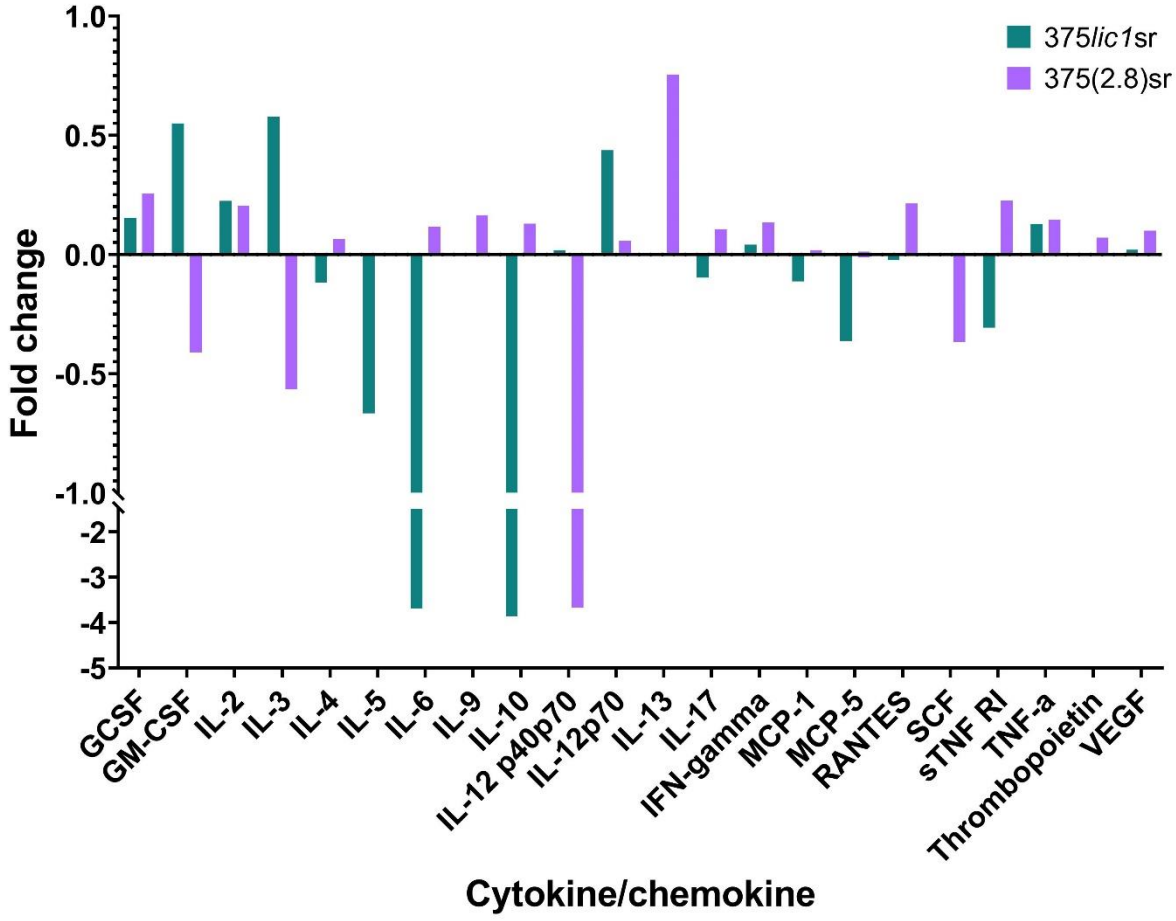

Figure 6.14. Chemokine and cytokine levels in *Junbo* mouse nasal passage wash day 1 post-inoculation with NTHi 375 strains. Fold change for NTHi 375*lic1*sr and 375(2.8)sr was calculated relative to NTHi 375sr. Data represented as log2 fold change (n=1 nasal passage wash sample per NTHi 375 strain)

6.2.10. PCho presence and position on the NTHi surface influences production of pro-inflammatory cytokines that increase blood neutrophil levels

Biomarkers in the serum are used to help diagnose AOM and identify the type of pathogen causing the disease (Schilder *et al.*, 2016). We compared the cytokine/chemokine levels in the serum at day 1 post-infection of *Junbo* mice with NTHi 375 strains. Appendix figure 5 shows the preliminary cytokine/chemokine profile from NI and NTHi 375sr infected *Junbo* mouse serum samples. We compared the cytokine/chemokine levels in the serum samples 1 day post-infection with NTHi 375*lic1*sr or NTHi 375(2.8)sr with NTHi 375sr infection (figure 6.15).

GM-SCF, IL-3, IFN-γ and MCP-1 were upregulated more than 2-fold after 1 day infection of the *Junbo* mouse with NTHi 375*lic1*sr compared to NTHi 375sr infection. IL-3 is produced by activated T cells and activates mature neutrophils and macrophages. Neutrophil and monocyte cell proportions were higher in blood from NTHi 375*lic1*sr compared to NTHi 375sr infected mice (figure 6.8B). MCP-1 directs the migration and filtration of monocytes and memory T cells at the site of infection. (Singh, Anshita and Ravichandiran, 2021). MCP-1 also regulates monocyte differentiation into dendritic cells. Macrophages are one of the primary cells producing MCP-1. CD4 T helper, CD8 cytotoxic and NK cells produce IFN-γ. IFN-γ leads to activation of macrophages and induces the expression of major histocompatibility complex. CD8+ T cells and NK cells were elevated in the blood from the *Junbo* mouse inoculated with NTHi 375*lic1*sr compared to NTHi 375sr inoculated mice (figure 6.9). This suggests that the elevated proportion of CD8+ T and NK cells could be responsible for the elevated IFN-γ production observed.

GM-CSF and SCF levels increased in the serum by over 1.5-fold following infection with NTHi 375*lic1*sr compared to NTHi 375sr. GM-CSF is produced by macrophages, T cells and NK cells to recruit neutrophils and monocytes. Neutrophils had one of the most elevated cell proportions of in the blood from the *Junbo* mouse following 1-day infection with NTHi

375(2.8)sr (figure 6.8B). Monocytes were also elevated in the NTHi 375sr infected *Junbo* mouse blood (figure 6.8B). SCF is involved in haematopoiesis and heightens the proliferation of the adaptive immune or innate immune cells. SCF also promotes mast cell growth and degranulation functions (Mak and Saunders, 2006).

In conclusion, PCho presence and position on the NTHi surface produces pro-inflammatory cytokines that could be correlated with the observed increase in blood neutrophil levels following infection of the *Junbo* mouse (figure 6.8).

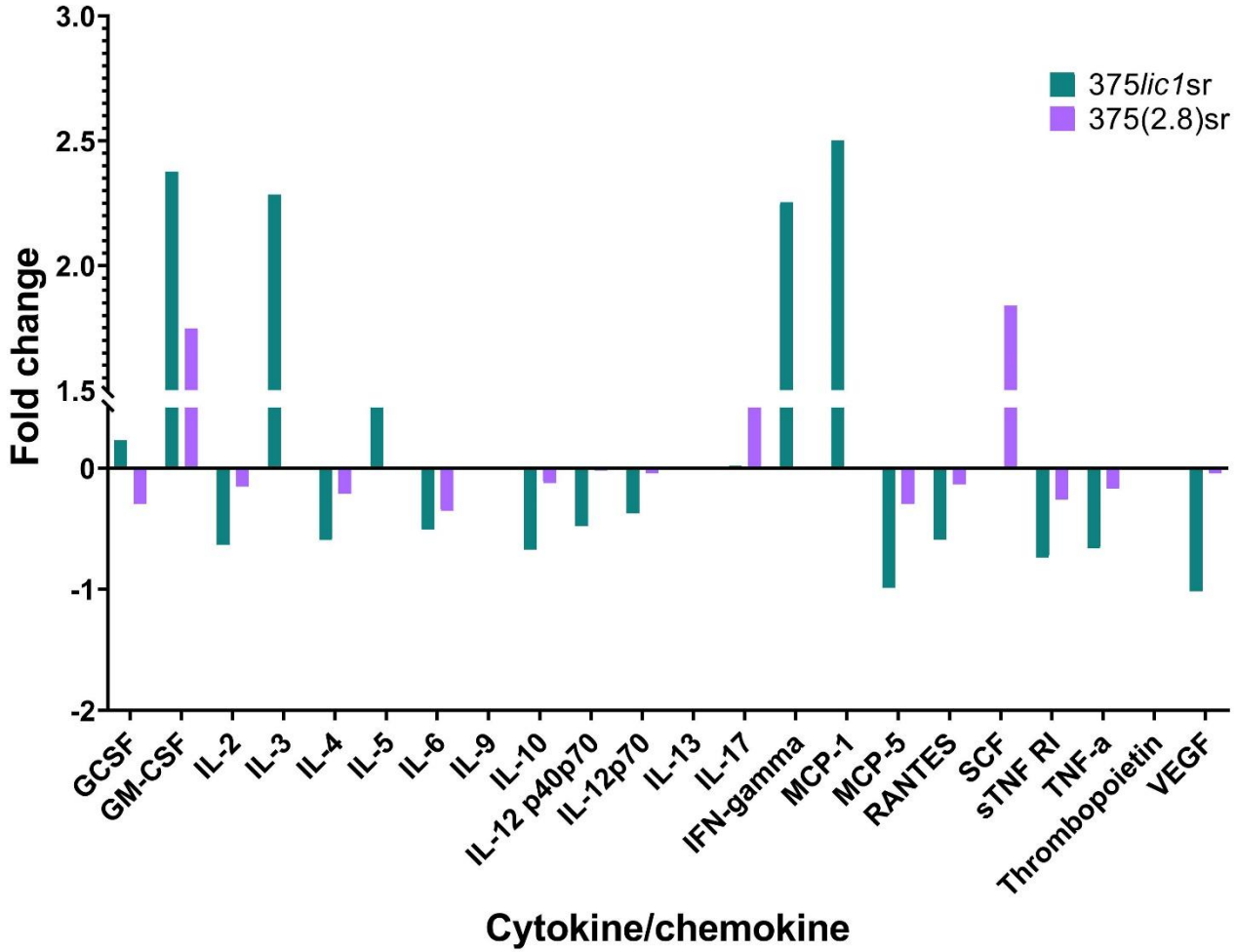

Figure 6.15. Chemokine and cytokine levels in *Junbo* mouse serum day 1 post-inoculation with NTHi 375 strains. Fold change for NTHi 375*lic1*sr and 375(2.8)sr was calculated relative to NTHi 375sr.Data represented as log2 fold change (n=1 serum sample per NTHi 375 strain).

6.2.11. 1 day post-inoculation of the Junbo mouse with NTHi 375 strains is too early a time-point to study all potential cytokine/chemokine changes

NALT is analogous to Waldeyer's ring in human and is important for the generation of mucosal immunity. Appendix figure 8 shows the preliminary cytokine/chemokine profile of NALT from *Junbo* mice infected with NTHi 375sr, 375*lic1*sr or 375(2.8)sr. We compared the cytokine/chemokine levels in the NALT samples obtained 1 day following infection with NTHi 375*lic1*sr or NTHi 375(2.8)sr with NTHi 375sr infection (figure 6.16). We did not observe any major differences in the levels of cytokines and chemokines after infection with either of the three NTHi 375 strains. IFN-γ was reduced 3.9-fold following infection with NTHi 375(2.8)sr compared to NTHi 375sr. SCF was reduced 3.1 fold following both NTHi 375*lic1*sr and 375(2.8)sr inoculations compared to NTHi 375sr infection. Day 1 post-infection infection may be too early a time-point to see any significant changes in the NALT cytokine and chemokine profiles.

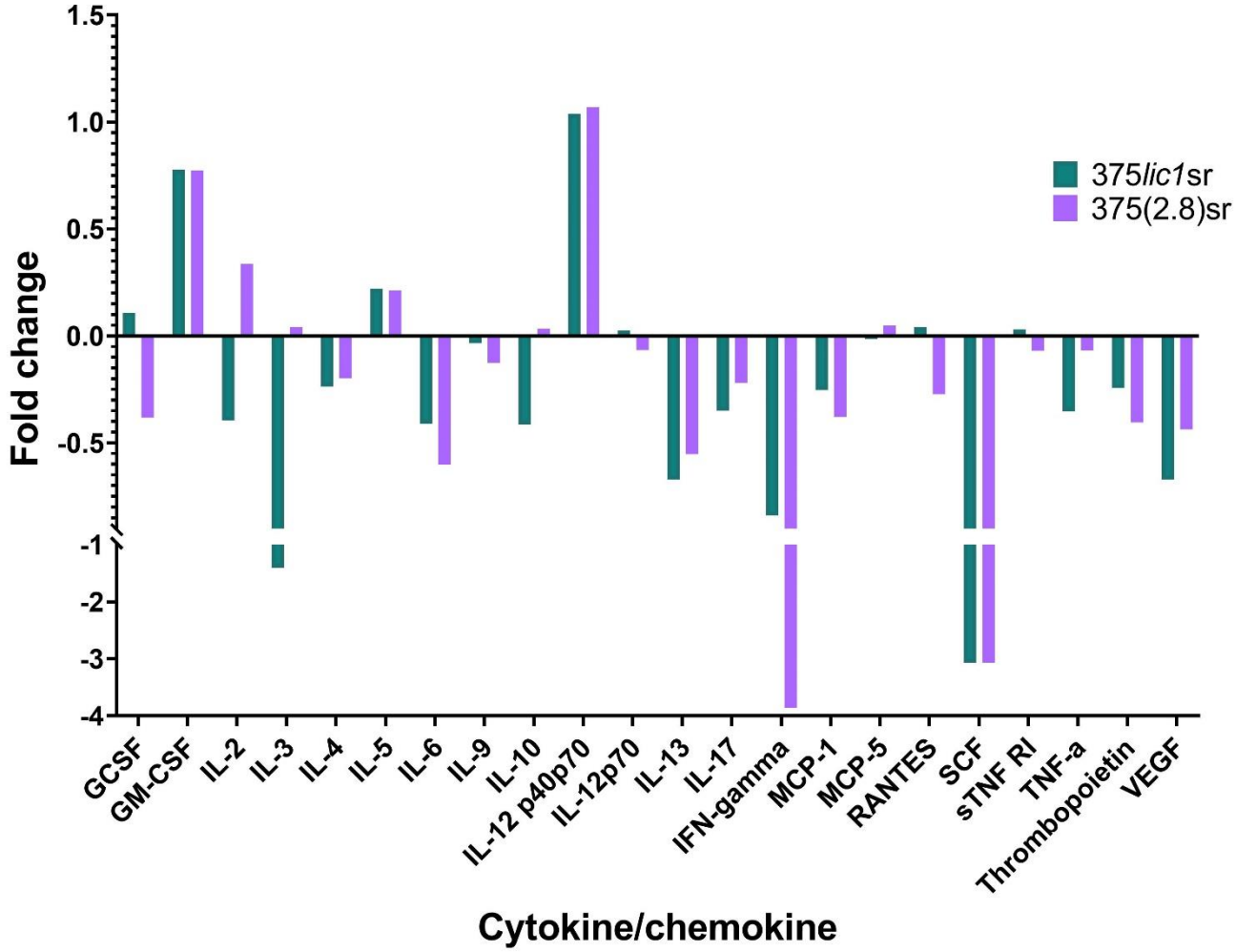

Figure 6.16. Chemokine and cytokine levels in *Junbo* mouse NALT 1 day post-inoculation with NTHi 375 strains. Fold change for NTHi 375*lic1*sr and 375(2.8)sr was calculated relative to NTHi 375sr.Data represented as log2 fold change (n=1 NALT sample per NTHi 375 strain)

6.3. Discussion

We used the *Junbo* mouse infection model to investigate how the presence and position of PCho on the surface of NTHi influences host-pathogen interactions relevant to commensal and disease behaviour of the bacteria. A single intranasal inoculation with NTHi 375 strains results in high rates of infection in the pre-existing inflamed ME of the *Junbo* mouse. Previous studies by our research group have reported that the composition of the *Junbo* mouse MEF influences both NTHi infection rate and bacterial titre attained in the ME (Hood *et al.*, 2016; Vikhe *et al.*, 2019). A similar infection strategy was adopted in this study. These properties of the model enabled us to study changes in infection rate, bacterial titre, acute phase response, immune cell and cytokine/chemokine composition following 1 day of infection with NTHi 375 strains, which differed in their patterns of PCho expression and position.

Even although CRP is not considered as the main acute phase protein in the mouse, changes in CRP levels post-inflammatory stimuli have been reported (Patterson and Higginbotham, 1965; Whitehead *et al.*, 1990). Transgenic mice expressing the human CRP gene have been used to study the action of CRP in inflammation and infection. However, as both human and mouse CRPs are present in these transgenic mice, it cannot be ruled out that the presence of both mouse and human CRP together may affect the apparent functions of the protein (Torzewski, Waqar and Fan, 2014). Furthermore, function of the transgenic CRP and its interaction within the murine environment such as cellular receptors and the extracellular matrix are not fully understood. Infection of the *Junbo* mouse with NTHi 375sr days 1, 3 and 7 post-inoculations showed that CRP levels are highest at day 1 of infection, whereas at day 3 and 7, the levels of CRP dropped. This is because CRP is an acute phase protein whose concentrations in the human increase dramatically at the onset of inflammation. The half-life of CRP in humans is 19-hours in health and disease (Pepys and Hirschfield, 2003). In human, serum CRP concentrations rise by 6 hours and peak

around 48 hours following the onset of inflammation or disease. The half-life of mouse CRP is not known, however, our data suggests mouse CRP levels are highest at day 1 post-NTHi infection. Baseline concentrations of CRP in the NI *Junbo* mouse and C3H/HeH mouse MEFs were similar, suggesting that the *Evi1* mutation does not affect the CRP levels observed in the *Junbo* mouse. The pre-existing inflammation in the *Junbo* mouse ME permits infection with NTHi. Whereas, NTHi does not infect C3H/HeH mice. C3H/HeH mice do not develop OM and therefore do not have MEF, thus, ME washes were used to determine CRP levels following NTHi infection. Similarly, ME washes were performed in *Junbo* mice that had clear MEs (*i.e*. no MEF present). CRP levels in the ME washes from clear MEs following NTHi infection in the *Junbo* mouse had similar baseline CRP levels to MEF of NI *Junbo* and ME washes from C3H/HeH mice. This confirms that the presence of NTHi per se causes elevated MEF CRP levels in the *Junbo* mouse. ME washes from C3H/HeH mice inoculated with NTHi 375sr did not have elevated CRP levels. The *Junbo* mouse is therefore a robust animal model to study CRP following NTHi infection.

Junbo mice were infected with NTHi 375 strains to investigate the effect of PCho presence and position on the NTHi surface on CRP levels and the host cellular response. Both mouse and human CRP are similar in structure and bind to PCho in a calcium dependent manner (Lu *et al.*, 2018). The *Junbo* mouse develops OM around 4 to 5 weeks of age. We used 5-week old *Junbo* mice to determine if CRP levels change at the onset of OM. We showed that CRP levels in the 5-week old *Junbo* mouse increase around the time of development of OM and that CRP levels increase further in 5-week old *Junbo* mice with OM when inoculated with NTHi 375sr. However, at 5-weeks of age, many of the *Junbo* mice have not developed OM yet and only a 50% ME infection rate were observed 1 day post-inoculation with NTHi 375sr. By 11-weeks of age, most *Junbo* mice have bilateral OM and constant MEF. We used IHC to visualise CRP staining in the MEF for *Junbo* mice infected with NTHi 375sr post day-1 inoculation. We do indeed observe staining in the MEF; however, it is unclear where this CRP is coming: is it produced locally by immune cells or epithelial cells

or is it transported from the liver? CRP is known to be expressed in epithelial cells in respiratory mucosal surfaces (Jane M. Gould and Weiser, 2001; Ramage, Proudfoot and Guy, 2004) and evidence exists that CRP is transported by immune cells (Melnikov *et al.*, 2020). However, which one of these is dominant for the observations we report is unclear. Further investigation is needed to understand this; for example, staining of immune and epithelial cells in the MEF can provide novel insight into mechanisms by which CRP enters at sites of inflammation.

Finally, we had an over 90% infection rate at day 1 post-inoculation with NTHi 375sr. Therefore, we used 11-week old *Junbo* mice as the best model to study the host-pathogen interactions relevant to NTHi infection and AOM.

The infection rate observed for both NTHi 375sr and 375(2.8)sr in the *Junbo* mouse ME was over 90%, compared to 50% for NTHi 375*lic1*sr, a PCho non-expressing mutant. Bacterial titres in the MEF were also higher for PCho expressing NTHi 375sr and 375(2.8)sr bacteria compared to NTHi 375*lic1*sr. Bacteria were pre-determined whether they are expressing PCho or not. Bacteria from the *Junbo* mouse NPW and MEF continue to express PCho on their surface even in the presence of CRP in the *Junbo* mouse ME (appendix figure 3). This suggests that expression of PCho by NTHi in the MEF provides a selective advantage for bacteria, even in the presence of CRP that can primarily target PCho. CRP levels were highest at day 1 post-inoculation with NTHi 375*lic1*sr compared to infection with PCho expressing NTHi 375 strains. The reason for this might be that the mouse CRP ELISA measures only unbound CRP (*i.e*. CRP not bound to PCho or other ligands) in the mouse samples. The higher CRP concentration observed following NTHi 375*lic1*sr infection of the mouse could be due to less CRP binding to bacteria, as there is no PCho expressed on their surface.

The immune cellular content is directly related to the grade of the MEF. We measured CRP levels and NTHi titre across the different grades of MEF. The highest bacterial titre for NTHi

375sr was found in MEFs that are more opaque and viscous higher grade and where the highest concentrations of CRP were found. Whereas, for NTHi 375(2.8)sr infection of the *Junbo* mice resulted in higher CRP levels in lower grades of MEF. NTHi 375(2.8)sr titres were lower when levels of CRP were higher, suggesting that PCho off heptose I enables the NTHi to survive better in higher grade, MEFs; *i.e*. in the presence of more immune cells. PCho off heptose III on the surface of NTHi 375(2.8)sr has a negative correlation with CRP levels and grade of MEF. Higher bacterial titres were measured in higher grade MEFs, where there was a lower concentration of CRP. Thus, NTHi bacteria expressing PCho off heptose III survive better in MEFs where there is less CRP present. Therefore, PCho off heptose III could be promoting NTHi clearance in the presence of CRP. This is a similar effect to that we observed in the SBA. NTHi 375(2.8)sr was killed more in serum containing CRP but survived better in CRP-depleted serum. PCho off heptose I on the NTHi surface seemingly promotes better bacterial survival in the presence of CRP in the *Junbo* mouse MEF.

NTHi infection of the ME can induce cell death in the MEF and higher grade MEFs have the most dead immune cells (Vikhe *et al.*, 2019). CRP binds to damaged or apoptotic cell membranes in order to facilitate their clearance by the immune system (Gershov *et al.*, 2000; Alnaas *et al.*, 2017). The grade of the MEF can influence bacterial survival in the presence of CRP, where higher CRP levels in the lower grade MEF could be more efficient at clearing away NTHi than CRP in higher grade MEF. Elevated CRP levels in higher-grade MEF infected with NTHi 375sr could be part of a host response to activate the immune system to clear away the greater number of dead cells.

PCho is the primary binding ligand for CRP. However, although NTHi 375sr expresses PCho on its surface, in chapter 3, we showed that CRP does not bind strongly to NTHi 375sr but binds NTHi 375(2.8)sr very well and this could influence bacterial survival in the *Junbo* mouse. MEF obtained from mice at day 1 post-inoculation with NTHi had the highest

concentration of CRP; therefore, we immunophenotyped cells in the *Junbo* mouse MEF at that time point. Neutrophils were the most abundant cells in the MEF of NI and NTHi inoculated mice. Infection with PCho expressing NTHi 375sr and 375(2.8)sr led to higher proportions of neutrophils than did infection with the PCho mutant strain, 375*lic1*sr, which had similar numbers to NI mouse MEFs. These observations are concordant with those from previously published NTHi infection studies in the *Junbo* mouse (Vikhe *et al.*, 2019). Neutrophils engulf and kill bacteria. Activated neutrophils de-granulate and release antimicrobial factors into their environment (Brinkmann *et al.*, 2004). Neutrophil death, NETosis, leads to the release of extracellular nucleic acids, encompassing histones and granular proteins that form NETs (Schachern *et al.*, 2017). NETs are more prevalent in higher grade MEF from the *Junbo* mouse and influence the MEF viscosity (Vikhe *et al.*, 2019). NTHi can promote the formation of NETs which, in combination with NTHi bacteria, can form a biofilm (Hong *et al.*, 2007). NTHi present within the NETs are resistant to extracellular killing by other immune cells and phagocytic activity by incoming neutrophils (Juneau *et al.*, 2011). NET formation increases with the duration of NTHi infection, and is commonly observed in recurrent and chronic OM (Val *et al.*, 2016). We did not focus our study on NETs in the MEF of *Junbo* mice inoculated with NTHi 375 strains at day 1 post-infection. Future work should investigate the relationship between PCho presence and position on NET formation to better understand the role of PCho on biofilm formation and persistence in AOM.

A number of studies have investigated the role of PCho on the NTHi surface to better understand the commensal and pathogenic behaviour of NTHi. Surface expressed PCho has been suggested to contribute to the persistence of NTHi in the respiratory tract of human (Weiser *et al.*, 1998a). The presence of PCho offers NTHi a selective advantage in the upper respiratory tract, whereas, in the blood, it disadvantages the bacteria by exposing them to enhanced immune clearance (Langereis *et al.*, 2019). The mechanism by which PCho on the NTHi surface influences NTHi survival in the presence of immune cells is not

well characterised. Using the *Junbo* mouse, we carried out a detailed study of relevant fluids and tissues by comparing the immune profiles and cellular response, as appropriate, of the MEF, serum, nasal wash and NALT obtained from NI and NTHi infected mice. We did not observe any significant changes in the MEF myeloid cells; therefore, the presence PCho off heptose III on NTHi surface and PCho mutant gave rise to similar innate immune cell responses. However, MEF following infection with NTHi 375(2.8)sr had more monocytes and CD11b+ DCs in higher grade MEFs compared to infection with NTHi 375sr. In the mouse, classical DCs (cDCs) represent 1-5% of tissue cells, depending on the organ and CD11b+ DCs are one subset of these cells (Merad *et al.*, 2013). CD11b+ DCs are potent inducers of CD4+ T cell proliferation and induce both Th2 and Th17 responses to allergens and extracellular pathogens in the lung and the intestine (Plantinga *et al.*, 2013; Ginhoux and Schlitzer, 2014). The number of CD11b+ DCs are elevated in the MEF of the *Jeff* mouse, another mouse model of OM (Vikhe *et al.*, 2020) and in the *Junbo* mouse over the 7 days after infection with NTHi bacteria (Vikhe *et al.*, 2019). However, their function in the MEF and their role in OM and NTHi infection are unknown. The elevated level of CD11b+ DCs in the *Junbo* mouse MEF after inoculation with NTHi 375(2.8)sr, when compared to NTHi 375sr infection, suggests that NTHi 375(2.8)sr induces a similar response to that observed in allergy. Even though CD11b+ DCs are known to induce a Th17 or Th2 cellular response, IL-17 and IL-4 (a key Th2 cytokine) were not elevated in mouse MEF. Levels of IL-17 and IL-4 were higher in MEFs infected with NTHi 375sr compared to NTHi 375(2.8)sr. CD11b+ DCs are very heterogeneous in nature and the maturity of these cells determine their cellular response (Izumi *et al.*, 2021). Future work should look at the potential function of CD11b+ DCs after infection of the *Junbo* mouse with NTHi 375 strains in antigen presentation and the T cell response.

NTHi infection increased the proportion of Treg cells in the *Junbo* mouse MEF. These are immuno-modulating cells. We therefore investigated this further and confirmed NTHi infection could induce Treg cells *in vitro*. In other studies, sustained NTHi infection and

inflammation of the mouse ME following direct inoculation of the ME with NTHi after blocking the Eustachian tube, induces Treg mediated immune suppression, therefore contributing to the immune tolerance against NTHi infection (Hirano *et al.*, 2015). Levels of Treg cells were lowest in higher grade MEFs following infection with NTHi 375sr compared to NTHi 375*lic1*sr infection. Whereas all the grade of MEFs from NTHi 375*lic1*sr infected mice had similar Treg cell proportions. Furthermore, IL-10, a cytokine produced by Treg cells was also found at lower levels in high grade MEF from *Junbo* mice infected with NTHi 375*lic1*sr compared to MEFs from *Junbo* mice infected with NTHi 375sr. Infection with NTHi 375(2.8)sr also resulted in lower levels of Treg cells in higher grade MEFs. Therefore, the presence of PCho, regardless of its position on the NTHi surface, causes a reduction in the number of Treg cells in higher grade MEF at day 1 post-NTHi inoculation of the *Junbo* mouse.

NTHi 375sr and 375(2.8)sr had higher bacterial titres in the ME of the *Junbo* mouse than did NTHi 375*lic1*sr. The enhanced cytokine/chemokine response in grade 3/4 or above MEFs from *Junbo* mouse infected by NTHi 375sr permitted bacterial survival in the presence of a higher inflammatory response compared to NTHi 375(2.8)sr and 375*lic1*sr infection. CRP could play a role in the cellular response and NTHi survival. In the circulatory system, CRP is produced and secreted as a soluble pentamer by the liver. It is present in secretions of the human respiratory tract where human respiratory epithelial cells are able to express CRP, thus potentially contributing to bacterial clearance in the respiratory tract (Jane M. Gould and Weiser, 2001). The isoform of CRP influences the leukocyte response. Pentameric CRP (pCRP) has anti-inflammatory properties, driving M2 (anti-inflammatory) and Th2 (response against extracellular bacteria) responses, whereas monomeric CRP (mCRP) is pro-inflammatory and promotes M1 (pro-inflammatory) and Th1 responses (response against intracellular bacteria) (Trial, Potempa and Entman, 2016). The biological relevance of CRP in the MEF for the mouse could be affected by which isoform is present. NTHi infection with 375sr strains elicited a more M2-like phenotype of the macrophages in

the MEF. *In vitro,* PCho bound CRP promotes M2 macrophage differentiation via IL-13 and is associated with a Th2 response (Trial, Cieslik and Entman, 2016). Furthermore, NTHi 375sr infection in the *Junbo* mouse elicited more Th2 cytokines/chemokines compared to infection with NTHi 375*lic1*sr and 375(2.8)sr.. Therefore, CRP in the *Junbo* mouse MEF infected with NTHi 375sr could be promoting M2 macrophage differentiation that may have result in an anti-inflammatory influence despite the predominantly pro-inflammatory environment. The isoform of CRP could further be influencing the cellular response in the *Junbo* mouse MEF following a day 1 inoculation with NTHi. In the serum, NTHi 375(2.8)sr infection resulted in more M1 like macrophages, however serum CRP levels day 1 post-inoculation with NTHi 375sr and 375(2.8)sr were similar to each other. The differences in the proportion macrophage phenotype could be driven by the isoform of CRP present in the serum. Future work should investigate what type of isoform is present following NTHi 375 strain infection in the *Junbo* mouse. Monomeric CRP has been shown to promote M1 macrophage development (McFadyen *et al.*, 2018). Knowledge of the CRP isoform predominant following different NTHi infections in the *Junbo* mouse could help us understand why some NTHi bacteria survive better in the presence of CRP.

Inoculation with NTHi 375sr produced a heterogeneous T cell response in the *Junbo* mouse MEF. Th1 (IFN-γ), Th2 (IL-4) and Th17 (IL-17) T helper cytokines were each found in higher grade MEFs following NTHI 375sr infection. This was not observed for NTHi 375*lic1*sr and 375(2.8)sr, therefore indicating that PCho off heptose I on the NTHi surface may help promote NTHi survival by activating a T helper response. However, we were unable to predict which of these T helper responses will be dominant 1 day post-infection. In previous studies with the *Junbo* mouse, NTHi infection was reported to promote a Th2 response (Vikhe *et al.*, 2019). Other microbes also utilise PCho to modify the host immune response, for example, ES-62, a PCho containing glycoprotein secreted by *Acanthocheilonema viteae*, a filarial nematode that causes tropical infection, induces a Th2 response with increased IL-4 and decreased IFN-γ levels (Whelan *et al.*, 2000). PCho therefore, plays a

role in host T cell responses. Future experiments should investigate the cytokine/chemokine response at later time points, initially day 3 and then day 7 to confirm if NTHi 375sr also induces a Th2 response. To our knowledge, we are the first to report the changes in cellular response day 1 post-inoculation of the mouse with NTHi 375 strains, which differ only according to the presence and position of PCho. We show that NTHi expressing PCho off heptose I survived better in the presence of inflammatory cytokines compared to NTHi with PCho off heptose III or no PCho.

CRP is predominantly produced by the liver and is transported to inflammatory sites via the blood. Serum CRP levels in the *Junbo* mice were 50-fold less than the MEF at day 1 post-inoculation with NTHi. This suggests that CRP is transported from the blood to MEF, where it concentrates and localises with NTHi infection and OM in the *Junbo* mouse. By the time we had collected the samples from *Junbo* mouse at day 1 post NTHi infection, increased CRP already localises to the MEF, where NTHi is present. Increased CRP was also present in the NPW and NALT indicating that CRP can also perfused into these tissues from the blood. CRP levels in the NPW and NALT did not change at day 1 post-inoculation with NTHi 375 strains, confirming the CRP response in the *Junbo* mouse MEF is due to NTHi infection. The CRP response in the *Junbo* mouse is likely driven by NTHi infection in the MEF. In human, CRP levels following infection are usually measured using patient blood. Serum CRP levels in AOM are usually not accurate in predicting bacterial infection (Tejani *et al.*, 1995). CRP is not usually measured in AOM patient MEF and the concentration of CRP in MEF from human is under-reported. In the human MEF, CRP levels during AOM range from between 6 to 150 mg/L (Principi *et al.*, 1986). In the *Junbo* mouse CRP levels are influenced by the grade of MEF and are correlated with NTHi survival depending on the presence and position of PCho on the NTHi surface. Therefore, CRP levels in human AOM patients should be measured and low levels of CRP should be not disregarded but rather used to study the host immune-pathogen interaction.

The cytokine/chemokine profiles of NPW, blood and NALT did not show much difference following infection of the *Junbo* mouse with NTHi 375. NTHi 375sr infection resulted in more IL-6 and IL-10 in NPW than NTHi 375*lic1*sr infected mice NPW. This suggests that infection with NTHi 375sr that expresses PCho off heptose I promotes T cell dysfunction in the NPW when compared to the PCho non-expressing mutant, 375*lic1*sr. This observation is similar to that in otitis prone children during AOM are characterised by early and constitutive activation of pro-inflammatory signalling in the nasopharynx and a Th2- and Treg cell-dominated profile (Morris *et al.*, 2020).

Following NTHi infection, the most prominent cytokine/chemokine response was in the MEF when compared to other tissues of fluids of the *Junbo* mouse. NTHi ascends up the ET from the NP to the ME from as early as 1 hour post NTHi inoculation (Hood *et al.*, 2016). Therefore, the initial immune response could be a localised response to the NTHi in the MEF at day 1 post-inoculation. Following this, the adaptive immune response would become activated and we would expect to see differences in cellular responses in the blood and NALT at time point later than day 1 post-NTHi inoculation. The NP is where NTHi is normally found in the healthy human and therefore, the lack of a cellular response in the NP of the *Junbo* mouse is consistent with what is expected from a good commensal.

In conclusion, the presence or absence and position of PCho on the NTHi bacterium can influence survival in the *Junbo* mouse. NTHi induces a dampened immune response through T reg cells and M2-like macrophages in the MEF, which can contribute to NTHi survival. However, the cytokine/chemokine response is critical in elucidating why NTHi expressing PCho have higher infection rates and bacterial titres in the *Junbo* mouse MEF. Finally, NTHi 375sr which expresses PCho off heptose I on its surface enhances the inflammatory environment in the *Junbo* mouse MEF and survives in the presence of CRP. Whereas, NTHi 375(2.8)sr, which expresses PCho off heptose III does not induce an inflammatory cytokine/chemokine profile in the *Junbo* MEF and does not survive in the

presence of high CRP levels. CRP present in the MEF containing NTHi 375sr bacteria could be acting to dampen the immune response elicited by NTHi 375sr, thus allowing NTHi 375sr to survive better in the presence of CRP. These data show that PCho on the NTHi surface influences clearance of NTHi by the host. CRP binding to PCho on the NTHi surface is influenced by the PCho position, were bacteria expressing PCho off heptose III interact with and bind well to CRP, and are also cleared away from the MEF in the presence of CRP. Whereas, PCho off heptose I does not bind CRP well and permits NTHi survival even in the presence of CRP in the *Junbo* mouse MEF. The role of CRP and host immune cells in the presence of NTHi is complex and highly influenced by PCho position on the bacteria. This sets the foundation to explore avenues to identify further specific host-pathogen interactions that influence bacterial survival in AOM.

6.4. Future work

We have shown that the presence and position of PCho influences NTHi survival in the presence of CRP in the *Junbo* mouse. We looked at the NTHi infection rates and bacterial titres day 1 post infection with NTHi 375 strains. Although NTHi 375sr and 375(2.8)sr both had high infection rates and bacterial titres in the mouse ME, longer time periods, particularly at days 3 and 7 post-infection study should be studied to see how the position of PCho effects bacterial survival in the *Junbo* over time.

In the mouse, SAP is a major acute phase protein. SAP is also an acute phase protein in the human (Lu *et al.*, 2018). Our preliminary data shows that SAP levels in the *Junbo* mice are influenced by NTHi infection (appendix figure 7). Future work can investigate further the role of SAP in AOM in the *Junbo* mouse.

The innate and adaptive immune responses should be investigated at later time points following NTHi infection of the mouse to study the cellular responses once adaptive immunity is activated. We measured CRP levels at days 3 and 7 post-inoculation. Future work should look at the immune cell profiles and immune cell response day 3 and 7 post

inoculation with NTHi in the *Junbo* mouse. We confirmed that NTHi 375sr expressing PCho survives in the presence of CRP in the NP and MEF from the *Junbo* mouse. Future infection studies should investigate phase variation on NTHi 375(2.8)sr. This can explain the role of CRP in NTHi survival/killing upon PCho position changes on the NTHi surface.

Cytokine/chemokine responses in the MEF were most changed at day 1 post-inoculation with NTHi 375 strains. Most of the innate and adaptive immune cells were similar in proportion for all NTHi 375 strain infections. However, we did observe significant differences in the cytokine/chemokine responses in the ME between the NTHi strains, which suggests that PCho presence and position does influence the cellular response in the *Junbo* mouse. Single-cell spatial transcriptomics could be used to measure total gene activity in a tissue sample and map where the activity is occurring. This would provide more in-depth understanding of how PCho on the NTHi bacterium influences individual gene expression profiles of individual host cells.

Statistical analysis could not be performed on the data from the cytokine/chemokine assays on the tissues from the *Junbo* mouse due to limited biological replicas as we only had time to carry out preliminary experiments. More biological replicates (*e.g.* n=3) will help us to understand if the differences in the cytokine/chemokine responses that we observe are statistically significant.

Finally, other NTHi strains that naturally express PCho off different heptoses should be used to infect the *Junbo* mice to investigate if the acute phase response, the immune cell profile and immune cell response are similar to what we observed using our NTHi 375 strains and its PCho expressing isogenic variants.

Chapter 7. Discussion

Acute otitis media (AOM) remains a significant global burden. AOM is the leading cause of antibiotic prescription in paediatric patients, adding to developing antibiotic resistance (Williams *et al.*, 2018). Non-Typeable *Haemophilus influenzae* (NTHi) is one of the leading otopathogens in AOM (Schilder *et al.*, 2016). NTHi is a common commensal of the human nasopharynx; however, as well as causing AOM it is associated with other infectious diseases including exacerbations of chronic obstructive pulmonary disease (COPD), sinusitis and conjunctivitis.

The lipopolysaccharide (LPS) is the main glycolipid on the surface of NTHi and is comprised of carbohydrate and non-carbohydrate molecules. It plays an important role in host-pathogen interaction in commensal and disease settings. Phosphocholine (PCho) is one component of the LPS on the NTHi surface that is involved in commensal and disease behaviour of the bacterium. NTHi acquires choline from the host, phosphorylates it and adds it to the LPS using the *lic1* operon. NTHi express PCho on their surface in a phase variable manner (PCho on or off). This is a random and a pre-existing condition on the bacteria that allows them to be better suited for the environment they are found in. For example, blood isolates are commonly found to have no PCho expression on their surface (phase variation off), whereas, in the upper respiratory tract, NTHi tend to express PCho (phase variation on) (Schweda *et al.*, 2007b; Langereis *et al.*, 2019). The phase variable expression of PCho allows the bacterial population to adapt quickly to their environment, therefore playing an important role in both health and disease. PCho on the NTHi surface helps the bacteria to colonise by binding to platelet-activating factor receptor on host cells and survive in the presence of host immune factors, including CRP.

We investigated the roles of CRP and PCho on the NTHi surface in AOM. CRP is the main acute phase protein in the human. CRP, primarily binds PCho, but bind at lower affinity to other molecules such as phosphoethanolamine (PEtn) and galactose, both components of

NTHi LPS (Culley *et al.*, 2000; Singh, Suresh, Praither, *et al.*, 2008). The central dogma in the literature states that CRP binds PCho in a calcium dependent manner. CRP binding to bacterial surfaces can lead to clearance of bacteria either through opsonisation and uptake by phagocytes or through the direct activation of the classical complement pathway. Although NTHi can express PCho on their surface, bacteria have been shown to survive in the presence of CRP (Langereis, van der Pasch and de Jonge, 2019). Therefore, we investigated the roles of PCho on NTHi surface in bacterial survival in AOM.

As well as the presence or absence, the position of PCho on the LPS molecule can influence CRP binding and CRP mediated killing of NTHi bacteria (E. Lysenko *et al.*, 2000; Langereis *et al.*, 2019). In chapter 3, we showed using our in-house developed indirect ELISA that PCho expressed off heptose I binds CRP the least compared to other PCho positions on the NTHi strains. PCho off heptose III binds most CRP, followed by PCho off heptose II. In chapter 4, using the serum bactericidal assay (SBA), we showed that PCho presence and position influences bactericidal killing, where NTHi expressing PCho off heptose III, NTHi 375(2.8)sr, was the most sensitive strain. Serum mediated killing is generally associated with CRP and antibodies (Clark *et al.*, 2012; Langereis, van der Pasch and de Jonge, 2019). To understand how much of the killing in the SBA is influenced by CRP, we removed CRP from the normal human serum (NHS) and showed that bacterial killing does not change significantly for NTHi expressing PCho off heptose I, NTHi 375sr, and the PCho mutant strain, NTHi 375*lic1*sr. The removal of CRP from the NHS enabled NTHi 375(2.8)sr to become as resistant to SBA killing as NTHi 375sr. Another NTHi 375 isogenic strain, NTHi 375(12.1)sr, which contains a *lic1D* gene with the potential to add PCho off heptose II, influenced serum mediated killing of the bacteria. NTHi 375(12.1)sr also bound more CRP when compared to NTHi 375sr. The NTHi 375 parent strain did not have a hexose off heptose II to permit PCho addition at that position. However, immunoblotting for PCho expression using PCho specific antibody, TEPC-15, for NTHi 375(12.1)sr confirmed that some PCho was present for this strain. A PCho specific

antibody, 12D9, which only recognises PCho off heptose III, indicated some low level antibody binding (Cody *et al*., unpublished). Further analysis of the LPS of this strain would be needed to understand where PCho is positioned on the surface of this bacterium. In addition to this, immunoblotting of NTHi 375 strains (figure 3.3D) showed that the levels of PCho on the NTHi surface are different in NTHi 375 strains. Future work should investigate why these differences in immunoblot staining exists if the NTHi variants are structurally similar.

PCho complexed with CRP interacts with complement protein, C1q, and consequently activates the classical complement pathway in human. As CRP is not a major acute phase protein in the mouse, its role in the activation of the complement pathway is not well understood in this animal. To overcome this, studies have used human CRP in the mouse, either by creating transgenic mice (Szalai *et al.*, 2000; Singh, Ngwa and Agrawal, 2020) or through injection of human CRP into the mouse (Suresh *et al.*, 2006). However, the human CRP is a foreign protein in the mouse and it is not clear what its functional role is in the mouse (Torzewski, Waqar and Fan, 2014). Similar limitations apply for transgenic mice where there is limited knowledge on human CRP and its interactions with mouse cellular receptors. We infected the *Junbo* mouse (chapter 6), a mouse model for OM, with NTHi 375 strains (which differed in the presence and position of PCho on their surface) and measured serum CRP, C1q and C5a concentrations. C1q is the first subcomponent of the classical pathway and complement activation. We show that PCho presence and position influenced CRP, C1q and C5a levels in the *Junbo* mouse serum (figure 4.4). To our knowledge, this has not been reported previously. C1q levels were lower for NTHi 375sr and 375(2.8)sr, compared to NTHi 375*lic1*sr. Classical complement pathway activation by human CRP is limited to the early proteins of the complement pathway, with limited consumption of C3 to C9 complement proteins (Siegel, Rent and Gewurz, 1974). Therefore, the presence of C5a suggests that the terminal complement proteins may be activated, where after C3 convertases are formed, C3b binds to C5. Activation of C5 by C5

convertases leads to the formation of C5a and C5b. C5a is a strong chemoattractant involved in the recruitment of inflammatory cells. C5a facilities phagocytosis and regulates Fox-P3 induced T regulatory cells (Frank, 2017). C5b combines with the next complement protein, C6, to initiate the formation of the membrane attack complex (MAC). We did not measure other classical pathway complement proteins, and the formation of the MAC, therefore, these should be studied in future experiments. Information on these further complement proteins will help us to understand the mechanism of bacterial killing in the presence of CRP in the serum-mediated killing. The role of CRP in the mouse needs to be investigated to understand if it leads to the formation of MAC or if it behaves similarly to human CRP. Antibody mediated classical complement pathway leads to MAC formation, therefore, future work should investigate serum mediated killing in the absence of antibodies. This will provide more insight into the precise role of CRP in classical complement pathway activation and serum mediated killing of NTHi.

CRP can also function as an opsonin to activate opsonophagocytosis. In chapter 5, we showed preliminary data on the role of PCho presence and position on the surface of NTHi in uptake and survival in the macrophage and activation of these cells. NTHi 375sr, which expresses PCho off heptose I, had higher bacterial survival post 2-hour infection of macrophages than did NTHi 375*lic1*sr and 375(2.8)sr (figure 5.3). The M1 macrophage expression of genes IL-1β, TNF-α and iNOS were all upregulated suggesting NTHi infection elicited a pro-inflammatory response in macrophages. IL-10, a M2 macrophage gene, was also upregulated for all the NTHi 375 strains, with the highest expression post 2-hour infection with NTHi 375sr. IL-10 plays an important role in down regulating the inflammatory macrophage response, including inhibiting phagocytosis (Moore *et al.*, 2001; Redford, Murray and O'Garra, 2011). IL-10 upregulation could be a potential mechanism used by NTHi to minimise macrophage killing. To study if serum from AOM inflammation could influence bacterial uptake into macrophages, we added serum from the *Junbo* mouse infected with NTHi. We did not have access to human AOM serum samples; therefore,

serum from the *Junbo* mouse was used as this model shares similar immune response to NTHi in AOM as AOM patients (Vikhe *et al.*, 2019). The effect of adding *Junbo* mouse serum that were inoculated with different NTHi strains was similar to our data on the SBA. The addition of serum from *Junbo* mice inoculated with NTHi 375sr induced an inflammatory response in bone marrow derived macrophages for both NTHi 375sr and 375(2.8)sr. This suggests that serum from different NTHi infections have different immune components that may influence bacterial killing and phagocytosis. It is not clear what the role of CRP in the *Junbo* mouse serum is and this should be further investigated. PCho-bound CRP interacts with macrophages can lead to the activation of phagocytosis. Future work should investigate the differences between CRP and NTHi along uptake. Furthermore, we are unclear about what receptors and down-stream signalling pathways that are associated with CRP binding to NTHi is still unclear and therefore should be investigated further.

Our *in vitro* assays confirmed that the presence and position of PCho on the NTHi surface influences CRP binding, serum mediated killing (in the presence and absence of CRP) and macrophage response. The host-pathogen interactions in health and disease are complex. There is limited understanding on the role of PCho presence and position on the NTHi surface on the host immune cell molecular pathways. CRP is an under-studied and under-reported protein in the mouse. In chapter 6, we confirm that CRP levels are highest at day 1 post NTHi infection in the *Junbo* mouse, and that CRP is a localised response to NTHi infection in the MEF of the *Junbo* mouse. To our knowledge, we are first to report this novel finding. Even though the *Junbo* mouse had a pre-existing inflammation, we confirmed that infection with NTHi induced CRP production in the mouse. The NTHi infection in pre-existing inflammation is similar to NTHi infection in human. In the human, viral infection leads to inflammation response in the URI and usually pre-disposes children to NTHi infection in AOM (section 1.1.7). Even though liver is the primary location for CRP production, serum CRP levels were 50-fold lower than MEF CRP levels. At day 1 post inoculation in the *Junbo* mouse, CRP may have perfused from the blood into the *Junbo*

mouse MEF, which could be the reason why are observed higher levels of CRP in the MEF. CRP may localise to the ME from the blood through the blood vessels in the ME. NTHi infection in AOM has been reported to increase angiogenesis and vascular permeability that permits infiltration of immune proteins and leukocytes (François, 1997; Husseman *et al.*, 2012). Future work can investigate the main source of CRP in the *Junbo* mouse. Earlier infection time periods *e.g.* 6 hours post NTHi infection could be used to study CRP levels in the *Junbo* mouse tissues and fluids. In the mouse, when the CRP levels start to increase following infection is not reported, therefore time-period for CRP elevation from the human for initial experiments. In the human, CRP levels increase within 6-hours of an inflammatory stimuli (Pepys and Hirschfield, 2003). In addition of CRP being a localised response in the *Junbo* mouse MEF, we confirmed that CRP changes in the *Junbo* mouse MEF were correlated with NTHi infection (sections 6.2.1, 6.2.3.2 and 6.2.3.3).

Bacterial titres in the *Junbo* mouse were correlated with MEF opacity and viscosity. PCho expressing NTHi strains 375sr and 375(2.8)sr had higher infection rates and bacterial titres than the PCho mutant strain, NTHi 375*lic1*sr, therefore confirming PCho on the NTHi surface provides an advantage for NTHi survival in the MEF of *Junbo* mouse. CRP levels were highest in MEF from 1 day post inoculation with NTHi 375*lic1*sr compared to NTHi 375sr and 375(2.8)sr. Higher levels of CRP 1 day post inoculation with NTHi 375*lic1*sr could be due to limited binding sites for CRP, as shown through our CRP binding ELISA (chapter 3). We measured differences in CRP levels between NTHi 375sr (increases with opacity and viscosity) and 375(2.8)sr (decreases with opacity and viscosity). In the presence of CRP, lower MEF bacterial titres of NTHi 375(2.8)sr were measured. This confirms that PCho off heptose III on the NTHi surface makes the NTHi more susceptible to killing in the presence of CRP.

The immune cell response in young children contributes to the development of OM and influences recurrent AOM (Liu *et al.*, 2013; Sharma and Pichichero, 2013; Morris *et al.*,

2020; Pichichero, 2020). Immune profiling of the cells in the *Junbo* mouse MEF 1 day post inoculation with NTHi 375 strains confirms that NTHi infection dampens the immune cell response. M2-like (anti-inflammatory) macrophages and T regulatory (Treg) cells (suppress immune response) were elevated following day 1 post inoculation with NTHi 375 strains compared to MEF from non-inoculated mice. Further, we confirm that *in vitro,* NTHi infection induced Treg cells. NTHi infection in the *Junbo* mouse led to a decrease in the proportion of MEF dendritic cells, especially for NTHi 375*lic1*sr. In the blood, neutrophilia is markedly different between NTHi 375sr and NTHi 375*lic1*sr, where it was the highest 1 day post inoculation with NTHi 375*lic1*sr, implying PCho is inhibiting the neutrophilia. In the NALT, the antigen presenting cells macrophage (and to a lesser extent CD8+DC in NALT) is highest 1 day post inoculation with NTHi 375sr. To our knowledge, we are first to report these findings and confirm that PCho presence and position influences the immune cell content in the *Junbo* mouse. In the human, presence of NTHi in the MEF influences immune cell response. These findings are pivotal in understanding the host-pathogen interaction in AOM. Finally, the cytokine/chemokine profiling of the *Junbo* mouse MEF 1 day post inoculation with NTHi 375 strains shows that NTHi 375sr elicits a greater T cell response whereas NTHi 375*lic1*sr and 375(2.8)sr do not. PCho off heptose I on NTHi 375sr therefore survives in the *Junbo* MEF by inducing a dysfunctional immune cell response where we observed Th1, Th2 and Th17 responses simultaneously.

These findings show that NTHi 375sr elicited a much more inflammatory response in the *Junbo* mouse MEF than NTHi 375lic1sr and 375(2.8)sr. CRP is a double-edge sword, where it has both pro- and anti-inflammatory properties (Sproston and Ashworth, 2018). Therefore, in the MEFs with NTHi 375sr, CRP could be acting to dampen the inflammatory response to NTHi. Whereas, for NTHi 375(2.8)sr, CRP binding to the bacteria may influence bacterial clearance in the MEF. However, this needs to be further investigated. Other immune components can also add to this. The immune cell response in the MEF is complex where NTHi survival and killing could be correlated with CRP and/or other immune

components. It remains unclear if NTHi survival in AOM is correlated to CRP interaction or if the presence of CRP influences NTHi survival in the presence of immune cells. We do not have a clear mechanist link between presence and absence of CRP. Therefore, further experiments are needed to understand the molecular role of CRP in NTHi survival in AOM. The use of CRP mutant mice can help understand the role of CRP in AOM. CRP mutant mice fail to clear away other bacterial infections (Paul Simons *et al.*, 2014). Future studies could look at bacterial survival in the presence or absence of CRP in the mouse. Mice homozygous for allele lacking CRP in the serum are available (*Crp MGI Mouse Gene Detail - MGI:88512 - C-reactive protein, pentraxin-related*, no date). The CRP mutant mouse can be crossed with the *Junbo* mouse to allow the mice to be infected with NTHi to investigate the potential role of CRP in the mouse.

The immune system is highly complex, with many cell states (pro- and anti- inflammatory) existing in parallel with diverse immune cell molecular pathways that all interact in a highly dynamic and coordinated manner. We have shown that the immune cell profile is influenced by NTHi 375 strain infection in the *Junbo* mouse. However, this is a piece of a much more complex biological picture, where other cells of the immune system could also be influencing the immune cell response in AOM. For this, high-throughput and high-resolution omics technologies can provide a deeper insight into host-pathogen interactions in AOM. Transcriptomic technology has been previously used to discover novel genes and pathways in AOM and other genomics technologies have been used to characterise disease pathophysiology in OM (Hernandez *et al.*, 2015; Giese *et al.*, 2020; Rao *et al.*, 2021). Single cell spatial transcriptomics, which incorporates single-cell RNA sequencing (that revels gene expression profiles of individual cells) and spatial transcriptomics (that provides positional information of the RNA or nuclei), is more recently being used to understand the cellular response within a particular tissue at the single cell level for various infections (Stubbington *et al.*, 2017; Dar *et al.*, 2021). We confirm that CRP is a localised response to NTHi infection in the MEF and that immune cell profiles change depending on the PCho

presence and position on the NTHi bacterial surface. The techniques used to obtain these findings rely on processing the tissue, where some biological information may be lost or missing due to cell stress, aggregation or cell death. Single cell spatial transcriptomics would use the intact tissue. The position of any given cell, relative to other cells and non-cellular structures within the tissue and fluid can be helpful in defining the cell phenotype, cell state and cell function. Spatial transcriptomics can reveal features from healthy tissue-wide patterning from disease sites (Williams *et al.*, 2022), therefore providing potential cellular and molecular targets for therapeutics.

In the mouse, serum amyloid protein (SAP) is considered a more important acute phase protein. We show that SAP levels increased following NTHi infection, but we are not sure the relevance of this protein in NTHi infection and AOM in the *Junbo* mouse. Therefore, future work can look at the role of SAP and CRP in NTHi infection in AOM in the *Junbo* mouse. SAP is also an acute phase protein in the human (Clos, 2013), but CRP is the major acute phase protein in the human. As NTHi is a human specific pathogen and both mouse and human CRP bind PCho, we focused our work on CRP.

Other phosphorylated molecules such as PEtn off heptose II on the NTHi surface can also interact with CRP binding to the NTHi surface (chapter 3). This could explain why NTHi may survive in the presence of CRP in AOM. Future work should include infecting the *Junbo* mouse with PEtn mutant strains and PEtn-PCho double mutants to investigate the CRP levels and immune cell profile and response. It will be interesting to see if a similar immune cell response as NTHi 375(2.8)sr is elicited for NTHi 375sr when PEtn off heptose II is removed.

7.1. Conclusion

Host-pathogen interaction in AOM is complex. The presence and position of PCho on the surface of NTHi influences CRP binding, serum mediated killing, uptake, survival and macrophage phenotype in opsonophagocytosis. PCho off heptose I on the NTHi surface allows the bacteria to survive in the presence of CRP, immune cells and inflammatory cytokines. Whereas, bacteria expressing PCho off heptose III and no PCho do not survive well in the presence of CRP, immune cells and inflammatory cytokines. Therefore, the presence and position of PCho on NTHi influences bacterial survival in the presence of CRP in AOM.

References

Ackland, J. *et al.* (2019) 'Macrophage inflammatory responses to Non-typeable Haemophilus influenzae (NTHi) are strain-dependent', in *European Respiratory Journal*. European Respiratory Society (ERS), p. PA5440. Available at: https://doi.org/10.1183/13993003.congress-2019.pa5440.

Ackland, J. *et al.* (2021) 'Dual RNASeq Reveals NTHi-Macrophage Transcriptomic Changes During Intracellular Persistence', *Frontiers in Cellular and Infection Microbiology*, 11, p. 740. Available at: https://doi.org/10.3389/fcimb.2021.723481.

Agrawal, A. *et al.* (2001) 'Topology and Structure of the C1q-Binding Site on C-Reactive Protein', *The Journal of Immunology*, 166(6), pp. 3998–4004. Available at: https://doi.org/10.4049/jimmunol.166.6.3998.

Alnaas, A.A. *et al.* (2017) 'Conformational Changes in C-Reactive Protein Affect Binding to Curved Membranes in a Lipid Bilayer Model of the Apoptotic Cell Surface', *Journal of Physical Chemistry B*, 121(12), pp. 2631–2639. Available at: https://doi.org/10.1021/acs.jpcb.6b11505.

Arason, V.A. *et al.* (2005) 'Otitis media, tympanostomy tube placement, and use of antibiotics: Cross-sectional community study repeated after five years', *Scandinavian Journal of Primary Health Care*, 23(3), pp. 184–191. Available at: https://doi.org/10.1080/02813430510031298.

Arason, V.A. and Sigurdsson, J.A. (2010) 'The problems of antibiotic overuse', *Scandinavian Journal of Primary Health Care*. Taylor & Francis, pp. 65–66. Available at: https://doi.org/10.3109/02813432.2010.487652.

Austeng, M.E. *et al.* (2013) 'Otitis media with effusion in children with in Down syndrome', *International Journal of Pediatric Otorhinolaryngology*, 77(8), pp. 1329–1332. Available at: https://doi.org/10.1016/j.ijporl.2013.05.027.

Avadhanula, V. *et al.* (2006) 'Nontypeable Haemophilus influenzae adheres to intercellular adhesion molecule 1 (ICAM-1) on respiratory epithelial cells and upregulates ICAM-1 expression', *Infection and Immunity*, 74(2), pp. 830–838. Available at: https://doi.org/10.1128/IAI.74.2.830-838.2006.

Badimon, L. *et al.* (2018) 'C-reactive protein in atherothrombosis and angiogenesis', *Frontiers in Immunology*. Frontiers Media S.A., p. 430. Available at: https://doi.org/10.3389/fimmu.2018.00430.

Bantroch, S., Buhler, T. and Lam, J.S. (1994) 'Appropriate coating methods and other conditions for enzyme-linked immunosorbent assay of smooth, rough, and neutral lipopolysaccharides of Pseudomonas aeruginosa', *Clinical and Diagnostic Laboratory Immunology*, 1(1), pp. 55–62. Available at: https://doi.org/10.1128/cdli.1.1.55-62.1994.

Barenkamp, S.J. (2015) 'Editorial Commentary: Respiratory Viruses and Otitis Media in Young Children', *Clinical Infectious Diseases*, 60(1), pp. 10–11. Available at: https://doi.org/10.1093/cid/ciu716.

Barsig, J. *et al.* (1995) 'Lipopolysaccharide-induced interleukin-10 in mice: role of endogenous tumor necrosis factor-α', *European Journal of Immunology*, 25(10), pp. 2888–2893. Available at: https://doi.org/10.1002/eji.1830251027.

Behrouzi, A. *et al.* (2017) 'Vaccine candidates against nontypeable Haemophilus influenzae: A review', *Iranian Biomedical Journal*. Pasteur Institute of Iran, pp. 69–76. Available at: https://doi.org/10.18869/acadpub.ibj.21.2.69.

Berger, A. (2000) ‘Science commentary: Th1 and Th2 responses: What are they?’, *British Medical Journal*. British Medical Journal Publishing Group, p. 424. Available at: https://doi.org/10.1136/bmj.321.7258.424.

Berman, S., Gewurz, H. and Mold, C. (1986) ‘Binding of C-reactive protein to nucleated cells leads to complement activation without cytolysis.’, *Journal of immunology (Baltimore, Md. : 1950)*, 136(4), pp. 1354–9. Available at: http://www.ncbi.nlm.nih.gov/pubmed/3944459 (Accessed: 14 September 2022).

Bhutta, M.F. (2012) ‘Mouse models of otitis media: Strengths and limitations’, *Otolaryngology - Head and Neck Surgery (United States)*. Otolaryngol Head Neck Surg, pp. 611–614. Available at: https://doi.org/10.1177/0194599812449986.

Binks, M.J. *et al.* (2011) ‘Viral-bacterial co-infection in australian indigenous children with acute otitis media’, *BMC Infectious Diseases*, 11(1), p. 161. Available at: https://doi.org/10.1186/1471-2334-11-161.

Black, S., Kushner, I. and Samols, D. (2004) ‘C-reactive protein’, *Journal of Biological Chemistry*. Elsevier, pp. 48487–48490. Available at: https://doi.org/10.1074/jbc.R400025200.

Brinkmann, V. *et al.* (2004) ‘Neutrophil Extracellular Traps Kill Bacteria’, *Science*, 303(5663), pp. 1532–1535. Available at: https://doi.org/10.1126/science.1092385.

Brugger, S.D. *et al.* (2019) ‘Age-Dependent Dissimilarity of the Nasopharyngeal and Middle Ear Microbiota in Children With Acute Otitis Media’, *Frontiers in Genetics*, 10(JUN), p. 555. Available at: https://doi.org/10.3389/fgene.2019.00555.

Cao, X.E. *et al.* (2022) ‘A diagnostic platform for rapid, simultaneous quantification of procalcitonin and C-reactive protein in human serum’, *eBioMedicine*, 76, p. 103867. Available at: https://doi.org/10.1016/j.ebiom.2022.103867.

Chonmaitree, T. *et al.* (2008) ‘Viral upper respiratory tract infection and otitis media complication in young children’, *Clinical Infectious Diseases*, 46(6), pp. 815–823. Available at: https://doi.org/10.1086/528685.

Clark, S.E. *et al.* (2012) ‘Phosphorylcholine Allows for Evasion of Bactericidal Antibody by Haemophilus influenzae’, *PLoS Pathogens*. Edited by N. Salama, 8(3), p. e1002521. Available at: https://doi.org/10.1371/journal.ppat.1002521.

Clark, S.E. and Weiser, J.N. (2013) ‘Microbial modulation of host immunity with the small molecule phosphorylcholine’, *Infection and Immunity*. American Society for Microbiology (ASM), pp. 392–401. Available at: https://doi.org/10.1128/IAI.01168-12.

Clementi, C.F. and Murphy, T.F. (2011) ‘Non-Typeable Haemophilus influenzae Invasion and Persistence in the Human Respiratory Tract’, *Frontiers in Cellular and Infection Microbiology*, 1, p. 1. Available at: https://doi.org/10.3389/fcimb.2011.00001.

Du Clos, T.W. (2000) *Function of C-reactive protein*, *Annals of Medicine*. Available at: https://doi.org/10.3109/07853890009011772.

Clos, T.W. Du (2013) ‘Pentraxins: Structure, Function, and Role in Inflammation’, *Hindawi*, 2013. Available at: https://doi.org/https://doi.org/10.1155/2013/379040.

Costerton, J.W. *et al.* (1995) ‘Microbial biofilms’, *Annual Review of Microbiology*. Annual Reviews Inc., pp. 711–745. Available at: https://doi.org/10.1146/annurev.mi.49.100195.003431.

Craig, J.E. *et al.* (2001) ‘Survival of nontypeable Haemophilus in £ uenzae in

macrophages', 203, pp. 55–61.

Crp MGI Mouse Gene Detail - MGI:88512 - C-reactive protein, pentraxin-related (no date). Available at: http://www.informatics.jax.org/marker/MGI:88512 (Accessed: 27 September 2022).

Culley, F.J. *et al.* (2000) 'C-reactive protein binds to phosphorylated carbohydrates', *Glycobiology*, 10(1), pp. 59–65. Available at: https://doi.org/10.1093/glycob/10.1.59.

Dar, D. *et al.* (2021) 'In situ single-cell activities of microbial populations revealed by spatial transcriptomics', *bioRxiv*, p. 2021.02.24.432792. Available at: https://doi.org/10.1101/2021.02.24.432792.

Davidoss, N.H., Varsak, Y.K. and Santa Maria, P.L. (2018) 'Animal models of acute otitis media – A review with practical implications for laboratory research', *European Annals of Otorhinolaryngology, Head and Neck Diseases*. Elsevier Masson SAS, pp. 183–190. Available at: https://doi.org/10.1016/j.anorl.2017.06.013.

Debertin, A.S. *et al.* (2003) 'Nasal-associated lymphoid tissue (NALT): Frequency and localization in young children', *Clinical and Experimental Immunology*, 134(3), pp. 503–507. Available at: https://doi.org/10.1111/j.1365-2249.2003.02311.x.

Deegan, O. *et al.* (2003) 'Quantitative detection of C-reactive protein using phosphocholine-labelled enzyme or microspheres', *Analytical Biochemistry*, 312(2), pp. 175–181. Available at: https://doi.org/10.1016/S0003-2697(02)00439-6.

Deguine, J. and Barton, G.M. (2014) 'MyD88: A central player in innate immune signaling', *F1000Prime Reports*, 6. Available at: https://doi.org/10.12703/P6-97.

Diagnosis | Diagnosis | Otitis media - acute | CKS | NICE (no date). Available at: https://cks.nice.org.uk/topics/otitis-media-acute/diagnosis/diagnosis/ (Accessed: 30 July 2022).

Duell, B.L., Su, Y.-C. and Riesbeck, K. (2016) 'Host-pathogen interactions of nontypeable *Haemophilus influenzae* : from commensal to pathogen', *FEBS Letters*, 590(21), pp. 3840–3853. Available at: https://doi.org/10.1002/1873-3468.12351.

Elder, B.L., Boraker, D.K. and Fives-Taylor, P.M. (1982) 'Whole-bacterial cell enzyme-linked immunosorbent assay for Streptococcus sanguis fimbrial antigens', *Journal of Clinical Microbiology*, 16(1), pp. 141–144. Available at: https://doi.org/10.1128/jcm.16.1.141-144.1982.

Van Eldere, J. *et al.* (2014) 'Non-typeable Haemophilus influenzae, an under-recognised pathogen', *The Lancet Infectious Diseases*, 14(12), pp. 1281–1292. Available at: https://doi.org/10.1016/S1473-3099(14)70734-0.

Elke K.H. Schweda1, Brigitte Twelkmeyer1, J.L. (2008) 'Profiling structural elements of short-chain lipopolysaccharide of non-typeable Haemophilus influenzae', *Innate Immunity*, 14(4), pp. 199–211. Available at: https://journals.sagepub.com/doi/pdf/10.1177/1753425908095958.

Ercoli, G. *et al.* (2015) 'Development of a serological assay to predict antibody bactericidal activity against non-typeable Haemophilus influenzae', *BMC Microbiology*, 15(1), p. 87. Available at: https://doi.org/10.1186/s12866-015-0420-x.

Ernst, O. *et al.* (2019) 'Exclusive Temporal Stimulation of IL-10 Expression in LPS-Stimulated Mouse Macrophages by cAMP Inducers and Type I Interferons', *Frontiers in Immunology*, 10, p. 1788. Available at: https://doi.org/10.3389/fimmu.2019.01788.

Erwin, A.L. and Smith, A.L. (2007) 'Nontypeable Haemophilus influenzae: understanding virulence and commensal behavior', *Trends in Microbiology*, 15(8), pp. 355–362. Available at: https://doi.org/10.1016/j.tim.2007.06.004.

Fitzsimmons, L.F., Hampel, K.J. and Wargo, M.J. (2012) 'Cellular choline and glycine betaine pools impact osmoprotection and phospholipase C production in Pseudomonas aeruginosa', *Journal of Bacteriology*, 194(17), pp. 4718–4726. Available at: https://doi.org/10.1128/JB.00596-12.

Fox, K.L. *et al.* (2008) 'Duplicate copies of lic1 direct the addition of multiple phosphocholine residues in the lipopolysaccharide of Haemophilus influenzae', *Infection and Immunity*, 76(2), pp. 588–600. Available at: https://doi.org/10.1128/IAI.00748-07.

Foxwell, A.R., Kyd, J.M. and Cripps, A.W. (1998) 'Nontypeable Haemophilus influenzae: Pathogenesis and Prevention', *Microbiology and Molecular Biology Reviews*, 62(2), pp. 294–308. Available at: http://mmbr.asm.org/content/62/2/294%5Cnhttp://mmbr.asm.org/content/62/2/294.full.pdf%5Cnhttp://www.ncbi.nlm.nih.gov/pubmed/9618443.

François, M. (1997) 'New views on the pathogenesis of acute otitis media and its complications', *Clinical Microbiology and Infection*. Blackwell Publishing Ltd, pp. 3S5-3S12. Available at: https://doi.org/10.1016/s1198-743x(14)64946-6.

Frank, M.M. (2017) 'Complement in Control of Infectious Agents', in *Principles and Practice of Pediatric Infectious Diseases*. Elsevier Inc., pp. 624–103. Available at: https://doi.org/10.1016/B978-0-323-40181-4.00103-1.

Gang, T.B. *et al.* (2012) 'The phosphocholine-binding pocket on C-reactive protein is necessary for initial protection of mice against pneumococcal infection', *Journal of Biological Chemistry*, 287(51), pp. 43116–43125. Available at: https://doi.org/10.1074/jbc.M112.427310.

Gaultier, G.N. *et al.* (2017) 'The Immunostimulatory Capacity of Nontypeable Haemophilus influenzae Lipooligosaccharide', *Pathogens & Immunity*, 2(1), p. 34. Available at: https://doi.org/10.20411/PAI.V2I1.162.

Gershov, D. *et al.* (2000) 'C-reactive protein binds to apoptotic cells, protects the cells from assembly of the terminal complement components, and sustains an antiinflammatory innate immune response: Implications for systemic autoimmunity', *Journal of Experimental Medicine*, 192(9), pp. 1353–1363. Available at: https://doi.org/10.1084/jem.192.9.1353.

Giese, A.P.J. *et al.* (2020) 'Genomics of Otitis Media (OM): Molecular Genetics Approaches to Characterize Disease Pathophysiology', *Frontiers in Genetics*. Frontiers Media S.A., p. 313. Available at: https://doi.org/10.3389/fgene.2020.00313.

Ginhoux, F. and Schlitzer, A. (2014) 'CD11b+ DCs rediscovered: Implications for vaccination', *Expert Review of Vaccines*. Expert Reviews Ltd., pp. 445–447. Available at: https://doi.org/10.1586/14760584.2014.893196.

Gould, J. M. and Weiser, J.N. (2001) 'Expression of C-reactive protein in the human respiratory tract', *Infection and Immunity*, 69(3), pp. 1747–1754. Available at: https://doi.org/10.1128/IAI.69.3.1747-1754.2001.

Guo, R.F. and Ward, P.A. (2005) 'Role of C5a in inflammatory responses', *Annual Review of Immunology*. Annu Rev Immunol, pp. 821–852. Available at: https://doi.org/10.1146/annurev.immunol.23.021704.115835.

Haapasalo, K. and Meri, S. (2019) 'Regulation of the Complement System by Pentraxins', *Frontiers in Immunology*, 10, p. 1750. Available at: https://doi.org/10.3389/fimmu.2019.01750.

Hafrén, L. *et al.* (2015) 'Predisposition to Childhood Otitis Media and Genetic Polymorphisms within the Toll-Like Receptor 4 (TLR4) Locus', *PLOS ONE*. Edited by Y.-G. Yao, 10(7), p. e0132551. Available at: https://doi.org/10.1371/journal.pone.0132551.

Hampton, T. *et al.* (2021) 'Recurrent acute otitis media: A survey of current management in England', *Journal of Laryngology and Otology*, 135(10), pp. 855–857. Available at: https://doi.org/10.1017/S0022215121001924.

Hardison, R.L. *et al.* (2018) 'Transient Nutrient Deprivation Promotes Macropinocytosis-Dependent Intracellular Bacterial Community Development', *mSphere*, 3(5). Available at: https://doi.org/10.1128/msphere.00286-18.

Hermansson, A. *et al.* (1988) 'A rat model for bacterial otitis media', *Acta Oto-Laryngologica*, 105(S457), pp. 144–147. Available at: https://doi.org/10.3109/00016488809138898.

Hernandez, M. *et al.* (2008) 'Myeloid differentiation primary response gene 88 is required for the resolution of otitis media', *Journal of Infectious Diseases*, 198(12), pp. 1862–1869. Available at: https://doi.org/10.1086/593213.

Hernandez, M. *et al.* (2015) 'The transcriptome of a complete episode of acute otitis media', *BMC Genomics*, 16(1), p. 259. Available at: https://doi.org/10.1186/s12864-015-1475-7.

Hirano, T. *et al.* (2007) 'Role of Toll-like receptor 4 in innate immune responses in a mouse model of acute otitis media', *FEMS Immunology & Medical Microbiology*, 49(1), pp. 75–83. Available at: https://doi.org/10.1111/j.1574-695X.2006.00186.x.

Hirano, T. *et al.* (2015) 'Accumulation of regulatory T cells and chronic inflammation in the middle ear in a mouse model of chronic otitis media with effusion induced by combined eustachian tube blockage and nontypeable Haemophilus influenzae infection', *Infection and Immunity*, 84(1), pp. 356–364. Available at: https://doi.org/10.1128/IAI.01128-15.

Hong, W. *et al.* (2007) 'Phosplioiylclioline decreases early inflammation and promotes the establishment of stable biofilm communities of nontypeable Haemophilus influenzae strain 86-028NP in a chinchilla model of otitis media', *Infection and Immunity*, 75(2), pp. 958–965. Available at: https://doi.org/10.1128/IAI.01691-06.

Hood, D. *et al.* (2016) 'A new model for non-typeable Haemophilus influenzae middle ear infection in the Junbo mutant mouse', *Disease Models & Mechanisms*, 9(1), pp. 69–79. Available at: https://doi.org/10.1242/dmm.021659.

Huang, C.F. *et al.* (2019) 'A reporter mouse for non-invasive detection of toll-like receptor ligands induced acute phase responses', *Scientific Reports*, 9(1), pp. 1–9. Available at: https://doi.org/10.1038/s41598-019-55281-w.

Husseman, J. *et al.* (2012) 'The role of vascular endothelial growth factors and fibroblast growth factors in angiogenesis during otitis media', *Audiology and Neurotology*, 17(3), pp. 148–154. Available at: https://doi.org/10.1159/000333805.

Van Ingen, G. *et al.* (2016) 'Genome-wide association study for acute otitis media in children identifies FNDC1 as disease contributing gene', *Nature Communications*, 7(1), pp. 1–7. Available at: https://doi.org/10.1038/ncomms12792.

Iuchi, H. *et al.* (2019) 'Role of phosphorylcholine in Streptococcus pneumoniae and

nontypeable Haemophilus influenzae adherence to epithelial cells', *Auris Nasus Larynx*, 46(4), pp. 513–519. Available at: https://doi.org/10.1016/j.anl.2018.11.003.

Izumi, G. *et al.* (2021) 'CD11b+ lung dendritic cells at different stages of maturation induce Th17 or Th2 differentiation', *Nature Communications*, 12(1), pp. 1–16. Available at: https://doi.org/10.1038/s41467-021-25307-x.

Juneau, R.A. *et al.* (2011) 'Nontypeable haemophilus influenzae initiates formation of neutrophil extracellular traps', *Infection and Immunity*, 79(1), pp. 431–438. Available at: https://doi.org/10.1128/IAI.00660-10.

Jung, S.Y. *et al.* (2021) 'Toll-like receptors: Expression and roles in otitis media', *International Journal of Molecular Sciences*. MDPI. Available at: https://doi.org/10.3390/ijms22157868.

Kadry, N.A. *et al.* (2021) 'Immunization with HMW1 and HMW2 adhesins protects against colonization by heterologous strains of nontypeable Haemophilus influenzae', *Proceedings of the National Academy of Sciences of the United States of America*, 118(32), p. e2019923118. Available at: https://doi.org/10.1073/pnas.2019923118.

Kahlenberg, J.M. and Kaplan, M.J. (2013) 'Little Peptide, Big Effects: The Role of LL-37 in Inflammation and Autoimmune Disease', *The Journal of Immunology*, 191(10), pp. 4895–4901. Available at: https://doi.org/10.4049/jimmunol.1302005.

Kaur, R. *et al.* (2014) 'Correlation of nasopharyngeal cultures prior to and at onset of acute otitis media with middle ear fluid cultures', *BMC Infectious Diseases*, 14(1), p. 640. Available at: https://doi.org/10.1186/s12879-014-0640-y.

Kaur, R., Casey, J. and Pichichero, M. (2016) 'Differences in innate immune response gene regulation in the middle ear of children who are otitis prone and in those not otitis prone', *American Journal of Rhinology and Allergy*, 30(6), pp. e218–e223. Available at: https://doi.org/10.2500/ajra.2016.30.4393.

Kerr, M.A. (1981) 'The complement system', *Biochemical Education*, 9(3), pp. 82–88. Available at: https://doi.org/10.1016/0307-4412(81)90207-7.

Ketterer, M.R. *et al.* (1999) 'Infection of primary human bronchial epithelial cells by Haemophilus influenzae: Macropinocytosis as a mechanism of airway epithelial cell entry', *Infection and Immunity*, 67(8), pp. 4161–4170. Available at: https://doi.org/10.1128/iai.67.8.4161-4170.1999.

Kim, E. *et al.* (2013) 'Protein-Directed Immobilization of Phosphocholine Ligands on a Gold Surface for Multivalent C-Reactive Protein Binding', *Current Topics in Medicinal Chemistry*, 13(4), pp. 519–524. Available at: https://doi.org/10.2174/1568026611313040012.

Kodama, H. *et al.* (1999) 'Cellular immune response of adenoidal and tonsillar lymphocytes to the P6 outer membrane protein of non-typeable Haemophilus influenzae and its relation to otitis media', *Acta Oto-Laryngologica*, 119(3), pp. 377–383. Available at: https://doi.org/10.1080/00016489950181422.

Kubinyecz, O. *et al.* (2020) 'The Jeff Mouse Mutant Model for Chronic Otitis Media Manifests Gain-of-Function as Well as Loss-of-Function Effects', *Frontiers in Genetics*, 11. Available at: https://doi.org/10.3389/fgene.2020.00498.

Landerholm, M.K. *et al.* (2004) 'Characterization of novel structural features in the lipopolysaccharide of nondisease associated nontypeable Haemophilus influenzae', *European Journal of Biochemistry*, 271(5), pp. 941–953. Available at:

https://doi.org/10.1111/j.1432-1033.2004.03996.x.

Langereis, J.D. *et al.* (2019) 'Nontypeable Haemophilus influenzae Invasive Blood Isolates Are Mainly Phosphorylcholine Negative and Show Decreased Complement-Mediated Killing That Is Associated with Lower Binding of IgM and CRP in Comparison to Colonizing Isolates from the Oropharynx', *Infection and immunity*. Edited by S.M. Payne, 87(2). Available at: https://doi.org/10.1128/IAI.00604-18.

Langereis, J.D., van der Pasch, E.S. and de Jonge, M.I. (2019) 'Serum IgM and C-Reactive Protein Binding to Phosphorylcholine of Nontypeable Haemophilus influenzae Increases Complement-Mediated Killing.', *Infection and immunity*, 87(8), pp. e00299-19. Available at: https://doi.org/10.1128/IAI.00299-19.

Lappan, R. *et al.* (2018) 'A microbiome case-control study of recurrent acute otitis media identified potentially protective bacterial genera', *BMC Microbiology*, 18(1), pp. 1–20. Available at: https://doi.org/10.1186/s12866-018-1154-3.

Laurent, P. *et al.* (1985) 'Rapid enzyme immunoassay for quantification of C-reactive protein (CRP)', *Clinical Biochemistry*, 18(5), pp. 272–275. Available at: https://doi.org/10.1016/S0009-9120(85)80030-8.

Lavillegrand, J.R. *et al.* (2021) 'Elevated plasma IL-6 and CRP levels are associated with adverse clinical outcomes and death in critically ill SARS-CoV-2 patients: inflammatory response of SARS-CoV-2 patients', *Annals of Intensive Care*, 11(1), p. 9. Available at: https://doi.org/10.1186/s13613-020-00798-x.

Lee, R.T., Takagahara, I. and Lee, Y.C. (2002) 'Mapping the binding areas of human C-reactive protein for phosphorylcholine and polycationic compounds. Relationship between the two types of binding sites', *Journal of Biological Chemistry*, 277(1), pp. 225–232. Available at: https://doi.org/10.1074/jbc.M106039200.

Leichtle, A. *et al.* (2009) 'TLR4-mediated induction of TLR2 signaling is critical in the pathogenesis and resolution of otitis media', *Innate Immunity*, 15(4), pp. 205–215. Available at: https://doi.org/10.1177/1753425909103170.

Lim, D.J. *et al.* (1979) 'Otitis Media With Effusion: Cytological and Microbiological Correlates', *Archives of Otolaryngology*, 105(7), pp. 404–412. Available at: https://doi.org/10.1001/archotol.1979.00790190030006.

Liu, K. *et al.* (2013) 'Transcriptome signature in young children with acute otitis media due to non-typeable *Haemophilus influenzae*', *International Immunology*, 25(6), pp. 353–361. Available at: https://doi.org/10.1093/intimm/dxs154.

Lu, J. *et al.* (2018) 'Pentraxins and Fc receptor-mediated immune responses', *Frontiers in Immunology*, 9(NOV). Available at: https://doi.org/10.3389/fimmu.2018.02607.

Luo, Y. *et al.* (2012) 'Sensitive and rapid quantification of C-reactive protein using quantum dot-labeled microplate immunoassay', *Journal of Translational Medicine*, 10(1), p. 24. Available at: https://doi.org/10.1186/1479-5876-10-24.

De Lusignan, S. *et al.* (2017) 'RCGP Research and Surveillance Centre Annual Report 2014-2015: Disparities in presentations to primary care', *British Journal of General Practice*, 67(654), pp. e29–e40. Available at: https://doi.org/10.3399/bjgp16X688573.

Lysenko, E. *et al.* (2000) 'The position of phosphorylcholine on the lipopolysaccharide of Haemophilus influenzae affects binding and sensitivity to C-reactive protein-mediated killing', *Molecular Microbiology*, 35(1), pp. 234–245. Available at: https://doi.org/10.1046/j.1365-2958.2000.01707.x.

Lysenko, E.S. *et al.* (2000) 'Bacterial phosphorylcholine decreases susceptibility to the antimicrobial peptide LL-37/hCAP18 expressed in the upper respiratory tract', *Infection and Immunity*, 68(3), pp. 1664–1671. Available at: https://doi.org/10.1128/IAI.68.3.1664-1671.2000.

Majewski, K. *et al.* (2018) 'Serum concentrations of antimicrobial peptide cathelicidin LL-37 in patients with bacterial lung infections', *Central European Journal of Immunology*, 43(4), pp. 453–457. Available at: https://doi.org/10.5114/ceji.2018.81355.

Mak, T.W. and Saunders, M.E. (2006) 'Cytokines and Cytokine Receptors', in *The Immune Response*. Elsevier, pp. 463–516. Available at: https://doi.org/10.1016/b978-012088451-3.50019-3.

Månsson, M. *et al.* (2003) 'Structural diversity in lipopolysaccharide expression in nontypeable *Haemophilus influenzae*', *European Journal of Biochemistry*, 270(4), pp. 610–624. Available at: https://doi.org/10.1046/j.1432-1033.2003.03399.x.

Marnell, L., Mold, C. and Du Clos, T.W. (2005) *C-reactive protein: Ligands, receptors and role in inflammation*, *Clinical Immunology*. Available at: https://www.sciencedirect.com/science/article/pii/S1521661605002809?via%3Dihub (Accessed: 11 September 2019).

Marom, T., Nokso-Koivisto, J. and Chonmaitree, T. (2012) 'Viral-bacterial interactions in acute otitis media', *Current Allergy and Asthma Reports*. Nature Publishing Group, pp. 551–558. Available at: https://doi.org/10.1007/s11882-012-0303-2.

Martí-Lliteras, P. *et al.* (2009) 'Nontypeable Haemophilus influenzae clearance by alveolar macrophages is impaired by exposure to cigarette smoke', *Infection and Immunity*, 77(10), pp. 4232–4242. Available at: https://doi.org/10.1128/IAI.00305-09.

Martines, F. *et al.* (2016) 'Factors influencing the development of otitis media among Sicilian children affected by upper respiratory tract infections', *Brazilian Journal of Otorhinolaryngology*, 82(2), pp. 215–222. Available at: https://doi.org/10.1016/j.bjorl.2015.04.002.

Massa, H.M., Spann, K.M. and Cripps, A.W. (2021) 'Innate Immunity in the Middle Ear Mucosa', *Frontiers in Cellular and Infection Microbiology*. Frontiers Media S.A. Available at: https://doi.org/10.3389/fcimb.2021.764772.

McFadyen, J.D. *et al.* (2018) 'Dissociation of C-reactive protein localizes and amplifies inflammation: Evidence for a direct biological role of C-reactive protein and its conformational changes', *Frontiers in Immunology*. Frontiers Media S.A., p. 1351. Available at: https://doi.org/10.3389/fimmu.2018.01351.

Melnikov, I. *et al.* (2020) 'Crp is transported by monocytes and monocyte-derived exosomes in the blood of patients with coronary artery disease', *Biomedicines*, 8(10), pp. 1–12. Available at: https://doi.org/10.3390/biomedicines8100435.

Merad, M. *et al.* (2013) 'The dendritic cell lineage: Ontogeny and function of dendritic cells and their subsets in the steady state and the inflamed setting', *Annual Review of Immunology*. NIH Public Access, pp. 563–604. Available at: https://doi.org/10.1146/annurev-immunol-020711-074950.

Mestas, J. and Hughes, C.C.W. (2004) 'Of Mice and Not Men: Differences between Mouse and Human Immunology', *The Journal of Immunology*, 172(5), pp. 2731–2738. Available at: https://doi.org/10.4049/jimmunol.172.5.2731.

Mittal, R. *et al.* (2014) 'Role of innate immunity in the pathogenesis of otitis media',

International Journal of Infectious Diseases. Elsevier, pp. e259–e267. Available at: https://doi.org/10.1016/j.ijid.2014.10.015.

Mittal, R. *et al.* (2018) 'Microbial otitis media: recent advancements in treatment, current challenges and opportunities', *Journal of Medical Microbiology*, 67(10), pp. 1417–1425. Available at: https://doi.org/10.1099/jmm.0.000810.

Molins, B. *et al.* (2018) 'C-reactive protein as a therapeutic target in age-related macular degeneration', *Frontiers in Immunology*. Frontiers Media S.A. Available at: https://doi.org/10.3389/fimmu.2018.00808.

Monasta, L. *et al.* (2012) 'Burden of disease caused by otitis media: systematic review and global estimates.', *PloS one*, 7(4), p. e36226. Available at: https://doi.org/10.1371/journal.pone.0036226.

Moore, K.W. *et al.* (2001) 'Interleukin-10 and the interleukin-10 receptor', *Annual Review of Immunology*. Annual Reviews 4139 El Camino Way, P.O. Box 10139, Palo Alto, CA 94303-0139, USA , pp. 683–765. Available at: https://doi.org/10.1146/annurev.immunol.19.1.683.

Morey, P. *et al.* (2011) 'Evidence for a non-replicative intracellular stage of nontypable Haemophilus influenzae in epithelial cells', *Microbiology*, 157(1), pp. 234–250. Available at: https://doi.org/10.1099/mic.0.040451-0.

Morey, P. *et al.* (2013) 'Relative contributions of lipooligosaccharide inner and outer core modifications to nontypeable haemophilus influenzae pathogenesis', *Infection and Immunity*, 81(11), pp. 4100–4111. Available at: https://doi.org/10.1128/IAI.00492-13.

Morris, M.C. *et al.* (2020) 'Immune Network Modeling Predicts Specific Nasopharyngeal and Peripheral Immune Dysregulation in Otitis-Prone Children', *Frontiers in Immunology*, 11, p. 1168. Available at: https://doi.org/10.3389/fimmu.2020.01168.

N O Ku 1, R.F.M. (1993) 'The Mouse C-reactive Protein (CRP) Gene Is Expressed in Response to IL-1 but Not IL-6', *Cytokine*, 5(4), pp. 319–326. Available at: https://doi.org/10.1016/1043-4666(93)90063-b.

Naylor, E.J. *et al.* (2007) 'Haemophilus influenzae induces neutrophil necrosis: A role in chronic obstructive pulmonary disease?', *American Journal of Respiratory Cell and Molecular Biology*, 37(2), pp. 135–143. Available at: https://doi.org/10.1165/rcmb.2006-0375OC.

Nehring, S.M. *et al.* (2021) *C Reactive Protein [Updated 2021 May 10]*, *StatPearls*. StatPearls Publishing. Available at: http://www.ncbi.nlm.nih.gov/pubmed/28722873 (Accessed: 9 August 2022).

Ngo, C.C. *et al.* (2016) *Predominant bacteria detected from the middle ear fluid of children experiencing otitis media: A systematic review*, *PLoS ONE*. Edited by S. Reid. Public Library of Science. Available at: https://doi.org/10.1371/journal.pone.0150949.

Ngo, C.C. *et al.* (2022) 'Predominant Bacterial and Viral Otopathogens Identified Within the Respiratory Tract and Middle Ear of Urban Australian Children Experiencing Otitis Media Are Diversely Distributed', *Frontiers in Cellular and Infection Microbiology*, 12, p. 14. Available at: https://doi.org/10.3389/fcimb.2022.775535.

Nishinarita, S., Sawada, S. and Horie, T. (1990) 'Phosphorylcholine antibodies in pulmonary infection', *Medical Microbiology and Immunology*, 179(4), pp. 205–214. Available at: https://doi.org/10.1007/BF00195251.

Nokso-Koivisto, J., Marom, T. and Chonmaitree, T. (2015) 'Importance of viruses in acute

otitis media', *Current Opinion in Pediatrics*. Lippincott Williams and Wilkins, pp. 110–115. Available at: https://doi.org/10.1097/MOP.0000000000000184.

Oh, J.K. *et al.* (2018) 'The influence of surface chemistry on the kinetics and thermodynamics of bacterial adhesion', *Scientific Reports*, 8(1), pp. 1–13. Available at: https://doi.org/10.1038/s41598-018-35343-1.

Oswald, I.P. *et al.* (1992) 'Interleukin 10 inhibits macrophage microbicidal activity by blocking the endogenous production of tumor necrosis factor α required as a costimulatory factor for interferon γ-induced activation', *Proceedings of the National Academy of Sciences of the United States of America*, 89(18), pp. 8676–8680. Available at: https://doi.org/10.1073/pnas.89.18.8676.

P02741.1 (2022). Available at: https://www.ncbi.nlm.nih.gov/protein/P02741/ (Accessed: 4 May 2020).

Parkinson, N. *et al.* (2006) 'Mutation at the Evi1 locus in Junbo mice causes susceptibility to otitis media', *PLoS Genetics*, 2(10), pp. 1556–1564. Available at: https://doi.org/10.1371/journal.pgen.0020149.

Parra, M.M. *et al.* (2011) 'Bacterial etiology and serotypes of acute otitis media in Mexican children', *Vaccine*, 29(33), pp. 5544–5549. Available at: https://doi.org/10.1016/j.vaccine.2011.04.128.

Pathak, A. and Agrawal, A. (2019) 'Evolution of C-Reactive Protein.', *Frontiers in immunology*, 10, p. 943. Available at: https://doi.org/10.3389/fimmu.2019.00943.

Patterson, L.T. and Higginbotham, R.D. (1965) 'Mouse C-reactive protein and endotoxin-induced resistance.', *Journal of Bacteriology*, 90(6), pp. 1520–1524. Available at: https://doi.org/10.1128/jb.90.6.1520-1524.1965.

Paul Simons, J. *et al.* (2014) 'C-reactive protein is essential for innate resistance to pneumococcal infection', *Immunology*, 142(3), pp. 414–420. Available at: https://doi.org/10.1111/imm.12266.

Peltola, H. (2000) ' Worldwide Haemophilus influenzae Type b Disease at the Beginning of the 21st Century: Global Analysis of the Disease Burden 25 Years after the Use of the Polysaccharide Vaccine and a Decade after the Advent of Conjugates ', *Clinical Microbiology Reviews*, 13(2), pp. 302–317. Available at: https://doi.org/10.1128/cmr.13.2.302.

Peñaloza, H.F. *et al.* (2018) 'Expanding the Current Knowledge About the Role of Interleukin-10 to Major Concerning Bacteria', *Frontiers in Microbiology*, 9(SEP), p. 2047. Available at: https://doi.org/10.3389/fmicb.2018.02047.

Pepys, M.B. and Hirschfield, G.M. (2003) 'C-reactive protein: a critical update', *Journal of Clinical Investigation*, 111(12), pp. 1805–1812. Available at: https://doi.org/10.1172/JCI18921.

Pichichero, M.E. (2020) 'Immunologic dysfunction contributes to the otitis prone condition', *Journal of Infection*, 80(6), pp. 614–622. Available at: https://doi.org/10.1016/j.jinf.2020.03.017.

Piltcher, O.B. *et al.* (2002) 'A rat model of otitis media with effusion caused by eustachian tube obstruction with and without Streptococcus pneumoniae infection: Methods and course', *Otolaryngology - Head and Neck Surgery*, 126(5), pp. 490–498. Available at: https://doi.org/10.1067/mhn.2002.124935.

Plantinga, M. *et al.* (2013) 'Conventional and Monocyte-Derived CD11b+ Dendritic Cells

Initiate and Maintain T Helper 2 Cell-Mediated Immunity to House Dust Mite Allergen', *Immunity*, 38(2), pp. 322–335. Available at: https://doi.org/10.1016/j.immuni.2012.10.016.

Prendecki, M. *et al.* (2020) 'Temporal changes in complement activation in haemodialysis patients with COVID-19 as a predictor of disease progression', *Clinical Kidney Journal*, 13(5), pp. 889–896. Available at: https://doi.org/10.1093/CKJ/SFAA192.

Principi, N. *et al.* (1986) 'C-reactive protein in acute otitis media', *Pediatric Infectious Disease*, 5(5), pp. 525–527. Available at: https://doi.org/10.1097/00006454-198609000-00007.

Rajab, I.M., Hart, P.C. and Potempa, L.A. (2020) 'How C-Reactive Protein Structural Isoforms With Distinctive Bioactivities Affect Disease Progression', *Frontiers in Immunology*. Frontiers Media S.A. Available at: https://doi.org/10.3389/fimmu.2020.02126.

Ramage, L., Proudfoot, L. and Guy, K. (2004) 'Expression of C-reactive protein in human lung epithelial cells and upregulation by cytokines and carbon particles', *Inhalation Toxicology*, 16(9), pp. 607–613. Available at: https://doi.org/10.1080/08958370490464599.

Rao, Y. *et al.* (2021) 'Single-Cell Transcriptome Profiling Identifies Phagocytosis-Related Dual-Feature Cells in A Model of Acute Otitis Media in Rats', *Frontiers in Immunology*, 12. Available at: https://doi.org/10.3389/fimmu.2021.760954.

Redford, P.S., Murray, P.J. and O'Garra, A. (2011) 'The role of IL-10 in immune regulation during M. tuberculosis infection', *Mucosal Immunology*, 4(3), pp. 261–270. Available at: https://doi.org/10.1038/mi.2011.7.

Riesbeck, K. (2020) 'Complement evasion by the human respiratory tract pathogens *Haemophilus influenzae* and *Moraxella catarrhalis*', *FEBS Letters*, 594(16), pp. 2586–2597. Available at: https://doi.org/10.1002/1873-3468.13758.

Rosa-Olivares, J. *et al.* (2015) 'Otitis media: To treat, to refer, to do nothing: A review for the practitioner', *Pediatrics in Review*. American Academy of Pediatrics, pp. 480–486. Available at: https://doi.org/10.1542/pir.36-11-480.

Rosales, C. and Uribe-Querol, E. (2017) 'Phagocytosis: A Fundamental Process in Immunity', *BioMed Research International*. Hindawi Limited. Available at: https://doi.org/10.1155/2017/9042851.

Rosenberg, M. (1981) 'Bacterial adherence to polystyrene: A replica method of screening for bacterial hydrophobicity', *Applied and Environmental Microbiology*, 42(2), pp. 375–377. Available at: https://doi.org/10.1128/aem.42.2.375-377.1981.

Rowley, D. and Wardlaw, A.C. (1958) 'Lysis of gram-negative bacteria by serum.', *Journal of general microbiology*, 18(2), pp. 529–533. Available at: https://doi.org/10.1099/00221287-18-2-529.

Ruohola, A. *et al.* (2006) 'Microbiology of acute otitis media in children with tympanostomy tubes: Prevalences of bacteria and viruses', *Clinical Infectious Diseases*, 43(11), pp. 1417–1422. Available at: https://doi.org/10.1086/509332.

Sarafi, M.N. *et al.* (1997) 'Murine monocyte chemoattractant protein (MCP)-5: A novel CC chemokine that is a structural and functional homologue of human MCP-1', *Journal of Experimental Medicine*, 185(1), pp. 99–109. Available at: https://doi.org/10.1084/jem.185.1.99.

Schachern, P.A. *et al.* (2017) 'Neutrophil extracellular traps and fibrin in otitis media:

Analysis of human and chinchilla temporal bones', *JAMA Otolaryngology - Head and Neck Surgery*, 143(10), pp. 990–995. Available at: https://doi.org/10.1001/jamaoto.2017.1320.

Schilder, A.G.M.M. *et al.* (2016) 'Otitis media', *Nature Reviews Disease Primers*, 2(1), p. 16063. Available at: https://doi.org/10.1038/nrdp.2016.63.

Schwechheimer, C. and Kuehn, M.J. (2015) 'Outer-membrane vesicles from Gram-negative bacteria: Biogenesis and functions', *Nature Reviews Microbiology*. Nature Publishing Group, pp. 605–619. Available at: https://doi.org/10.1038/nrmicro3525.

Schweda, E.K.H. *et al.* (2003) 'Structural profiling of lipopolysaccharide glycoforms expressed by non-typeable Haemophilus influenzae: Phenotypic similarities between NTHi strain 162 and the genome strain Rd', *Carbohydrate Research*, 338(23), pp. 2731–2744. Available at: https://doi.org/10.1016/S0008-6215(03)00385-9.

Schweda, E.K.H. *et al.* (2007) 'Expression and structural diversity of the lipopolysaccharide of Haemophilus influenzae: Implication in virulence', *International Journal of Medical Microbiology*, 297(5), pp. 297–306. Available at: https://doi.org/10.1016/j.ijmm.2007.03.007.

Searight, F.T., Singh, R. and Peterson, D.C. (2022) *Otitis Media With Effusion*, *StatPearls*. StatPearls Publishing. Available at: http://www.ncbi.nlm.nih.gov/pubmed/30855877 (Accessed: 30 September 2022).

Seppanen, E. *et al.* (2018) 'Evidence of functional cell-mediated immune responses to nontypeable Haemophilus influenzae in otitis-prone children', *PLOS ONE*. Edited by R. Borrow, 13(4), p. e0193962. Available at: https://doi.org/10.1371/journal.pone.0193962.

Sharma, S.K., Casey, J.R. and Pichichero, M.E. (2011) 'Reduced Memory CD4+ T-Cell Generation in the Circulation of Young Children May Contribute to the Otitis-Prone Condition', *The Journal of Infectious Diseases*, 204(4), pp. 645–653. Available at: https://doi.org/10.1093/infdis/jir340.

Sharma, S.K., Casey, J.R. and Pichichero, M.E. (2012) 'Reduced serum IgG responses to pneumococcal antigens in otitis-prone children may be due to poor memory B-cell generation', *Journal of Infectious Diseases*, 205(8), pp. 1225–1229. Available at: https://doi.org/10.1093/infdis/jis179.

Sharma, S.K. and Pichichero, M.E. (2013) 'Cellular immune response in young children accounts for recurrent acute otitis media', *Current Allergy and Asthma Reports*, 13(5), pp. 495–500. Available at: https://doi.org/10.1007/s11882-013-0370-z.

Shrive, A.K. *et al.* (1996) 'Three dimensional structure of human C-reactive protein', *Nature Structural Biology*, 3(4), pp. 346–354. Available at: https://doi.org/10.1038/nsb0496-346.

Siboo, R. and Kulisek, E. (1978) 'A fluorescent immunoassay for the quantification of C-reactive protein', *Journal of Immunological Methods*, 23(1–2), pp. 59–67. Available at: https://doi.org/10.1016/0022-1759(78)90109-6.

Siegel, J. *et al.* (1975) 'Interactions of C reactive protein with the complement system. II. C reactive protein mediated consumption of complement by poly L lysine polymers and other polycations', *Journal of Experimental Medicine*, 142(3), pp. 709–721. Available at: https://doi.org/10.1084/jem.142.3.709.

Siegel, J., Rent, R. and Gewurz, H. (1974) 'Interactions of C-reactive protein with the complement system: I. Protamine-induced consumption of complement in acute phase

sera', *Journal of Experimental Medicine*, 140(3), pp. 631–647. Available at: https://doi.org/10.1084/jem.140.3.631.

Singh, S., Anshita, D. and Ravichandiran, V. (2021) 'MCP-1: Function, regulation, and involvement in disease', *International Immunopharmacology*. Elsevier B.V., p. 107598. Available at: https://doi.org/10.1016/j.intimp.2021.107598.

Singh, S.K., Suresh, M. V., Prayther, D.C., *et al.* (2008) 'Phosphoethanolamine-complexed C-reactive protein: A pharmacological-like macromolecule that binds to native low-density lipoprotein in human serum', *Clinica chimica acta; international journal of clinical chemistry*, 394(1–2), p. 94. Available at: https://doi.org/10.1016/J.CCA.2008.04.015.

Singh, S.K., Suresh, M. V., Voleti, B., *et al.* (2008) 'The connection between C-reactive protein and atherosclerosis', *Annals of Medicine*. NIH Public Access, pp. 110–120. Available at: https://doi.org/10.1080/07853890701749225.

Singh, S.K., Ngwa, D.N. and Agrawal, A. (2020) 'Complement Activation by C-Reactive Protein Is Critical for Protection of Mice Against Pneumococcal Infection', *Frontiers in Immunology*, 11, p. 1812. Available at: https://doi.org/10.3389/fimmu.2020.01812.

Slack, M.P.E. (2015) 'A review of the role of Haemophilus influenzae in community-acquired pneumonia', *Pneumonia*, 6(1), pp. 26–43. Available at: https://doi.org/10.15172/pneu.2015.6/520.

Smith-Vaughan, H. *et al.* (2006) 'Measuring nasal bacterial load and its association with otitis media', *BMC Ear, Nose and Throat Disorders*, 6(1), p. 10. Available at: https://doi.org/10.1186/1472-6815-6-10.

Sojo-Dorado, J. and Rodríguez-Baño, J. (2017) 'Gentamicin', in *Kucers the Use of Antibiotics: A Clinical Review of Antibacterial, Antifungal, Antiparasitic, and Antiviral Drugs, Seventh Edition*. CRC Press, pp. 964–991. Available at: https://doi.org/10.1201/9781315152110.

Sproston, N.R. and Ashworth, J.J. (2018) 'Role of C-Reactive Protein at Sites of Inflammation and Infection.', *Frontiers in immunology*, 9, p. 754. Available at: https://doi.org/10.3389/fimmu.2018.00754.

Steimle, A., Autenrieth, I.B. and Frick, J.S. (2016) 'Structure and function: Lipid A modifications in commensals and pathogens', *International Journal of Medical Microbiology*. Elsevier GmbH, pp. 290–301. Available at: https://doi.org/10.1016/j.ijmm.2016.03.001.

Stubbington, M.J.T. *et al.* (2017) 'Single-cell transcriptomics to explore the immune system in health and disease', *Science*. American Association for the Advancement of Science, pp. 58–63. Available at: https://doi.org/10.1126/science.aan6828.

Suresh, M. V. *et al.* (2006) 'Role of the Property of C-Reactive Protein to Activate the Classical Pathway of Complement in Protecting Mice from Pneumococcal Infection', *The Journal of Immunology*, 176(7), pp. 4369–4374. Available at: https://doi.org/10.4049/jimmunol.176.7.4369.

Suzuki, K. and Bakaletz, L.O. (1994) 'Synergistic effect of adenovirus type 1 and nontypeable Haemophilus influenzae in a chinchilla model of experimental otitis media', *Infection and Immunity*, 62(5), pp. 1710–1718. Available at: https://doi.org/10.1128/iai.62.5.1710-1718.1994.

Suzuki, S. *et al.* (2022) 'Association between C-reactive protein and risk of overall and 18

site-specific cancers in a Japanese case-cohort', *British Journal of Cancer*, 126(10), pp. 1481–1489. Available at: https://doi.org/10.1038/s41416-022-01715-8.

Swinkels, M. *et al.* (2018) 'C-reactive protein and pentraxin-3 binding of factor H-like protein 1 differs from complement factor H: Implications for retinal inflammation', *Scientific Reports*, 8(1), pp. 1–12. Available at: https://doi.org/10.1038/s41598-017-18395-7.

Swords, W.E. *et al.* (2000) 'Non-typeable Haemophilus influenzae adhere to and invade human bronchial epithelial cells via an interaction of lipooligosaccharide with the PAF receptor', *Molecular Microbiology*, 37(1), pp. 13–27. Available at: https://doi.org/10.1046/j.1365-2958.2000.01952.x.

Swords, W.E. *et al.* (2001) 'Binding of the non-typeable Haemophilus influenzae lipooligosaccharide to the PAF receptor initiates host cell signalling', *Cellular Microbiology*, 3(8), pp. 525–536. Available at: https://doi.org/10.1046/j.1462-5822.2001.00132.x.

Szalai, A.J. *et al.* (2000) 'Human C-reactive protein is protective against fatal Salmonella enterica serovar Typhimurium infection in transgenic mice', *Infection and Immunity*, 68(10), pp. 5652–5656. Available at: https://doi.org/10.1128/IAI.68.10.5652-5656.2000.

Tejani, N.R. *et al.* (1995) 'Use of C-Reactive Protein in Differentiation Between Acute Bacterial and Viral Otitis Media', *Pediatrics*, 95(5), pp. 664–669. Available at: https://doi.org/10.1542/peds.95.5.664.

Tesmer, L.A. *et al.* (2008) 'Th17 cells in human disease', *Immunological Reviews*. NIH Public Access, pp. 87–113. Available at: https://doi.org/10.1111/j.1600-065X.2008.00628.x.

Thomssen, H., Kahan, M. and Londei, M. (1995) 'Differential effects of interleukin-10 on the expression of HLA class II and CD1 molecules induced by granulocyte/macrophage colony-stimulating factor/interleukin-4', *European Journal of Immunology*, 25(9), pp. 2465–2470. Available at: https://doi.org/10.1002/eji.1830250909.

Tillett, W.S. and Francis, T. (1930) 'Serological reactions in pneumonia with a nonprotein somatic fraction of pneumococcus', *Journal of Experimental Medicine*, 52(4), pp. 561–571. Available at: https://doi.org/10.1084/jem.52.4.561.

Torzewski, M., Waqar, A.B. and Fan, J. (2014a) 'Animal models of C-reactive protein.', *Mediators of inflammation*, 2014, p. 683598. Available at: https://doi.org/10.1155/2014/683598.

Torzewski, M., Waqar, A.B. and Fan, J. (2014b) 'Animal models of C-reactive protein', *Mediators of Inflammation*, 2014. Available at: https://doi.org/10.1155/2014/683598.

Trial, J., Cieslik, K.A. and Entman, M.L. (2016) 'Phosphocholine-containing ligands direct CRP induction of M2 macrophage polarization independent of T cell polarization: Implication for chronic inflammatory states.', *Immunity, inflammation and disease*, 4(3), pp. 274–88. Available at: https://doi.org/10.1002/iid3.112.

Trial, J., Potempa, L.A. and Entman, M.L. (2016) 'The role of C-reactive protein in innate and acquired inflammation: new perspectives.', *Inflammation and cell signaling*, 3(2). Available at: http://www.ncbi.nlm.nih.gov/pubmed/27738646 (Accessed: 11 September 2019).

Trune, D.R. and Zheng, Q.Y. (2009) 'Mouse models for human otitis media.', *Brain research*, 1277, pp. 90–103. Available at: https://doi.org/10.1016/j.brainres.2009.02.047.

TSUJIMOTO, M., INOUE, K. and NOJIMA, S. (1980) 'C-Reactive Protein Induced

Agglutination of Lipid Suspensions Prepared in the Presence and Absence of Phosphatidylcholine1', *The Journal of Biochemistry*, 87(5), pp. 1531–1537. Available at: https://doi.org/10.1093/oxfordjournals.jbchem.a132894.

Tugirimana, P.L. *et al.* (2009) 'A new turbidimetric method for assaying serum C-reactive protein based on phosphocholine interaction', *Clinical Chemistry and Laboratory Medicine*, 47(11), pp. 1417–1422. Available at: https://doi.org/10.1515/CCLM.2009.312.

Uribe-Querol, E. and Rosales, C. (2020) 'Phagocytosis: Our Current Understanding of a Universal Biological Process', *Frontiers in Immunology*. Frontiers Media S.A., p. 1066. Available at: https://doi.org/10.3389/fimmu.2020.01066.

Val, S. *et al.* (2016) 'Proteomic Characterization of Middle Ear Fluid Confirms Neutrophil Extracellular Traps as a Predominant Innate Immune Response in Chronic Otitis Media', *PLOS ONE*. Edited by N. Palaniyar, 11(4), p. e0152865. Available at: https://doi.org/10.1371/journal.pone.0152865.

Vanneste, P. and Page, C. (2019) 'Otitis media with effusion in children: Pathophysiology, diagnosis, and treatment. A review', *Journal of Otology*. PLA General Hospital Department of Otolaryngology Head and Neck Surgery, pp. 33–39. Available at: https://doi.org/10.1016/j.joto.2019.01.005.

Vergison, A. (2008) 'Microbiology of otitis media: A moving target', *Vaccine*, 26(SUPPL. 7), p. G5. Available at: https://doi.org/10.1016/j.vaccine.2008.11.006.

Verhoeff, M. *et al.* (2006) 'Chronic suppurative otitis media: A review', *International Journal of Pediatric Otorhinolaryngology*. Elsevier, pp. 1–12. Available at: https://doi.org/10.1016/j.ijporl.2005.08.021.

Vikhe, P.P. *et al.* (2019) 'Cellular content plays a crucial role in Non-typeable *Haemophilus influenzae* infection of preinflamed *Junbo* mouse middle ear', *Cellular Microbiology*, 21(1), p. e12960. Available at: https://doi.org/10.1111/cmi.12960.

Vikhe, P.P. *et al.* (2020) 'Mutation in Fbxo11 Leads to Altered Immune Cell Content in Jeff Mouse Model of Otitis Media', *Frontiers in Genetics*, 11. Available at: https://doi.org/10.3389/fgene.2020.00050.

Volanakis, J.E. and Wirtz, K.W.A. (1979) 'Interaction of C-reactive protein with artificial phosphatidylcholine bilayers [20]', *Nature*, pp. 155–157. Available at: https://doi.org/10.1038/281155a0.

Wang, X. *et al.* (2002) ' Toll-Like Receptor 4 Mediates Innate Immune Responses to Haemophilus influenzae Infection in Mouse Lung ', *The Journal of Immunology*, 168(2), pp. 810–815. Available at: https://doi.org/10.4049/jimmunol.168.2.810.

Watson, J. *et al.* (2019) 'Predictive value of inflammatory markers for cancer diagnosis in primary care: a prospective cohort study using electronic health records', *British Journal of Cancer*, 120(11), pp. 1045–1051. Available at: https://doi.org/10.1038/s41416-019-0458-x.

Weiser, J.N. *et al.* (1998) 'Phosphorylcholine on the lipopolysaccharide of Haemophilus influenzae contributes to persistence in the respiratory tract and sensitivity to serum killing mediated by C-reactive protein.', *The Journal of experimental medicine*, 187(4), pp. 631–40. Available at: https://doi.org/10.1098/rsif.2012.0904.

Weiser, J.N., Love, J.M. and Moxon, E.R.R. (1989) 'The molecular mechanism of phase variation of H. influenzae lipopolysaccharide', *Cell*, 59(4), pp. 657–665. Available at: https://doi.org/10.1016/0092-8674(89)90011-1.

Weiser, J.N. and Pan, N. (1998) ‘Adaptation of *Haemophilus influenzae* to acquired and innate humoral immunity based on phase variation of lipopolysaccharide’, *Molecular Microbiology*, 30(4), pp. 767–775. Available at: https://doi.org/10.1046/j.1365-2958.1998.01108.x.

West-Barnette, S., Rockel, A. and Swords, W.E. (2006) ‘Biofilm growth increases phosphorylcholine content and decreases potency of nontypeable Haemophilus influenzae endotoxins’, *Infection and Immunity*, 74(3), pp. 1828–1836. Available at: https://doi.org/10.1128/IAI.74.3.1828-1836.2006.

Whelan, M. *et al.* (2000) ‘A Filarial Nematode-Secreted Product Signals Dendritic Cells to Acquire a Phenotype That Drives Development of Th2 Cells’, *The Journal of Immunology*, 164(12), pp. 6453–6460. Available at: https://doi.org/10.4049/jimmunol.164.12.6453.

Whitehead, A.S. *et al.* (1990) ‘Mouse C-reactive protein. Generation of cDNA clones, structural analysis, and induction of mRNA during inflammation’, *Biochemical Journal*, 266(1), pp. 283–290. Available at: https://doi.org/10.1042/bj2660283.

Wieland, C.W. *et al.* (2005) ‘ The MyD88-Dependent, but Not the MyD88-Independent, Pathway of TLR4 Signaling Is Important in Clearing Nontypeable Haemophilus influenzae from the Mouse Lung ’, *The Journal of Immunology*, 175(9), pp. 6042–6049. Available at: https://doi.org/10.4049/jimmunol.175.9.6042.

Williams, C.G. *et al.* (2022) ‘An introduction to spatial transcriptomics for biomedical research’, *Genome Medicine*. BioMed Central Ltd, p. 68. Available at: https://doi.org/10.1186/s13073-022-01075-1.

Williams, M.R. *et al.* (2018) ‘Antibiotic prescribing quality for children in primary care: An observational study’, *British Journal of General Practice*, 68(667), pp. e90–e96. Available at: https://doi.org/10.3399/bjgp18X694409.

Willrich, M.A. V. (2020) ‘The complement system’, in *Contemporary Practice in Clinical Chemistry*. Elsevier, pp. 391–412. Available at: https://doi.org/10.1016/B978-0-12-815499-1.00023-5.

Wolbink, G.J. *et al.* (1996) ‘CRP-mediated activation of complement in vivo: assessment by measuring circulating complement-C-reactive protein complexes.’, *Journal of immunology (Baltimore, Md. : 1950)*, 157(1), pp. 473–9. Available at: http://www.ncbi.nlm.nih.gov/pubmed/8683153 (Accessed: 26 May 2022).

Wong, J.B. *et al.* (2019) ‘B-1a cells acquire their unique characteristics by bypassing the pre-BCR selection stage’, *Nature Communications*, 10(1), pp. 1–15. Available at: https://doi.org/10.1038/s41467-019-12824-z.

Wu, Y. *et al.* (2015) ‘C-reactive protein and inflammation: conformational changes affect function’, *Biological Chemistry*, 396(11), pp. 1181–1197. Available at: https://doi.org/10.1515/hsz-2015-0149.

Xu, Q. *et al.* (2017) ‘Nasopharyngeal polymicrobial colonization during health, viral upper respiratory infection and upper respiratory bacterial infection’, *Journal of Infection*, 75(1), pp. 26–34. Available at: https://doi.org/10.1016/j.jinf.2017.04.003.

Yamanaka, T. *et al.* (1982) ‘Immunologic aspects of otitis media with effusion: Characteristics of lymphocyte and macrophage reactivity’, *Journal of Infectious Diseases*, 145(6), pp. 804–810. Available at: https://doi.org/10.1093/infdis/145.6.804.

Yoshida, T. *et al.* (2020) ‘C reactive protein impairs adaptive immunity in immune cells of patients with melanoma’, *Journal for ImmunoTherapy of Cancer*, 8(1), p. e000234.

Available at: https://doi.org/10.1136/jitc-2019-000234.

Young, N.M., Foote, S.J. and Wakarchuk, W.W. (2013) 'Review of phosphocholine substituents on bacterial pathogen glycans: Synthesis, structures and interactions with host proteins', *Molecular Immunology*, 56(4), pp. 563–573. Available at: https://doi.org/10.1016/j.molimm.2013.05.237.

Yuan, Y. *et al.* (2017) 'Surface characteristics influencing bacterial adhesion to polymeric substrates', *RSC Advances*, 7(23), pp. 14254–14261. Available at: https://doi.org/10.1039/c7ra01571b.

Zeisel, S.H. and da Costa, K.-A. (2009) 'Choline: an essential nutrient for public health.', *Nutrition reviews*, 67(11), pp. 615–23. Available at: https://doi.org/10.1111/j.1753-4887.2009.00246.x.

Zhang, L. *et al.* (2018) 'An ELISA Assay for Quantifying Monomeric C-Reactive Protein in Plasma', *Frontiers in Immunology*, 9(MAR), p. 511. Available at: https://doi.org/10.3389/fimmu.2018.00511.

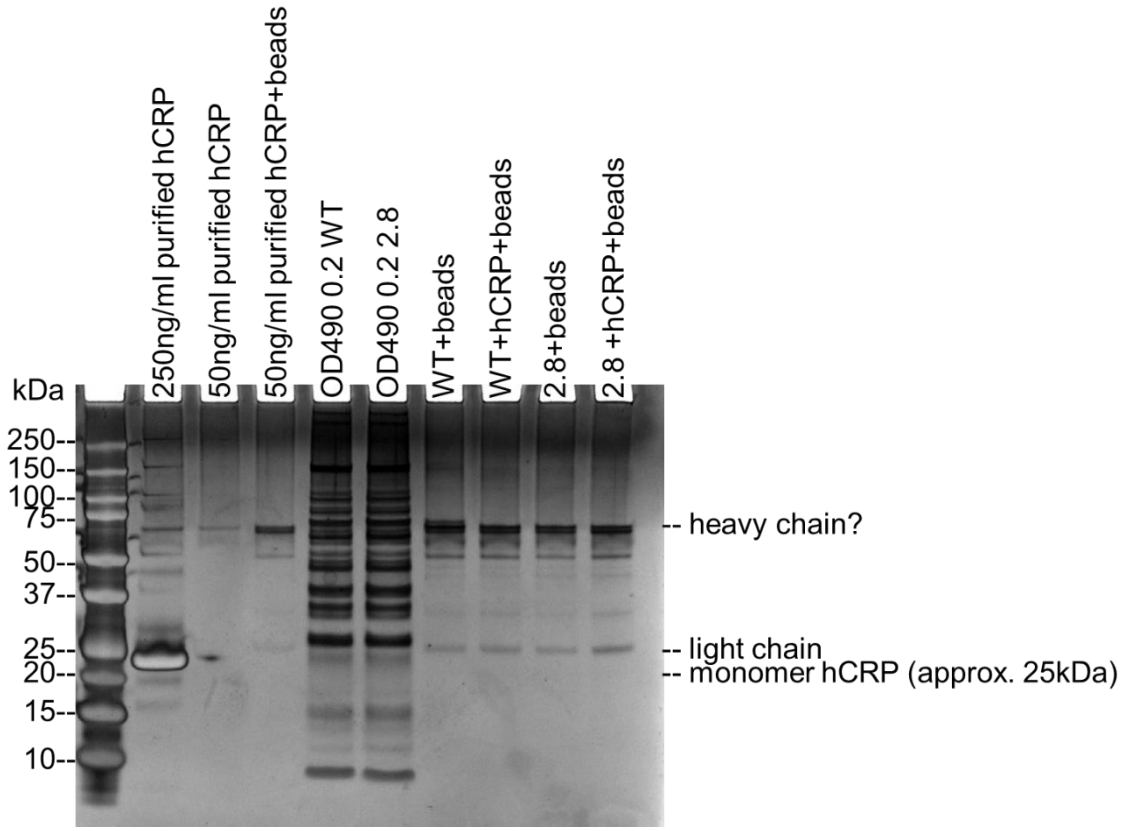

Appendix figure 1. SDS-PAGE gel for co-immunoprecipitation of NTHi-bound human CRP (hCRP).

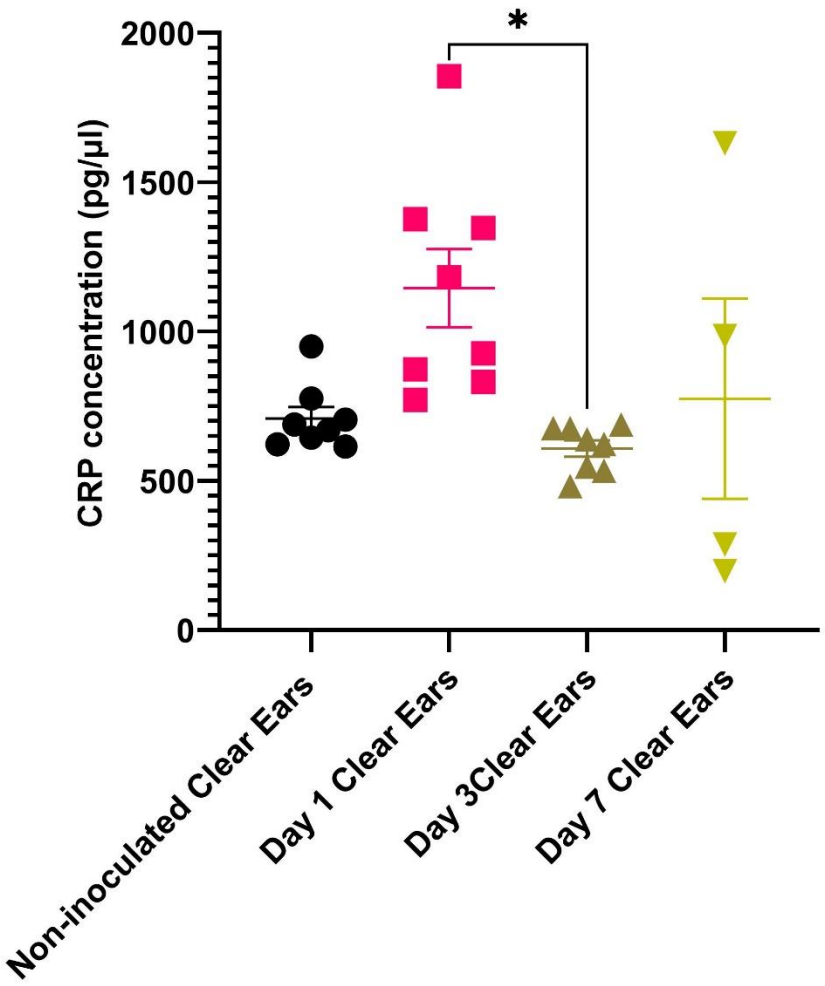

Appendix figure 2. CRP levels in the middle ear of C3H/HeH mice infected with NTHi 375sr.

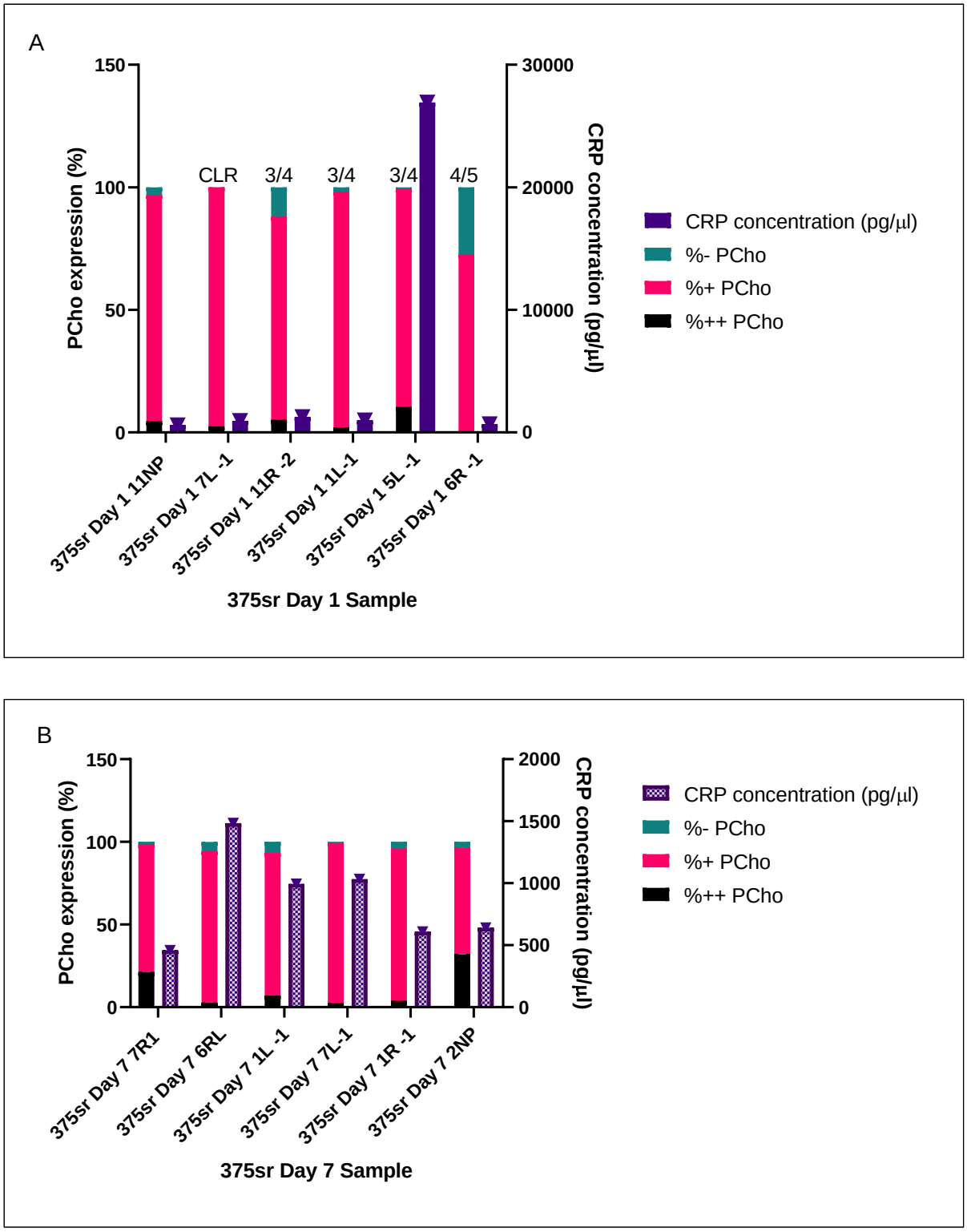

Appendix figure 3. PCho expression on NTHi from NP and MEF from the *Junbo* mice day 1 and 7 post inoculation with NTHi 375sr. (A) PCho expression day 1 post inoculation in the *Junbo* mouse NP and MEF. (B) PCho expression day-7 post inoculation NP and MEF.

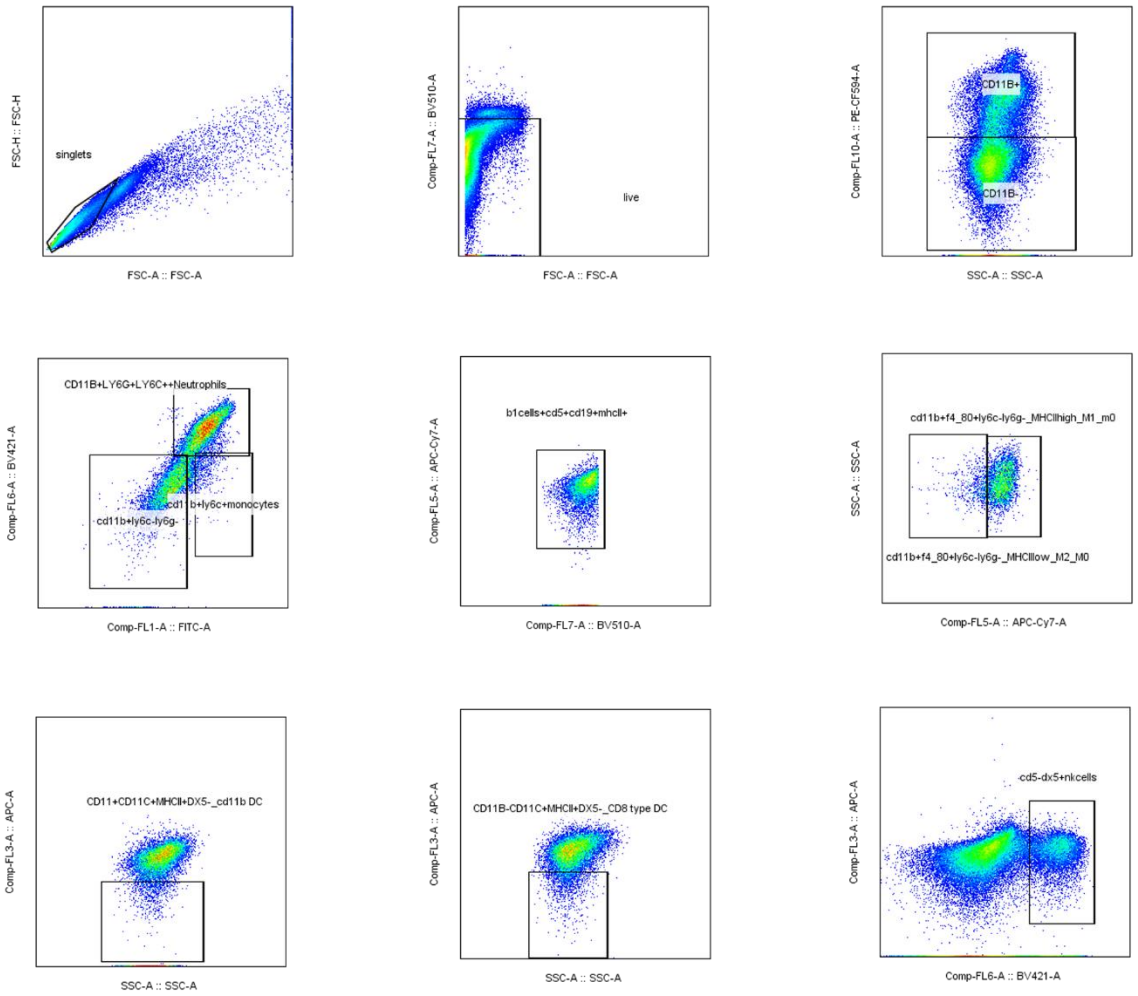

Appendix figure 4. Gating strategy for innate immune cell profiling in the *Junbo* mouse tissues and fluids

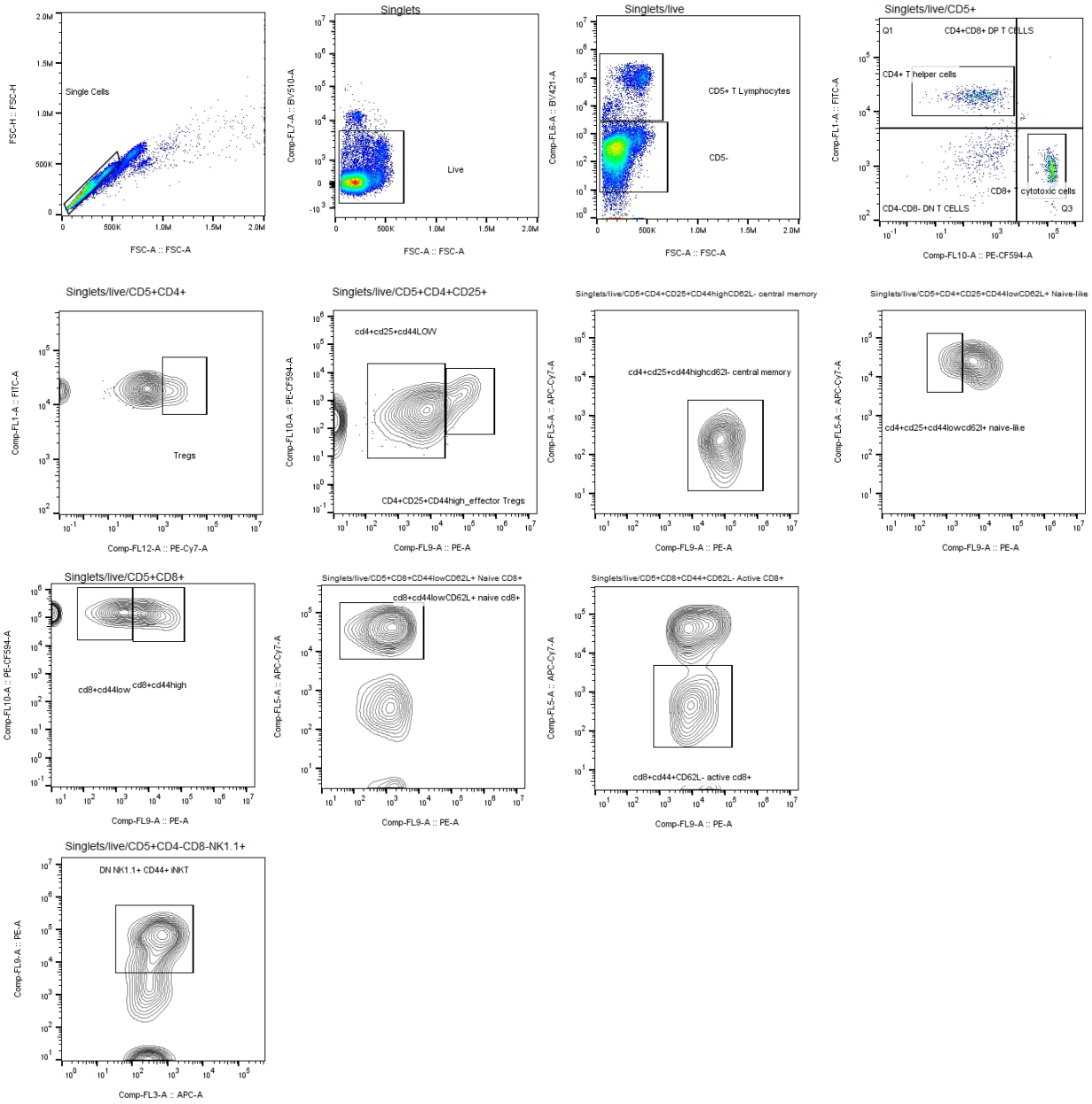

Appendix figure 5. Gating strategy for adaptive immune cell profiling in the *Junbo* mouse tissues and fluids

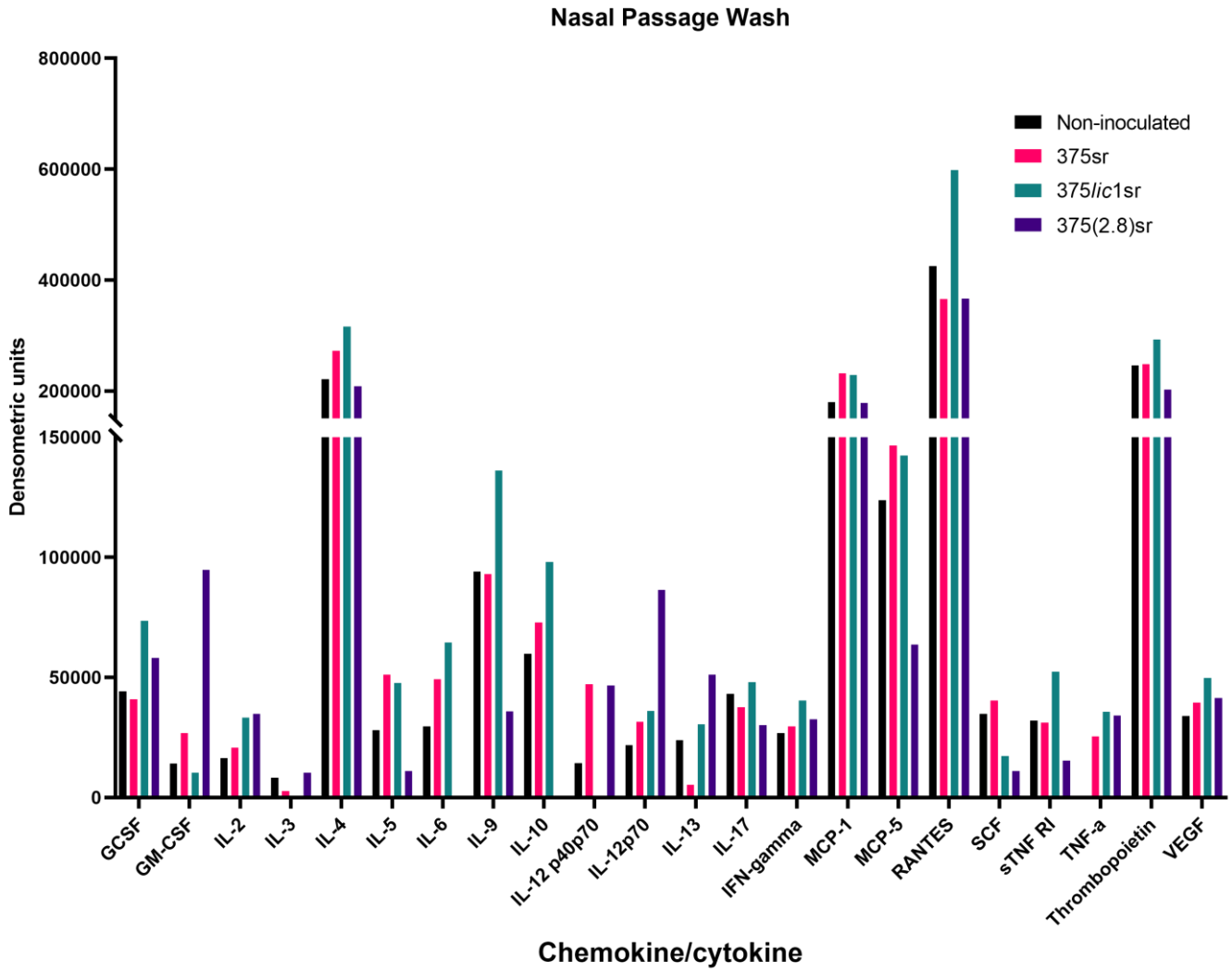

Appendix figure 6. Cytokine and chemokine expression levels in the *Junbo* mouse NP following infection with NTHi 375 strains

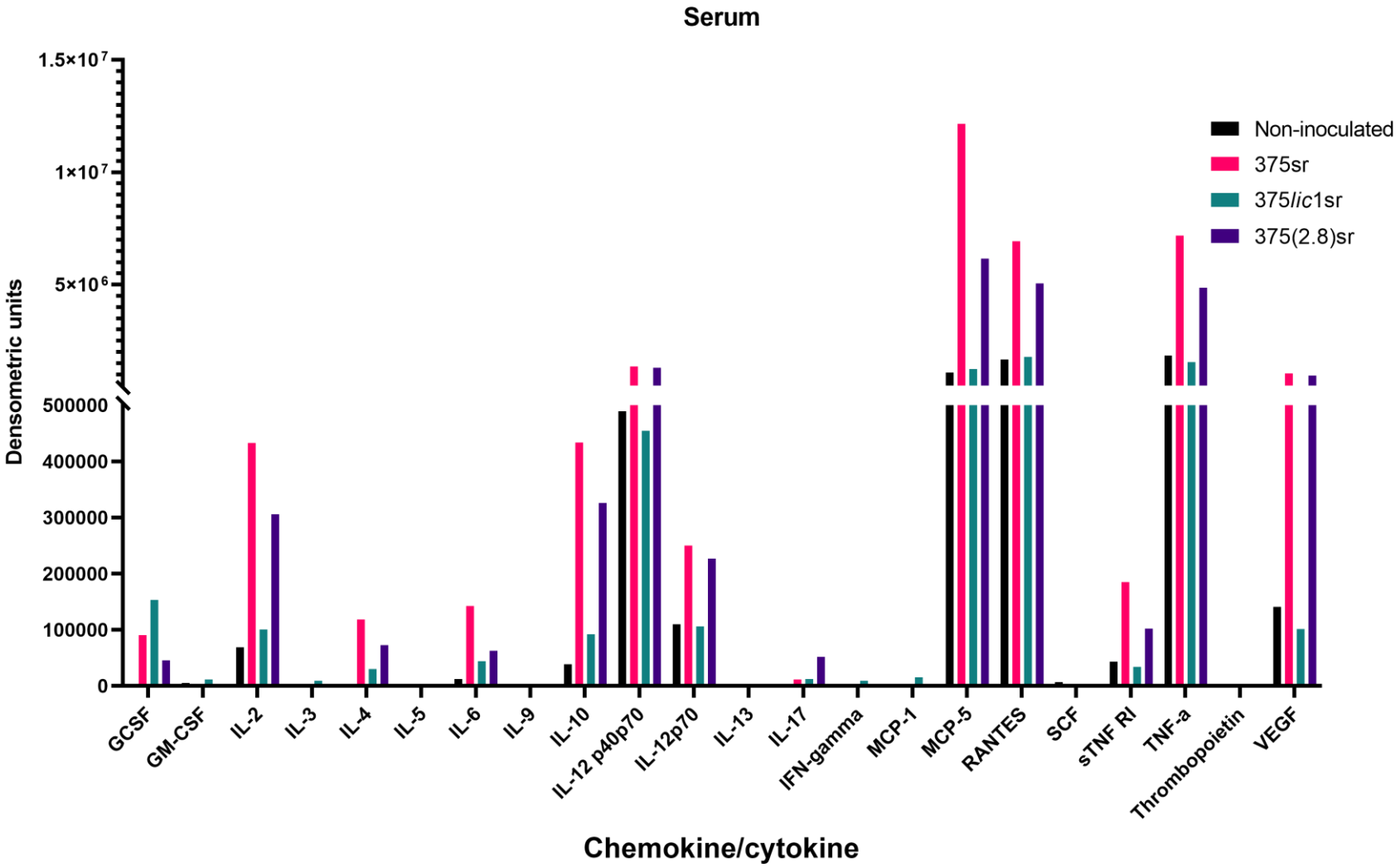

Appendix figure 7. Cytokine and chemokine expression levels in the *Junbo* mouse blood following infection with NTHi 375 strains

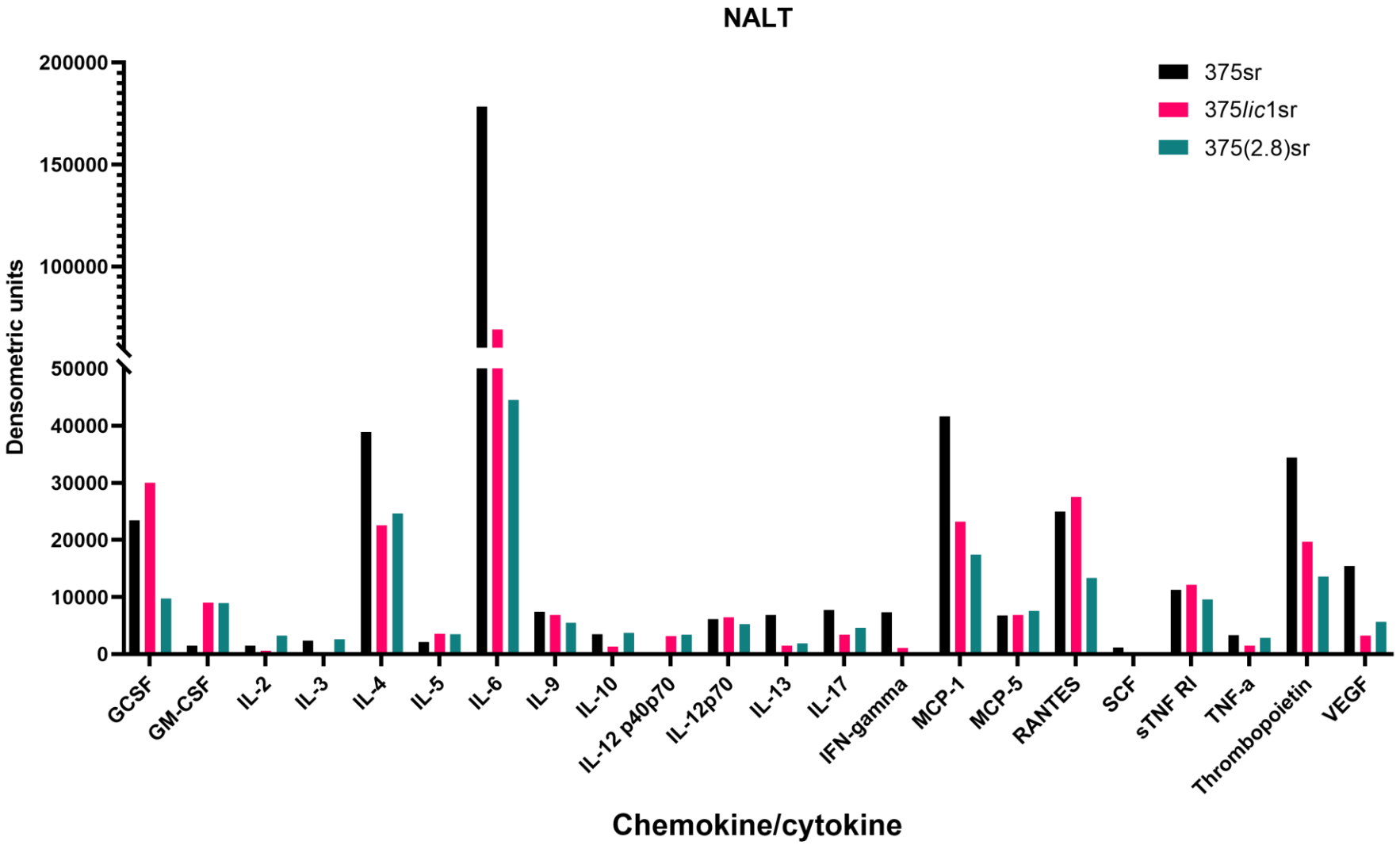

Appendix figure 8. Cytokine and chemokine expression levels in the *Junbo* mouse NALT following infection with NTHi 375 strains

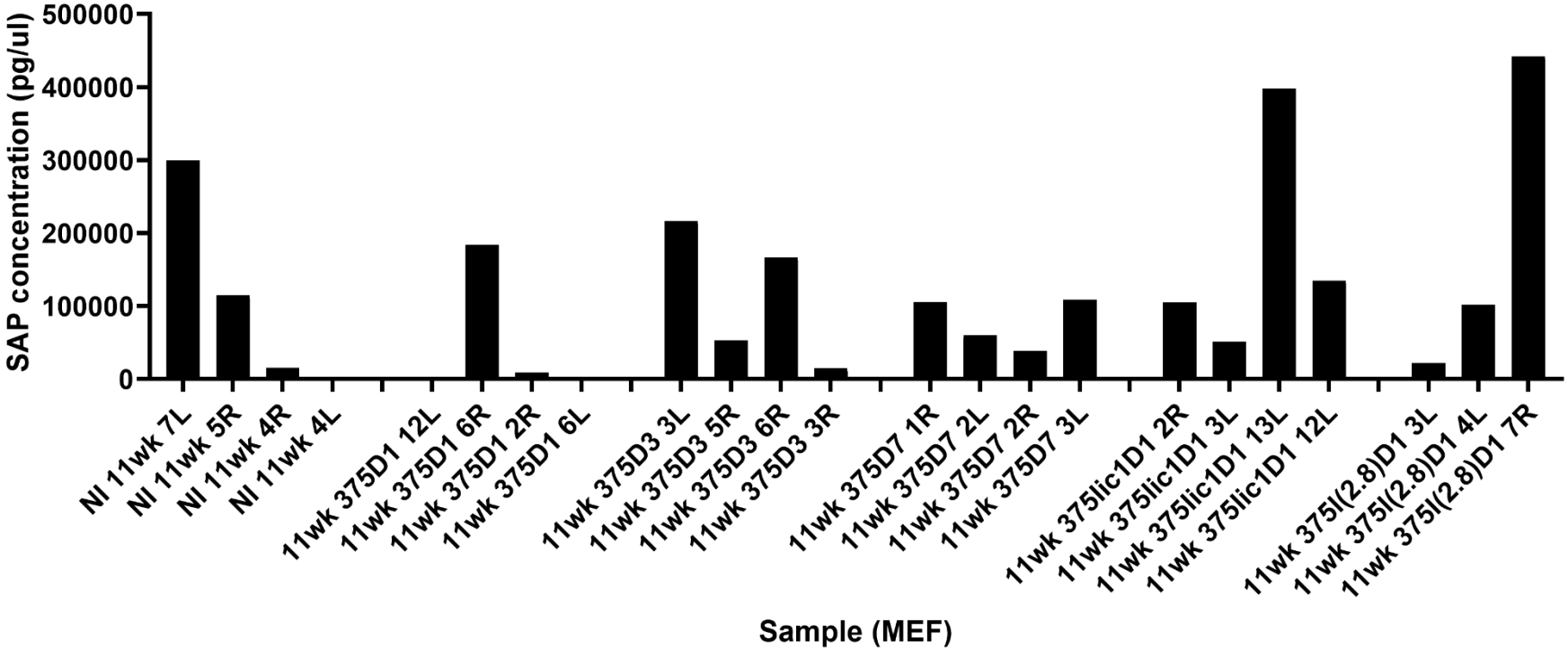

Appendix figure 9. SAP levels in the *Junbo* mouse middle ear fluids following infection with NTHi 375 strains

Appendix table 1 Immune cell markers defining specific innate and adaptive immune cells

Immune cell	Positive immune cell markers
Neutrophils	CD11b+Ly6G+Ly6C+
Monocytes	Ly6G-CD11b+Ly6C+
Macrophages	Ly6C-Ly6G-CD11b+SSClowF4/80+
M1-like macrophages	Ly6C-Ly6G-CD11b+SSClowF4/80+MHCIIhigh
M2-like macrophages	Ly6C-Ly6G-CD11b+SSClowF4/80+MHCIIlow
CD8+ dendritic cells	DX5-CD11b- CD11C+MHCII+
CD11b+ dendritic cells	DX5-CD11C+MHCII+CD11b+
Eosinophils	Ly6C-Ly6G-CD11b+SSC-Ahigh
B1a cells	CD11b-CD5+CD19+MHCII+
Invariant natural killer cells	CD4-CD8-NK1.1+CD44+
Natural killer cells	CD5+CD44+DX5+
T helper (CD4)+ cells	CD8-CD5+CD4+
T helper (CD4)+ effector cells	CD8-CD5+CD4+CD44+
T helper (CD4)+ resting cells	CD8-CD5+CD4+CD44lowCD62L-
T cytotoxic (CD8+) cells	CD4-CD5+CD8+
T cytotoxic (CD8+) naïve cells	CD4-CD5+CD8+CD62L+CD44-
T cytotoxic (CD8+) effector cells	CD4-CD5+CD8+CD62L-CD44+
T cytotoxic (CD8+) resting cells	CD4-CD5+CD8+CD62L+CD44+
T regulatory cells	CD8-CD5+CD4+CD25+
T regulatory effector cells	CD8-CD5+CD4+CD25+CD44+
T regulatory memory cells	CD4+CD25+CD44+CD62L-